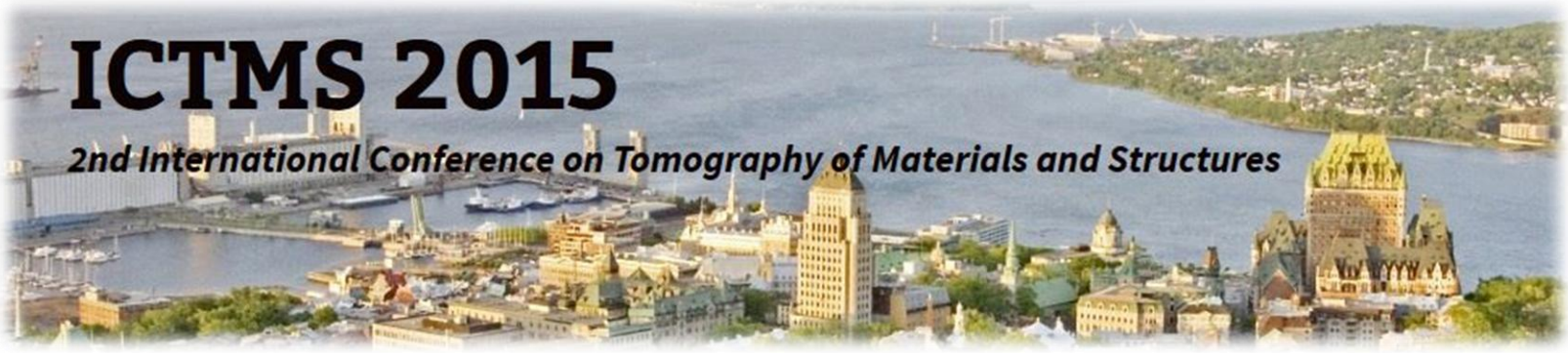

PROGRAM

2nd International Conference on Tomography of Materials and Structures

June 29th – July 3rd, 2015

Québec, Canada

INRS
UNIVERSITÉ DE RECHERCHE
A RESEARCH UNIVERSITY

Lab CT Scan
Laboratoire multidisciplinaire de tomodensitométrie
pour les ressources naturelles et le génie civil

Contents

Welcome

The conference Organizing Committee welcomes you to the second International Conference on Tomography of Material and Structure. This conference is held every two years. The first one was hosted by the Ghent University in Gent, Belgium, in 2013.

The International Conference on Tomography of Materials and Structures is dedicated to CT-Scanning for non-medical applications. This four full-day congress will bring together an international group of scientists to discuss a broad range of issues related to the use of computed tomography in materials and structures and all its related topics.

The main focus of this conference will be:

- X-ray and neutron tomography acquisition hardware, software and set-ups:
- Advances in reconstruction algorithms:
- 3D image analysis
- Applications of recent advances in CT imaging.
- New equipment (Medical CT, Micro-Scan, Nano-Scan)
- 10 specifics themes including Hydraulics and sediment transport, Geomaterial,
- Materials, Structures and Mineralogy, Wood, Sediments structures, ancient and Modern, Innovative geotechnical Applications, Concrete & building rocks, Porous Material, Hydrogeology, water infiltration and Pollution, Archaeology, Petroleum core analysis

New studies and contributions from universities, governmental agencies and industry are presented.

92 oral presentations and 70 poster presentations will be done. The allocated time for each presentation will be 20 minutes (15 minutes for the presentation itself and 5 minutes for questions).

The abstracts are included inside this program and all the extended abstracts will be provided on a USB stick.

We expect that a special issue of some international journal will be produced to include the 15 more promising papers.

Enjoy the conference, and have a great time in Quebec City, the Oldest city of North America!

ICTMS2015 Organizing Committee

Committees

Chairs:

Prof Dr. Bernard Long – INRS, Québec, Canada (Chair)
Prof Dr. Pierre Francus – INRS, Québec, Canada (Co-chair)

Local organising committee:

Regis Xhardé – INRS
Stéphane Montreuil – INRS
Louis-Frédéric Daigle – INRS
Mathieu Des Roches – INRS
Sally J. Selvadurai – McGill
Geneviève Treyvaud – INRS
Michel Malo – lNRS
Mathieu Duchesne – NRCan, Québec
Richard Martel – lNRS
Corinne B.-Brunelle – INRS

Scientific committee:

Prof Dr. Robert Aller – Stony Brook University, USA
Prof Dr. Khalid Alshibli – University of Tennessee, USA
Prof Dr. Richard W.C. Arnott – University of Ottawa, Canada
Prof Dr. Reginald Auger – Université Laval, Québec, Canada
Dr. Frederic De Beer – NECSA, South Africa
Dr. Dominique Bernard – CNRS, Bordeaux France
Dr. Mattieu Boone – Ghent University, Belgium
Prof Dr. Jean-Yves Buffiere – INSA, Lyon, France
Prof Dr. Leslie Butler – LSU, Baton Rouge, USA
Prof Dr. Jan Carmeliet – ETH Zurich, Switzerland
Prof Dr. Veerle Cnudde – Ghent University, Belgium
Dr. Francesco De Carlo – Argonne National Laboratory, USA
Dr. Dominique Derome – Empa, Zurich, Switzerland
Prof Dr. Philippe Després – Université Laval, Canada
Prof Dr. Jacques Desrues – CNRS, laboratoire 3SR, Grenoble, France
Prof Dr. Subhasis Ghoshal – McGill University, Montréal, Canada
Prof Dr. Giovanni Grasselli – University of Toronto, Canada
Dr. Stephen Hall – Lund University, Sweden

Edited by:

INRS-ETE
ISBN – 978-2-89146-847-3

Thanks to our sponsors

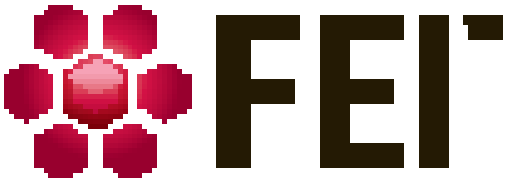

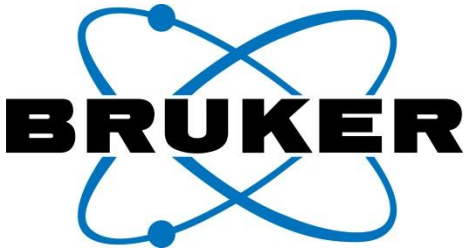

Conference Venue

Location

The 2nd International Conference on Tomography of Materials and Structures will be held at the Hilton Hotel, in the heart of Quebec City.

Hilton Hotel
1100, Rene-Levesque East, Quebec City,
Quebec, G1R 4P3 Canada
Tel : 418-647-2411 Fax : 418-647-6488

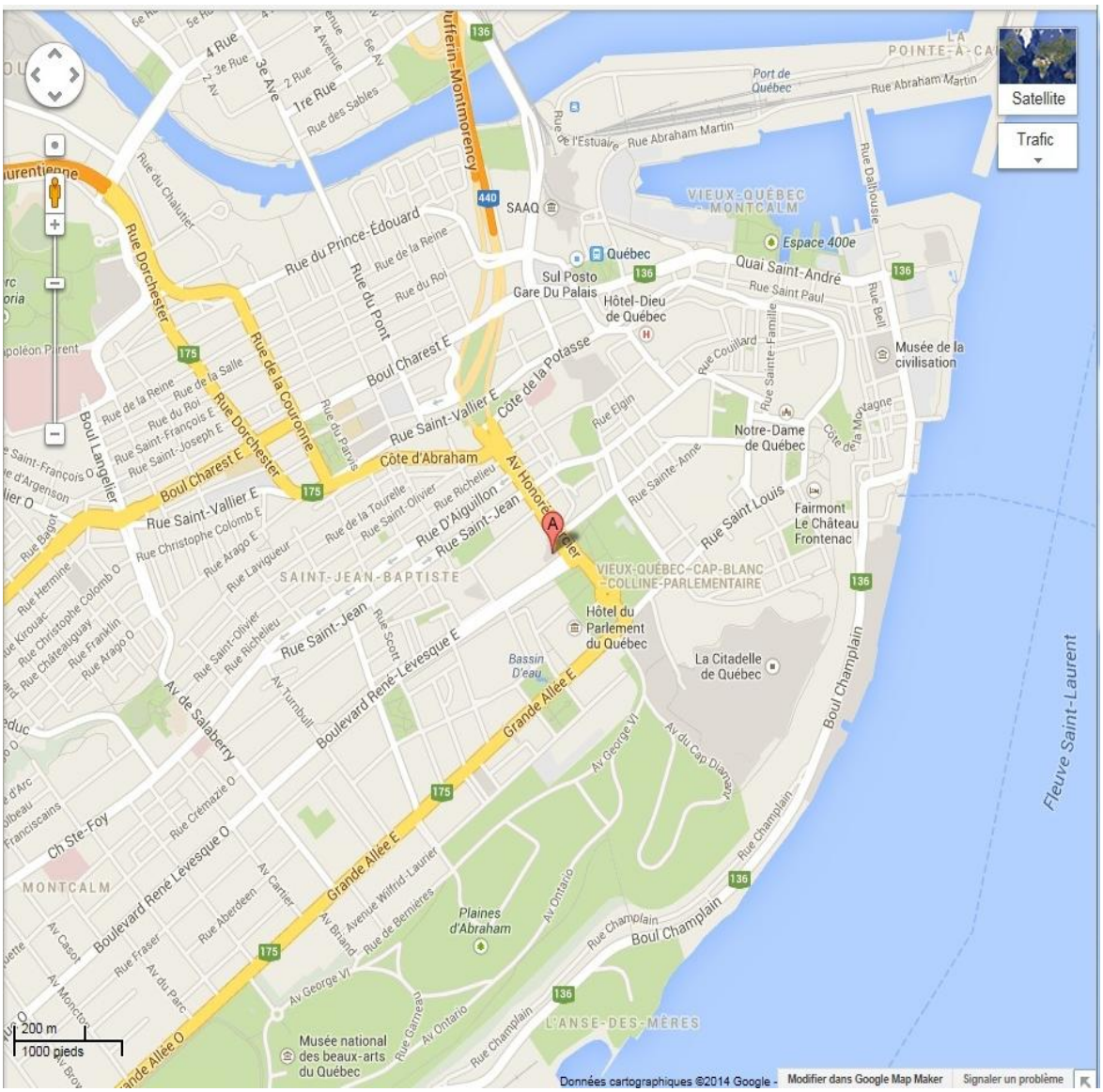

By Plane

Jean-Lesage International Airport, 16 km (10 miles) away from downtown Quebec City, can be reached via boulevard Wilfrid-Hamel (138) or autoroute Charest (440)
Phone : 418-640-3300
For all flight options from and to Quebec City, please refer to the Quebec City Jean-Lesage International Airport Flight Planner or the Air Accessibility Chart

Airlines

Air Canada
Direct flights from Toronto, Ottawa, Montreal, Gaspé, Sept-Îles, Îles-de-la-Madeleine and Wabush
Reservation : 1-888-247-2262, Info: 1-888-422-7533

Air Transat
Seasonal flights from Paris
Reservation : 1-866-391-6654, Info: 1-877-872-6728

Delta Air lines
Direct flights from New York JFK
Reservation : 1-800-241-4141

Porter Airlines
Direct flight from Toronto
Reservation : 1-888-619-8622

United Airlines
Direct flights from Chicago and Newark/New York
Reservation : 1-800-864-8331

U.S. Airways
Direct flights from Philadelphia
Reservation : 1-800-428-4322

Westjet
Direct flights from Toronto
Reservation and information : 1-877-956-6982

By Car

Highway 20 (autoroute Jean-Lesage) runs along the south shore of the St. Lawrence River, and Highway 40 (autoroute Félix-Leclerc) is the north shore access to the city
Travel Distances : Source: CAA data

Canadian Cities	Miles*	Kilometers
Halifax	1,069	1,069
Montreal	253	253
Ottawa	450	450
Toronto	766	766

American Cities	Miles*	Kilometers
Atlanta	1401	2,241
Boston	381	610
Chicago	1,016	1,625
Detroit	728	1,164
New York	524	839
Philadelphie	617	987
Washington D.C.	749	1,199

By Bus

Espacebus.com

Espacebus.com gives you the schedule and details for all bus services going to Quebec City from any departure point

Intercar

Intercar links Quebec City with Saguenay, Lac-Saint-Jean, Charlevoix, and all destinations along the North Shore (Côte-Nord)

Orléans Express

Orleans Express Coach Lines provide daily service between Quebec City, Montreal, and other destinations in the province

Greyhound

Visitors travelling by bus from the USA come into Montreal via Greyhound, then transfer to Orléans Express bus for Quebec City

Quebec City Bus Stations, Gare du Palais Bus Terminal

320, rue Abraham-Martin, Quebec : 418-525-3000

Sainte-Foy Terminal

3001, Chemin des Quatre-Bourgeois, borough of Sainte-Foy–Sillery–Cap-Rouge. 418-650-0087

By Train

VIA Rail Canada

Daily VIA Rail Canada service between Toronto, Ottawa, Montreal and Quebec City
Phone : 1-888-842-7245
Visitors traveling by train from the USA come into Montreal via Amtrak, then transfer to VIA Rail Canada trains for Quebec City

Amtrak

Phone : 1-800-USA-RAIL (1-800-872-7245)

Quebec City Train Stations

Gare du Palais (Central Station) : 450, rue de la Gare-du-Palais, Quebec
Phone : 1-888-842-7245
Gare de Sainte-Foy : 3255, chemin de la Gare, borough of Sainte-Foy–Sillery–Cap-Rouge
Phone : 1-888-842-7245

Electricity

Quebec's electrical current is 60 cycles, 110 volts. An adapter is needed for electrical appliances using another type of current, such as the 220-volt European system

Emergency

For any type of medical emergency
Health Info line (daily, 24 hours/day, answering service provided by qualified nurses) : 8-1-1
Enfant-Jésus Hospital : 1401, 18e rue, Québec, 418-649-5555
Hôtel-Dieu Hospital : Côte du Palais, Vieux-Québec, 418-691-5042
Jeffery Hale Hospital : 1250, chemin Sainte-Foy, Québec, 418-684-5333
Saint-François d'Assise Hospital : 10, rue de l'Espinay, Québec, 418-525-4388
Saint-Sacrement Hospital : 1050, chemin Sainte-Foy, Québec, 418-682-7515
Laval University Hospital (C.H.U.Q.) : 2705, boulevard Laurier, Sainte-Foy, 418-654-2114
Poison Control Center : (daily, 24 hours/day) 418-656-8090, 1-800-463-5060
Tel-Aide Crisis Center : (open every day: anxiety, emotional crisis, depression) 418-686-2433
Dentist : 418-666-4363 / 7 days a week and statutory holidays.
Other 24 hour/day emergencies : Police, fire and ambulance 9-1-1

Quebec Provincial Police

(Sûreté du Québec) 418-623-6262 or 310-4141 (anywhere in the province of Quebec).

Free Wireless Internet Connection

Thanks to ZAP Quebec, the Quebec region has several access points throughout the city.

Gratuities

With very few exceptions, tips are not included in the final tabulation of restaurant bills. Tips are usually 15% of the total bill, excluding taxes.

Language

French is the official language of Québec but English is widely spoken in tourist areas (attractions, hotels, restaurants and boutiques in tourist areas).

Money

Canadian and American dollars are not at par. American currency is accepted in most establishments at variable exchange rates.
Legal tender is the Canadian dollar, which divides into 100 cents. Bills come in the following denominations: 5, 10, 20, 50 and 100 dollars. The coins in use are of the following denominations: 5, 10 and 25 cents, as well as one and two dollars.

Banks and Caisses Populaires (credit unions)

Normal banking hours are from 10 a.m. to 3 p.m., Monday through Friday, with extended hours on Thursday, Friday and Saturday at some locations. Traveler's cheques, ideally in Canadian funds, are the safest way to carry money and are accepted by banks and major commercial establishments.

Credit Cards

Major credit cards such as American Express, MasterCard and Visa are accepted almost everywhere.
With the advent of automated teller machines, visitors can do banking through network systems like "Plus", "Circus", "Interac", etc. and enjoy excellent rates of exchange.

No Smoking Regulations

The Tobacco Law forbids smoking in all public buildings, including bars and restaurants.

Taxes

The federal tax on goods and services (GST) is 5% and applies to most goods and services in Canada. The provincial sales tax (PST) is 9.975% and is charged on the selling price not including the federal tax and applies to most goods and services purchased in Québec.

Conference Information

Registration Information

The Welcome desk is open Monday from 14:00 to 17:30pm and other day from 8:00 to 17:30. Delegate will be provided with a name badge, a bag with the program and abstract book. For security reasons, the name badges must be visible at any time to get access to the sessions, the posters, the booths, lunch buffets and refreshments, and receptions.

Welcome Cocktail

A Welcome Cocktail, courtesy of GE is offered to all participants on Monday evening from 18:30 in the Hilton Hotel.

Lunch Buffets and Refreshments

Refreshment will be served every day in the morning and in the afternoon.
Lunch buffet will be serving at all participants in the central room between 12:10 and 13:40.

Gala Dinner

The Gala Dinner will be served in the south room of the Hilton Hotel on Thursday July 2nd at 19:00.

IntAC Meeting

The IntAC Meeting will be held on Wednesday July 1st in the Palais room from 17:10 to 18:30 pm.

Workshop

A workshop titled "*Avizo 3D analysis software for materials science*" will be held by FEI and will be presented by Nicholas Vito, FEI Avizo expert. Join the FEI team for a workshop introducing advanced 3D visualization and processing solutions for materials analysis. After a quick introduction, attendees will have the opportunity to ask questions, see live demonstrations and use Avizo software.The topics covered at the Avizo workshop will include:

- General introduction to Avizo software
- 3D visualization (slicing, volume rendering)
- 3D image processing and segmentation
- Quantification and advanced measurements - incl. porosity
- Fiber analysis
- Surface and 3D mesh generation, skeletonization, and image-to-simulation workflows
- Material properties simulation - e.g. permeability
- Tasks automation

General Conference Program

<table>
<tr><th></th><th>Mon | 29 June</th><th>Tue | 30 June</th><th>Wed | 1 July</th><th>Thur | 2 July</th><th>Fri | 3 July</th></tr>
<tr><td>8:00</td><td></td><td>Registration</td><td>Registration</td><td>Registration</td><td>Registration</td></tr>
<tr><td>8 :45</td><td></td><td>Opening & Keynote speaker (8:30)</td><td>Keynote speaker</td><td>Keynote speaker</td><td>Keynote speaker</td></tr>
<tr><td>9 :45</td><td></td><td>Coffee Break</td><td>Coffee Break</td><td>Coffee Break</td><td>Coffee Break</td></tr>
<tr><td>10 :10</td><td></td><td>*Session 101 Session 201</td><td>*Session 103 Session 313</td><td>*Session 203/309 Session 302</td><td>*Session 306 Session 301/310</td></tr>
<tr><td>12 :10</td><td></td><td>Lunch</td><td>Lunch</td><td>Lunch</td><td>Lunch</td></tr>
<tr><td>13:40</td><td rowspan="3">Registration, Booth and Poster set-up (14:00)</td><td>*Session 102 Session 308</td><td>Keynote speaker</td><td>*Session 204 Session 205</td><td>*Session 202 Session 303/311</td></tr>
<tr><td>15:20</td><td>Coffee Break</td><td rowspan="2">Coffee Break
Poster session Workshop (14:20)</td><td>Coffee Break</td><td>Coffee Break</td></tr>
<tr><td>15 :50</td><td>*Session 102 Session 304</td><td>*Session 204 Session 205</td><td>Excursions</td></tr>
<tr><td></td><td>Ice Breaker (18:30)</td><td></td><td>IntACT General Meeting (17 :10)</td><td>Gala Dinner (19:00)</td><td></td></tr>
</table>

*** Sessions in the Kent room (see page 13)**

Authors Instructions:

Oral Presentations
- The time allocated for oral presentation is 20 minutes, 15 minutes for the presentation and 5 minutes for discussion.
- Presentation will be done on Windows with Microsoft Office 2010 (Power Point). Pdf presentation can be accepted. Make sure your presentation is compatible.
- You must upload your presentation on the computers at least 15minutes before your session in the room you are presenting.

Poster Presentations
Poster should be produced on portrait format on 3' x 5' (90cm x 150 cm).
Poster will be displayed throughout the conference and you must be at your poster for discussion the Wednesday afternoon and during the coffee breaks.

Free workshop, Wednesday July 1st afternoon – Avizo 3D analysis software for materials science *by Nicholas Vito, FEI Avizo expert* (Inscriptions at the registration desk)

Conference Plan

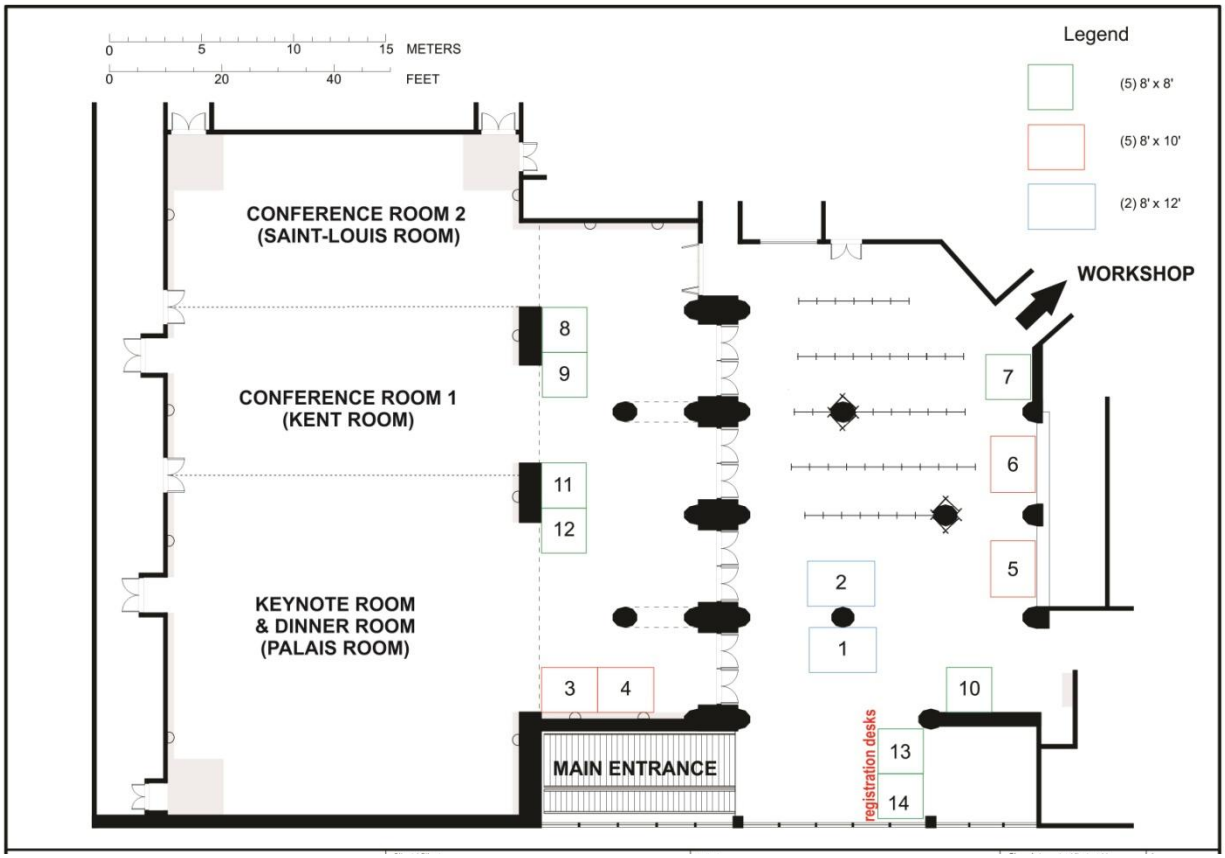

Booth 1 – Zeiss
Booth 2 – General Electrics
Booth 3 – Petrolia
Booth 4 – FEI
Booth 5 – ORS
Booth 6 – Bruker
Booth 7 – INRS
Booth 8 – Trikon
Booth 9 – FPInnovations
Booth 10 – NR Can
Booth 11 – Excillum
Booth 12 – Scanco Medical
Booths 13 & 14 – Registration desks
Room 15: FEI Workshop (room Courville – see page 14)

Main Floor

1st Floor (ICTMS Conference)

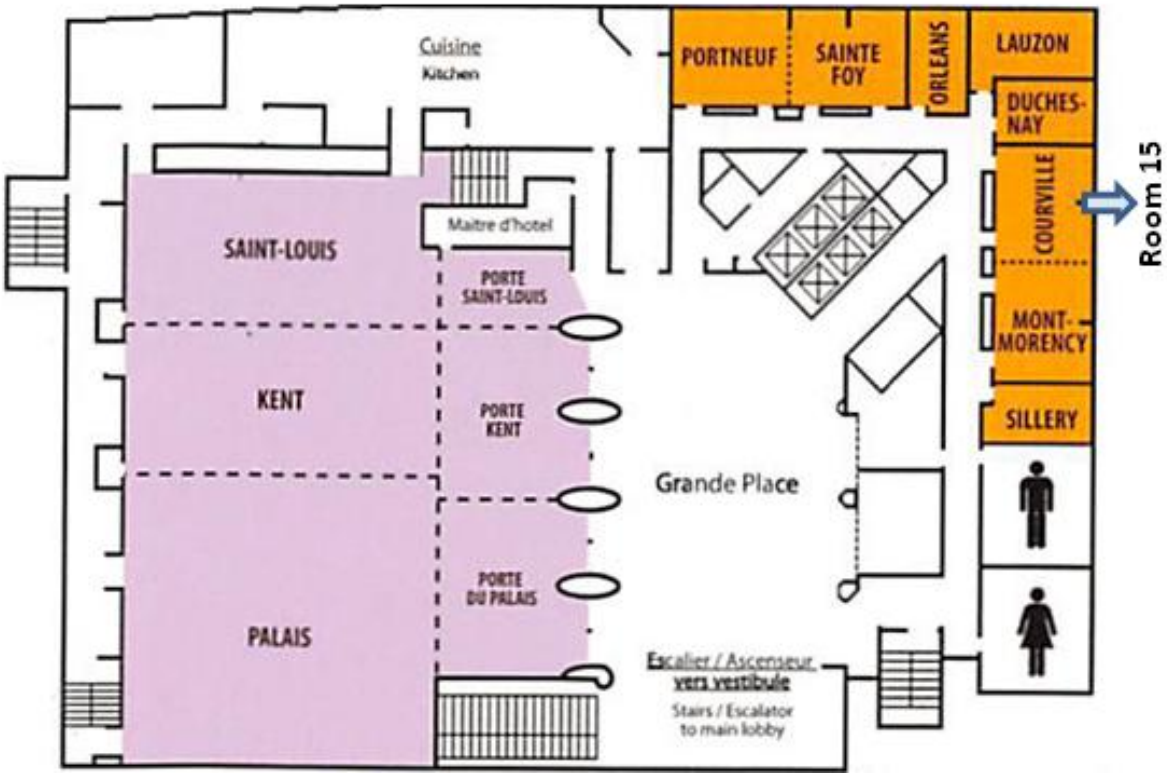

Keynote Speakers

Dr. KARL STIERSTORFER (Siemens Healthcare, Forchheim, Germany)

Born in 1963, Karl Stierstorfer studied Physics, finishing with a PhD thesis in the field of many-particle physics in Erlangen. In 1991 he joined Siemens Medical. His first project was the design of a Monte Carlo simulation program for X-ray scatter simulation. The results of this project were the programs MOCASSIM and DRASIM which are still being used in Siemens Medical and by cooperation partners. After joining the business unit CT, Karl Stierstorfer worked mainly in the fields of data preprocessing, CT reconstruction and iterative reconstruction. Since 2007, he is head of the CT physics team which is responsible for concepts of new medical CT scanners. Karl has a list of over 30 publications and holds more than 50 patents.

In this keynote talk, Dr. Stierstorfer will give an overview of the technologies and capabilities of medical CT. Since its invention in the early 1970s, medical Computed Tomography (CT) has gone through a dramatic evolution from a device that could image a patient's head in a scan time of several minutes to a tool that can scan whole patients within a few seconds and is fast enough to image a moving heart. The purpose of this talk is to review the current state of the art in medical CT, to give some examples for advanced medical applications and finally, to present a few examples of scans of non-medical objects.

Dr. GREG BANIAK (BP CANADA, CALGARY CANADA)

Originally from Saskatoon, Saskatchewan, Canada, Greg Baniak completed his B.Sc. Honors degree in Geology from the University of Saskatchewan in 2008. Following this, he moved west to Edmonton, Alberta, Canada where he worked on his PhD under the supervision of Drs. George Pemberton and Murray Gingras. His thesis focused on characterizing permeability and porosity distributions within bioturbated intervals using both carbonates and siliciclastics as case studies. All of his thesis work has been published in peer-reviewed journals such as Sedimentology, Marine and Petroleum Geology, Journal of Sedimentary Research, and Ichnos. Following the completion of his PhD in 2013, Greg moved south to Calgary, Alberta, Canada to begin working full-time as a Petroleum Geologist with BP Canada. Since March 2015, Greg has been seconded from BP Canada to Devon Energy where he is working as a Project Geologist on the joint venture Pike Oil Sands asset.

In this keynote talk, Dr. Baniak will present the application of X-ray micro-CT to bulk reservoir permeability. In the Pine Creek gas field, the primary reservoir intervals occur in the Upper Devonian Wabamun Group. A prominent feature within the Wabamun Group is the presence of the dolomitized burrow fabrics that have permeabilities ranging between 1 and 350 millidarcies (mD), while the adjacent lime mudstone-wackestone have permeabilities of less than 1 mD. To better understand the influence of bioturbation on bulk reservoir permeability, high-resolution X-ray microtomography (micro-CT) and helical computed tomography (helical-CT) imaging techniques were used.

Prof. David Cooper (UNIVERSITY OF SASKATCHEWAN, SASKATOON, CANADA)

Dr. Cooper is an Associate Professor and Canada Research Chair in Synchrotron Bone Imaging within the Department of Anatomy and Cell Biology at the University of Saskatchewan. During his training, he completed two degrees at the University of Saskatchewan, Paleobiology (1998) and Anatomy and Cell Biology (2000), before earning his PhD in Archaeology and Medical Science at the University of Calgary (2005) and then pursuing post-doctorate training at the University of British Columbia within the Centre for Hip Health. Dr. Cooper's interdisciplinary research focuses on high resolution imaging of cortical bone microarchitecture and related applications in the study of bone adaptation, aging and disease. In recent years, these pursuits have increasingly focused on the unique capabilities of synchrotron-based imaging.

In this keynote talk, Dr. Cooper will present the BioMedical Imaging and Therapy (BMIT) facility. This facility provides synchrotron-specific imaging and radiation therapy capabilities. There are two separate endstations used for experiments: the Bending Magnet (BM) 05B1-1 beamline and the Insertion Device (ID) 05ID-2 beamline. Examples of imaging techniques devloped at BMIT include: K-edge subtraction imaging (KES), phase contrast imaging (PCI) and Diffraction Enhanced Imaging (DEI, also known as Analyzer-Based Imaging, or ABI) both in projection and CT modes. The BM endstation provide monochromatic (15-40 keV) or a pink beam (~50 keV peak) for samples up to 50 kg, and the ID endstation extend the program to higher energies (up to 120 keV) and a higher capacity positioning system (up to 450 kg). The beam in both endstations is up to 200 mm wide and 10 mm high. Core research programs include human and animal reproduction, cancer imaging and therapy, spinal cord injury and repair, cardiovascular and lung imaging and disease, bone and cartilage growth and deterioration, mammography, developmental biology, gene expression research as well as the introduction of new imaging methods.

Prof. Oleg Shpyrko (UNIVERSITY OF CALIFORNIA AT SAN DIEGO)

Dr. Shpyrko is associate professor at the department of physics, UC San Diego. He have a PhD in Physics, Harvard University, Department of Physics. PhD Advisor: Prof. Peter S. Pershan in 2004, he was after that Posdoctoral Fellow at Havard University, between 2004 and 2005, and CNM Distinguished Post doctor Argonne National Laboratory, Center for Nanoscale Materials. Advisor: Prof. Eric D. Isaacs, 2005-2007, and Professor at University of California San Diego, Department of Physics, 2007-present.
The center of interest are: Experimental condensed matter physics using scattering probes ; X-ray synchrotron scattering and nanoscale imaging ; Strongly Correlated Systems: Metal-Insulator Transition, Magnetism in Correlated Oxides, Charge and Spin Density Wave systems, Search for Novel High-Temperature Superconducting materials ; Magnetic Thin Films and Nanostructures, Magnetoelectric heterostructures, Magnesium-Ion Battery materials ; Surface and interfacial properties of liquids, soft and biologically relevant materials ; Dynamics and structure of materials in nanoscale confinement ; Light scattering and microscopy studies of capillary phenomena and self-assembly. Attempts to produce focusing x-ray optics date back to the days

of Roentgen, however, it was not until the past decade that X-ray Microscopy has finally been able to achieve sub-100 nm resolution.
In this keynote talk, Dr. Shpyrko will introduce a novel X-ray microscopy technique, which relies on coherent properties of X-ray beams, and eliminates the need for focusing optics altogether, replacing it with a computational algorithm. He has applied this technique to image magnetic domains, as well as to image the distribution of lattice strain in nanostructures. I will also discuss recent results of in-operando imaging of lithium ion diffusion and dislocation dynamics in lithium ion energy storage devices. He will discuss applications of these novel X-ray imaging methods in context of new generation of fully coherent X-ray sources.

Prof Gioacchino (Cino) Viggiani (UNIVERSITÉ JOSEPH FOURIER, GRENOBLE, FRANCE)

Cino Viggiani was born in Napoli (Italy), where he obtained a B.S. in Civil Engineering (1988), a Ph.D. in Geotechnical Engineering at the University of Roma “La Sapienza” (1994), and a H.D.R. (Habilitation) in Mechanics at Université Joseph Fourier, Grenoble, France (2004), where he is full Professor since 2004. In 2012 he was advanced to the rank of Professeur de Classe Exceptionnelle by the French National Council of Universities (CNU). He served in the capacity of Vice-President for Research in Physics and Engineering, and he is the Head of Laboratoire 3SR since 2013. He is Editor of the International Journal Acta Geotechnica (Springer) since 2006. He is the author of about 120 scientific papers and delivered numerous keynotes and invited lectures worldwide. His research involves experimental investigations as well as theoretical and numerical modeling of the behavior of geomaterials, including localized failure and hydro-mechanical coupling. Applications are principally in geoenvironmental, petroleum, and civil engineering. On the experimental side, he has been using quite a range of soils and rock testing apparatus, including plane strain compression devices for soils and rocks equipped with ultrasonic tomography / acoustic emission systems, and a generalized shear apparatus with principal stress rotation. Advanced methods such as Digital Image Correlation and X-ray tomography have been developed, and they are applied to experimentally detect the onset of localized deformation.
In this keynote talk, Dr. Viggiani will discuss about X-ray tomography for granular materials: current trends and perspectives. Combining X-ray tomography and three-dimensional (3D) image analysis has finally opened the way for experimental micro-(geo)mechanics, allowing access to different scales of interest. When these correspond to a scale that has been imaged at high spatial resolution, high-quality measurements can be obtained (*e.g.*, 3D displacements and rotations of individual grains of sand sample under load). However, there are issues when the scale of interest is smaller, for example the characterization of grain-to-grain contacts (their orientations and evolution) or production of fines by grain breakage. This paper presents a short selection of new grain-scale measurements obtained using existing techniques. The challenges associated with smaller scale measurements on the same images are also discussed through a few examples from ongoing work.

Oral Presentations

Monday, June 29th

Day One

- 14:00 – 18:30 Registration

- 14:00 – 18:30 Booth and poster set-up

- 18:30 – 21:00 Ice Breaker

Tuesday, June 30th

Day Two

- 08:30 – 08:45 Introduction : Bernard Long & Dominique Bernard

- 08:45 – 09:45 Keynote speaker : **Dr. Stierstorfer, Siemens Germany** "What Medical Computed Tomography can do for Material Science (and what not)?"

- 09:45 - 10:10 **Coffee break**

Session 101 - Synchrotron

Chairs: Robert Winarski & Jean Carmeliet

- 10:10 – 10:30 (090) : Taming the flood: Distributed image processing made easy on large tomographic datasets *by *K. Mader[1,2,3], R. Mokso[1], A. Patera[1], M. Stampanoni[1,2] from [1]Paul Scherrer Institut, Switzerland, [2]University of Zurich, Zurich, [3]4Quant, Zurich, Switzerland.*

- 10:30 – 10:50 : (109) PSICHE: A new synchrotron tomography beam line for materials science at SOLEIL *by *A. King[1], N. Guigno[1], P. Zerbino[1], K. DesjardinS[1], N. Lenoir[2], M. Borner[3], J.-P. Itié[1] from [1]Synchrotron SOLEIL, Gif-sur-Yvette, France, [2]PLACAMAT, UMS3626-CNRS/Université de Bordeaux, France, [3]Laboratoire NAVIER, UMR8205- CNRS/ENPC/ IFSTTAR/ Université Paris-Est, Champs-sur-Marne, France.*

- 10:50 – 11:10 (130) : Studying water/porous materials interactions with X-ray tomography *by *D. Derome[1], A. PAtera[2 3], M.Dash[4,1], M. Parada[4,1], S. Lal[1], J. Carmeliet[4,1] from [1]Swiss Federal Laboratories for Materials Science and Technology, EMPA, Dübendorf, Switzerland, [2]Paul Scherrer Institute, Switzerland, [3]EPFL de Lausanne, Lausanne, Switzerland, [4]ETH Zurich, Switzerland.*

- 11:10-11:30 (159) : Time-resolved (4D) *in situ* X-ray tomographic microscopy at TOMCAT: Understanding the dynamics of materials ***by*** **J. L. Fife[1], F. Marone[1], R. Mokso[1], M.*

Stamponi[1,2] from [1]Swiss Light Source, Paul Scherrer Institut, Villigen PSI, Switzerland, [2]University of Zurich

- 11:30-11-50 (169) : High speed and time resolved tomography of fluid flow in porous media at Diamond Light Source Beamline I12 *by *R. C. Atwood[1], S. B. Coban, K. J. Dobson[2], D. Kazantsev[3,4], S. A. McDonald[3], N.T. Vo[1], P.J. Withers[3] from [1]Diamond Light Source, Didcot, UK, [2]Ludwig-Maximilians University, Germany, [3]University of Manchester, Manchester UK, [4]The Manchester X-Ray Imaging Facility, Research Complex at Harwell, Didcot, UK.*

- 11:50-12:10 (190) : Magnetic contrast nanotomography *by *R. Winarski from Argonne National Laboratory, ILL. USA.*

Session 201 - Advance in reconstruction algorithms

Chairs: Andrew Kingston & Philippe Després

- 10:10-10:30 (012) : Computed tomography from limited data using a robust discrete algebraic reconstruction technique *by *X. Zhugei, K. J. Batenburg[123] from [1]Centrum Wiskunde & Informatica (CWI), Science Park Amsterdam, The Netherlands, [2]Leiden University, Leiden, The Netherlands, [3]University of Antwerp, Antwerp, Belgium.*

- 10:30-10:50 (148) : A new method for measuring grain displacements in granular materials by X-ray computed tomography *by *M. H. Khalili, S. Brisard, M. Bornert, J. M. Pereira, M. Vandamme, J. N. Roux from Université Paris-Est, Marne-la-Vallée, France.*

- **10:50-11:10 (158) : Assessment and reduction of the scatter effects in an industrial 300kV micro-focus CT system** *by *M. Plamondon[1], P. Schuetz[2], T. Luethi[1], J. Hofmann[1], A. Flisch[1] from [1]Empa, Swiss Federal Laboratories, Dübendorf, Switzerland and [2]Lucern University, Horw, Switzerland.*

- 11:10-11:30 (163) : Accurate measurements of features near the resolution limit of tomographic data: extension to heterogeneous matrix, multiple feature types, and shape determination *by *R. A. Ketcham, A. S. Mote fromThe University of Texas at Austin, Austin TX, USA.*

- 11:30-11:50 (179) : Material discrimination using dual energy computed tomography *by *M. Pazireshi, B. Recuri, G. Myersi, A. Kingston from Dept. Applied Mathematics, RSPE, ANU 6201, Australia.*

- 11:50-12:10 (198) : Recent advances in X-ray computed tomography and potential impact for non-medical applications *by P. Després from Laval University, Québec, Qc. Canada.*

- 12:10 – 13:40 Lunch

Session 102 (Part I)- Micro CT

Chairs: Matthieu Boone, Giovani Grasselli & Adrian Sheppard

- 13:40-14:00 (014) : 3D chemical imaging in the laboratory by X-ray absorption edge microtomography *by C. K. Egan[1],* S. D. M. Jacques[1,2], A. M. Beale[2,3], R. A. D. Pattrick[4], P. J. Withers[1], R. J. Cernik[1] from [1]University of Manchester, Manchester, UK, [2]UK Catalysis Hub, at Harwell, Didcot, UK, [3]University College London, London, UK, [4]University of Manchester, Manchester,UK.*

- 14:00-14:20 (019) : Mapping grains in 3D by laboratory X-ray diffraction contrast tomography *by *S. A. McDonald[1], C. Holzner[2], P. Reischig[3], E. M. Lauridsen[3], P. J. Withers[1], A. Merkle[2], M. Feser[2] from [1]University of Manchester, Manchester, UK, [2]Carl Zeiss X-ray Microscopy Inc., Pleasanton, CA, USA and [3]Xnovo Technolog, Køge, Denmark.*

- 14:20-14:40 (032) : Liquid-metal-jet X-ray tube technology and tomography applications *by *E. Espes, F. Björnsson, C. Gratorp, B. Hansson, O. Hemberg, G. Johansson, J. Kronstedt, M. Otendal, P. Takman, R. Terfelt, T. Tuohimaa from Excillium, Kista, Sweden.*

- 14:40-15:00 (055) : Arion: a realistic projection simulator for optimizing laboratory and industrial micro-CT *by *J. Dhaene[1], E. Pauwels[1], T. De Schryver[1], A. De Muynck[1], M. Dierick[1], L. Van Hoorebeke[1] from [1]UGCT, Ghent University, Gent, Belgium.*

- 15:00-15:20 (098) : NanoCT imaging with a prototype nanofocus source and a single-photon counting detector *by *M. Müller[1], S. Ferstl[1], S. Allner[1], M. Dierolf[1], P. Takman[2], T. Tuohimaa[2], B. Hansson[2], F. Pfeiffer[1] from [1]Technische Universität München, Garching, Germany and [2]Excillum AB, Kista, Sweden.*

- 15:20-15:40 (150) : Rock deformation and micro-CT analyses *by N. Tisato, Q. Zhao, G. Grasselli from University of Toronto, Toronto, Canada.*

Session 308 - Concrete & building rocks

Chairs: Jacques Marchand & Veerle Cnudde

- 13:40-14:00 (026) : Non-destructive integrated CT-XRD method developed for hardened cementitious material *by *T. Sugiyama[1], T. Hitomi[2], K. Kajiwara[3] from [1]Hokkaido University, Sapporo, Hokkaido, Japan, [2]Obayashi Co. Lt., Kiyose, Tokyo, Japan, [3]Japan Synchrotron Radiation Research Institute, Sayo-cho, Hyogo, Japan.*

- 14:00-14:20 (096) : Salt crystallization dynamics in building rocks: a 4D study using laboratory Xray micro-CT *by *H. Derluyn[1], M. A. Boone[1,2], M. N. Boone[3], T. De Kock[1], S. Peetermans[4], J. Desarnaud[5], N.Shahidzadeh[5], L. Molari[6], S. De Miranda[6], V. Cnudde[1] from [1]UGCT – Ghent University,Gent, Belgium [2]XRE – X-ray Engineering bvba, Gent, Belgium [3]UGCT, Ghent University, Gent, Belgium [4]NIAG, Spallation Neutron Source Division, Paul Scherrer Insitute, Switzerland [5]University of Amsterdam, Amsterdam, The Netherlands [6]University of Bologna, Bologna, Italy.*

- 14:20-14:40 (123) : Use of X-ray scan to assess the extent of defects in concrete elements *by *J. Marchand[1], R. Cantin[1], E. Samson[1] from [1]SIMCO Technologies Inc., Québec (QC) Canada.*

- 14:40-15:00 (132) : A 3D Investigation of Interface Porosity and Fracture Characteristics of Cement-Based Composites *by C. Gangsa, L. Flanders, *E. Landis from University of Maine Orono Maine USA.*

- 15:00-15:20 (151) : Freeze-thaw decay in sedimentary rocks: a laboratory study with CT under controlled ambient conditions *by *T. De Kock[1], M.A. Boone[1,2], T. De Schryver[3], H. Derluyn[1], J. Van STappen[1], D. Van Loo[2], B. Masschaele[2,3], V. Cnudde[1] from [1]UGCT –Ghent University, Ghent, Belgium, [2]X-ray Engineering, Ghent, Belgium [3]UGCT, Ghent University, Ghent, Belgium.*

- 15:20 – 15:50 Coffee break

Session 102 (Part II) - Micro CT

Chairs: Matthieu Boone, Giovani Grasselli & Adrian Sheppard

- 15:50-16:10 (153) : A laboratory micro-CT setup for fast continuous scanning: applications for pore scale fluid flow research *by M. A. Boone[1,2], *J. Van Stappen[1], T. Bultreys[1], M. N. Boone[3], T. De Schryver[3], B. Masschaele[2,3], D. Van Loo[2], L. Van Hoorebeke[3], V. Cnudde[1] from [1]UGCT – PProGRess, Dept. Geology and Soil Science, Ghent University, Gent, Belgium, [2]XRE – X-ray Engineering bvba, Gent, Belgium, and [3]UGCT, Dept. Physics and Astronomy, Ghent University, Gent, Belgium.*

- 16:10-16:30 (172) : Multi-Energy Nano Computed Tomography Phase Retrieval for Material Discrimination *by *H. Li[1], A. Kingston[1], G. Myers[1], B. Recur[1], A. Sheppard[1] from [1]Australian National University, Canberra, Australia.*

- 16:30-16:50 (022) : Investigation of carbon nanostructure in copper covetics by X-ray nanotomography *by B. Ma[1], R. P. Winarski[2], J. Wen[2], D. J. Miller[2], C. U. Segre[3], U. (Balu) Balachandran[1], D. R. Forrest[4] from [1]Energy Systems Division, Argonne National Laboratory, Argonne, IL, [2]Nanoscience and Technology Division, Argonne National Laboratory, Argonne, IL, [3]Department of Physics, Illinois Institute of Technology, Chicago, IL and [4]U.S. Department of Energy, Advanced Manufacturing Office, Washington, DC, USA.*

Session 304 - Sedimentary structures: modern and ancients

Chairs: Richard Ketcham & Patric Selvadurai

- 15:50-16:10 (029) : Dynamic micro-CT analysis of fracture formation in rock specimens subjected to multi-phase fluid flow *by *J. Van Stappen[1], T. Bultreys[1], M.A. Boone[1], E. Verstrynge[2], V.Cnudde[1] from [1]PProGRess – UGCT –Ghent Universtiy, Ghent, Belgium and [2]Unit of Architecture and Building Techniques – Campuses Sint-Lucas Brussels and Ghent – Dept. of Architecture – KU Leuven, Leuven, Belgium.*

- 16 :10-16 :30 (185) : CT-Scan analysis of bioturbation structures: from intertidal mudflat to young mangrove forest in French Guiana (South America) *by A. Aschenbroich[1], E Michaud[1], F Fromard[2], L. F Daigle[3], B Long[3], G Thouzeau[1] from [1]Laboratoire des Sciences de l'Environnement Marin (LEMAR, UMR 6539, CNRS-IRD-UBO), IUEM, PLOUZANE, France, Laboratoire*

d'écologie fonctionnelle et Environnement, Université Paul Sabatier, Toulouse, France.[3]Institut national de la recherche scientifique, Québec (Québec), Canada

- 16:30-16:50 (110) : Computerized coaxial tomography (CT-Scanning) in paleoclimatic studies *by P. Francus[1,2], F. Lapointe[1,2], C. Massa[3,] D. Fortin[4], K. Kanamaru[5], G. St-Onge[6,2] from [1]Institut National de la Recherche Scientifique and GEOTOPE Québec, Canada, [3]Lehigh University, Bethlehem, PA, USA, [4]Northern Arizona University, AZ, USA, [5]University of Massachusetts, Amherst, MA, USA and [6]ISMER, UQAR, Rimouski, Québec, Canada.*

- 16:50-17:10 (136) : Assessment of a new method to estimate the thermal conductivity of permafrost using CT scan analyses *by *M. A. Ducharme[1,2], M. Allard[1,2], J. Côté[3], E. L'hérault[2] from [1]Université Laval, Faculté de foresterie, géographie et de géomatique, [2]Centre d'études nordiques, [3]Université Laval.*

Wednesday, July 1st

Day three

- 8:45 - 09:45 Keynote speaker : **Dr. Baniak, Greg**, BP Canada
''Using micro-CT and helical-CT to image permeability and porosity variations in bioturbated hydrocarbon reservoirs. Examples from shoreface, deep-water and carbonate depositional systems''

- 09:45 - 10:10 **Coffee break**

Session 103 - Interferometry

Chairs: Leslie Butler & De Carlo Francesco

- 10:10-10:30 (003) : Laser interactive 3D computer graphics *by *J. B. Bellet[1], I. Berechet[2], S. Berechet[2], G. Berginc[3], G. Rigaud[1] from [1]Université de Lorraine, Metz, France, [2]Société SISPIA, Vincennes, France, [3]Thales Optronique, Elancourt, France.*

- 10:30-10:50 (079) : A study on the hydration processes in cementitious material based on X-ray dark-field imaging *by *F. Prade[1], F. Malm [2], C. Grosse[2], F. Pfeiffer[1] from [1]Medizintechnik, Technische Universität München, Germany, [2]Universität München, München, Germany [3]Empa, Swiss Federal Laboratories for Materials Science and Technology, Dübendorf, Switzerland.*

- 10:50-11:10 (103) : Biomedical and materials science applications of grating-based phase-contrast imaging using synchrotron and conventional X-ray sources *by *J. Herzen[1], M. Willner[1], L. Birnbacher[1], M. Viermetz[1], K. Scherer[1], F. Prade[1], A. Sarapata[1], A. Fingerle[2], P. Noël[2], E. Rummeny[2], H. Hetterich[3], T. Saam[3], M. Reiser[3], F. Pfeiffer[1] from [1]Technische Universität München, Germany, [2]Technische Universität München, Munich, Germany and [3]Ludwig-Maximilians-Universität München, Germany.*

- 11:10-11:30 (143) : Grating based differential phase contrast imaging of an interpenetrating AlSi12/Al_2O_3 metal matrix composite *by *J. Maisenbacher[1], F. Prade[2], J. Gibmeier[1], F. Pfeiffer[2] from [1]Institute for Applied Materials (IAM-WK), Karlsruhe Institute for Technology, Karlsruhe, Germany, [2]Echnische Universität München, Germany.*

- 11:30-11:50 (165) : Single-grating interferometer for high-resolution phase-contrast imaging at synchrotron radiation sources *by *A. Hipp[1], J. Herzen[2], I. Greving[1], J. U. Hammel[1], P. Lytaev[1], A. Schreyer[1], F. Beckmann[1] from [1]Helmholtz-Zentrum Geesthacht, Geesthacht, Germany and [2]Technische Universität München, Garching, Germany.*

- 11:50-12:10 (182) : Grating-based X-ray phase-contrast imaging at PETRA III *by *A. Hipp[1], F. Beckmann[1], I. Greving[1], J. U. Hammel[1], P. Lytaev[1], A. Schreyer[1], J. Herzen[2] from [1]Helmholtz-Zentrum Geesthacht, Geesthacht, Germany and [2]Technische Universität München, Garching, Germany.*

Session 313 - Petroleum core analysis

Chairs: Michel Malo & Patric Jacobs

- 10:10-10:30 : to be determined

- 10:30-10:50 (052) : Construction of complex 3D digital rock models *by *I. V. Yakimchuk[1], I. A. Varfolomeev[1,2], N. V. Evseev[1], B. D. Sharchilev[1], O. A. Kovaleva[2], D. A. Lisicin[1,2], D. A. Korobkov[1], S. S. Safonov[1] from [1]Schlumberger, Moscow, Russia and [2]Moscow Institute of Physics and Technology, Dolgoprudny, Russia.*

- 10:50-11:10 (063) : Sensitivity analysis for micro-tomography data segmentation in digital rock physics *by H. Berthet, *M. Blanchet, R. Rivenq from TOTAL, Pau, France*.

- 11:10-11:30 (145) : Characterization of reservoir quality in the upper devonian wabamun group using micro-CT and helical-CT imaging techniques *by *G. M. Baniak from BP Canada Energy Group ULC, Calgary, Alberta, Canada.*

- 11:30-11:50 (211) : How computerized tomography can improve the remote detection of hydrocarbons using seismic methods? *by *M. J. Duchesne[1], B. Giroux[2] from [1]Geological Survey of Canada, Québec, Qc. Canada, [2]INRS-ETE, Québec, Qc. Canada.*

- 12:10 – 13:40 **Lunch**

- 13:40 – 14:20 Keynote speaker : **Dr D.M.L Cooper,** University of Saskatchewan
''CT imaging Capabilities at BMIT at the Canadian Light Source''

- 14:20 - 17:10 Poster presentations and booth visits

- 14:20 - 17:10 **Workshop - Avizo 3D analysis software for materials science** *by Nicholas Vito, FEI Avizo expert*

- 17:10 – 18:30 IntACT general meeting

Thursday, July 2nd

Day four

- 08:45 - 09:45 Keynote speaker : **Prof Dr. Oleg G. Shpyrko**
University of California at San Diego (UCSD)
Coherent X-Ray nanovision

- 9:45 - 10:10 **Coffee break**

Sessions 203 & 309 - Multi-tissue quantitative Imaging technique & Porous Material

Chairs 203: Eric Landis & Sabine Rolland de Roscoat
Chairs 309: Nicolas Lenoir & Takafumi Sugiyama

- 10:10-10:30 (018) : to be determined

- 10:30-10:50 (021) : Metal artifact reduction using confidence maps and patch-based method *by *L. Frédérique[1,3,] B. Recur[2], S. Genot[3], J. P. Domenger[1], P. Desbarats[1] from [1]LaBRI, Université de Bordeaux / CNRS, Talance, France, [2]Australian National University, Dept. Applied Maths, RSPE, Canberra Australia, [3]Tomo Adour, Zone Europa, Pau, France.*

- 10:50-11:10 (091) : 3D-imaging by synchrotron X-ray micro tomography of ferroelectric composite materials and numerical modelling of their physical properties *by *J. Lesseur[1,2], C. Elissalde[1,2], C. Estournes[3], R. Epherre[3], P. Veber[1,2], M. Gayot[1,2], M. Maglione[1,2], D. Bernard[1,2] from [1]CNRS, ICMCB, UPR9048, - Pessac, France, [2]Univ. Bordeaux, ICMCB, UPR 9048, Pessac, France, [3]CIRIMAT et Plateforme Nationale CNRS de Frittage flash, PNF2 MHT, Univ. Paul Sabatier, Toulouse, France.*

- 11:10-11:30 (133) : From 3D X-ray micro tomography images of porous materials to pore network: Image processing and fluid flow modelling *by *D. Bernard[1,2], N. Combaret[3], J. Lesseur[1,2,] A.K. Diouf[1,2], E. Plougonven[4] from [1]CNRS, ICMCB, UPR9048, Pessac, France, [2]Univ. Bordeaux, ICMCB, UPR9048, Pessac, France, [3]VSG, Visualization Science Group an FEI Company, Mérignac, France, [4]Univ. Liège, Lab. Chemical Engineering, Liège, Belgium.*

- 11:30-11:50 (134) : Phase-contrast synchrotron X-ray fast tomography of wicking in yarns *by *M. Parada[1,2], D. Derome[2], R. M. Rossi[3], J. Carmeliet[1,2] from [1]Chair of Building Physics. ETHZ, Swiss Federal Institute of Technology in Zurich. Zürich, Switzerland, [2]Laboratory for Multiscale Studies for the Built Environment. Empa, Swiss Federal Laboratories for Materials Science and Technology. Dübendorf, Switzerland, [3]Laboratory for Protection and Physiology. Empa, Swiss Federal Laboratories for Materials Science and Technology. St. Gallen, Switzerland.*

- 11:50-12:10 (192) : Neutron imaging of coupled deformation and fluid flow in sandstones *by E. Tudisco[1], *S. A.Hall[1,2], J. Hovind[3], N. Khardjilov [4], E. M. Charalampidou[5], H. Sone[6] from [1]Division of Solid Mechanics, Lund University, Lund Sweden, [2]European Spallation Source AB,*

Lund, Sweden, [3]Paul Scherrer Institute, Villigen, Switzerland, [4]Helmholtz Zentrum Berlin, Germany, [5]Institute of Petroleum Engineering, Heriot Watt University, Edinburgh, UK, and [6]GFZ-Potsdam, Germany.

Session 302 - Geomaterial, Materials, Structures and Mineralogy

Chairs: Yosuke Higo and Mathieu Duchesne

- 10:10-10:30 (006) : Through-porosity induced corrosion under a Fe-based amorphous coating revealed by in-situ X-ray tomography *by *S. G.Wang[1], S. D. Zhang[1], J. Q.Wang[1], S. C.Wang[1], L. Zhang[1] from [1]Shenyang National Laboratory for Materials Science, Institute of Metal Research, China and Academy of Sciences, Shenyang, PR China.*

- 10:30-10:50 (007) : Characterization of three-dimensional fatigue pre-crack propagation for 316L stainless steel with lab-based X-ray tomography *by *S. G.Wang[1], L. Xiong[1], S. C.Wang[1], L. Zhang[1] from [1]Shenyang National Laboratory for Materials Science, Institute of Metal Research, Chinese and Academy of Sciences, Shenyang, PR China.*

- 10:50-11:10 (020) : Microstructural characterization of SiC foams used as solar absorber devices *by J. Mollicone[1], *B. Duployer[1], P. Lenormand[1], C. Tenailleau[1], J. Vicente[2], F. Ansart[1] from [1]CIRIMAT, UMR - CNRS 5085, Université de Toulouse, Toulouse, France and [2]Laboratoire IUSTI, Marseille, France.*

- 11:10-11:30 (078) : *In-operando* fast tomography of lithium-ion batteries during operation and failure *by D. P. Finegan[1]*, M. Scheel[2], J. Robinson[1], B. Tjaden[1], I. Hunt[3], M. Di Michiel[2], G. Offer[3], G. Hinds[4], D. J.L. Brett[1], P. R. Shearing[1] from [1]Department of Chemical Engineering, University College London, London, UK, ESRF, [2]The European Synchrotron, Grenoble, France, [3]Imperial College London, South London, UK, and [4]National Physical Laboratory, Teddington, UK.*

- 11:30-11:50 (112) : Carbon anodes investigation through computed tomography *by *D. Picard[1], H. Alamdari[1], D. Ziegler[2], L. F. Daigle[3], M. Fafard[1] from [1]Université Laval, Aluminium Research Centre, Québec (Québec), Canada, [2]Alcoa Primary Metals, Alcoa Technical Center –Alcoa Centre, PA, USA, and [3]INRS-ETE, Environmental Technology Laboratories, Québec (Québec), Canada.*

- 11:50-12:10 (187) : Coarsening in phase-separated silicate melts observed by in-situ tomography *by D. Bouttes[1], *E. Gouillart[2], W. Woelffel [2], E. Boller[3], L. Salvo[4], P. L'Huissier[4], D.Vandembroucq[1] from [1]Laboratoire PMMH, UMR 7636 CNRS/ESPCI/Univ. Paris,UPMC/Univ. Paris Diderot, Paris, France, [2]Surface du Verre et Interfaces, UMR 125 CNRS/Saint-Gobain, Aubervilliers, France, [3]European Synchrotron Radiation Facility (ESRF), Grenoble, France, [4]SIMAP, GPM2 group, CNRS UMR 5266, University of Grenoble, Saint Martin d'Hères, France.*

- 12:10 – 13:40 Lunch

Session 204 (Part I) - 3D imaging

Chairs: Dominique Bernard & Khalid Alshibi

- 13:40-14:00 : to be determined

- 14:00-14:20 (030) : Edge illumination X-ray phase contrast computed tomography: implementations at synchrotrons and in standard laboratories *by *C. K. Hagen[1], A. Zamir[1], F. A. Vittoria[1], P.C. Diemoz[1], M. Endrizzi[1], A. Olivo[1] from [1]Department of Medical Physics and Biomedical Engineering, University College London, Malet Place, Gower Street, London, United Kingdom.*

- 14:20:14:40 (041) : Projection-based digital volume correlation: application to crack propagation *by T. Taillandier-Thomas,[1] H. Leclerc,[1] *S. Roux,[1], F. Hild[1] from [1]LMT, ENS-Cachan, CNRS, Univ. Paris-Saclay, Cachan, France.*

- 14:40:15:00 (056) : 4D quantification and tracking of time dependent features *by *L. Courtois[1,2], P. D.Lee[1,2], K. J. Dobson[3], Q. Lin[4], S. J. Neethling from [1]Manchester x-ray imaging facility, school of Materials, University of Manchester, UK, [2]Research Complex at Harwell,Rutherford Appleton Laboratory, Didcot, Oxfordshire, UK, [3]Earth & Environmental Sciences, LMU Munich, Munich, Germany, [4]Department of Earth Science and Engineering, Imperial College London, UK.*

- 15:00-15:20 (076) : 'Fast shear' phenomena in ductile fracture assessed by Digital Volume Correlation on Laminography synchrotron volumes *by T. Taillandier-Thomas[1,2], *T. F. Morgeneyer[2], L. Helfen[3,4], S. Roux[1], F. Hild[1] form [1]LMT, ENS-Cachan, CNRS, Univ. Paris-Saclay, France [2]MINES ParisTech, PSL Research University, MAT - Centre des matériaux, CNRS UMR 7633, France [3]ANKA/Institute for Photon Science and Synchrotron Radiation, Karlsruhe Institute of Technology (KIT), Germany, [4]European Synchrotron Radiation Facility (ESRF), BP 220, Grenoble Cedex, France.*

Session 205 (Part I) - Developing image analysis tools for synchrotron

Chairs: Xianghui Xiao & Ross Harder

- 13:40-14:00 (048) : A Computational toolbox for the data processing pipeline of four-dimensional data from phase contrast X-ray tomography *by A. J. Shahani[1], E. Begum Gulsoy[1], J. W. Gibbs[1,2], J. L. Fife[3], X. Xiao[4] and P. W. Voorhees[1] from [1]Department of Materials Science and Engineering, Northwestern University, Evanston, IL, USA, [2]Materials Science and Technology Division, Los Alamos National Laboratory, Los Alamos, NM, USA, [3]Swiss Light Source, Paul Scherrer Institute, Villigen, Switzerland, and [4]X-ray Science Division, Argonne National Laboratory, Lemont, IL USA.*

- 14:00-14:20 (049) : Advanced noise-reduction and segmentation methods in X-ray computed microtTomography *by *S. S. Singh[1], J. C. E. Mertens[1], J. J. Williams[1], P. Hruby[1], A. Kirubanandham[1], X. Xiao[2], F. De Carlo[2], N. Chawla[1], *from [1]Materials Science and Engineering, Arizona State University, Tempe, AZ, USA, [2]Advanced Photon Source, Argonne National Laboratory, Argonne, IL, USA.*

- 14:20-14:40 (111) : Upgraded ID01@ESRF: Nanodiffraction, full field diffraction microscopy and coherent diffraction imaging *by S. J. Leake[1], P. Boesecke[1], H. Djazouli[1], G. A.Chahine[1], J. Hilhorst[1], M. Elzo[1], M. I. Richard[1], G. Bussone[1], R. Grifone[!], S.Fernandez[1], T. U.Schulli[1] from [1]ESRF- The European Synchrotron, Grenoble, France.*

- 14:40-15:00 (149) : Tomography activities at advanced photon source *by X. Xiao from Advanced Photon Source, Argonne National Laboratory.*

- 15:00-15:20 (155) : Bilateral denoising and region merging segmentation for micro-CT images *by *S. J. Latham[1], A. M. Kingston[1], A. P. Sheppard[1] from [1]Department of Applied Mathematics, The Australian National University.*

- 15:20 – 15:50 Coffee break

Session 204 (Part II) - 3D imaging

Chairs: Dominique Bernard & Khalid Alshib

- 15:50-16:10 (077) : THz imaging versus X-ray tomography: Applications to material inspection ***by*** **B. Recur[1], H. Balacey[2], J. Bou Sleiman[3], J. B. Perraud[3,] J. P. Guillet[3], P. Mounaix[3] from [1]Australian National University, Dept. Applied Maths, RSPE, Canberra, Australia [2]Noctylio SAS, Bordeaux, France [3]IMS, Bordeaux University, CNRS UMR 5218, Talence, France.*

- 16:10-16:30 (080) : Scanning-SAXS tensor tomography: accessing the orientation of nanostructures in 3D *by *M. Liebi[1], M. Georgiadis[2], A. Menzel[1], O. Bunk[1], M. Guizar-Sicairos[1] from [1]Swiss Light Source, Paul Scherrer Institut, Villigen, Switzerland, and [2]Insitute for Biomechanics, ETH Zurich, Zurich, Switzerland.*

- 16:30-16:50 (161) : 3D *in situ* characterisation of the impregnation of model fibre networks using real time synchroton X-ray microtomography *by S. Rolland Du Roscoat[1,2,3]*, P. J. J. Dumont[4,5,6,] P. Carion[1,2,4,5,6], L. Orgeas[1,2], J. F. Bloch,[5,6], C. Geindreau[1,2], M. Terrien[4,5,6], P. Charrier[1,2], P. J. Liotier[7], S. Drapier[7], M. Pucci[7] from [1]Univ. Grenoble Alpes, 3SR, Grenoble, France, CNRS, 3SR, Grenoble, France, [3]ESRF, ID 19 Topography and Microtomography Group, Grenoble, France, [4]Univ. Grenoble Alpes, LGP2, Grenoble, France, [5]CNRS, LGP2, Grenoble, France, [6]Agefpi, LGP2, Grenoble, France, [7]Ecole des Mines de Saint-Etienne, Saint-Etienne, France.*

- 16:50-17:10 (183) : Combining nano X-ray Tomography and X-ray Fluorescence for In Situ Observations and 3D Chemical Segmentation *by T. Ley[1], Q. Hu[1], T. Kim[1], M.Moradian[1], J. Hanan[1], V. Rose[2,] R. Winarski[3], J. Gelb[4] from [1]- Oklahoma State University, [2]Argonne National Laboratory, Advanced Photon Source, [3]- Argonne National Laboratory, Center for Nanoscale Materials, and [4]– Zeiss X-ray Microscopy, USA.*

Session 205 (Part II) - Developing image analysis tools for synchrotron

Chairs: Xianghui Xiao & Ross Harder

- 15:50-16:10 (162) : CRAFT, a software tool to standartize CT environment *by *R. Vescovi[1], E. Miqueles[1], M. Cardoso[1] from [1]Laboratório Nacional de Luz Síncrotron, Rua Giuseppe Máximo Scolfaro, 10000, Campinas - State of São Paulo, Brazil.*

- 16:10-16-30 (176) : The study of fluid-rock interaction in 4D *by *F. Fusseis[1], W. Zhu[2], H. Lisabeth[2], J. Bedford[3], H. Leclére, X. Xiao from [1]School of Geosciences, The University of Edinburgh, Edinburgh, UK, [2]Department of Geology, University of Maryland, College Park, USA, [3]School of Environmental Sciences, University of Liverpool, UK, and [4]Advanced Photon Source, Argonne National Laboratory, USA.*

- 16:30-16:50 (186) : scikit-image and the Python ecosystem for 3-D image processing *by S. Van Der Walt1[1], *E. Gouillart[2], J. Nunez-Iglesias[2] from [1]Division of Applied Mathematics, Stellenbosch University, Stellenbosch, South Africa, [2]Surface du Verre et Interfaces, UMR 125 CNRS/Saint-Gobain, Aubervilliers, France, [3]Victorian Life Sciences Computation Initiative, Carlton, VIC, Australia.*

- 16:50-17:10 (196) : Multi-resolution characterisation of grain-based measurements from X-ray tomography *by *E. Andò[1,2], A. Tengattini[1,2,3], M. Wiebicke[1,2,4], G. Viggiani[1,2], S. Salager[1,2] from [1]Univ. Grenoble Alpes, 3SR, Grenoble, France, [2]CNRS, 3SR, Grenoble, France, [3]School of Civil Engineering, The University of Sydney, Sydney, NSW, Australia, [4]Technische Universität Dresden, Institute of Geotechnical Engineering, Germany.*

19:00 – Gala diner

Friday, July 3rd

Day five

- 08:45 - 09:45 Keynote speaker **Dr. Gioacchino (Cino) Viggiani**, Grenoble University «X-ray tomography for granular materials: current trends and perspectives»

- 9:45 - 10:10 **Coffee break**

Session 306 - Innovative Geotechnical Applications

Chairs: Jun Otani & Gino Viggiani

- 10:10-10:30 (013) : X-ray computed tomography investigation of structures in claystone at large scale and high speed *by *G. Zacher[1], A. Kaufhold[2], M. Halisch[3], J. Urbanski[4] from [1]GE Sensing & Inspection Technologies GmbH, phoenix|x-ray,Wunstorf, Germany, [2]Federal Institute for Geosciences and Natural Resources, Hannover, Germany, [3]Leibniz Institute for Applied Geophysics, Hannover, Germany and [4]GE Inspection Technologies, Road, Lewistown, PA, USA.*

- 10:30-10:50 (046) : Crack localization in digital volume correlation: Regularization with a damage law *by A. Bouterf[1], *S. Roux[1], F. Hild[1] from [1]LMT, ENS-Cachan, CNRS, Univ. Paris-Saclay, Cachan., France.*

- 10:50-11:10 (057) : A microstructural finite element analysis of cement damaging on Fointainebleau Sandstone *by *S. Nadimi[1], J. Fonseca[1], P. Bésuelle[2], G. Viggianil[2] from [1]City University London, UK, [2]Laboratoire 3SR, Grenoble, France.*

- 11:10-11:30 (069) : X-ray CT evaluation method for filling of permeable repair material into porous asphalt mixture *by *T. Fumoto[1], S. Motomatsu[2], M. Ohara[3], K. Uesaka[4], A. Adachi[5] from [1]Kinki University, Faculty of Science and Engineering, Department of Civil & Environmental Engineering, Higashiosaka, Osaka, Japan, [2]West Nippon Expressway Company Limited, Technical Development Bureau, Dojima Avanza, Osaka, Japan, [3]West Nippon Expressway Company Limited, Technical Development Bureau,Dojima Avanza, Osaka, Japan, [4]Showa Rekisei Industries Co., Ltd. Hyogo Japan, [5]Showa Rekisei Industries Co.,Ltd. Hyogo, Japan.*

- 11:30-11:50 (084) : Topological characterisation of pore deformations in dense granular packings and geomaterials *by *M. Saadatfar[1], H. Takeuchi[2], M. Hanifpour[3], N. Francois[1], V. robbins[1], Y. Hiraoka[2] from [1]Department of Applied Mathematics, Research School of Physics and Engineering, Ausralian National University, Canberra – Australia, [2]AIMR, Tohoku University, Japan, [3]Department of Physics, College of Sciences, Tehran University, Iran.*

- 11:50-12:10 (085) : Observation of ground displacement and strain field around the driven open-section piles *by *T. Sato[1], K.Onda[2], J.Otani[1] from [1]X-Earth Center, Kumamoto University, Kumamoto, Japan, [2]JFE Steel Corporation, Kawasaki, Japan.*

Session 301 & 310 - Hydraulics and sediment transport & Hydrogeology, Water infiltration and pollution

Chairs 301: William Arnott & Bernard Long
Chairs 310: Richard Martel, Subhasis Ghoshal

- 10:10-10:30 (194) : X-ray measurement of sand ripples bedload transport *by S. Montreui, B.Long from INRS-ETE, Québec, QC. Canada.*

- **10:30-10:50 (199) : The internal density structure of sediment-propelled turbidity currents as revealed by CT imagery** *by R. W. C. Arnott[1], M. Tilston[1], C. Rennie[1], B. Long[2] from [1]Ottawa University, Ottawa, ON., Canada, [2]INRS-ETE, Québec, QC. Canada.*

- 10:50-11:10 (203) : The influence of grain size on the velocity and sediment concentration profiles and depositional record of turbidity currents *by M. Tilston[1], R.W.C. Arnott[1], C. D. Rennie[2], B. Long[3] from [1]Department of Earth Sciences, University of Ottawa, Ottawa ON, Canada, [2]Department of Civil Engineering, University of Ottawa, Ottawa, ON, Canada, and [3]Centre Eau Terre Environnement, INRS, Québec City QC Canada.*

- 11:10-11:30 (121) : Evolution of soil hydraulic properties under saturated conditions *by *Y. Périard[1], S. José Gumière [1], B. Long[2], A. N. Rousseau[2], J. Caron[1] from [1]Department of Soils and Agri-Food Engineering, Laval University, Québec, QC, Canada, and [2]Institut national de la recherche scientifique : Centre Eau, Terre et Environnement, Québec, QC, Canada.*

- 11:50-12:10 (146) : Characterization of intra-aggregate bioaccessible porosity *by *A. Akbari[1], S. Ghoshal[1] from [1]Department of Civil Engineering, McGill University, Montreal, Québec, Canada.*

- 12:10-12:30 (177) : Frequency mapping of local degree of saturation in partially saturated sand subjected to drying and wetting process *by *Y. Higo[1], G. Khaddour[2], S. Salager[2], R. Morishita[3]†, R. Kido[3] from [1]Department of Urban Management, Kyoto University, Kyoto Japan, [2]Grenoble-INP, UJF, CNRS UMR5521, Laboratoire 3SR, Saint Martin d'Hères, Grenoble, France, [3]Department of Civil and Earth Resources Engineering, Kyoto University, Kyoto Japan, † Currently in Oil, Gas and Metals National Corporation (JOGMEC), Japan.*

- 12:10 – 13:40 Lunch

Session 202 - Geotechnic

Chairs: Jacques Desrues & Stephen Hall

- 13:40-14:00 (025) : Influence of particle morphology on strain localization of sheared sand *by A. M. Druckrey[1], K. A. Alshibli[2], M. Jarrar[3] from [1]Dept. of Civil & Env. Engineering, University of Tennessee, Knoxville, TN, USA, [2]Dept. of Civil & Env. Engineering, University of Tennessee, Knoxville, TN, USA, [3]Dept. of Civil & Env. Engineering, University of Tennessee, Knoxville, TN, USA.*

- 14:00-14:20 (104) : Wormhole development in carbonate rocks during CO_2 acidized water flow *by A. P. S. Selvadurai, C. Couture from Department of Civil Engineering and Applied Mechanics, McGill University, Montréal, QC, Canada.*

- 14:20-14:40 (120) : Characterisation of force chains in granular media through combined 3DXRD and X-ray tomography *by *S. A. Hall[1,2], R. C Hurley[3], J. Wright[4] from [1]Division of Solid Mechanics, Lund University, Lund Sweden, [2]European Spallation Source AB, Lund, Sweden, [3]Mechanical and Civil Engineering, California Institute of Technology, Pasadena, CA, USA, [4]European Synchrotron Radiation Facility, Grenoble, France.*

- 14:40-15:00 (204) : Characterization of rock discontinuity morphology during shearing using X-ray micro-CT *by B. S. A. Tatone[1], *N. Tisato[2], G. Grasselli[2] from [1]Geomechanica Inc.,Toronto, Toronto, ON, Canada, and [2]Department of Civil Engineering, University of Toronto, Toronto, ON, Canada.*

- 15:00-15:20 (024) : Insight into 3D fracture behavior of silica sand *by M. B. Cil[1], K. A. Alshibli[1] from [1]Dept. of Civil & Env. Engineering, University of Tennessee, Knoxville, TN, USA, [2]Dept. of Civil & Env. Engineering, University of Tennessee, Knoxville, TN, USA.*

Session 303 & 311 - Wood & Archaeology

Chairs 303: Dominique Delorme and Jan Van Den Bulcke
Chairs 311 Réginald Auger & Geneviève Treyvaud

- 13:40-14:00 (045) : *In-situ* study of wood hygro-mechanical behaviour by phase contrast X-ray tomography at cellular and sub-cellular scales *by *A. Patera[1,2], D. Derome[3], J. Carmeliet[3,4], M. Stampanoni[1,5] from [1]Swiss Light Source, Paul Scherrer Institute, Villigen, Switzerland, [2]Centre d'Imagerie BioMedicale, Ecole Polytechnique Federale de Lausanne, Lausanne, Switzerland, [3]Laboratory for Building Science and Technology, Swiss Federal Laboratories for Materials Scienceand Technology, EMPA, Dübendorf, Switzerland, [4]Chair of Building Physics, ETH Zurich, Switzerland and [5]Institute of Biomedical Engineering, University and ETH Zürich, Switzerland.*

- 14:00-14:20 (047) : Non-destructive research on wooden musical instruments: From macroscale to submicron imaging with lab-based XCT systems *by *J. Van den Bulcke[1], D. Van Loo[2,3], M. Dierick[2,3], B. Masschaele[2,3], M.N. Boone[2], L. Van Hoorebeke[2], J. Van Acker[1] from [1]UGCT - Laboratory of Wood Technology, Department of Forest and Water Management, Faculty of Bioscience Engineering, Ghent University, Gent, Belgium, 2GCT – Dept. Physics and Astronomy, Ghent University, Gent, Belgium and [3]XRE, X-Ray Engineering bvba, Gent, Belgium.*

- 14:20-14:40 (072) : Using X-ray microtomography to assess the vulnerability to drought-induced embolism in plants *by N. Lenoir[1*], S. Delzon[2], E. Badel[3], R. Burlett[2], B. Choat[4], H. Cochard[3], S. Jansen[5], J. M. Torres-Ruize[2] from [1]PLACAMAT, UMS3626 CNRS-Univ. of Bordeaux, Pessac (FRANCE), [2]INRA, UMR BIOGECO, Talence, France, [3]INRA, UMR PIAF, Clermont-Ferrand, France, [4]University of Western Sydney, Sydney, Australia, [5]University of ULM, ULM, Germany.*

- 14:40-15:00 (207) : Low-resolution high-speed CT scanning for sawmill log sorting and grading *by *Y. An[1], G.S. Schajer[2], C. Ristea[3], B. Lehmann[4], D. Wong[5], Z. Pirouz[6] from [1,3,4,5,6]FPInnovations, Vancouver, BC, V6T 1Z4 and [2]Department of Mechanical Engineering, UBC, Vancouver, BC, Canada.*

- **15:00-15:20 (039) : Celtic drum fibula morphology, preparation technique and conservation state determined by X-ray computed tomography** by **C. Tenailleau[1], E. Dubreucq [2], B. Duployer[1], L. Severac[1], P. Y. Milcent [2], L. Robbiola[2] from [1]CIRIMAT, UMR - CNRS 5085, Université de Toulouse, Toulouse, France and [2]TRACES, UMR - CNRS 5608, Université de Toulouse, Toulouse, France.*

- 15:20-15:40 (074) : Micro-CT characterization of archaeological bones *by H. Coqueugniot[1,2], A. Colombo[2,1], C. Rittemard[3], O. Baker[3], B. Dutailly[1], O. Dutour[3,1,4], *N. Lenoir[5,1] from [1]UMR 5199 PACEA, Bat B8, Université de Bordeaux, Pessac, France [2]Department of Human Evolution, Max Planck Institute for Evolutionary Anthropology, Leipzig, Germany,[3]Laboratoire d'Anthropologie biologique Paul Broca, Ecole Pratique des Hautes Etudes, France [4]Department of Anthropology, University of Western Ontario, Canada and [5]UMS 3626 PLACAMAT, Pessac, France.*

- 15:40 – 16:00 Coffee break

- 16:00 – 17:30 Visit of the laboratory facilities or of Old City

Poster Presentations

Session 101

- **011 : CT imaging capabilities at BMIT at the canadian light source** ***by*** *M. A. Webb[1], G. Belev[1], D. Miller[1], T. W. Wysokinski[1], N. Zhu[1], *B. Long[2], M. London[3], D. Chapman [4], D. M. L Cooper[4] from[1] Canadian Light Source Inc., Saskatoon, SK, Canada, [2]INRS-ETE, Québec Qc. Canada, [3]Alberta Innovates – Technology Futures, Edmonton, Alberta, Canada and [4]University of Saskatchewan, Saskatoon SK, Canada.*

- **108 : Ultrafast data post processing pipeline for real-time tomographic imaging at TOMCAT** *by F. Marone[1], A. Studer[2,] H. Billich[2], L. Sala[2], T. Zamofing[3], R. Mokso[1], *M. Stampanoni[1,4] from [1]Swiss Light Source, Paul Scherrer Institute, Villigen, Switzerland, [2]Information Technology Division AIT, Paul Scherrer Institute, Villigen, Switzerland, [3]Controls Group, Paul Scherrer Institute, Villigen, Switzerland, [4]University and ETH Zurich, Zurich, Switzerland.*

- 157 : High resolution muon computed tomography at neutrino beam facilities *by *B. Suerfl[1], C. Tully[2] from [1]Physics Department, Princeton University, Princeton, New Jersey and [2]Physics Department, Princeton University, Princeton, New Jersey.*

Session 102

- 036 : Micro-CT of ultra-high molecular weight polyethylene: Enhancing contrast between polyethylene and polyurethane *by *J. M. Sietins[1] from [1]U.S. Army Research Laboratory, Aberdeen Proving Ground, MD, USA.*

- 062 : Modelling of X-ray tube spot size and heel effect in Arion *by J. Delepierre[1], *J. Dhaene[1], M. N. Boone[1], M. Dierick[1], L. Van Hoorebeke[1] from [1]UGCT, Department of Physics and Astronomy, Ghent University, Gent, Belgium.*

- 068 : Optimization of scanner parameters for dual energy micro-CT *by *E. Pauwels[1], J. Dhaene[1], A. De Muynck[1], M. Dierick[1], L. Van Hoorebeke[1] from [1]UGCT-Dept. Physics and Astronomy, Ghent University, Gent, Belgium.*

- **089 : Phase-contrast imaging applied on biological and material samples using a commercial X-ray system** *by P. Bidola[1], K. Achterhold[1], F. Pfeiffer[1] from [1]*
nchen, Garching, Germany.

- 092 : Automated processing of series of micro-CT scans *by *A. De Muynck[1], M.N. Boone[1], M. Dierick[1], I. Cambré[2], E. Louagie[2], D. Elewaut[2], L. Van Hoorebeke[1] from [1]UGCT - Dept. Physics and Astronomy, Ghent University, Gent, Belgium, and [2]Laboratory for Molecular Immunology and Inflammation, Faculty of Medicine and Health Sciences, Ghent University, Ghent, Belgium.*

- 113 : Evaluation of the absorbed dose in X-ray microtomography *by *A. De Muynck[1], S. Bonte[1], J. Dhaene[1], M. Dierick[1], K. Bacher[2], L. Van Hoorebeke[1] from [1]UGCT - Department of Physics and Astronomy, Ghent University, Gent, Belgium, and [2]Department of Basic Medical Sciences, Division of Medical Physics-Gent, Ghent University, Ghent, Belgium.*

- 138 : Application of micro/nano-CT to material characterization for industrial R&D using a very versatile tomography system *by A. Singhal from General Electric Global Research Center, Niskayuna, NY, USA.*

Session 103

- 178 : Construction and preliminary results from a 70 keV X-ray tomography beamline with a stepped-grating interferometer *by K. Ham[1], W. W. Johnson[2], K. L. Matthews II[2], G. Knapp[3], J. Yuan[3], J. Ge[4], A. Brooks[3], D. van Loo[5], *L. G. Butler[3] from [1]CAMD, Louisiana State University, Baton Rouge, LA, USA, [2]Department of Physics & Astronomy, Louisiana State University, Baton Rouge, LA, USA, [3]Department of Chemistry, Louisiana State University, Baton Rouge, LA, USA, [4]CCT, Louisiana State University, Baton Rouge, LA, USA and [5]X-Ray Engineering (XRE) bvba, Gent, Belgium.*

- 195 : *In situ* analysis of 3D printing processes using grating-based X-ray interferometry *by *O. Kio[1], P. Davis[2], X. Li[3], J. Ge[4], M. Mathis[5], K. Ham[6], L. Butler[7]from [1]Department of Chemistry, Louisiana State University. [2]Department of Construction Management, Louisiana State University, [3]School of Electrical Engineering and Computer Science (EECS), and Center for Computation and Technology (CCT), Louisiana State University, [4]Center for Computation and Technology (CCT), Louisiana State University, [5]Comparative Biomedical Sciences, School of Veterinary Medicine, Louisiana State University, [6]Center for Advanced Microstructures & Devices, Louisiana State University, Baton Rouge, LA, and [7]Department of Chemistry, College of Science, Louisiana State University, USA.*

Session 201

- **061 : Evaluation of phase correction algorithms outside the validity boundaries** *by *M. N. Boone, L. Van Hoorebeke from UGCT – Dept. Physics and Astronomy, Ghent University, Gent, Belgium.*

- 095 : Effect of an initial solution in iterative reconstruction of dynamically changing objects *by M. Heyndrickx[1], T. De Schryver[1], M. Dierick[1], *M. N. Boone[1], T. Bultreys[2], V. Cnudde[2], L. Van Hoorebeke[1] from [1]UGCT – Dept. Physics and Astronomy, Ghent University, [1]Gent, Belgium and [2]UGCT / ProgRess – Dept. Geology and Soil Science, Ghent University, Gent, Belgium.*

- 117 : Semi-empirical beam-hardening correction of dense materials using a bio- medical scanner *by *D.R. Edey[1], S.I. Pollmann[2], D.Lorusso[2,4], M. Drangova[2,5,6], R.L. Flemming[3], D.W. Holdsworth[2,5,6] from [1]Department of Geological Sciences, University of Texas at Austin, Austin, TX, USA, [2]Imaging Research Laboratories, Schulich School Of Medicine &Dentistry, Western University, London, ON, Canada, [3]Department of Earth Sciences, Western University, London, Canada, [4]Department of Physiology and Pharmacology, Schulich School Of Medicine & Dentistry, Western University, London, ON, and [5]Department of Surgery; Schulich School of Medicine & Dentistry, Western University, London, ON, and [6]Department of Medical Biophysics; Schulich School of Medicine & Dentistry, Western University, London, ON, Canada.*

- 140 : A provenance management system for tomography data processing and visualization *by G. Knapp[1], *J. Yuan[2], L. Butler[3], N. Navejar[3], M. B. Olatinwo[3], J. Ge[4] from Department of Chemistry, Louisiana State University, Baton Rouge, LA, USA*

- 168 : CT reconstruction with automated component and specimen motion corrections *by *B. Recur, A. K. S. Lathami, G. M. A. Sheppard from Australian National University, Dept. Applied Maths, RSPE, Canberra, Australia.*

- 101 : X-ray tomography imaging application for the study of soft matter systems *by C. Xia1, J. Li1, Y. Cao1, B. Kou1, *Y. Wang1, X. Xiao2, K. Fezzaa2 from 1Department of Physics and Astronomy, Shanghai Jiao Tong University, Shanghai China and 2Advanced Photon Source, Argonne National Laboratory, Argonne, IL USA.*

Session 203

- 017 : Novel contrast agents for contrast-enhanced CT to visualize in 3D the blood vessel network and fat cell distribution in bone marrow *by G. Kerckhofs[1,2], A. Sap[3], E. Plougonven[4], N. Van Gastel[1,5], M. Durand[1,2], R. Vangoitsenhoven[5], B. Van Der Schueren[5], A. Léonard[4], K. Vandamme[1,6], G. Carmeliet[1,5], T. N. Parac-Vogt[3], F.P. Luyten[1,2], L. Geris[1,7,8] from [1]Prometheus, Division of Skeletal Tissue Engineering, KU Leuven, Leuven, Belgium; [2]Dept. Development and Regeneration - Skeletal Biology and Engineering Research Center, KU Leuven, Leuven, Belgium; [3]Dept. Chemistry - Molecular Design and Synthesis, KU Leuven, Leuven, Belgium; [4]Dept. Applied Chemistry, Université de Liège, Liège, Belgium; [5]Dept. Clinical and Experimental Medicine - Clinical and Experimental Endocrinology, KU Leuven, O&N 1, Leuven, Belgium; [6]Dept. Oral Health Sciences - BIOMAT, KU Leuven, Leuven, Belgium; [7]Biomechanics Research Unit, Université de Liege, Liège, Belgium; [8]Dept. Mechanical Engineering - Biomechanics Section, KU Leuven, Heverlee, Belgium.*

- 102 : Quantitative three-dimensional tissue imaging of lipid, protein, and water contents via X-ray phase-contrast tomography *by *M. Willner1, M. Viermetz1, M. Marschner1, J. Herzen1, C. Braun2, A. Fingerle3, P. Noel3, E. Rummeny3, F. Pfeiffer1 from 1Department of Physics and Institute of Medical Engineering, Technische Universität München, Germany, 2Institute of Forensic Medicine, Ludwig-Maximilians-Universität München, München, Germany and 3Department of Diagnostic and Interventional Radiology, Technische Universität München, München, Germany.*

Session 204

- 040: A small step beyond resolution *by E. Zelinger[1], D. Podea[2] and V. Brumfeld[3] from [1]The Hebrew University of Jerusalem, Israel [2]"Vasile Goldis" Western University of Arad, [3]Romania and The Weizmann Institute of Science, Israel.*

- 066 : X-ray tube spectrum determination for quantitative interpretation of reconstructed Micro-CT images *by *O. A. Kovaleva[1], D. A. Korobkov[2], I. V. Yakimchuk[2] from [1]Moscow Institute of Physics and Technology, Dolgoprudny, Russian Federation and [2]Schlumberger Moscow Research, Russian Federation.*

- 099 : Laboratory nano-CT using geometric magnification *by *P. Stahlhut[1,3], A. Hoelzing[1,2], J. Engels[1,2], R. Hanke[1,2] from [1]Chair of X-ray Microscopy, University Wuerzburg, Wuerzburg, Germany, [2]Fraunhofer Development Center X-ray Technology EZRT, Fuerth and [3]Zentralinstitut fuer Neue Materialien und Prozesstechnik, Fuerth, Gernamy.*

- 124 : Commerical lithium-ion batteries, neutron tomography and diffraction, PCA-MCR, and SNARK *by *A. Brooks, J. Yuan, L. Butler from Department of Chemistry, Louisiana State University, 232 Choppin Hall, Baton Rouge, LA, USA.*

- 126 : New capabilities in X-ray microscopy for understanding microstructural evolution over time and length scales *by *W. Harris[1], A. Merkle[1], J. Gelb[1], L. Lavery[1], C. Holzner[1] from [1]Carl Zeiss X-ray Microscopy, Inc., Pleasanton, CA, USA.*

- 127 : Diffraction contrast tomography as an additional characterization modality on a 3D laboratory X-ray microscope *by *C. Holzner[1], A. Merkle[1], P. Reischig[2], E. M. Lauridsen[2], M. Feser[1] from [1]Carl Zeiss X-ray Microscopy, Pleasanton, CA, USA, [2]Xnovo Technology ApS, Køge, Denmark.*

- 174 : Nanoscale 4-D imaging during mechanical testing: application to crack growth in dentin *by X. Lu[1], R. S. Bradley[1], B. Hornberger[2], M. Leibowitz[2], A. Tkachuk[2], S. Etchin[2], P. J. Withers[1] from [1]Henry Moseley X-ray Imaging Facility, School of Materials, The University of Manchester, UK and [2]Carl Zeiss X-ray Microscopy, Pleasanton, CA, USA.*

Session 205

- 009 : Feasibility of iterative phase contrast tomography *by N. T. Vo*, R. C. Atwood, M. Drakopoulos from Diamond Light Source, Harwell Science and Innovation Campus, Didcot, Oxfordshire, UK.*

- 044 : Towards the reconstruction of the mouse brain vascular networks with high resolution synchrotron radiation X-ray tomographic microscopy *by *A. Patera[1,2], A. Astolfo[1], K. S. Mader[1,3], M. Schneider[4,5], B. Weber[5], M. Stampanoni,[3] from [1]Swiss Light Source, Paul Scherrer Institute, Villigen, Switzerland, [2]Centre d'Imagerie Bio Medicale, Ecole Polytechnique Federale de Lausanne, Lausanne, Switzerland, [3]Institute of Biomedical Engineering, University and ETH Zürich, Switzerland, [4]Computer Vision Laboratory, ETH Zurich, Zurich, Switzerland, [5]Institute of Pharmacology and Toxicology, University of Zurich, Zurich, Switzerland.*

- 088 : Cost-effective image analysis in the cloud: A case study using 1300 mouse femur samples *by *K. Mader[1,2,3], M. Stampanoni[1,2] from [1]Swiss Light Source, Paul Scherrer Institute, Villigen, Switzerland, [2]Institute of Biomedical Engineering, Swiss Federal Institute of Technology and University of Zurich, Zurich, Switzerland and [3,4]Quant, Zurich, Switzerland.*

- 119 : Analysis of flame retardancy in polymer blends synchrotron X-ray K-edge tomography and interferometric phase contrast movies *by *M. B. Olatinwo[1], H. Kyungmin[2], J. McCarney[3], S. Marathe[4], L. G. Butler[1] from [1]Chemistry Department, Louisiana State University, Baton Rouge, LA, [2]Center for Advanced Microstructures & Devices, Lousiana State University, Baton Rouge, LA, [3]Albemarle Corporation, Baton Rouge, LA, [4]Advanced Photon Source, Argonne National Laboratory, Argonne, IL, USA.*

- 156 : Coherent X-ray diffraction imaging of strain on the nanoscale *by *R. Harder[1] from [1]Argonne National Laboratory, Argonne, IL, USA*

- 175 : Use of distance transforms and correlation maps for advanced 3D analysis of impact damage in composite panels *by *F. Leonard[1], J. Stein[2] from [1]BAM – Federal Institute for Materials Research and Testing, Berlin,Germany and [2]TWI Ltd., Granta Park, Great Abington, Cambridge, UK.*

- 201 : Proposal of a data evaluation chain for the inspection of thermoplast clips *by *U. Hassler[1], W. Holub[1], M. Rehak[1], E. Penne[1], T. Grulich[1] from [1]Fraunhofer IIS/EZRT/AMS/RBV, Fuerth, Germany.*

- 210 : In-situ 3D nano-imaging at the advanced photon source *by V. De Andrade, M. Wojcik, D. Gursoy, A. Deriy, F. De Carlo from Advanced Photon Source, Argonne National Laboratory, Lemont, Il, USA.*

Session 301

- 118 : Wave-sediment interaction imaging with X-ray tomography: A small-scale experiment to characterize the artefacts *by C. B. Brunelle[1], B. Long[1], Pi. Francus[1], L. F. Daigle[1], M. Des Roches[1], H. Takayama[2] from INRS-ETE, Québec, Canada and [2]Kumamoto University, Japan.*

- 187 : Evolution of the ripple field under a wave regime on the offshore of the breaker bar, along the beach profile: Experiment using CT-Scan imaging *by H. Takayama[1], B. Long[2], T. Mukunoki[1], C. B. Brunelle[2] from [1]Kumamoto University, Kumamoto City, Japan and [2]Institut national de la recherche scientifique, Québec, Canada.*

Session 302

- 010 : Ptychographic tomography of geological samples – Pushing the spatial resolution limits *by *W. De Boever[1], H. Derluyn[1], J. Van Stappen[1], J. Dewanckele[1], T. Bultreys[1], M. Boone[2], T. De Schryver[2], E. T. B. Skjønsfjell[3], A. Diaz[4], M. Holler[4], V. Cnudde[1] from [1]PProGRess – UGCT – Dept. Of Geology and Soil Science – Ghent University, Ghent, Belgium, [2]Radiation Physics group - UGCT – Dept. Of Physics and Astronomy – Ghent University, Ghent, Belgium, [3]Dept. of Physics – Norwegian University of Science and Technology – Norway, [4]Paul Scherrer Institute – Villigen, Switzerland.*

- 038 : $BaTiO_3$-based composite materials for Electronics characterized by X-ray computed tomography *by *C. Tenailleau[1], S. Dupuis[1], P. Dufour[1], B. Duployer[1], S. Guillemet-Fritsch[1] from [1]CIRIMAT, UMR - CNRS 5085, Université de Toulouse, Toulouse, France.*

- 065 : Mineralogy Mapping on 3D Digital Rock Models Based on X-ray Micro-CT and Electron Microscopy Techniques *by I. V. Varfolomeev[1,2], *O. A. Kovaleva[1,2], I. V. Yakimchuk[2] from [1]Moscow Institute of Physics and Technology, Dolgoprudny, Russia and [2]Schlumberger, Moscow, Russian Federation.*

- 115 : Measuring in-situ fragment size distributions caused by melt inclusion decrepitation and other mechanisms using HRXCT *by *T. Clow[1], R. A. Ketcham[1] from [1]University of Texas at Austin, Department of Geological Sciences, University Austin, Texas, USA*

- 125 : Evaluation by Computed Tomography of the Quality of Carbon Anodes Used in Aluminum Industry *by S. Amrani*[1], D. Kocaefe[1], Y. Kocaefe[1], D. Bhattacharyay[1], M. Bouazara[1], B. Morais[2] , [1] University of Québec at Chicoutimi 555 Boulevard de l'Université, Chicoutimi, Québec, Canada.*

- 189 : Pore engineering of copper foams made by space holder technique through XMCT characterization *by A. M. Parvanian[1], M. Saadatfar[2,*], M. Panjepour[1], M. H. Shahzeydi[1] from [1]Department of Materials Engineering, Isfahan University of Technology, Isfahan, Iran and Research School of Physics and Engineering, [2]The Australian National University, Canberra, Australia.*

- 193 : Neutron imaging of coupled deformation and fluid flow in sandstones *by E. Tudisco[1], *S.A.Hall[1,2], J. Hovind[3], N. Khardjilov[4], E-M. Charalampidou[5], H. Sone[6] from [1]Division of Solid Mechanics, Lund University, Lund Sweden, [2]European Spallation Source AB, Lund, Sweden, [3]Paul Scherrer Institute, Villigen, Switzerland, [4]Helmholtz Zentrum Berlin, Germany, [5]Institute of Petroleum Engineering, Heriot Watt University, Edinburgh, UK and [6]GFZ-Potsdam, Germany.*

Session 303

- 212: Effect temperature and tree species on the damage progression of whitespotted sawyer, Monochamus scutellatus scutellatus (Say), larvae in recently burned logs, by X-Ray CT measurement *by S. Bélanger[1], É. Bauce[2], C. Hébert[2], B. Long[4], R. Berthiaume[2], J. Labrie[4], L. F. Daigle[4] from [1]Ministère de la Forêt, de la Faune et des Parcs, [2]Laboratoire Entomologie forestière (Consortium iFor), Université Laval, Canada [3]Ressources naturelles Canada, Centre de foresterie des Laurentides, Québec, Canada [4]Institut national de la recherche scientifique, Centre Eau, Terre & Environnement, Québec Canada.*

- **206** : **Cricket bat characterization based on X-Ray Computed Tomography and image processing** *by *J. Tao[1], P. Evans[2], M. Saadatfar[1], [1] Department of Applied Mathematics, [2] Faculty of Forestry, Australian National University, Australia.*

Session 304

- **141 : Application of X-ray interferometry to a highly structured calcium carbonate shell (Foraminifera)** *by G. Knapp[1], *J. Yuan[2], L. Butler[3], N. Navejar[3], M. B. Olatinwo[3], J. Ge[4] from Department of Chemistry, Louisiana State University, Baton Rouge, LA, USA.*

- 152 : **The potential of CT-scan as a high-resolution tool to identify laminated sediments from deep lakes in the Côte-Nord region, Quebec** *by *O. Nzekwe[1,2], P. Francus[1,2], G. St-Onge[2,3], P. Lajeunesse[2,4] from [1]Institut national de la recherche scientifique, Centre Eau Terre et Environnement, Québec, Canada, [2]GEOTOP Research Centre, Montréal, Canada, [3]Institut des sciences de la mer de Rimouski (ISMER), Université du Québec à Rimouski, Canada and [4]Centre d'études nordiques, Département de géographie, Université Laval, Québec, Canada.*

- 154 : **Acquisition of the natural remanent magnetization in varved sediments: laboratory redeposition experiments, CT-Scan imaging and modeling** *by *E. G. H. Philippe[1,2], G. St-Onge[1], J. P. Valet[2], P. Francus[3] from [1]Institut des sciences de la mer de Rimouski (ISMER), Université du Québec à Rimouski, Rimouski, QC, Canada, [2]Institut de Physique de Globe de Paris, Paris, France, [3]Institut national de la recherche scientifique, Centre Eau Terre Environnement (INRS-ETE), QC, Canada.*

- 209 : Ferrous iron in bioturbated sedimentary deposits: a three-dimensional exploratory analysis using planar optodes coupled to tomographic reconstructions *by J. Soto Neira[1], E. Michaud[2], B. Long[3], *R. Aller[1] from [1]Stony Brook University, Stony Brook, NY, USA. [2]Université de Bretagne Occidentale, Institut Universitaire Européen de la Mer, Brest, France. [3]Institut National de la Recherche Scientifique, Québec, Canada.*

- 067 : Evaluation of experimental dissolution of dolomite using X-ray computed tomography *by *B. Bagley[1], B. M. Tutolo[1], A. J. Luhmann[1], M. O. Saar[1,2], W. E. Seyfried, Jr.[1] from [1]University of Minnesota, Department of Earth Sciences, Minneapolis, MN USA and [2]ETH-Zurich, Department of Earth Sciences, Zurich, Switzerland.*

- 037 : Determination of the REDOX paleoconditions: A MCT study of micro pyrite *by *V. Cardenes[1], J. Dewanckele[1], W. de Boever[1], J. P. Cnudde[1], V. Cnudde[1] from [1]Pore-scale Processes in Geomaterials Research Team (PProGRess), Geology Department, Ghent University, Ghent, Belgium.*

Session 306

- 005 : Study on displacement and strain field analysis in wheel-tracking test of asphalt mixture using X-ray CT and digital image correlation *by *S. Taniguchi[1], J. Otani[2], T. Sato[3], T. Kimura[1] from [1]Civil Engineering Research Institute for Cold Region, Public Works Research Institute, 1-3-1-34, Hiragishi, Toyohira-ku, Sapporo, JAPAN, [2]X-earth Center, Graduate School of Science and Technology, Kumamoto University, Kumamoto, Japan and [3]X-earth Center, Faculty of Engineering, Kumamoto University, Kumamoto, Japan.*

- 008 : Nanoscale mechanical properties of chalk from X-ray tomography *by D. Müter[1], *H. O. Sørensen[1], K. N. Dalby[1,] S. L. S. Stipp[1] from [1]Nano-Science Center, Dept. of Chemistry, University of Copenhagen, Denmark.*

- 050 : FE-analysis of granular materials based on X-ray CT data *by D. Takano[1], *Y. Miyata[2] from [1]Port and Airport Research Institute, Yokosuka, Japan and [2]National Defence Academy of Japan, Yokosuka, Japan.*

- 070 : Measurement of three-dimensional deformation inside construction material using X-ray CT and particle tracking velocimetry *by *T. Fumoto[1], K. Takehara[2] from [1]3-4-1 Kowakae, Higashi-Osaka, Japan and [2]3-4-1 Kowakae, Higashi-Osaka, Japan.*

Session 308

- 051 : Application of X-ray CT to the observation of cracking in a corroded RC bridge Slab *by *J. Chandra Kuri[1], I. Zafar[2], T. Sugiyama[3] from [1]Environmental Material Engineering Laboratory, Graduate School of Engineering, Hokkaido University. [2]Environmental Material Engineering Laboratory, Graduate School of Engineering, Hokkaido University and [3]Environmental Material Engineering Laboratory, Faculty of Engineering, Hokkaido University, Japan.*

- 058 : Evaluation of fiber characteristics and crack structures in conventional and high-performance concretes using X-ray computed tomography *by *T. Oesch[1], *E. Landis[2], D. Kuchma[3] from [1]U.S. Army Engineer Research and Development Center (ERDC), Vicksburg, MS, [2]Department of Civil and Environmental Engineering, University of Maine, Orono, ME, and [3]Department of Civil and Environmental Engineering, Tufts University, Medford, MA, USA.*

Session 309

- 015 : MicroCT as a tool during the development of pharmaceutical tablets *by *J. Klinzing[1] from [1]Merck & Co., Inc., West Point, Pennsylvania, USA.*

- 075 : Study on the effects of porous structure on carbon composites manufacture based on synchrotron X-ray CT imaging and 3D visualization analysis *by N. Vito[1], M. Lei[1], J. Olson[2] from [1]FEI-VSG, Houston, USA and [2]Canadian Light Source, Saskatoon, SK, Canada.*

- 082 : Solid-phase structural characterizacion in polymeric foams: Synchrotron µ-CT in the limits of resolution *by S. Perez-Tamarit[1], *E. Solórzano[1], A. Hilger[2], I. Manke[2], M. A. Rodriguez-perez[1] from [1]CellMat Laboratory, University of Valladolid, Valladolid, Spain and [2]Helmholtz-Zentrum Berlin für Materialien und Energie, Berlin, Germany.*

- 128 : 3D detection of damage evolution in porous brittle cement or plaster based materials *by T. T. Nguyen[1,2], M. Bornert[1], *C. Chateau[1], J. Yvonnet[2], Q. Z. Zhu[2] from [1]Université Paris-

Est, Laboratoire Navier, CNRS UMR8205, ENPC, IFSTTAR, Marne-la-Vallée Cedex, France and [2]Université Paris-Est, Laboratoire Modélisation et Simulation Multi Echelle, Marne-la-Vallée, France.

Session 310

- 122 : Predicting soil hydraulic properties from tomodensitometric analysis and particle size distribution *by *Y. Périard[1], S. José Gumière[1], A. N. Rousseau[2], J. Caron[1], D. W. Hallema[1,3] from [1]Department of Soils and Agri-Food Engineering, Laval University, QC, Canada, [2]Institut national de la recherche scientifique : Centre Eau, Terre et Environnement, Québec, QC, Canada and [3]Eastern Forest Environmental Threat Assessment Center, USDA Forest Service, Raleigh, NC, USA.*

- 164 : A combination of radiography and micro-tomography X-ray techniques for studying shear-induced migration of particles in yield stress fluids *by *S. Hormozi[1], M. Gholami[1], N. Lenoir[2], G. Ovarlez[2] from [1]Department of Mechanical Engineering, Ohio University, Athens, OH, USA. [2]PLACAMAT, UMS3626-CNRS/University of Bordeaux, Pessac, France.*

- 191 : Discrete analysis of water phase evolution within unsaturated soil *by G. Khaddour[1,2], *S. Salager[1,2], Y. Higo[3], E. Andò[1,2], J. Derues[1,2],*Y. Higo[1], G. Khaddour[2], S. Salager[2], R. Morishita[3†], R. Kido[3] From [1]Univ. Grenoble Alpes, [3]sr, Grenoble, France, [2]CNRS, [3]SR, Grenoble, France and [3]Separtment of Urban Management, Kyoto University, Kyoto, Japan.*

Session 311

- 100 : The use of metals and metal products on urban and rural archaeological sites: reconstructing technologies employed by native american and european artisans in new france during the 17th and 18th centuries *by G.Treyvaud from INRS ETE, Québec, Qc., Canada.*

- 205 : Development of the X-ray CT data base for the paleopathological analysis : Example of the saint-matthew protestant churchyard, Quebec City (1771- 1861) *by Z. Houle-Wierzbicki[2], G. Treyvaud[1], E. Raguin i[2], R. Auger[1], I. Ribot[2] from [1]Université Laval, Québec and [2]Université de Montréal. Qc., Canada.*

Session 313

- 067 : Evaluation of experimental dissolution of dolomite using X-ray computed tomography *by *B. Bagley[1], B. M. Tutolo[1], A. J. Luhmann[1], M. O. Saar[1,2], W. E. Seyfried, Jr.[1] from [1]University of Minnesota, Department of Earth Sciences, Minneapolis, MN USA, and [2]ETH-Zurich, Department of Earth Sciences, Zurich, Switzerland.*

- 129 : Image restoration for oil bearing sandstones *by *S. Bruns[1], S. S. Hakim[1], H. O. Sørensen[1], S. L. S. Stipp[1] from [1]University of Copenhagen, Department of Chemistry, Copenhagen, Denmark.*

- 135 : Porosity assessment of sandstones of the Potsdam Group, St. Lawrence Platform, Quebec, Canada: utilisation of the CT scanning techniques *by *J. F. Grenier[1], M. Malo[2], B. Long[2], D. Lavoie[3] from [12]INRS-ETE, Québec, Canada, and [3]Geological Survey of Canada, Québec, Canada.*

Book of Abstracts

Keynote Speaker

What medical CT can do for material science (and what not)

K. STIERSTORFER

KARL.STIERSTORFER@SIEMENS.COM

Siemens Healthcare, Siemensstr. 1, D 91301 Forchheim, Germany

Keywords: Computed Tomography, spatial resolution, temporal resolution

Since its invention in the early 1970s, medical Computed Tomography (CT) has gone through a dramatic evolution from a device that could image a patient's head in a scan time of several minutes to a tool that can scan whole patients within a few seconds and is fast enough to image a moving heart. The purpose of this talk is to give an overview of the technologies and capabilities of medical CT. The current state of the art in medical CT is reviewed and some examples for advanced medical applications are given. Finally, a few examples of scans of non-medical objects are presented.

Limitations of medical CT for non-medical applications

Certainly limitations of medical CT have to be considered when it comes to using it for non-medical applications:

- The system geometry is fixed,
- the beam hardening correction is optimized for water,
- the tube voltage is limited to 140 or 150 kV,
- the user interface is made for medical users,
- the image format is DICOM, a standard for medical images, jpeg exporting is possible,
- systems will typically be sold to non-medical customers on a take-it-or-leave-it basis
- regulatory system release is for medical usage. Issues may arise for other usages.

Using micro-CT and helical-CT imaging techniques to evaluate reservoir quality in bioturbated hydrocarbon reservoirs

G. M. BANIAK
greg.baniak@bp.com

BP Canada Energy Group ULC, Calgary, Alberta, Canada

For many decades, considerable efforts by subsurface petroleum specialists were devoted to understanding how parameters such as cementation, diagenesis, fracturing, and lithology impacted reservoir quality at the core (meter to centimeter) and thin-section (millimeter) scale. In more recent years, however, considerable advancements have been made in both academia and the petroleum industry to understand the distribution of porosity and permeability within reservoirs at the micron scale using high-resolution imaging techniques. Among others, the ability to evaluate rock samples using two- and three-dimensional (2D and 3D) imaging techniques has allowed geologists to better understand the impact bioturbation has on reservoir quality.

In short, bioturbation is the result of organisms (e.g., earthworms, amphipods) altering the sorting characteristics and diagenetic composition of the substrate. Because the burrows formed by these organisms are infilled with sediment that differs lithologically and geochemically from the surrounding sedimentary media, the end result is generally either an enhancement or reduction of the permeabilities and porosities in the burrows as compared to the unburrowed surrounding matrix. Herein, X-ray microtomography (micro-CT) and helical computed tomography (helical-CT) imaging techniques are discussed as a technique to evaluate the distribution of density contrasts associated with bioturbation at high resolutions (1 to 34 µm). Coupled with sedimentological data and spot-permeametry measurements, both of the imaging techniques proved valuable in mapping the distribution of permeability within bioturbated sediments. Carbonate datasets from Western Canada (Mississippian Debolt Formation and Devonian Wabamun Group) and siliclastics datasets from offshore Norway (Jurassic Ula Formation) are used as examples.

Within the studied datasets, spot-permeametry measurements revealed that the burrows are typically higher in permeability relative to the surrounding matrix. With knowledge of the lithological and sedimentological data, histograms of the attenuation coefficients for scanned samples within the micro-CT and helical-CT can be used to differentiate the matrix and burrows in 2-D and 3-D. As a result, the permeability measurements can be linked with the micro-CT and helical-CT data to build a spatial model that predicts the distribution of permeability in 2-D and 3-D. From this data, more accurate numerical models regarding bulk reservoir permeability can be constructed.

CT imaging capabilities at BMIT at the Canadian light source

*D. M. L. COOPER[1], M. A. WEBB[2], G. BELEV[2], D. MILLER[2], T. W. WYSOKINSKI[2], N. ZHU[2], D. CHAPMAN[1]
dml.cooper@usask.ca

[1] Anatomy and Cell Biology, University of Saskatchewan, Saskatoon, SK, Canada
[2] Canadian Light Source Inc., 44 Innovation Boulevard, Saskatoon SK S7N 2V3, Canada

The BioMedical Imaging and Therapy (BMIT) facility provides synchrotron-specific imaging and radiation therapy capabilities [1-5]. There are two separate endstations used for experiments: the Bending Magnet (BM) 05B1-1 beamline [3] and the Insertion Device (ID) 05ID-2 beamline [4-5]. Examples of imaging techniques devloped at BMIT include: K-edge subtraction imaging (KES), phase contrast imaging (PCI) and Diffraction Enhanced Imaging (DEI, also known as Analyzer-Based Imaging, or ABI) both in projection and CT modes. The BM endstation provide monochromatic (15-40 keV) or a pink beam (~50 keV peak) for samples up to 50 kg, and the ID endstation extend the program to higher energies (up to 120 keV) and a higher capacity positioning system (up to 450 kg). The beam in both endstations is up to 200 mm wide and 10 mm high. Core research programs include human and animal reproduction, cancer imaging and therapy, spinal cord injury and repair, cardiovascular and lung imaging and disease, bone and cartilage growth and deterioration, mammography, developmental biology, gene expression research as well as the introduction of new imaging methods.

There has been an active user program on the 05B1-1 beamline since its user program began 4 years ago. This is is now expanding with the comissioning of the insertion device based beamline 05ID-2. The CT program in particular has grown rapidly and is expected to grow not only in terms of the number of proposals but also in terms of greater complexity, desire for greater speed with higher resolution and the imaging of live animals. CT scans can range from imaging of the piglet with 200 µm resolution to imaging of bone samples with resolution on the scale of 2-3 µm.

This presentation will provide an overview of CT capabilities of the BMIT facility. The flexibility and dynamic nature of the equipment are simultaneously a great strength and a great challenge. Looking forward, BMIT is adding new capabilities such as a larger vertical beam, faster detectors and access to higher energies. At the same time, the workhorse bend-magnet based beamline will continue to provide a stable platform for CT experiments.

Coherent X-ray Nanovision

Oleg Shpyrko
oshpyrko@physics.ucsd.edu

Dept. of Physics, UC San Diego

Attempts to produce focusing x-ray optics date back to the days of Roentgen, however, it was not until the past decade that X-ray Microscopy has finally been able to achieve sub-100 nm resolution. In my talk I will introduce a novel x-ray microscopy technique, which relies on coherent properties of x-ray beams, and eliminates the need for focusing optics altogether, replacing it with a computational algorithm. We have applied this technique to image magnetic domains, as well as to image the distribution of lattice strain in nanostructures. I will also discuss recent results of in-operando imaging of lithium ion diffusion and dislocation dynamics in lithium ion energy storage devices. I will discuss applications of these novel x-ray imaging methods in context of new generation of fully coherent x-ray sources.

X-ray tomography for granular materials: current trends and perspectives

G. Viggiani[1,2] and E. Andò*[1,2]

cino.viggiani@3sr-grenoble.fr

[1] Univ. Grenoble Alpes, 3SR, F-38000 Grenoble, France
[2] CNRS, 3SR, F-38000 Grenoble, France

Keywords: x-ray tomography, granular materials

Combining x-ray tomography and three-dimensional (3D) image analysis has finally opened the way for experimental micro-(geo)mechanics, allowing access to different scales of interest. When these correspond to a scale that has been imaged at high spatial resolution, high-quality measurements can be obtained (*e.g.*, 3D displacements and rotations of individual grains of sand sample under load). However, there are issues when the scale of interest is smaller, for example the characterization of grain-to-grain contacts (their orientations and evolution) or production of fines by grain breakage. This paper presents a short selection of new grain-scale measurements obtained using existing techniques. The challenges associated with smaller scale measurements on the same images are also discussed through a few examples from ongoing work.

In conclusion this paper has attempted to highlight some of the challenges that arise when smaller-than-grain-scale measurements are required in the characterization of the deformation of a granular material. This is quite a natural requirement: in situ x-ray tomography combined with advanced image processing now allows experimental micro-geomechanics. The application of this tool can reveal different scales of interest.

When imaging the samples discussed in this paper, a trade-off had to be made between sample size and the precision of the description of each grain. Objects at a smaller scale are therefore described less precisely than would ideally be the case, but sample size cannot be safely reduced in order to benefit from a larger zoom. Consequently, the simplest approach is to accept the images as they are and try to meet the challenges of paucity of information with advanced techniques.

In the case of the natural progression from grain kinematics to the measurement of contact orientations and their evolution, the ‘ordinary’ approach to the orientation of a contact plane between two grains imaged at this scale has been shown to introduce extreme bias into the measurements to the extent that they are no longer usable. Close collaboration with experts in image processing has allowed this measurement to be made successfully using very advanced techniques.

At higher mean stresses, imaging of the production of fines during shearing is exciting. Although local porosity can be calculated from these images, measurement of a grain size distribution from these images remains a challenge that requires the development of new tools.

Session 101 - Synchrotron

(090) Taming the flood: Distributed image processing made easy on large tomographic datasets

*K. MADER[1,2,3], R. MOKSO[1], A. PATERA[1], M. STAMPANONI[1,2]
mader@biomed.ee.ethz.ch

[1] Swiss Light Source, Paul Scherrer Institut, Villigen, Switzerland
[2] Institute of Biomedical Engineering, Swiss Federal Institute of Technology and University of Zurich, Zurich, Switzerland
[3] 4 Quant, Zurich, Switzerland

The combination of improving detector technologies, more efficient measurements, and parallel acquisition have increased both the amount and the rate of data being produced in tomographic measurements. By contrast, the tools available for analyzing these ever growing datasets have remained relatively static. Additionally, with the latest acquisitions having sustained rates of 8GB/s [Mokso, 2009], the memory of even most powerful workstations is fully saturated after 1 minute of collection. Furthermore, while transistor count has continued to grow at an exponential rate, the speed of processors has been relatively stagnant since the early 2000s. The accumulation of these effects demand a radical change in the approach to handling large datasets.

While the growth in tomography has been unique in the sheer magnitude of data produced, the fields of bioinformatics [Altintas, 2013], and web analytics [Dean, 2008] have experienced similar growth spurts and made significant progress on developing flexible, scalable frameworks for processing massive datasets in a distributed, fault-tolerant manner. Using the Apache Spark framework developed in [Zaharia, 2012], we have implemented a series of image processing tools for common image processing tasks like segmentation.

The framework we developed, Spark Image Layer, is built on top of the Apache Spark framework which provides the cloud-support, distribution, and fault-tolerance. The layer currently includes a range of basic image processing operations including filtering / noise reduction, segmentation, contouring, distance / thickness map generation, shape, distribution, and texture analysis as described in [Mader, 2012]. The various components can then be pipelined into a workflow using scripts written in Java, Python, or Scala. Alternatively the tools can be run from a web-based interface. The status of the analysis and the results can be queried interactively from the web interface which provides both image, rendered, and plotted visualizations based on the type of analysis being performed. Given access to enough computational resources, the analysis can even be run in a streaming mode to process the images in real-time rather than single static analyses after the data are measured and saved.

The framework can be applied to a wide variety of datasets with successful results, but where the tools really excel is the area where no existing approach provides a viable solution. Specifically we have focused on two major projects. The first is imaging of full adult Zebra fish at cellular resolution having a final volume of 11500 x 2800 x 628 → 20-40GVx / sample. The second is a full measurement of the mouses brain vasculature with capillary resolution ≈ 10,000 x 10,000 x 10,000 → 1000 GVx / sample. While the information content of the images is very different, the same sorts of analyses will need to be performed on both. In order to convert an overwhelming mass of image data into a deeper understanding, many different segmentation

and analysis techniques will need to be tested and validated quickly. We demonstrate how these data can be segmented and how machine learning algorithms can be leveraged to further improve the reliability and automation of such analyses.

References :
1.Mokso, R., Marone, F. & Stampanoni, M. Real-Time Tomography at the Swiss Light Source. in AIP conf. proc. (SRI2009, 2009).
2.Altintas, I. Workflow-driven programming paradigms for distributed analysis of biological big data. in 2013 iEEE 3rd international conference on computational advances in bio and medical sciences (iCCABS) 1–1 (IEEE, 2013). doi:10.1109/ICCABS.2013.6629243
3.Dean, J. & Ghemawat, S. MapReduce: simplified data processing on large clusters. Communications of the ACM 51, 107 (2008).
4.Matei Zaharia, M. J. F., Mosharaf Chowdhury. Spark: Cluster computing with working sets. at http://citeseerx.ist.psu.edu/viewdoc/summary?doi=10.1.1.180.9662 (2012)
5.Mader, K., Mokso, R. & Raufaste, C. Quantitative 3D Characterization of Cellular Materials: Segmentation and Morphology of Foam. Colloids and Surfaces A: 415, 230–238 (2012).

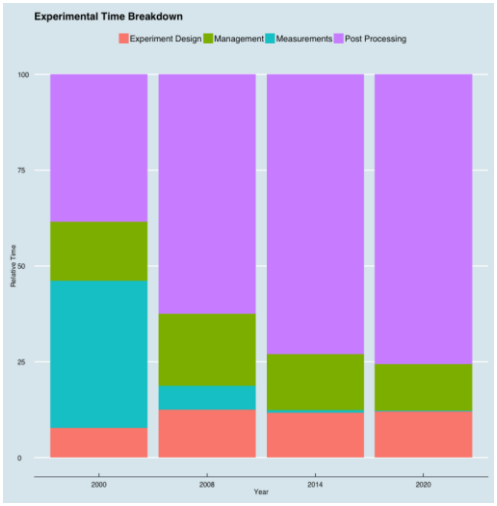

Figure 1. The graph illustrates the rapid change in the distribution of experiment time, particularly when examining the proportion used up by post-processing.

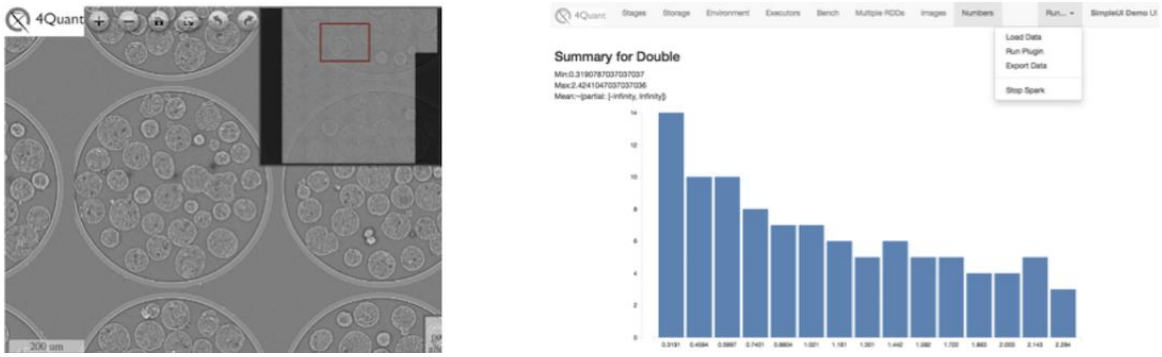

Figure

Figure 2. The GUI interface for the Spark Image Layer tools. The left panel shows the DeepZoom-based tool to explore a multi-gigabyte dataset using a web-browser. The right panel shows the D3.js-based visualizations showing histograms.

(109) PSICHE: A new synchrotron tomography beam line for materials science at SOLEIL

*A. KING[1], N. GUIGNOT[1], P. ZERBINO[1], K. DESJARDINS[1], N. LENOIR[2], M. BORNERT[3], J. P. ITIÉ[1]
king@synchrotron-soleil.fr

1 Synchrotron SOLEIL, St Aubin, Gif-sur-Yvette, 91192, France
2 PLACAMAT, UMS3626-CNRS/Université de Bordeaux, Pessac, 33608, France
3 Laboratoire NAVIER, UMR8205-CNRS/ENPC/IFSTTAR/Université Paris-Est, Champs-sur-Marne, 77200, France

PSICHE is the high-energy beam line for imaging and diffraction at the French national synchrotron SOLEIL. The tomography instrument has just entered service, with the first experiments successfully performed in September 2014. The tomograph has been optimized for in-situ materials science experiments, with a high speed, high load capacity rotation stage and white beam compatible optics. The instrument uses parallel beam geometry for imaging with pixel sizes from 0.325 to 8 microns. Beam energies from 20 to >80 keV are available, and a full dataset can be acquired in ~10 seconds in pink beam mode. It has already proven equally useful for life science and cultural heritage applications. The beam line also hosts diffraction experiments from samples at extreme pressures in both energy dispersive and angular dispersive modes. Consequently, many possibilities exist for combining diffraction and imaging in order to obtain more complete knowledge of a given sample or process. This presentation will introduce the beam line to potential future users, and give examples of results that have been obtained so far, including experiments combining imaging with diffraction and extreme conditions. Future perspectives and plans will be presented, both for extending the scope of tomography measurements, but also for combining imaging and reciprocal space information with grain mapping or correlative tomography approaches for unique and innovative experiments.

(130) Studying water/porous materials interactions with X-ray tomography

*D. DEROME[1], A. PATERA[2,3], M.DASH[4,1], M. PARADA[4,1], S. LAL[1], J. CARMELIET[4,1]
dominique.derome@empa.ch

[1] Laboratory for Multiscale studies for the built environment, Swiss Federal Laboratories for Materials Science and Technology, EMPA, Dübendorf, Switzerland
[2] Swiss Light Source, Paul Scherrer Institute, Villigen, Switzerland
[3] Centre d'Imagerie BioMedicale, Ecole Polytechnique Federale de Lausanne, 1015 Lausanne, Switzerland
[4] Chair of Building Physics, ETH Zurich, Switzerland

Water, a common fluid, displays a wide range of interactions with porous materials. We use X-ray tomography to capture the configuration of the porous material and of the liquid, in a variety of experiments. We often couple these investigations with neutron imaging, most often in projection, for moisture quantification. The datasets acquired are designed to validate advanced computational models. We investigate here porous materials of the following classes: cellular (with vapor), fibrilar and aggregate agglomerate (both with liquid water), at scales ranging from a few hundreds of nanometers to millimeters.

Many biological and engineering materials are essentially cellular, a feature which provides them with a low density, ~~a~~ high strength and ~~a~~ high toughness. The deformation of cellular materials in response to environmental stimuli such as changes in relative humidity, is of practical interest to evaluate, amongst others, their durability. We have used wood, more specifically xylem, as a "model" material for such hygroscopic cellular materials. Using phase-contrast synchroton-radiation X-ray tomographic microscopy, we isolated different tissues, i.e. pure earlywood or latewood of different porosity, to look at the configuration of the cellular structure at different moisture contents, due to exposure to different relative humidities. Such investigation allowed to quantify a swelling anisotropy dependent on porosity and to identify the total absence of hysteresis of swelling for homogeneous tissues [1]. Using nanotomography, we could isolate components of the cell wall and study their swelling behavior.This multiscale investigation of the complex hierarchical structure of wood shows that its configuration reduces the swelling/shrinkage strains and increases its dimensional stability in a humid environment. Similar work is being carried out on the living tissue of the tree, phloem.

Yarns and textile are porous, highly deformable materials which configuration induces a strong directionality on liquid water flow. Within hydrophilic yarns, the rapid water uptake is captured using phase contrast synchrotron-radiation X-ray fast tomographic microscopy, where three full scans are acquired per second. This technique provides the actual configuration of water amongst the fibers, and leads to the novel capacity of tracking several capillaries. Parallel paths and mergers of paths can be identified, providing a sub-yarn-scale understanding of capillary flow in fibrilar materials.

Porous asphalt, made of bonded aggregates and with a porosity of up to 20%, has the particular behavior to allow gravity-driven drainage. We use neutron imaging to acquire the spatial distribution of liquid water in porous asphalt during drainage and controlled drying. Neutron imaging provides ~~a~~ quantitative information of very high resolution in terms of moisture content in porous materials with high resolution. Nevertheless, a full understanding of the water flow could only be performed by combining the saturation degree distribution obtained by neutron radiography with the exact 3D geometry of the sample obtained with lab-based X-ray tomography [2]. Thus, the actual path of water during drainage and drying could be identified.

The measurements were performed at the TOMCAT beamline of the Swiss Light Source, headed by Prof Marco Stampanoni, and at the NEUTRA and ICON beamlines of SINQ, headed by Dr. Eberhard Lehmann, at Paul Scherrer Institute, Villigen, Switzerland. We acknowledge the invaluable help of their scientific teams.

References :

[1] Patera, A., Derome, D., Griffa, M., & Carmeliet, J. (2013). Hysteresis in swelling and in sorption of wood tissue. Journal of Structural Biology, 182(3), 226–234.

[2] Lal S, Poulikakos L, Sedighi Gilani M, Jerjen I, Vontobel P, Partl M, Carmeliet J, Derome D.(2014) Investigation of Water Uptake in Porous Asphalt Concrete Using Neutron Radiography, Transport in Porous Media, 105 (2), 431-450.

(159) Time-resolved (4D) *in situ* X-ray tomographic microscopy at TOMCAT: Understanding the dynamics of materials

*J. L. FIFE[1], F. MARONE[1], R. MOKSO[1], M. STAMPANONI[1,2]
julie.fife@psi.ch

[1] Swiss Light Source, Paul Scherrer Institut, Villigen PSI, Switzerland
[2] Institute for Biomedical Engineering, Swiss Federal Institute of Technology and University of Zurich, Zurich, Switzerland

Non-destructive synchrotron-based x-ray tomographic microscopy is ideal for studying various materials systems in three and four dimensions (3D and 4D, respectively), and the TOMCAT beamline[1] at the Swiss Light Source is one of the premier beamlines in the world for such experiments. Spatial resolution ranges from 1-20µm with fields-of-view from 1-15mm, and temporal resolution is as fast as 0.1s for a full 3D data acquisition[2]. Contrast varies from standard absorption, typically used in metal and composite systems, to propagation- and grating-based phase contrast, predominantly used for biological and other traditionally low-contrast materials. The efficient image processing pipeline provides a full 3D reconstruction within a few seconds[3], making visualization of selected slices close to real time. To exploit these state-of-the-art capabilities and to explore the dynamics of materials at elevated temperatures, a dedicated laser-based heating system has been developed[4] and a mechanical testing device is being commissioned. This talk will summarize the novel capabilities available at TOMCAT, as well as focus on recent achievements in dynamic, time-resolved experimentation. Particularly, it will highlight the results that have been achieved when using the gigaFROST detector[5]; a worldwide unique system that provides true dynamic experimentation with continuous image acquisition up to 7.7GB/s and decouples the temporal resolution from the total imaging time. Other results like the vesiculation of bubbles in geological materials at high temperatures under simple dead-weight compression, 4D self-healing of ceramics and 4D solidification of metals will be discussed. Since dynamic experimentation generates large amounts of data, typically on the order of terabytes, *automated* tools for visualizing and characterizing the resulting phenomena are necessary. This talk will also underscore these developments and summarize the future of time-resolved, 4D imaging at TOMCAT.

References :
[1] Stampanoni, M, Groso, A, Isenegger, A, et al. (2006) : Trends in synchrotron-based tomographic imaging: the SLS experience.—Proceedings of the SPIE, 6318: 63180M-1—63180M-14.
[2] Mokso, R, Marone, F, Stampanoni, M, et al. (2010) : Real time tomography at the Swiss Light Source.—AIP Conference Proceedings, 1234: 87- 90.
[3] Marone, F, Stampanoni, M. (2012) : Regridding reconstruction algorithm for real-time tomographic imaging.—Journal of Synchrotron Radiation, 19: 1029-1037.
[4] Fife, JL, Rappaz, M, Pistone, M, et al. (2012) : Development of a laser-based heating system for *in situ* synchrotron-based x-ray tomographic microscopy.—Journal of Synchrotron Radiation, 19: 352-358.
[5] Mokso, R, et al. (2015) : SRI Proceedings, in preparation.

(169) High speed and time resolved tomography of fluid flow in porous media at Diamond Light Source Beamline I12

*R. C. ATWOOD[1], S. B. COBAN, K. J. DOBSON[2], D. KAZANTSEV[3,4], S. A. MCDONALD[3], N. T. VO[1], P. J. WITHERS[3]
robert.atwood@diamond.ac.uk

[1] Diamond Light Source, Didcot, UK
[2] Ludwig-Maximilians University, Department of Earth and Environmental Sciences„ Germany
[3] University of Manchester, Manchester UK
[4] The Manchester X-Ray Imaging Facility, Research Complex at Harwell, Didcot, UK

X-ray tomography has the ability to provide a detailed sample assessment in 3D, and quantification of porosity, grain orientations, fracture alignments, some information about the material compositoin, and many other features. Monochromatic synctrotron X-rays can provide imaging conditions allowing the discrimination of water, air and solid particles even at relatively high energy required to penetrate macroscopic samples of minerals. The images can be obtained quickly enough to provide tomography of a column of mineral particles while fluids are percolating through the intergranular spaces, with sub-second resolution.

This allows better understanding of the development and maintenance of flow pathways, which is of interest in diverse fields of geophysics, chemical engineering, mining and mineral processing, as well as life sciences. To capture such processes, recent work at I12 has focused on developing experimental capability for sample manipulation, data acqusition and processing, and at University of Manchester, on novel mathematical approaches for obtaining information about the process from the X-ray image data. In recent experiments, high speed synchrotron x-ray tomography has been used to acquire each 3D image in under 1 second, over a period of 5-20 seconds. Plain water and contrast-enhanced brine flowing in columns of natural aggregate and in well characterized glass spheres are imaged, and improvments in reconstructing the time-series by use of 4D reconstruction methods are illustrated.

(190) Magnetic contrast nanotomography

*R. WINARSKI[1]

[1] Center for Nanoscale Materials, Argonne National Laboratory, 9700 S. Cass Avenue, Argonne, Illinois, USA

We are using the X-ray polarization selectivity (linear, right and left circularly polarized) available at the Hard X-ray Nanoprobe Beamline to examine magnetic materials in three dimensions using magnetism as a contrast mechanism [1,2,3]. X-ray magnetic circular dichroism (XMCD) refers to the differential absorption of left and right circularly polarized (LCP and RCP) X-rays, induced in a sample by an applied magnetic field. By closely analyzing the difference in the XMCD absorption spectra, information can be obtained on the magnetic properties of the elements in the system, such as spin and orbital magnetic moments. Differences in the near-edge X-ray absorption spectra are proportional to the differences in spin densities of the unoccupied electron bands in the sample. We are measuring these differences in absorption contrast while controlling the polarization during nanotomography acquisition.

References :
[1] Winarski, R. P., Holt, M. V., Rose, V., Fuesz, P., Carbaugh, D., Benson, C., Shu, D., Kline, D., Stephenson, G. B., McNulty, I. and Maser, J. (2012), A hard X-ray nanoprobe beamline for nanoscale microscopy. Jnl of Synchrotron Radiation, 19: 1056–1060. doi: 10.1107/S0909049512036783
[2] J. C. Lang and G. Srajer, Rev. Sci. Instrum. 66, 1540 (1995).
[3] G. Schütz, W. Wagner, W. Wilhelm, P. Kienle, R. Zeller, R. Frahm, and G. Materlik, Phys. Rev. Lett. 58, 737

(011) CT imaging capabilities at BMIT at the Canadian light source

M. A. WEBB[1], G. BELEV[1], D. MILLER[1], T. W. WYSOKINSKI[1], N. ZHU[1], *B. LONG[2], M. LONDON[3], D. CHAPMAN [4], D. M. L. COOPER[4]
mike.london@albertainnovates.ca

1 Canadian Light Source Inc., 44 Innovation Boulevard, Saskatoon SK, S7N 2V3, Canada
2 INRS-ETE, University of Québec, Québec, G1K 9A9, Canada
3 Alberta Innovates – Technology Futures, 250 Karl Clark Road, Edmonton AB, T6N 1E4, Canada
4 Anatomy and Cell Biology, University of Saskatchewan, Saskatoon SK, Canada

The BioMedical Imaging and Therapy (BMIT) facility provides synchrotron-specific imaging and radiation therapy capabilities [1-5]. There are two separate endstations used for experiments: the Bending Magnet (BM) 05B1-1 beamline [3] and the Insertion Device (ID) 05ID-2 beamline [4-5]. Examples of imaging techniques devloped at BMIT include: K-edge subtraction imaging (KES), phase contrast imaging (PCI) and Diffraction Enhanced Imaging (DEI, also known as ABI) both in projection and CT modes. The BM endstation provide monochromatic (15-40 keV) or a pink beam (~50 keV peak) for samples up to 50 kg, and the ID endstation extend the program to higher energies (up to 120 keV) and a higher capacity positioning system (up to 450 kg). The beam in both endstations is up to 200 mm wide and 10 mm high. Core research programs include human and animal repro-duction, cancer imaging and therapy, spinal cord injury and repair, cardiovascular and lung imaging and disease, bone and cartilage growth and deterioration, mammography, developmental biology, gene expression research as well as the introduction of new imaging methods.

There has been an active user program on the 05B1-1 beamline since it started users program 4 years ago. This is is now expanding with the comissioning of the insertion device based beamline 05ID-2. The CT program in particular has grown rapidly and is expected to grow not only in terms of the number of proposals but also in terms of greater complexity, desire for greater speed with higher resolution and the imaging of live animals. CT scans can range from imaging of the piglet with 200 µm resolution to imaging of bone samples with submicron resolution.

In this poster, we present the CT capabilities of the BMIT facility. It is the flexibility and dynamic nature of the equipment that are simultaneously a great strength and a great challenge. Looking forward, BMIT is adding new capabilities such as a larger vertical beam, faster detectors and access to higher energies. At the same time, the workhorse bend-magnet based beamline will continue to provide a stable platform for CT experiments.

References :
1. Chapman LD, (2007) CLSI Doc. No. 26.2.1.1 Rev. 0.A
2. Chapman LD, (2006) CLSI Doc. No. 26.2.1.2 Rev. 0
3. Wysokinski TW et al. (2007) NIM A 582:73-76
4. Wysokinski TW et al. (2013) J. Phys: Conf Ser 425: 07
5. Wysokinski TW et al. (2015) NIM A 775:1-4.

(108) Ultrafast data post processing pipeline for real-time tomographic imaging at TOMCAT

F. MARONE[1], A. STUDER[2], H. BILLICH[2], L. SALA[2], T. ZAMOFING[3], R. MOKSO[1], *M. STAMPANONI[1,4]
federica.marone@psi.ch

[1] Swiss Light Source, Paul Scherrer Institute, Villigen, Switzerland
[2] Information Technology Division AIT, Paul Scherrer Institute, Villigen, Switzerland
[3] Controls Group, Paul Scherrer Institute, Villigen, Switzerland
[4] Institute for Biomedical Engineering, University and ETH Zurich, Zurich, Switzerland

At the TOMCAT beamline at the Swiss Light Source, the endstation, devoted to tomographic microscopy with sub-second temporal resolution, has been delivering new scientific results for few years. Dynamic processes (e.g. evolution of liquid foams and physiology in small living animals (Simon et al., 2014)) could for the first time be captured in 3D through time. Until recently, a major limitation for in-situ and in-vivo experiments has lain in the finite RAM (36 GB) of the used CMOS detector permitting only short continuous acquisition, typically only few seconds. To overcome the limited data transfer rates of commercially available detectors, we developed a new GIGAbit Fast Read-Out SysTem (Gigafrost). This new system has no on-board RAM: the sensor can be read out continuously in an unlimited manner providing rates as high as 8 GB/s.

To fully exploit the potential of the TOMCAT experimental endstation equipped with this innovative system, tools to look almost in real time at least at a slice selection of the tomographic volumes are mandatory. We report here on our recent scientific activities focused namely on the development of new strategies for efficient handling and fast post processing of large amount of data to optimally complement the hardware implementation. We are active on several fronts. Large efforts were spent on tomographic reconstruction algorithms, validating Fourier methods (in particular gridrec) as alternatives to the standard Filtered Back-Projection approach (Marone and Stampanoni, 2012). Furthermore, the entire post processing pipeline concept as originally implemented at the TOMCAT beamline has been completely revised to match the new challenging data rates. In this context, the data format has been optimized permitting fast I/O and compatibility with data from other synchrotron sources: we adopted the Scientific Data Exchange data format, based on the HDF5 technology (De Carlo et al, 2014). The original implementation of the algorithm computing corrected sinograms has been completely substituted by a more transparent and modular version, ensuring higher flexibility and scalability. For highest speed, I/O to disk is minimized and the reconstruction routine, gridrec in our case, can read computed sonograms directly from memory and the correct center of rotation is automatically estimated to ensure high-quality tomographic reconstructions. The raw data are typically first written to disk. The reconstruction parameters can be fully controlled and optimized via a user-friendly Graphical User Interface (GUI) implemented as a Fiji plugin and the reconstruction of the entire tomographic volume can be submitted to the reconstruction cluster per simple mouse click. The raw data can however also be streamed directly to the ultrafast post-processing pipeline with the aim of obtaining preliminary tomographic reconstruction of few selected slices almost in real time to better follow the acquisition process in 3D. This new pipeline can deliver about 20 tomographic slices in less than 3 s.

Python has been the language of choice, in combination with Message Passing Interface (MPI) for the implementation of this post-processing pipeline. Cython has been used to improve the computational performance of few selected parts. We use the Sun Grid Engine (SGE) batch

queuing system for optimal use of all available distributed computational resources. With this approach, efficient management of the priorities for online-user and offline work is facilitated.

Current work is also focussed on complementing the pipeline with tools aimed at offline post-processing at a later stage. On one hand, more sophisticated algorithms for the mitigation of artifacts typical to ultrafast tomographic volumes (e.g. sample instabilities, flatfield modulations, low signal-to-noise ratio) are needed. On the other hand, for highest quality results, the reconstruction of strongly undersampled tomographic datasets necessitates routines based on iterative algorithms and a priori information.

(157) High resolution muon computed tomography at neutrino beam facilities

*B. SUERFU[1], C. TULLY[2]
suerfu@princeton.edu

[1] Physics Department, Princeton University, Princeton, New Jersey 08544
[2] Physics Department, Princeton University, Princeton, New Jersey 08544

X-ray computed tomography (CT) has an indispensable role in constructing 3D images of objects made from light materials. However, limited by absorption coefficients, X-rays cannot deeply penetrate materials such as copper and lead. Here we show via simulation that muon beams can provide high resolution tomographic images of dense objects and of structures within the interior of dense objects. The effects of resolution broadening from multiple scattering diminish with increasing muon momentum. As the momentum of the muon increases, the contrast of the image goes down and therefore requires higher resolution in the muon spectrometer to resolve the image. The variance of the measured muon momentum reaches a minimum and then increases with increasing muon momentum. The impact of the increase in variance is to require a higher integrated muon flux to reduce fluctuations. The flux requirements and level of contrast needed for high resolution muon computed tomography are well matched to the muons produced in the pion decay pipe at a neutrino beam facility and what can be achieved for momentum resolution in a muon spectrometer. Such an imaging system can be applied in archaeology, art history, engineering, material identification and whenever there is a need to image inside a transportable object constructed of dense materials.

Session 102 - Micro CT

(014) 3D chemical imaging in the laboratory by X-ray absorption edge microtomography

C. K. EGAN[1], *S. D. M. JACQUES[1,2], A. M. BEALE[2,3], R. A. D. PATTRICK[4], P. J. WITHERS[1],R. J. CERNIK[1]
christopher.egan@manchester.ac.uk

[1] School of Materials, University of Manchester, Manchester, UK
[2] UK Catalysis Hub, Rutherford Appleton Laboratory, Research Complex at Harwell, Didcot, UK
[3] University College London, Department of Chemistry, 21 Gordon Street, London, UK
[4] School of Earth, Atmospheric and Environmental Sciences,University of Manchester, Manchester,UK

Spectroscopic X-ray imaging detectors can be easily interchanged with conventional detectors within a laboratory microtomography scanner such that the absorbed X-ray spectrum of a material can be measured. If this detector has sufficient energy resolution, X-ray absorption edges can be observed within the spectrum, the position of which identifies the atomic elemental composition integrated along that ray-path. Using standard computed tomography methods, the internal chemistry of a sample can be reconstructed and visualised in 3D. Semi-quantitative analysis can be employed by voxel-wise spectral fitting to give a measure of relative elemental concentrations from within the sample. We will present technical details on the development of this technique including information on detector technology, and we will demonstrate its application with a couple of case studies, including: the distribution of catalytic metals supported on porous substrates for industrial scale chemical processing; and mapping of chemical elements and minerals inside geological core samples.

(019) Mapping grains in 3D by laboratory X-ray diffraction contrast tomography

*S. A. McDonald[1], C. Holzner[2], P. Reischig[3], E. M. Lauridsen[3], P.J. Withers[1], A. Merkle[2], M. Feser[2]
sam.mcdonald@manchester.ac.uk

[1] School of Materials, University of Manchester, Manchester, M13 9PL, UK
[2] Carl Zeiss X-ray Microscopy Inc., 4385 Hopyard Road, Suite 100, Pleasanton, CA 94588, USA
[3] Xnovo Technology ApS, Galoche Alle 15, 4600 Køge, Denmark

The majority of metallic and ceramic engineering materials of interest are polycrystalline. The properties of these materials can be significantly affected by behaviour at the length scale of the crystalline grain structure. The ability to characterise this crystallographic microstructure, non-destructively and in three-dimensions, is thus a powerful tool for understanding many facets of materials performance. The technique of X-ray diffraction contrast tomography (DCT) using monochromatic X-ray beams of very high flux found at 3rd generation synchrotron sources has been shown to be capable of mapping crystal grains and their orientations in 3D non-destructively [Johnson *et al*., 2008; Ludwig *et al*., 2009; Ludwig *et al*., 2010]. Clearly given the much wider availability and accessibility of laboratory X-ray microtomography systems the development of a laboratory DCT technique is an attractive prospect. Here we describe a new commercial laboratory X-ray DCT modality which has been enabled and present some early experimental results.

Firstly we explore the capability of the technique by studying a titanium alloy (Ti-β21S) sample having an average grain size around 36 □m. The individual grain locations and orientations are reconstructed using DCT. These results are independently compared to measurements from both synchrotron and laboratory phase contrast tomography.

One of the advantages of DCT over destructive methods of mapping grain orientations in 3D is the ability to track grain orientations and sizes over time (e.g. '4D' studies). An example of this capability is provided by following the sintering of 100μm diameter copper particles at a temperature of 1050°C, through a series time lapse DCT measurments. Local diffusion and deformation-related shape changes of the sintering particles are captured using conventional absorption tomography. At the same time, DCT enables particle rearrangements (rotations and translations) as well as competitive grain growth from particle to particle through the sintering cycle to be tracked. This new laboratory based method could have a wide range of applications as well as supporting 3D polycrystalline modelling of materials performance.

References :
Johnson, G., King, A., Goncalves Honnicke, M., Marrow, J. & Ludwig, W. X-ray diffraction contrast tomography: a novel technique for three-dimensional grain mapping of polycrystals. II. The combined case. *J. Appl. Crystallogr.* **41**, 310–318 (2008).
Ludwig, W., Reischig, P., King, A., Herbig, M., Lauridsen, E.M., Johnson, G., Marrow, J. & Buffière, J.-Y. Three-dimensional grain mapping by X-ray diffraction contrast tomography and the use of Friedel pairs in diffraction data analysis. *Rev. Sci. Instrum.* **80**, 033905 (2009).
Ludwig, W., King, A., Herbig, M., Reischig, P., Marrow, J., Babout, L., Lauridsen, E.M., Proudhon, H. & Buffière, J.-Y. Characterisation of polycrystalline materials using synchrotron X-ray imaging and diffraction techniques. *JOM* **62**, 22–28 (2010).

(032) Liquid-metal-jet X-ray tube technology and tomography applications

*E. ESPES[1], F. BJÖRNSSON, C. GRATORP, B. HANSSON, O. HEMBERG, G. JOHANSSON, J. KRONSTEDT, M. OTENDAL, P. TAKMAN, R. TERFELT, T. TUOHIMAA
emil.espes@excillum.com

[1] Excillum

The power and brightness of electron-impact micro-focus X-ray tubes have long been limited by thermal damage in the anode. This limit is overcome by the liquid-metal-jet anode (MetalJet) technology that has previously demonstrated [1] brightness in the range of one order of magnitude above current state-of-the art sources. This is possible due to the regenerative nature of this anode and the fact that the anode is already molten, which allows for significantly higher e-beam power density than on conventional solid anodes.

Over the last years, the MetalJet technology has developed from prototypes into fully operational and stable X-ray tubes running in many labs over the world. Key applications include X-ray diffraction and scattering, but recently several publications [2,3,4,5] have also shown very impressive X-ray computed tomography results using the liquid-metal-jet anode technology, especially in phase contrast imaging.

This presentation will review the current status of the technology specifically in terms of stability, lifetime, flux and brightness, with a clear focus on its applicability for X-ray computed tomography. It will also discuss details of the liquid-metal-jet technology with a focus on the fundamental limitations of the technology. It will furthermore refer to some recent data from applications within X-ray computed tomography.

References :
[1] O. Hemberg, M. Otendal, and H. M. Hertz, Liquid-metal-jet anode electron-impact x-ray source, Applied Physics Letter, 2003, 83, 1483.
[2] D. H. Larsson; U. Lundström; U. Westermark; P. A. C. Takman; A. Burvall; M. Arsenian Henriksson; H. M. Hertz, Small-animal tomography with a liquid-metal-jet x-ray source, SPIE Proceedings Vol. 8313 Medical Imaging 2012: Physics of Medical Imaging
[3] Simon Zabler; Thomas Ebensperger; Christian Fella; Randolf Hanke, High-resolution X-ray imaging for lab-based materials research, Conference on Industrial Computed Tomography, Wels, Austria 2012
[4] T. Thüring; T. Zhou; U. Lundström; A. Burvall; S. Rutishauser; C. David; H. M. Hertz; M. Stampanoni, X-ray grating interferometry with a liquid-metal-jet source, Applied Physics Letters 103, 091105 (2013)
[5] Matthias Bartels; Victor H. Hernandez; Martin Krenkel; Tobias Moser; Tim Salditt, Phase contrast tomography of the mouse cochlea at microfocus x-ray sources, Applied Physics Letters 103, 083703 (2013)

(055) Arion: a realistic projection simulator for optimizing laboratory and industrial micro-CT

*J. DHAENE[1], E. PAUWELS[1], T. DE SCHRYVER[1], A. DE MUYNCK[1], M. DIERICK[1], L. VAN HOOREBEKE[1]
jelle.dhaene@ugent.be

[1] UGCT-Dept. Physics and Astronomy, Ghent University, Proeftuinstraat 86/N12, B-9000 Gent, Belgium, email: jelle.dhaene@ugent.be

At the 'Ghent University Centre for X-ray Tomography' (UGCT, www.ugct.ugent.be), a variety of samples, both in terms of size and composition, are scanned for a wide range of applications. In order to increase the quality of these scans and simultaneously reduce the scan time and thus cost of X-ray Computed Tomography (CT), the scanner parameters need to be optimized. This optimization is specific for a given geometry and composition of a sample due to the complexity of the imaging process. In X-ray micro-CT, the reconstructed sample is represented by a discrete 3D volume. Each voxel in this volume contains a calculated grey value which represents the linear attenuation coefficient μ in that voxel. This reconstructed attenuation coefficient is the product of the local mass attenuation coefficient μ/ρ and the local density ρ. The former depends both on the incident photon energy and on the atomic number of the element(s) present in the sample. Conventional laboratory-based X-ray micro-CT setups use polychromatic X-ray tubes in combination with energy-integrating detectors with an energy-dependent efficiency. Therefore, the calculated attenuation coefficient in a voxel of the reconstructed volume is dependent on the incident X-ray spectrum and spectral sensitivity of the detector. The incident polychromatic beam will significantly alter while it propagates through the sample, resulting in beam hardening of the spectrum.

Optimal scanning conditions will be different for each application. the influence of the different variables, such as emitted spectrum, detector response, beam filtration and the sample itself, needs to be taken into account to create these optimal conditions. A GPU-based simulation tool, Arion, has been developed to simulate realistic radiographic projections taking into account all these scan characteristics (Dhaene et al., 2015). The programme creates a virtual scan setup which consists of a source, detector and sample. For each of these components a position and orientation can be set. As such, there are no limitations to the geometry of the virtual scan setup. The polychromatic behaviour of the components needs to be known to simulate radiographic projections. These are obtained by performing Monte Carlo simulations for the X-ray tubes and energy-integrating detectors used at the UGCT by using BEAMnrc. The elemental attenuation data of the XCOM database of NIST was used during these simulations. In Arion, A ray-tracing technique is applied to determine the total attenuation in a ray and to calculate the contribution in every energy bin to the detector pixels using the datasheets of the source and detector obtained by the Monte Carlo simulations. In such way a polychromatic radiographic image is obtained.

Simulated and real scans using various scanner setups at the UGCT show good agreement. The results of the simulations can thus be used to determine the optimal scanning conditions in order to create the best signal-to-noise (SNR) or contrast-to-noise-ratio (CNR) for a certain application. Additionally, the simulation programme can be applied for the development of industrial CT scanners. In such setup, the geometry is often bound to stringent limitations. The wide range of possible geometries for the virtual scan setup allows to test which limited setup suits best for a certain application.

References :
Dhaene, J., Pauwels E., De Shryver, T., De Muynck, A., Dierick, M, Van Hoorebeke, L., *A realistic projection simulator for laboratory based X-Ray micro-CT*. Nuclear Inst. and Methods in Physics Research, B, Volume 342, p. 170-178, 2015

(098) NanoCT imaging with a prototype nanofocus source and a single-photon counting detector

*M. MÜLLER[1], S. FERSTL[1], S. ALLNER[1], M. DIEROLF[1], P. TAKMAN[2], T. TUOHIMAA[2], B. HANSSON[2], F. PFEIFFER[1]
mark_mueller@ph.tum.de

1 Department of Physics and Institute of Medical Engineering, Technische Universität München, James-Franck-Straße, 85748 Garching, Germany
2 Excillum AB, Torshamnsgatan 35, 16440 Kista, Sweden

In the last decade X-ray microCT (µCT) has gained importance in many research domains and is becoming a routine microscopy technique. Due to the recent development of transmission X-ray tubes with focal spot sizes below 1 micron, scientific setups[1] as well as commercially available microCT scanners[2,3] can nowadays achieve resolutions in the nanometer range. We present a novel microCT setup featuring a prototype nanofocus X-ray source and a single-photon counting detector. The system relies on mere geometrical magnification and can reach resolutions around 300 nm at its current state. The nanofocus X-ray tube (Excillum AB, Sweden) consists of a tungsten transmission target on a diamond layer and can so far reach focal spot sizes down to about 300 nm. The design of the head of the source allows for positioning of the object very close to the focal spot and consequently for high magnification factors (up to 1500).

The X-ray camera is a PILATUS 300K-W 20Hz detector with a 1000 µm silicon sensor. The image area of this camera consists of 1475 x 195 pixels with a pixel size of 172 x 172 µm[2]. In contrast to conventional CCD and flatpanel detectors, the single-photon counting detector has no readout or dark current noise and its point spread function is the pixel size. The detector is motorized and can be moved into x-, y-, and z-direction.

The sample is rotated on a high precision air bearing rotary stage that can be moved precisely into x-, y-, and z-direction. Additionally, it is possible to correct the sample position relative to the rotation axis. The entire sample motorization is mounted upside down to facilitate measurements of samples in solutions.

First results demonstrate that the focal spot of the tube is stable enough over the time of a CT scan (up to 15 hours) to permit imaging with submicron resolution. The small focal spot size also results in sufficient spatial coherence to exploit edge enhancement effects and to apply phase contrast imaging methods. Moreover, the first images indicate that image acquisition with a practically noise-free photon counting detector combined with a low-flux nanofocus tube can result in enhanced contrast compared to similar setups. We will show first applications comprising stained soft tissue samples as well as bone and tooth samples; e.g. a 3D data set of a piece of tooth, where the dentin tubules, micrometer-narrow channels extending from the dentin-enamel junction to the pulp chamber of the tooth[4], are clearly resolved (see attached image).

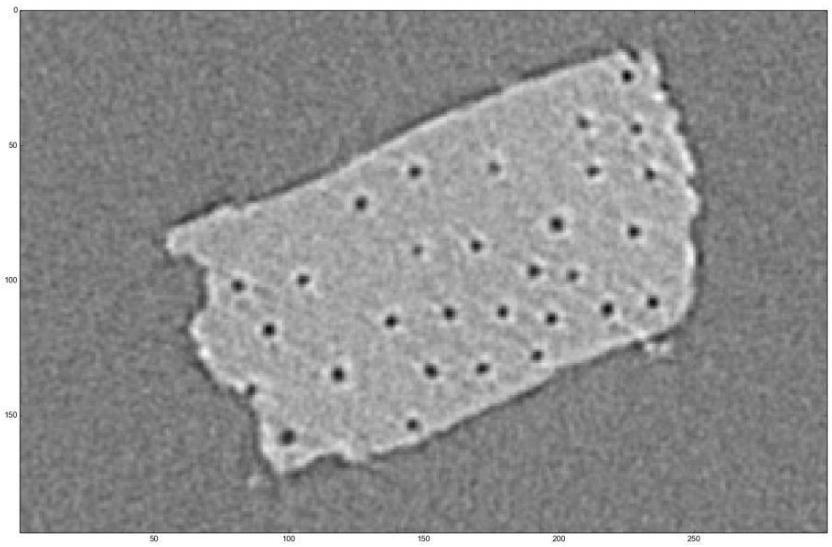

Figure 1. Transversal slice of tooth piece: The dentin tubules can be clearly identified as dark spots. Voxel size: 280nm. (Premature result: No postprocessing, standard Filtered Back Projection used for reconstruction.)

References :
1 Dierick, M. et al. 2014, Nuclear Instruments and Methods in Physics Research Section B: Beam Interactions with Materials and Atoms 324, 25-40
2 http://www.xradia.com
3 http://www.skyscan.be/products/2011.htm
4 Kinney, J. H. et al. 2013, Critical Reviews in Oral Biology and Medicine 14, 13–29

(153) A laboratory micro-CT setup for fast continuous scanning: applications for pore scale fluid flow research

M. A. BOONE[1,2], *J. VAN STAPPEN[1], T. BULTREYS[1], M. N. BOONE[3], T. DE SCHRYVER[3], B. MASSCHAELE[2,3], D. VAN LOO[2], L. VAN HOOREBEKE[3], V. CNUDDE[1]
matthieu.boone@ugent.be

[1] UGCT – PProGRess, Dept. Geology and Soil Science, Ghent University, Krijgslaan 281/S8, B-9000 Gent, Belgium
[2] XRE – X-ray Engineering bvba, De Pintelaan 111, B-9000 Gent, Belgium
[3] UGCT, Dept. Physics and Astronomy, Ghent University, Proeftuinstraat 86/N12, B-9000 Gent, Belgium

The migration of fluids through a porous material and the influence of those fluids migration processes on the porous material itself are crucial in numerous geological and engineering applications. In order to obtain a better understanding of the dynamics of these processes, a fast time-resolved 3D characterization of the pore space is required. In recent years, fast micro-CT imaging with sub-second temporal resolution has become available at synchrotron facilities. In laboratory based micro-CT imaging however the temporal resolution is often bound due to the limited X-ray flux. At the Centre for X-ray Tomography of the Ghent University (UGCT) a gantry-based micro-CT system (environmental micro-CT; EMCT) was developed in cooperation with XRE (www.xre.be) (Dierick et al., 2014). This setup allows a continuous acquisition with a spatial resolutions below 10 µm and a temporal resolution of 12s for a complete 360° scan. The EMCT setup is quite different compared to more common micro-CT setups as the X-ray tube and detector rotate in a horizontal plane around the sample which remain stationary. This setup is ideal to image fast dynamic processes using peripheral equipment such as a cooling stage, fluid flow cell, pressure cell, … in a top-bottom geometry.

Here we present the first results of fast dynamic imaging using the EMCT scanner and a specially designed flow cell to visualize single and multiphase flow in porous rocks. In the single phase flow experiment, advection and diffusion of a tracer salt in a water saturated limestone sample was monitored during fluid injection (animation: http://youtu.be/LfvL2-AUIrE). This illustrates the presence of preferential flow paths in the limestone which were dominated by advection and less connected pore bodies dominated by diffusion. In the multiphase flow experiment oil was injected in a brine saturated sandstone, which allow to visualize the pore scale displacement of water by oil in discrete drainage events (animation: http://youtu.be/H3Zf4xfUSbw). These first results illustrate the potential of this setup for fast dynamic micro-CT imaging in a laboratory environment.

References :
Dierick, M., Van Loo, D., Masschaele, B., Van den Bulcke, J., Van Acker, J., Cnudde, V., & Van Hoorebeke, L. (2014). Recent micro-CT scanner developments at UGCT. *Nuclear Instruments and Methods in Physics Research Section B: Beam Interactions with Materials and Atoms*, *324*, 35–40.

(172) Multi-energy nano computed tomography phase retrieval for material discrimination

*H. LI[1], A. KINGSTON[1], G. MYERS[1], B. RECUR[1], A. SHEPPARD[1]
lhy110@physics.anu.edu.au

[1] Department of Applied Mathematics, RSPE, Australian National University, Canberra, ACT 2601, AUSTRALIA

X-ray nano-CT is a useful tool to study the high-resolution features in a sample of interest. Most samples distort the x-ray phase non-uniformly, altering the intensity distribution during propagation from the object to the detector. This effect is known as phase contrast. Current tomographic reconstruction methods assume the effect of this phase shift on the recorded attenuation can be ignored. This assumption is not valid for the nano-CT system under construction at the ANU. To achieve high X-ray detection accuracy and efficiency, we used a 400mm wide 3k*3k pixel detector. Using such a large detector, and still achieving a voxel size of 300 nanometres for a 1 mm diameter sample, a fine-focus geometry nano-CT requires at least 0.5 metre of X-ray propagation after going through the object. Small voxel resolution coupled with long propagation distance create significant phase-contrast edge artefacts in the reconstructed volume.

Phase contrast can both improve and diminish the quality of certain types of CT reconstruction. On one hand, phase-contrast imaging is more sensitive to low-density and low-atomic-number materials. This enhances the transition edges between different materials in the reconstruction. On the other hand, without phase retrieval, it introduces edge artefacts in the reconstruction [1], making quantitative analysis difficult. There is much research to devise phase retrieval algorithms to both reduce these phase shift artefacts and obtain the phase shift information through the object. Currently used near-field phase retrieval algorithms include the Born's approximation approach [2], and Paganin's single material approach [1]. Generally, Paganin's approach is not appropriate at our ANU facility because samples are not single material, and Born's approximation approach is not applicable since our x-ray wave field is not slowly varying nor small in magnitude.

To obtain a phase retrieval algorithm with valid assumptions for our experimental setup, we started with the Transport of Intensity (TIE) formulation [3], collecting two monochromatic radiographs at the same propagation distance. We first derived a set of coupled intensity-propagation equations, in terms of density (ρ) and atomic number (Z) in the sample. We investigated the magnitude of higher-order phase contrast terms and found they were significant for our nano-CT set-up. We found this by comparing the higher-order influence on intensity for different X-ray energies, different X-ray propagation distances, and for different sample feature size.

We have decoupled the two propagation equations to obtain a single-variable second-order propagation equation, relating density (ρ) in the sample to measured intensity at the detector. This differs from other phase retrieval algorithms ([2] and [3]) only directly relating attenuation in the sample to measured intensity at the detector. We derive a phase-retrieval algorithm based on our single-variable propagation model, designed to calculate a 3D density (ρ) and atomic number (Z) map of a sample from radiographs collected at two different energies. We investigate the performance of this algorithm, for multi-material objects which violate the assumptions of Paganin's approach [1].

References :
[1] D. Paganin and et al., “Simultaneous phase and amplitude extraction from a single defocused image of a homogeneous object,” Journal of Microscopy 206, 33-46 (2002).
[2] T. Gureyev and et al., “Optical phase retrieval by use of first Born- and Rytov-type approximations,” Applied Optics 43, 2418-2430 (2004).
[3] M. Reed Teague, "Deterministic phase retrieval: a Green’s function solution," Journal of the Optical Society of America 73, 1434-1441 (1983).

(150) Rock deformation and micro-CT analyses

N. TISATO[1], Q. ZHAO[1], G. GRASSELLI[1]
nicola.tisato@utoronto.ca

[1] University of Toronto

Experimental methods for rock–mechanics and –physics have been greatly improved in the last century. These developments enhanced our understanding of deformation processes in geo-materials. Nevertheless, many questions have not yet been addressed and new challenges, such as energy extraction from unconventional reservoirs, pose new ones.

As many physical and mechanical properties of rocks are intimately related to microscopical features, such as grain orientation or pore distribution, one of the next frontier, which must be overcome, is to perform deformation experiments while imaging the internal structure of the specimen. Such technology will be extremely beneficial to understand how, for instance, granular materials fail or how dissolution and precipitation of new phases influence the apparent rock properties.

The present contribution presents the designs and the preliminary results obtained with a couple of new X-ray-transparent vessels which can be paired with the micro-CT system installed at the University of Toronto. Both vessels can confine cylindrical rock specimens up to 25 MPa.

The first machine was designed to measure complex elastic moduli (or 1/Q) in cylindrical samples and to relate such measurement with the fluid distribution and/or the dissolution/precipitation of new mineral phases. In particular, the principal aim is to measure 1/Q for dry, water and water-CO_2 saturated samples. 1/Q will be measured after different periods of time to depict the impact of chemical reactions on the rock-physical properties. This study will help geophysical methods to improve the monitoring and surveying of gas, oil and water reservoirs as subsurface imaging relies on rock elastic properties.

The second machine is provided with a rotary motor which allows spinning a cylindrical sample against a static sample while the normal stress is maintained. This vessel will serve to image the formation of a brittle shear zone while measuring the evolution of friction. These experiments will shed light on brittle failure of rocks and weakening mechanisms providing new insights for earthquake related studies.

(22) Investigation of carbon nanostructure in copper covetics by X-ray nanotomography

B. MA[1], R. P. WINARSKI[2], J. WEN[2], D. J. MILLER[2], C. U. SEGRE[3], U. (BALU) BALACHANDRAN[1], D. R. FORREST[4]
bma@anl.gov

[1] Energy Systems Division, Argonne National Laboratory, Argonne, IL 60439
[2] Nanoscience and Technology Division, Argonne National Laboratory, Argonne, IL 60439
[3] Department of Physics, Illinois Institute of Technology, Chicago, IL 60616
[4] U.S. Department of Energy, Advanced Manufacturing Office, Washington, DC 20585

Recent advancement in nanoscience and nanomaterials engineering have made it possible to incorporate carbon nanostructures into copper metal matrixes to achieve unique physical properties. This new class of materials, known as covetics, may be a game-changer for materials scientists and engineers who have long sought to combine high-strength carbon with metal in their pursuit to improve materials performance. The enhanced electrical and thermal conduction of copper covetics originate from carbon nanostructures dispersed in the metal. High-resolution TEM investigation revealed carbon nanostructures of a few nanometers inserted into Cu lattice planes. Full-field transmission imaging and hard X-ray nanotomography were utilized to examine the 3D carbon nanostructure networks. Details of the results will be presented and discussed. This work was supported by the U.S. Department of Energy, Energy Efficiency and Renewable Energy, Advanced Manufacturing Office, under Contract DE-AC02-06CH11357

* This work was supported by the U.S. Department of Energy, Energy Efficiency and Renewable Energy, Advanced Manufacturing Office, under Contract DE-AC02-06CH11357. The submitted manuscript has been created by UChicago Argonne, LLC, Operator of Argonne National Laboratory ("Argonne"). Argonne, a U.S. Department of Energy Office of Science laboratory, is operated under Contract No. DE-AC02-06CH11357. The U.S. Government retains for itself, and others acting on its behalf, a paid-up nonexclusive, irrevocable worldwide license in said article to reproduce, prepare derivative works, distribute copies to the public, and perform publicly and display publicly, by or on behalf of the Government

(036) Micro-CT of ultra-high molecular weight polyethylene: Enhancing contrast between polyethylene and polyurethane

*J. M. SIETINS[1]
jennifer.m.sietins.ctr@mail.mil

[1] U.S. Army Research Laboratory, Aberdeen Proving Ground, MD 21005

X-ray micro-computed tomography is a powerful tool for three-dimensional imaging and quantitative data analysis. Much progress has been made in recent years to improve image resolution, enhance contrast between materials of similar density, and minimize or correct scanning artifacts during the reconstruction process. A known difficulty, however, is obtaining adequate contrast between materials with similar mass attenuation coefficients without the use of phase contrast imaging. Ultra-high molecular weight polyethylene (UHMWPE) composite products used for soldier protection applications employ a thermoplastic polyurethane-based matrix, which exhibits a similar attenuation response to the UHMWPE fiber. The combination of the lower x-ray energies needed for improved constrast between the polymer constituents as well the high resolution required for clarity of the fibers and voids within the composite create long scan times. Frame averaging, x-ray power, and rotation step sizes were adjusted to determine the influence on scan times, artifacts, and resulting attenuation histograms. Recommended scanning parameters are presented to provide sufficient contrast between polyethylene and polyurethane with the shortest scan times.

(062) Modelling of X-ray tube spot size and heel effect in Arion

J. DELEPIERRE[1], *J. DHAENE[1], M. N. BOONE[1], M. DIERICK[1], L. VAN HOOREBEKE[1]

[1] UGCT, Department of Physics and Astronomy, Ghent University, Proeftuinstraat 86, 9000 Gent, Belgium, jolien.delepierre@ugent.be , jelle.dhaene@ugent.be

X-ray Computed Tomography (CT) is a non-destructive technology used to produce three-dimensional images of objects, allowing the user to visualize the inside of an object. This reconstructed object is represented by a discrete three-dimensional volume and each voxel inside this volume contains a grey value that represents a calculated linear attenuation coefficient μ. In laboratory-based X-ray CT polychromatic sources are used in combination with energy-integrating detectors. Changes in the emitted spectrum or use of different detectors will thus result in different reconstructed attenuation coefficients.

To optimize the scanner settings such as high voltage and filtration for a given sample, Arion, a fast and realistic projection simulator (Dhaene *et al.*, 2014) was developed at the 'Ghent University Centre for X-ray Tomography' (UGCT, www.ugct.ugent.be). This GPU accelerated polychromatic simulator takes into account scan characteristics such as emitted spectrum, detector energy response, beam filtration and the sample itself. It would also be very useful in iterative reconstruction methods which try to match a simulated projection of a solution to the actually measured projection.

Arion already takes into account the above described effects caused by the polychromatic nature of the imaging process. Although this description of a virtual scanner is sufficient in most cases, sometimes it is useful to take into account other effect such as finite spot size and a heel effect of the X-ray tube to perform the simulations. The finite spot size can result in a reduction of spatial resolution in the radiographic projection. The heel effect causes a gradient in the spectral distribution over the projection image, which may influence the above mentioned optimization.

A large spot size can either be caused by the use of the X-ray tube at a high power or by the internal structure of an X-ray tube (Boone *et al.*, 2012). Both effects are typically modelled by a two-dimensional profile. A convolution between this profile and the sharp projection acquired with an infinite small spot size results in the image that would be acquired from the finite spot size. However, radiation originating from the internal structure of a tube requires an extension of this method to account for the difference in X-ray spectrum and source position.

The heel effect is caused by the non perpendicular angle of attack of the electrons on the anode of a directional X-ray tube. In these tubes both the intensity and spectrum depend on the direction in which the X-rays escape from the target material as the probability for absorption depends on the distance the photons travel within the anode material. Due to the geometry of the anode, this distance depends on the direction of emission. This behaviour was simulated by performing Monte Carlo simulations using BEAMnrc and could be modelled by using the results from these simulations. This model can be used to correct the radiographic images obtained by Arion for a heel effect of a directional tube.

References :

Dhaene, J., Pauwels E., De Shryver, T., De Muynck, A., Dierick, M, Van Hoorebeke, L., *A realistic projection simulator for laboratory based X-Ray micro-CT*. Nuclear Inst. and Methods in Physics Research, B, Volume 342, p. 170-178, 2015

Boone M. N., Vlassenbroeck J., Peetermans S., Van Loo D., Dierick M., Van Hoorebeke L., *Secondary radiation in transmission-type x-ray tubes: Simulation, practical issues and solution in the context of x-ray microtomography*. Nucl. Instrum. Methods Phys. Res., Sect. A, 661(1) :7-12, 2012

(068) Optimization of scanner parameters for dual energy micro-CT

*E. PAUWELS[1], J. DHAENE[1], A. DE MUYNCK[1], M. DIERICK[1], L. VAN HOOREBEKE[1]

[1] UGCT-Dept. Physics and Astronomy, Ghent University, Proeftuinstraat 86/N12, B-9000 Gent, Belgium, email: elin.pauwels@ugent.be , jelle.dhaene@ugent.be

In X-ray Computed Tomography (CT), the reconstructed sample is represented by a discrete 3D volume. Each voxel in this volume contains a grey value that represents a linear attenuation coefficient μ. This is the product of the local mass attenuation coefficient μ/ρ, which is both energy and material dependent, and the local density ρ of the material. Therefore, the reconstructed linear attenuation coefficients of two materials of different composition can still have similar grey values, making them practically indistinguishable. Since the mass attenuation coefficient of a chemical element solely depends on the photon energy, a distinction between different materials with similar grey values can be made by combining information from scans performed at two or more different X-ray energies. This technique is called Dual Energy CT (DECT).

DECT yields very good results when a monochromatic X-ray source is used which is often the case in synchrotron imaging. However, when using a laboratory-based micro-CT, the polychromatic behaviour of the photon beam and detector sensitivity and efficiency complicates the choice of the appropriate scanning parameters for applications of DECT methods. A programme for simulating realistic radiographic projection images, Arion (Dhaene et al., 2015), has recently been developed at the 'Ghent University Centre for X-ray Tomography' (UGCT, www.ugct.ugent.be). This programme can also be used to identify optimal scanning parameters for different applications, including DECT.

The use of Arion to optimize these conditions will be presented. A virtual phantom of three aqueous solutions was created and used as a sample. These solutions contained $Pb(NO_3)_2$, PTA and KBr, which are typical staining materials used for the visualization of soft tissue with micro-CT. Simulations were made for different scanning conditions, which covered a range of voltages and filters. Varying these parameters will result in a broad range of different spectra. Covering this range is necessary to find the best signal-to-noise ratio (SNR) or contrast-to-noise ratio (CNR) for the materials inside the phantom for a specific application.

First, all single energy scans were studied in terms of distinctiveness between the three solutions. In most cases at least two out of three materials are not distinguishable. Then a post-reconstruction method (Granton et al., 2008) was applied for the range of simulations. This method allows to combine the information from scans performed at two different energies and calculate the volume fractions of the three materials present in the phantom. In this way, the best energies to perform DECT can be selected.

References :
Dhaene, J., Pauwels E., De Shryver, T., De Muynck, A., Dierick, M, Van Hoorebeke, L., *A realistic projection simulator for laboratory based X-Ray micro-CT*. Nuclear Inst. and Methods in Physics Research, B, Volume 342, p. 170-178, 2015.
Granton P.V., Pollmann S.I., Ford N.L., Drangova M., Holdsworth D.W. *Implementation of dual- and triple-energy cone-beam micro-CT for postreconstruction material decomposition. Med Phys.*2008 Nov;35(11):5030-42.

(089) Phase-contrast imaging applied on biological and material samples using a commercial X-ray system

P. BIDOLA[1], K. ACHTERHOLD[1], F. PFEIFFER[1]
pidassa.bidola@tum.de

[1] Department of Physics & Institute of Medical Engineering, Technische Universität Munchen, James-Franck-Str 1, 85748 Garching, Germany

The single distance propagation-based phase-contrast imaging is one of the improving phase-contrast imaging techniques available nowadays [1, 2]. For these imaging methods require coherent X-rays beams, they commonly have been used at synchrotrons. However, the development in tomography enabled it to translate some of them also to laboratories using polychromatic X-rays tubes [3, 4].

The improvement of phase-retrieval algorithms, extended to cone-beam geometry [5, 6] allow it to obtain the amplitude and phase images, which usually hold complementary information. In fact, the use of phase-contrast and phase-retrieval algorithms in a cone-beam geometry are successfully applicable on materials [7], and biological samples [8].

After the study of a new commercial X-ray device for tomography (versaXRM-500 by Carl Zeiss), we present the application of the single-distance propagation-based phase-contrast imaging (2D and 3D) including the phase-retrieval on selected biological and material samples.

References :
[1] Bonse et al. (1965), Applied Physics Letters, 6(8), 155-156.
[2] Fritzgerald et al. (2000), physics today, 53(7), 23-26.
[3] Pfeiffer et al. (2006), Nature physics, *2*(4), 258-261.
[4] Wilkins et al. (1996), Nature, 384, 335-338.
[5] Paganin et al. (2002), Journal of microscopy, 206, 33-40.
[6] Burvall et al. (2011), optic express, 19, N°11.
[7] Mayo et al. (2012), materials, 5, 937-965.
[8] Bartels et al. (2013), Applied Physics Letters, 103, 083703.

(092) Automated processing of series of micro-CT scans

*A. De Muynck[1], M. N. Boone[1], M. Dierick[1], I. Cambré[2], E. Louagie[2], D. Elewaut[2], L. Van Hoorebeke[1]
amelie.demuynck@ugent.be

[1] UGCT - Dept. Physics and Astronomy, Ghent University, Proeftuinstraat 86/N12, B-9000 Gent, Belgium
[2] Laboratory for Molecular Immunology and Inflammation, Department of Rheumatology, Faculty of Medicine and Health Sciences, Ghent University, De Pintelaan 185, B-9000 Ghent, Belgium

At the 'Centre for X-ray Tomography' of Ghent University (UGCT; www.ugct.ugent.be) a wide variety of samples is imaged at different state-of-the-art home built micro-CT systems. For some applications, a large number of similar samples need to be scanned in order to obtain statistical relevant results. This is quite common in (bio-) medical applications, where for example specific parts of small animals are imaged. Conventionally, these samples must be properly positioned and scanned one by one. Given the desired resolution and the sample size, the sample should be centered accurately on the rotational axis. Furthermore, the variation between samples and sample mounting requires human intervention in this step. This causes a large number of delays in the scanning procedure, and makes scanning without human supervision impossible. The goal of this research was to limit the amount of human intervention in CT scanning and processing and to even be able to scan and process multiple samples without intervention of the operator.

A simple method to improve efficiency without complicated automated sample mounting is by vertical stacking. In this method, multiple samples are mounted on top of each other and subsequently scanned. However, positioning systems mounted on the rotation stage often have no absolute positioning, hence automatic centering based on this cannot be separately performed for each sample. To overcome this issue, we have developed several methods to perform the centering for stacked objects without absolute positioning. This is possible at the home built scanners at UGCT, because they are controlled by in-house developed software, which gives the opportunity to modify the acquisition schemes.

Another issue with a large number of similar scans is the reconstruction and analysis. Previously, the data was reconstructed per scan using Octopus Reconstruction (Inside Matters, www.octopusimaging.eu). This allowed for a high degree of optimization, but is a time-consuming and tedious method. Additionally, this is prone to human error. We used the Software Development Kit (SDK) of Octopus Reconstruction to develop a framework to automate this process. This framework allows for setting the optimization parameters determined using the Octopus Reconstruction GUI, hence the reconstruction quality can remain similar.

In this presentation, we present the methods used for this automation in the context of a study for rheumatology research where a large number of mouse hind legs and knees were scanned at UGCT. Both the developments made to enable stacked scanning and the challenges and solutions in the framework for automated reconstruction will be presented.

(113) Evaluation of the absorbed dose in X-ray microtomography

*A. DE MUYNCK[1], S. BONTE[1], J. DHAENE[1], M. DIERICK[1], K. BACHER[2], L. VAN HOOREBEKE[1]
amelie.demuynck@ugent.be

1 UGCT - Department of Physics and Astronomy, Ghent University, Proeftuinstraat 86, 9000 Gent, Belgium
2 Department of Basic Medical Sciences, Division of Medical Physics-Gent, Ghent University, Ghent, Belgium

A drawback of X-ray imaging is the deposition of a radiation dose in the object being imaged. For medical applications, it is important to quantify this dose, because it can be harmful to the patients' health. In comparison to medical scans, micro-CT scans have a much higher resolution, which typically gives rise to a higher dose in the scanned object. Next to a higher resolution, micro-CT scanners have more degrees of freedom than medical CT scanners. In medical CT, the scan geometry is nearly always the same. The patient is placed between an X-ray source and a detector, which rotate simultaneously around the patient. The typical degrees of freedom are the tube voltage, tube power, collimation and filtration. In most micro-CT applications, the sample rotates between the source and detector. In modern systems, both the source to object distance (SOD) and source to detector distance (SDD) can be varied independently and are additional degrees of freedom, as well as the scan time, the type of source and the type of detector. Furthermore, micro-CT can be used in a large number of research domains, and the objects under investigation can vary strongly in size and composition. Both the extra degrees of freedom and the variety of samples make standardized dosimetry tests very difficult to define and perform.

Due to the differences between micro-CT and medical CT, the standardized dosimetry calculations and measurements of medical applications cannot be applied in micro-CT scans. An exception of course is small animal micro-CT scanners, which can be seen as mini medical CT scanners in which the animals, mostly rodents, are scanned alive and receive a radiation dose during the scan. Many studies have measured or simulated the absorbed dose for small animal CT. In contrast, for practically all other micro-CT scan applications very little information is available in literature about dose deposition in the samples. Sometimes, for non-living samples such as metal objects, the dose is less important, because the limited dose involved in laboratory-based micro-CT will not affect the sample. However, some samples are radiation sensitive, such as minerals of which the colour can change due to radiation or plants which need to be examined several times during growth. Although the plants do not die, they can stop growing after a single scan. These two examples prove that it can be important to know the exact dose (or at least an estimate) that the sample under investigation will obtain during the total scan time.

The aim of this study is to examine the absorbed dose in lab-based micro-CT. The dose is measured using an ionisation chamber during different scan protocols. These scans are also simulated using two different simulation programs. The first program is BEAMnrc, a Monte-Carlo based simulation tool, whereas the second program is the in-house developed set-up optimizer with which the absorbed dose can be estimated. This GPU-based program is based on the law of Lambert-Beer to determine the total attenuation. The results describe the accuracy of

simulations for fast dose estimation prior to scanning. This research is performed at HECTOR (Masschaele et al., 2013), one of the scanners at the 'Centre for X-ray Tomography' of Ghent University (UGCT; www.ugct.ugent.be). UGCT is a research facility specialized in high resolution X-ray computed tomography, where several home built modular micro- and nano-CT scanners are in use.

References :

HECTOR: A 240kV micro-CT setup optimized for research, B. Masschaele, M. Dierick, D. V. Loo, M. N. Boone, L. Brabant, E. Pauwels, V. Cnudde and L. V. Hoorebeke, Journal of Physics: Conference Series;463 (1), p. 012012

(138) Application of Micro/Nano-CT to material characterization for industrial R&D using a very versatile tomography system

*A. SINGHAL
singhal@ge.com

[1] General Electric Global Research Center, Niskayuna, NY, USA

Micro-computed X-ray tomography has gained increasing importance in the field of 3D materials characterization and inspection because of its non-destructive nature. The CT data is used to generate 3D views of the internal structure, which would otherwise be obtained only destructively. State-of-the-art laboratory-based Micro-CT X-ray tube-based systems, although suffering from some limitations, are now at par with synchrotron-based tomography. The measurement speed and quality of the data obtained has resulted in this technique being widely used in the vast area of materials science. In this talk, I will describe how Micro/Nano-CT is being used for materials characterization by showing examples of several materials which are of interest to GE. The tomography system used here is the vtomex M300 micro/nano-CT (GE Sensing and Inspection Technologies), which has a 300kVp micro-focus source and a 180kVp nano-focus source. The dual tube configuration makes this is a very verstalie system, and provides spatial resolution ranging from sub-micron level to about 150μm, allowing a wide variety of material systems, and parts of various sizes to be imaged.

First, I will talk about Nickel-base superalloys, a material system primarily used for aircraft engine blades. These blades are subjected to cyclic loading during the gas-turbine operation. The microfocus tube of the vtomex M 300 was used to image test specimens of this material. The x-ray beam parameters were optimized to achieve a high resolution of 11 μm. Such high resolution is difficult to achieve for a material of this high density since the X-ray tube power needed to penetrate these materials is rather high, which is often accompanied by a trade-off in spatial resolution. I will discuss how CT serves as a valuable tool to locate and measure the cracks that form as a result of this mechanical loading, and analyze their morphology. Such measurements are difficicult to do by traditional metallography techniques because of ambiguity in the location of the cut sections with respect to the deepest part of the cracks. I will also show how the lab micro-CT images on these specimens compare with those obtained using synchrotron tomography at the ESRF.

Second, I will discuss the imaging of Oil Sands Tailings. Tailings are generated as a waste byproduct from the oil sands extraction processes used in mining operations. Tailings consist of natural minerals, clay, residual bitumen and water. Tailings reduction operations, currently underway, include methods to speed up the transition of large ponds, where tailings are stored, into reclaimed land. The nanofocus tube of the vtomex M 300 was used to study the microstructural evolution of tailings for various mixing parameters during the addition of a flocculant. A unique feature of this system is that the X-ray detector of this system translates horizontally on rails, thus doubling its field of view. This enables the imaging of wide objects at high magnification. A novel method of imaging these specimens was developed whereby liquid specimens were imaged in a frozen state using a CT cooling stage. A high resolution of 5 μm was achieved for these specimens. The pore size distribution in the tailings was compared for the various mixing parameters of the flocculant, to obtain a better understanding of the flocculant addition.

Finally, I will discuss images of polymer-matrix composite specimens which are also used in jet engine components. I will show how both micro- and nano-focus tubes are used to study various length scales of this material system. The information from the CT images is used as feedback for fine-tuning the material processing steps and design of the composite architecture.

Session 103 - Interferometry

(003) Laser interactive 3D computer graphics

*J. B. BELLET[1], I. BERECHET[2], S. BERECHET[2], G. BERGINC[3], G. RIGAUD[1]
jean-baptiste.bellet@univ-lorraine.fr

1 Université de Lorraine, Institut Elie Cartan de Lorraine, UMR 7502, Ile du Saulcy, 57045 Metz Cedex 1, France
2 Société SISPIA, 18, Allée Henri Dunant, 94300 Vincennes, France
3 Thales Optronique, 2, Avenue Gay Lussac CS 90502, 78995 Elancourt Cedex, France

A non-conventional optical imaging technic of three-dimensional active laser imaging has emerged *[Berginc, Jouffroy, 2009]*. A scene is illuminated by a laser source, in the visible or near-infrared band (500-2200 nm). At the same time, a high pixel density detector collects the reflected radiation. Such a record provides a high-resolution image with a large dynamic range, and can be obtained in various experimental conditions: day, night, sun, fog,... Even better, combining a set of laser images provides a 3D reconstruction of the scene. Such a laser system could be applied in many areas, such as surveillance or robotic vision. New scientific and industrial challenges have arisen from laser imagery, including the need of mathematical algorithms and dedicated visualization tools. Concerning the algorithm, Computerized Tomography has been extended to 3D laser imaging in *[Berginc, Jouffroy, 2009-2011]*: the FDK algorithm maps a set of 2D laser images to a 3D volume which represents the scene. Numerical results show that the highest values in such a computed volume are features of the scene.

One of the challenges is mathematical. Filtered Back Projections, such as the FDK algorithm, are designed to invert Radon-kind transforms from transmission tomography. Since laser measurements result mainly from reflections on opaque surfaces, laser imaging extends the validity of FBP from transmission to reflection. Is there a mathematical proof? In this talk we proove that FBP of reflection data is equal to FBP of the deduced transmission data that are introduced in *[Knight* et al.*, 1989]*. The last part of this talk is devoted to visualization of laser FDK volumes. Since the voxels of interest are the most intense ones, the Maximum Intensity Projection *[Wallis, Miller, 1991]* is emphasized. A software has been developed in CUDA C to compute fastly the FDK volume on a GPU, and to compute/display interactively its MIPs. It enables virtual displacements in the scene in real-time; also objects of interest can be located, extracted and recognized *[Berechet* et al.*, 2014]*. This laser interactive 3D computer graphics approach is finally shown to be relevant on real images of a complex scene: vehicle under branches. The car and the branches are both recognizable:

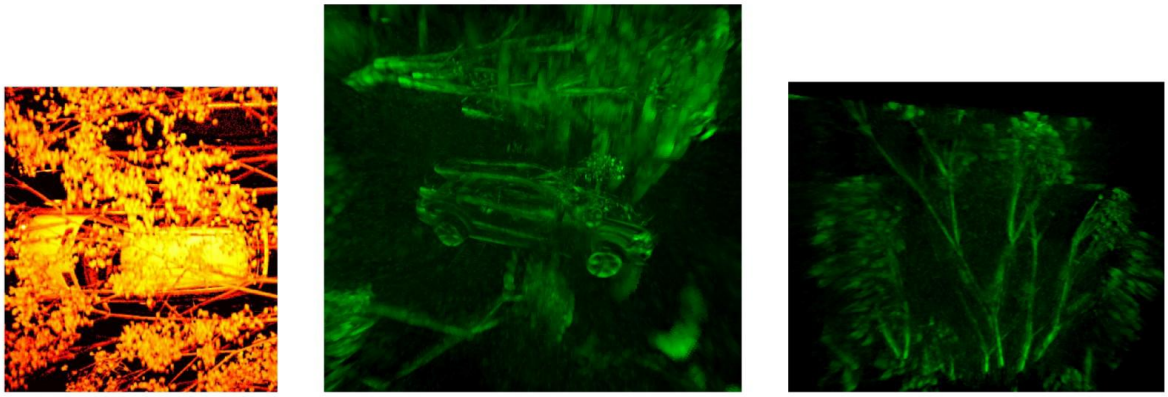

Figure: from left to right, real laser image (source: Thales), FDK volume, interactively extracted foliage.

References :
Berginc, G. and Jouffroy, M., *Simulation of 3D laser systems*, In Geoscience and Remote Sensing Symposium, IEEE International, IGARSS 2009, volume 2, pages 440—444, 2009.
Berginc, G. and Jouffroy, M., *Optronic system and method dedicated to identification for formulating three-dimensional images*, US patent 20110254924 A1, European patent 2333481 A1, FR 09 05720 B1, Nov. 11, 2009.
Berginc, G. and Jouffroy, M., *Simulation of 3D laser imaging*, PIERS Online 6(5), 415-419, 2010.
Berginc, G. and Jouffroy, M., *3D laser imaging*, PIERS Online 7(5), 411-415, 2011.
Knight, F., Kulkarni, S., Marino, R., and Parker, J., *Tomographic Techniques Applied to Laser Radar Reflective Measurements*, Lincoln Laboratory Journal, 2(2), 1989.
Wallis, J., and Miller, T., *Three-Dimensionnal Display in Nuclear Medicine and Radiology*, The Journal of Nuclear Medicine, 1991.
Berechet, S., Berginc, G., Bellet, J.-B., et Berechet, I., *Procédé d'identification et de discrimination par imagerie 3D d'objets dans une scène complexe*, Demande de brevet, 2014.
Ackowledgements: This work has been partially supported by the *DatDriv3D+* project, which is sponsored by the French Ministry of Economy: Directorate General of Competitiveness, Industry and Services; this project is part of program RAPID implemented by French Directorate General of Armament.

(079) A Study on the hydration processes in cementitious material based on X-ray dark-field Imaging

*F. PRADE[1], F. MALM[2], C. GROSSE[2], F. PFEIFFER[1]
friedrich.prade@ph.tum.de

1 Lehrstuhl für Biomedizinische Physik, Physik-Department & Institut für Medizintechnik, Technische Universität München, 85748 Garching, Germany
2 Lehrstuhl für Zerstörungsfreie Prüfung, Centrum Baustoffe und Materialprüfung, Technische Universität München, 81245 München
3 Empa, Swiss Federal Laboratories for Materials Science and Technology, Dübendorf 8600, Switzerland

In grating-based X-ray phase-contrast imaging three different contrast channels can be used in order to study complementary sample parameters. It has been shown that the dark-field contrast originates from X-ray scattering caused by unreasolvable microstructures within the sample [1]. In our work we utilized this effect to study the microstructural development in a cementitious material. The hardening of cementitious materials is driven by the development of crystalline structures which are formed due to the hydration of the dissolved base material. In the case of industrial cement this base material consists of a powder which contains particles with a size of 1-100 µm. To study the hydration process of this material we measured the evolution of the dark-field signal during the first 48 hours after the samples were prepared. Our results demonstrate that the hardening of the cement leads to a strong decrease in the dark-field signal [2]. Furthermore the time-resolved dark-field signal showed a strong correlation with ultrasound velocity measurements on the same material, thus indicating that the dark-field indeed detects changes within the microstructure of the cement.

Based on this finding we further tested our system for the detectability of the influence of temperature and admixtures on the hardening of the cement. For the temperature experiments our results showed that an acceleration and deceleration of the process caused by heating and cooling of the sample respectively can be spatially resolved by the time evolution of the dark-field signal. This result was expected since the chemical reactions within the sample and the diffusion of the material depends on the local temperature within the sample.

Further on, we tested limestone and quartz particles as an admixture to the cement. While for the quartz particles no influence on the dark-field signal was detected, we observed a change in the time evolution of the signal localized at the position of limestones of a certain type. The next challenging step is to perform several dark-field tomography scans during the hardening of cement to examine if this effect occurs just within the limestone itself or in the the vicinity of the limestone.In conclusion we demonstrate a new approach to study the hardening of cementitious materials with grating-based X-ray dark-field imaging and the possibility to test the influence of environmental parameters and admixtures on this process.

References :
1 Pfeiffer et al, Nature Materials, 2008.
2 Prade et al., submmitted to Cement and Concrete Research, 2014.

(103) Biomedical and materials science applications of grating-based phase-contrast imaging using synchrotron and conventional X-ray sources

*J. HERZEN[1], M. WILLNER[1], L. BIRNBACHER[1], M. VIERMETZ[1], K. SCHERER[1], F. PRADE[1], A. SARAPATA[1], A. FINGERLE[2], P. NOËL[2], E. RUMMENY[2], H. HETTERICH[3], T. SAAM[3], M. REISER[3], F. PFEIFFER[1]
julia.herzen@tum.de

[1] Department of Physics & Institute for Medical Engineering, Technische Universität München, Germany
[2] Department of Radiology, Klinikum rechts der Isar, Technische Universität München, Munich, Germany
[3] Department of Clinical Radiology, Ludwig-Maximilians-Universität München, Germany

In the last decade, X-ray phase-contrast imaging has been widely used to enhance the contrast for weakly absorbing materials, as for example in biological soft tissue. The extendibility to conventional polychromatic X-ray sources opened this modality to an even broader community. The most interesting aspect is the multimodality of the information provided by phase-contrast methods. It has the potential to improve clinical diagnostic as well as material characterization in non-destructive testing [Fingerle2014, Hetterich2014, Yang2014].

In this work we studied the multimodality of the grating-based X-ray phase-contrast method for a variety of applications from biomedical imaging to materials science. Its three signals – the attenuation, the phase-contrast and the dark-field signal – allow extracting complementary information on the objects inner structure from one single measurement. Here, the information gain using this imaging method at different length scales will be demonstrated for various human diseases and for materials analysis. Our results indicate that the combination of the signals can even help visualizing microstructural changes in two-dimensional radiographies avioding more time-consuming 3D tomography aquisitions.

References :
Fingerle AA, Willner M, Herzen J, Noël PB, and Pfeiffer F. „Quantitative x-ray phase-contrast computed tomography of simulated cystic kidney lesions – an in vitro phantom study“, Radiology 272(3) (2014), p. 739-48.
Hetterich H, Willner M, Fill S, Herzen J, Bamberg F, Hipp A, Schueller U, Adam-Neumaier S, Wirth S, Reiser M, Pfeiffer F, and Saam T. „X-Ray Phase-Contrast Computed Tomography: Qualitative and Quantitative Evaluation of Atherosclerotic Carotid Plaque“, Radiology 271(4) (2014), pp. 870-878.
Yang F, Prade F, Giffa M, Jerjen I, Di Bella C, Herzen J, Sarapata A, Pfeiffer F, and Lura P. „Dark-field X-ray imaging of unsaturated water transport in porous materials “,Applied Physics Letters 105 (2014), 154105-1-5.

(143) Grating based differential phase contrast imaging of an interpenetrating AlSi12/Al2O3 metal matrix composite

*J. MAISENBACHER[1], F. PRADE[2], J. GIBMEIER[1,] F. PFEIFFER[2]
jens.maisenbacher@kit.edu

[1] Institute for Applied Materials (IAM-WK), Karlsruhe Institute for Technology, 76131 Karlsruhe, Germany
[2] Physics Department (E17), Technische Universität München, 85748 Garching, Germany

Differential phase and dark field contrast imaging using a Talbot-Lau interferometer and a lab source is a well-known tool for investigations in the medical sector using soft X-rays. In recent time, also several possible applications for problems in material science have been shown, i.e. crack detection and the analysis of pore and or fibre orientations. While those results where mainly obtained using dark field contrast, a current investigation of metal-matrix / ceramics composites has shown a profitable application for phase contrast analysis. A three grating setup using a micro focus tube was used to obtain tomographic data in differential phase contrast for an interpenetrating AlSi12/Al_2O_3 metal-matrix composite.

The composite was fabricated by squeeze-casting AlSi12 melt in an open porous preform made by freeze-casting and drying of alumina suspension. Such composites exhibit a complex microstructure composed of lamellar domains as exhibited in the investigated sample. Knowledge about the 3D appearance of the microstructure is important with respect to the comprehension and the modelling of elastic-plastic deformation and internal load transfer in interpenetrating poly domain metal-matrix / ceramic composites. An investigation of the 3D structure using absorption based computed tomography so far did not yield satisfying results due to similar absorption properties of the constituent phases. Until now, the necessary characterisations of the 3D structure were carried out using (2D-)metallographic methods and making an assumption of the continuation of the structure in depth direction. However, this approach does not take into account connecting structures (sintering bridges) between the lamellae and therefore cannot yield a closing result. Additionally, explicit knowledge of the ceramics-matrix structures are needed in order to obtain effective, mechanical parameters such as Young's modulus and Poisson number. In this respect, interlamellar spacings, the lamellar orientation of individual ceramic domains and the form and distribution of sintering bridges are of particular interest.

The detailed 3D microstructure appearance of interpenetrating poly domain metal matrix AlSi12/Al_2O_3 composites was successfully provided by lab source differential phase contrast imaging.

(165) Single-grating interferometer for high-resolution phase-contrast imaging at synchrotron radiation sources

*A. HIPP[1], J. HERZEN[2], I. GREVING[1], J. U. HAMMEL[1], P. LYTAEV[1], A. SCHREYER[1], F. BECKMANN[1]
alexander.hipp@hzg.de

[1] Helmholtz-Zentrum Geesthacht, Max-Planck-Strasse 1, Geesthacht, Germany
[2] Technische Universität München, James-Frank Strasse 1, Garching, Germany

Phase-contrast imaging has proven to be a valuable tool when investigating weak absorbing material like soft tissue, due to its increased contrast compared to conventional absorption-contrast imaging. The most common type of grating interferometer consists of two gratings, a phase grating and an analyzer grating. Although a two-grating interferometer comes with a high sensitivity its performance is mainly restricted by the available aspect ratio of the analyzer-grating structres. The period of these structures (state of the art 2.4 µm) has to be smaller then the used pixel size and have to be highly absorbing which strongly limits the usable energy range.

In comparison to this, a single-grating interferometer comes with several advantages: The absence of an analyzer grating increases the photon flux at the detector plane by almost a factor of two and also allows to use this type of interferometer at any energy. Additionally, the setup itself is more stable and easy adjustable. With a single-grating interferometer it is also possible to use two different modes of phase-retrieval. The so-called stepping approach and the singe-shot or fringe analysis approach. This allows to use the same interferometer for high-resolution phase-contrast imaging and for very fast measurements.

Main requirement for this type of setup is a detector system with a high spatial resolution, that allows to resolve the interference pattern directly. The microtomography endstation at the beamline P05 is operated by the Helmholtz-Zentrum Geesthacht at the synchrotron radiation storage ring PETRA 3 at DESY, Hamburg, Germany. The imaging detector consists of a CCD-camera and a magnifying optics, which results in an effective pixel size between 0.3 µm and 2.4 µm. This is an ideal basis for high-resolution phase-contrast imaging using a single-grating interferometer.

Here we will present our investigations of a single-grating interferometer based on simulations. Focus of these calculations is on the reachable spatial resolution, depending on the grating period and the effective pixel size, as well as on the sensitivity of the setup. Additionally, we will prove the usability of the interferometer for high-resolution phase-contrast measurements with first experimental results obtained at the Imaging Beamline P05.

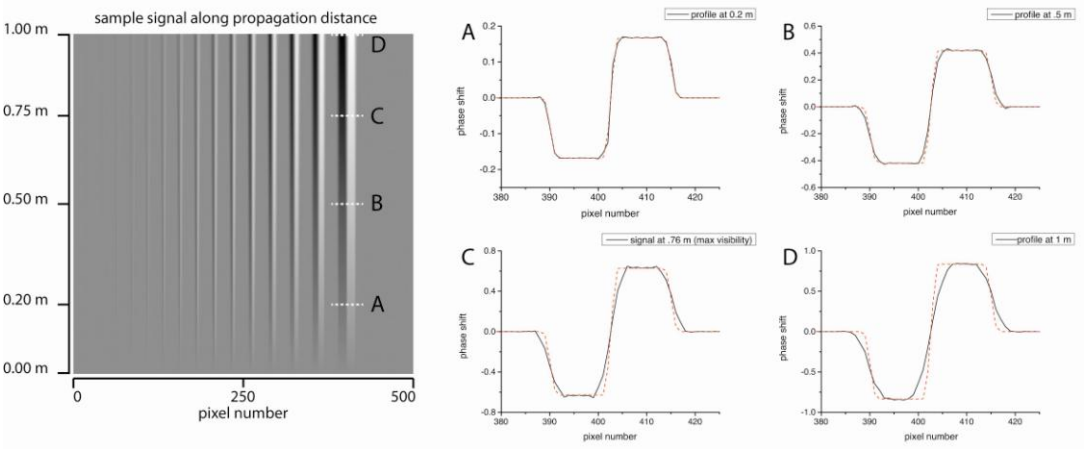

Figure 1. The image shows the simulated projected profile of the test sample along the propagation distance. The test sample consists of several PMMA rods with a squared cross-section sized between 1 µm and 60 µm. The phase-projection was retrieved from a stepping-scan with 5 steps and with a grating period of 10 µm. Structures below 5 µm are detectable. The plotted profiles of the largest rod at different distances (A,B,C,D) show significant blurring of the edges already at the 1st fractional Talbot distance (C). At short distances (A, B) the projected profile is in very good agreement with the expected signal (red dashed curve).

(182) Grating-based X-ray phase-contrast imaging at PETRA III

*A. HIPP[1], F. BECKMANN[1], I. GREVING[1], J. U. HAMMEL[1], P. LYTAEV[1], A. SCHREYER[1], J. HERZEN[2]
alexander.hipp@hzg.de

[1] Helmholtz-Zentrum Geesthacht, Max-Planck-Strasse 1, Geesthacht, Germany
[2] Technische Universität München, James-Frank Strasse 1, Garching, Germany

Conventional absorption-based imaging often lacks in good contrast at special applications like visualization of soft tissue or weak absorbing material in general. To overcome this limitation, several new X-ray phase-contrast imaging methods have been developed at synchrotron radiation facilities. Our aim was to establish the possibility of different phase-contrast imaging modalities at the Imaging Beamline (IBL, P05) and the High Energy Material Science beamline (HEMS, P07) at Petra III (DESY, Germany). We installed a grating interferometer (consisting of two gratings) with a fixed geometry usable at a large variety of without need of mechanical changes energies at the HEMS beamline. This has the strong advantage that measurements at different energies are directly comparable without any need for image registration.

We will present first results of a high-energy phantom sample obtained at different energies in the range from 33 up to 100 keV. Also first results on biomedical samples will be presented. By reference to those we will demonstrate the advantage of using a high-energy setup to avoid artifacts in the tomographic reconstruction usually occurring from phase-wrapping or too high absorbing samples.

(178) Construction and preliminary results from a 70 keV X-ray tomography beamline with a stepped-grating interferometer

K. HAM[1], W. W. JOHNSON[2], K. L. MATTHEWS II[2], G. KNAPP[3], J. YUAN[3], J. GE[4], A BROOKS[3], D. VAN LOO[5], *L. G. BUTLER[3]
higo.yohsuke.5z@kyoto-u.ac.jp

[1] CAMD, Louisiana State University, Baton Rouge, LA, 70806, USA
[2] Department of Physics & Astronomy, Louisiana State University, Baton Rouge, LA, 70803, USA
[3] Department of Chemistry, Louisiana State University, Baton Rouge, LA, 70803, USA
[4] CCT, Louisiana State University, Baton Rouge, LA, 70803, USA
[5] X-Ray Engineering (XRE) bvba, De Pintelaan 111, 9000 Gent, Belgium

An interferometer is being constructed at the LSU CAMD synchrotron, a 2nd generation synchrotron with a newly installed 7-Tesla, 11-pole wiggler and double crystal Laue monochromator. As this abstract is being written, the Laue monochromator is undergoing crystal alignment.

With 70 keV interferometry, new opportunities are opened in materials science imaging. We have experience since 2011 at the Advanced Photon Source with 20 to 35 keV interferometry, both stepped-grating and checkerboard single-shot interferometry. This low-energy interferometry has been extremely useful, but issues of phase wrap as well as excessive X-ray absorption in some samples have motivated the construction of the 70 keV system.

The APS work has also shown the sensitivity of X-ray interferometry to environmental factors, most notably, the susceptibility to temperature fluctuations. The LSU system is instrumented to measure temperature and vibrations during data collection. One of the team members has experience with the 4 km long optical interferometers used for the Laser Interferometer Gravitational-Wave Observatory (LIGO) project.

The three-grating, stepped-grating interferometer will be operated with the gratings oriented either horizontally or vertically with respect to the tomography sample. High precision rotation stages should enable rapid and reliable grating alignment. The two-directional differential phase contrast data will be used for improved tomography reconstructions. The two-directional dark-field images is expected to show anisotropic structure in materials science samples.

As is standard in some other facilities, the grating step motion will be with a piezoelectric translation stage. We will explore various step patterns with respect to the grating microfabrication support structure in an attempt to optimally sample the differential phase data with a minimum of interference from the support structure. The data analysis will use a new data analysis procedure.[1]

References :
[1] Marathe, S., L. Assoufid, X. Xiao, K. Ham, W. W. Johnson and L. G. Butler (2014). "Improved Algorithm for Processing Grating-Based Phase Contrast Interferometry Image Sets." Rev. Sci. Instrum. 85: art. no. 013704.

(195) *In situ* analysis of 3D printing processes using grating-based X-ray interferometry

*O. KIO[1], P. DAVIS[2], X. LI[3], J. GE[4], M. MATHIS[5], K. HAM[6], L. BUTLER[7]
okio1@tigers.lsu.edu

1 Department of Chemistry, College of Science, Louisiana State University
2 Department of Construction Management, College of Engineering, Louisiana State University
3 School of Electrical Engineering and Computer Science (EECS), and Center for Computation and Technology (CCT), Louisiana State University
4 Center for Computation and Technology (CCT), Louisiana State University
5 Comparative Biomedical Sciences, School of Veterinary Medicine, Louisiana State University
6 Center for Advanced Microstructures & Devices, Lousiana State University, 6980 Jefferson Hwy., Baton Rouge, LA 70806
7 Department of Chemistry, College of Science, Louisiana State University

In this research, the performances of 3D printers are evaluated through non-destructive analysis with a grating-based X-ray interferometer now under construction. The design parameters include operation with monochromatic X-rays at up to 70 keV with stepped-gratings at various Talbot orders and orientations (horizontal or vertical) of the linear gratings with respect to the sample.

The 70 keV interferometry is important to enable imaging of objects with highly absorbing materials—Al and Cu wiring—as well as weakly absorbing polymers. The phase contrast imaging technique is suitable for these mixtures as estimated X-ray phase shifts for a wide range of materials are more easily measured. The attenuation coefficients of metals and polymers span a wider range and lead to high absorption artifacts. The grating orientation with respect to printhead motion will be assessed for measurement of print speed defects and interlayer adhesion. The small angle scattering visible with dark-field imaging will also be assessed as a function of grating orientation. Several X-ray detectors are used with the interferometer; these will be evaluated for maximum frame rate possible with the synchrotron X-ray source, 7-Tesla wiggler, and high-throughput Laue monochromator.

Conventional X-ray absorption tomography has already been used to measure print quality with the Stanford Bunny, simple cubes, and algorithmic shapes (curved tubes following a quadratic equation). The print quality metrics have been assessed with the iterative closest point algorithm incorporated in Avizo version 9 as well as a new algorithm developed at LSU. With a low-cost 3D printer, errors in the Stanford Bunny are more noticeable for some features, for example, the ears, making a simple metric of printer performance complicated.

Session 201 - Advance in reconstruction algorithms

(012) Computed tomography from limited data using a robust discrete algebraic reconstruction technique

*X. ZHUGE[1], K. J. BATENBURG[1,2,3]

1 Centrum Wiskunde & Informatica (CWI), Science Park 123, 1098 XG Amsterdam, The Netherlands [email: zhuge@cwi.nl , joost.batenburg@cwi.nl]
2 Mathematical Institute, Leiden University, Niels Bohrweg 1, 2333 CA Leiden, The Netherlands
3 IMinds-Vision Lab, University of Antwerp (CDE), Universiteitsplein 1, Building N, 2610 Wilrijk, Antwerp, Belgium

Obtaining accurate reconstruction from a small number of projection images is of high importance in many tomography applications. Many advanced reconstruction techniques has been proposed in the past for limited data problems. Most of them achieve such goal by exploiting the prior information we have on the object under imaging. For example, it has been shown that if the object has rather sparse boundaries, significantly improved reconstructions can be obtained by applying the total variation minimization technique (Beck and Teboulle, 2009). In another type of problem, the object under test consists of only a few different materials, each produces an approximately constant gray value in the reconstructed image. By incorporating this knowledge as prior information, discrete tomography (Batenburg, 2005) can produce superior reconstructions using significantly less data comparing to conventional reconstruction methods such as the filtered backprojection (FBP).

Discrete Algebraic Reconstruction Technique (DART) is one of such algorithm that utilizes the discrete nature of the object. Assuming the gray values are known, DART alternates iteratively between discretization steps of segmentation based on gray values, and continuous steps of reconstruction on the boundary of segmented image (Batenburg and Sijbers, 2011). DART has been successfully applied for reconstructing samples from applications in CT (Van Aarle, et al., 2014) and ET (Van Aert, Batenburg, et al., 2011). Despite its success in many cases, DART encounter problems when the projection data contain noise. The fact that DART imposes strict constrains on the boundary pixels during iterations leads to noises being spread over these boundary pixels. As a result, the reconstruction of the boundary regions becomes less accurate in the results from DART under noisy conditions.

The main reason behind DART's problem of dealing with noisy projections is that the algorithm pushes abruptly the pixels toward discrete gray values in each iteration and fix the flat regions of the segmented image assuming these pixels are accurately reconstructed. This leads to spread of noise and errors in the boundary pixels. In this paper, we propose a robust discrete algebraic reconstruction technique (R-DART) which is performs more consistently against noise and mismatches than the original DART.

In the Robust DART, modifications are made on the procedure of algorithm. Firstly, the hard segmentation step is replaced with a soft segmentation function where the pixels are gently pushes toward the specified gray values. Second, the pixels that are greatly altered during the soft segmentation step are selected as free pixels, in contrast to the previous choice of boundary pixels. By smoothly steering the solution toward discrete gray values, the modified DART algorithm is less sensitive to noise and mismatches in the data than the original DART implementation.

Experimental μCT results show that the proposed algorithm yields accurate reconstructions under practical conditions. Figure 1 shows the reconstruction of a polyurethane foam taken with a SkyScan 1172 μCT scanner. As we compare the results of a single slice of the full 3D reconstruction from FBP and the proposed algorithm, it is clear that our modified DART is able to maintain a high level of accuracy even using only 25 projections, in contrast to the significantly degraded results from FBP. Complete numerical and experimental studies will be included in the final paper.

Acknowledgement
This work is supported in part by the Technology Foundation STW (Veni grant No. 13610), the Netherlands Organization for Scientific Research (NWO) (Vidi grant No. 639-072-005) and ExxonMobil Chemical. We would like to thank Prof. Jan Sijbers from iMinds - Vision Lab at the University of Antwerp for providing the μCT datasets. Networking support was provided by the EXTREMA COST Action MP1207.

(a)

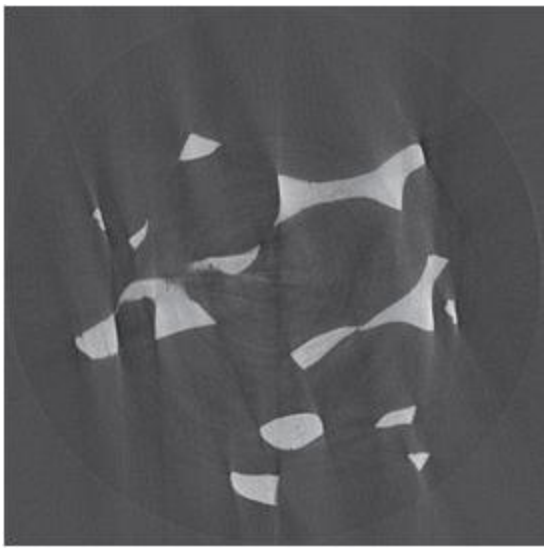

(b)

(c)

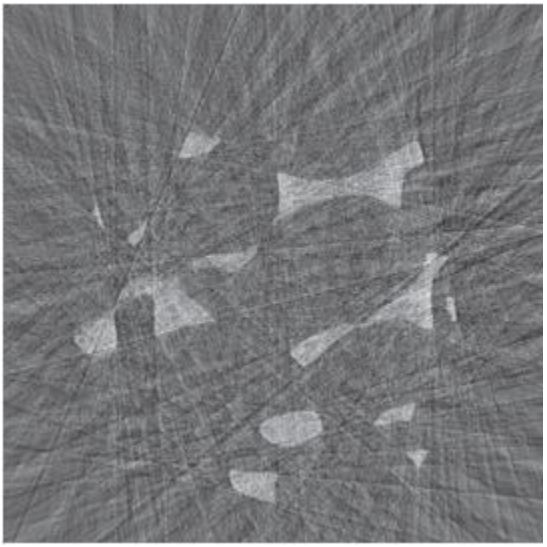

(d)

Figure 1: Comparison of reconstructions between FBP and the Robust DART using 500 and 25 projection images. (a) FBP using 500 projections, (b) Modified DART using 500 projections, (c) FBP using 25 projections, (d) Modified DART using 25 projections.

References :
Beck, A., and Teboulle, M. (2009). A Fast Iterative Shrinkage-Thresholding Algorithm for Linear Inverse Problems. SIAM Journal on Imaging Sciences 2, 183–202.
Batenburg, K.J. (2005). An evolutionary algorithm for discrete tomography, Discrete Appl. Math. 151 36-54.
Batenburg, K.J., Sijbers, J. (2011). DART: a practical reconstruction algorithm for discrete tomography, IEEE Trans. Image Process., vol. 20, no. 9, pp. 2542-2553.
Van Aarle, W., Batenburg, K.J., van Gompel, G., van de Casteele, E., Sijbers, J. (2014). Super-Resolution for Computed Tomography Based on Discrete Tomography, IEEE Trans. Image Process., vol. 23, pp. 1181-1193.
Van Aert, S., Batenburg, K.J., Rossell, M. D., Erni, R., and Van Tendeloo, G. (2011). Threedimensional atomic imaging of crystalline nanoparticles, Nature, 470, 374-377.

(148) A new method for measuring grain displacements in granular materials by X-ray computed tomography

*M. H. KHALILI[1], S. BRISARD[1], M. BORNERT[1], J. M. PEREIRA[1], M. VANDAMME[1], J. N. ROUX[1]
mohamed-hassan.khalili@enpc.fr

[1] Université Paris-Est, Laboratoire Navier (UMR 8205), CNRS, ENPC, IFSTTAR, F-77455 Marne-la-Vallée

We aim to measure the individual grain displacements in a granular material under constant load (creep). X-ray computed tomography imaging provides images of the granular medium microstructure during the experiment, and discrete volumetric image correlation (DV-DIC) [1] allows the determination of the grain individual rigid body motion from the reconstructed tomography images. However, for short-term creep, and time-resolved experiments in general, the sample evolutions can be very quick and occur before the tomography image acquisition is complete. Moreover, during long-term creep, the displacements of grains might be too tiny with respect to the accuracy of DV-DIC. This constitutes a serious limitation of standard experimental procedures for the investigation of the micromechanics of the creep of granular media at grain scale.

We present a new method for measuring grain displacements, that overcomes the above mentioned limitation. Indeed, in a granular material, assuming no fragmentation occurs, each grain undergoes a rigid body motion. Therefore, the displacement field reduces to a set of six degrees of freedom per grain. This suggests that the information contained in a full set of projections (necessary to perform an accurate 3D reconstruction) is excessively redundant for the determination of the grain displacements. Our method requires only few projections of the sample at its current state, thus reducing dramatically the acquisition time.

Displacements are estimated from the projections directly, without 3D reconstruction.

Our method is formulated as an inverse problem. A forward model based on Beer-Lambert's law is developed to efficiently perform numerical projections. The grain displacements are estimated by fitting the numerical projections to experimental projections of the current state of the sample. We also study the sensitivity of the estimated displacements to image noise, both numerically and through a theoretical model which highlights the influence of the setup parameters on the measurements. This model might be used as a tool to tune the experiment to reach the expected accuracy.

The method has been validated and its accuracy assessed against 2D numerical experiments on virtual microstructures.

When no noise is present in the projections, the applied displacements are retrieved exactly. Moreover, the error levels predicted by the theoretical model for various image noise levels are in agreement with the numerical results. Indeed, an accuracy similar to standard DV-DIC procedure is obtained with a significantly reduced number of projections; alternatively, higher accuracy is obtained when a conventional number of projections is used. An extension to the full 3D case, for both parallel (synchrotron tomography) and cone beam (laboratory setup) systems, is currently underway and will allow us to apply this methodology to real tests in a near future.

References :
[1] S. Hall, M. Bornert, J. Desrues, Y. Pannier, N. Lenoir, C. Viggiani and P. Bésuelle. Discrete and continuum analysis of localised deformation in sand using X-ray μCT and volumetric digital image correlation. Géotechnique (2010), 60(5), 315–322.

(158) Assessment and reduction of the scatter effects in an industrial 300kV micro-focus CT system

*M. PLAMONDON[1], P. SCHUETZ[2], T. LUETHI[1], J. HOFMANN[1], A. FLISCH[1]
mathieu.plamondon@empa.ch

[1] Empa, Swiss Federal Laboratories for Materials Science and Technology, Dübendorf, Switzerland
[2] Lucern University of Applied Sciences and Arts, Horw, Switzerland

High energetic X-ray photons are scattered in both the object and components of a computed tomography (CT) system and cause both artefacts and a loss in effective dynamic range. In this contribution, we investigate the influence of individual CT components on scattered radiation registered on the detector using Monte Carlo (MC) simulations. This assessment is performed on an upgraded system with a 300kV micro-focus source (Finetec FOMR300.0) and flat-panel detector (Perkin-Elmer XRD 1621 AN14 ES). A detailed GEANT4[1)] simulation framework of the source, detector and hall has been developed for this purpose. Applying the recipe from a previous study[2)], a 75% reduction of the hall scatter, i.e. the intensity of radiation scattered in the hall and detected on the flat panel, is estimated by the use of specially designed lined walls. Minimized in such a way by hardware modifications, the signal intensity of the hall scatter I_{hall} is kept below 0.5% of the flat-field level I_{flat}. Simple modifications to the detector housing would also allow reducing the internal detector scatter I_{det} by a factor 3 to less than 3% of I_{flat}. The strengths of these two scatter contributions, respectively $T_{hall}=I_{hall}/I_{flat}$ and $T_{det}=I_{det}/I_{flat}$, are expected to show weak spatial variations and can be characterized experimentally with in-situ measurements. The measured transmission T_{meas} is then decomposed in the following way

$$T_{meas} = \frac{I_{sig} + I_{obj+\mathrm{det}} + I_{hall}}{I_{flat} + I_{\mathrm{det}} + I_{hall}}$$

which leads to this expression to obtain the actual transmission signal T_{sig}:

$$T_{sig} = \frac{I_{sig}}{I_{flat}} = T_{meas} - \left(-T_{meas}\right)T_{hall} + T_{meas}T_{\mathrm{det}} - T_{obj+\mathrm{det}}$$

The last factor $T_{obj+det}$ depending on the complete object will typically dominate the other terms in the context of a 300 kV CT setup as illustrated in Figure 1. This example shows the marginal impact of the hall scatter (in blue) for moderately absorbing samples as well as the importance of the internal detector scattering (in green) if left at its current value of T_{det}=9%.

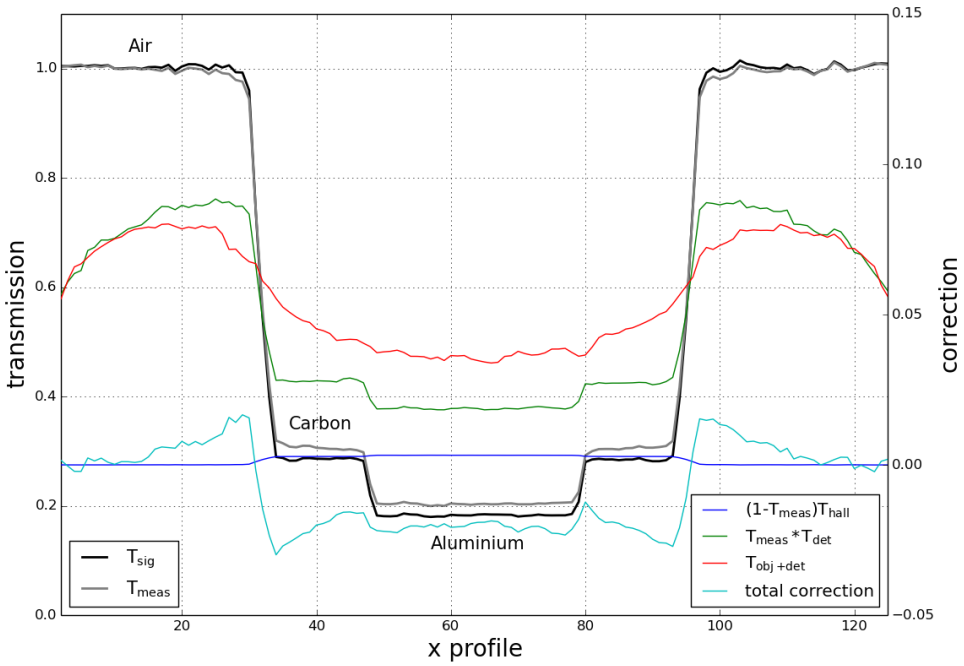

Figure 1 Illustrative example of the corrections applied to a given slice in the case of an object made of concentric cubes of carbon and aluminium.

In order to obtain an accurate assessment of $T_{obj+det}$, a correction scheme must take into account the scattering in both object and detector as well as the energy dependent detector response. The raw data from a CT measurement are first reconstructed with a conventional Feldkamp-Davis-Kress[3] algorithm. A simplified MC model is then presented, which allows to predict the object scatter from the reconstructed voxel model and subsequently correct this component. In this contribution, we show that the object scatter can be estimated in a sufficiently short time by swift combination of variance reduction techniques[4] and code parallelism. This indicates that the suggested algorithm is suitable for the integration into the workflow of an industrial CT appliance.

References :
IEEE Transactions on Nuclear Science 53 No. 1 (2006) 270-278.
Schütz, Philipp; Jerjen, I; Hofmann, J; Plamondon, M; Flisch, A & Sennhauser, U (2014). Correction algorithm for environmental scattering in industrial computed tomography. *NDT & E International,* 2014(64), 59-64.
L. A. Feldkamp, L. C. Davis, and J. W. Kress, *JOSA A*, Vol. 1, Issue 6, pp. 612-619 (1984).
Z Med Phys. 2014 Jun 24. pii: S0939-3889(14)00063-4. doi: 10.1016/j.zemedi.2014.04.001.

(163) Accurate measurements of features near the resolution limit of tomographic data: extension to heterogeneous matrix, multiple feature types, and shape determination

*R. A. KETCHAM[1], A. S. MOTE[1]
ketcham@jsg.utexas.edu

[1] Department of Geological Sciences, Jackson School of Geosciences, The University of Texas at Austin, Austin TX 78712, USA

In geological investigations utilizing X-ray computed tomography (XCT), the features of interest, such as trace phases, pores, and vesicles, are in many cases small compared to the data resolution. If at least one dimension of a feature subtends only a small number of voxels (generally, less than the point-spread function (PSF) width, as characterized by Ketcham et al. 2010 and Ketcham and Hildebrandt, 2014), then accurate segmentation and measurement is complicated by partial-volume and blurring effects. Typically, such features will appear relatively large compared to their true size, but their contrast with surrounding material will be diminished compared to larger instances of the same material. These complications can be addressed if one can make that simplifying assumption that the X-ray attenuation caused by the feature of interest is fully present in the CT data, but distributed over a larger volume.

If the "true" CT number of the material of interest can be ascertained, corresponding the the value it would achieve if unaffected by blurring, then the volume of a small feature can be accurately determined by summing the X-ray attenuation surplus or deficit associated with it relative to the surrounding matrix. This is demonstrated by scanning a series of gold particles of varying shapes and sizes at progressively lower resolution by surrounding them with progressively more quartz. Shape information is of course lost as resolution diminishes, but some can be recovered by only utilizing a subset of the voxels associated with the feature corresponding to its true volume. Orientation information can likewise be recovered, particularly when the long and/or short axis is distinct from the intermediate axis.

The measurement problem becomes yet more complicated if the matrix in which the features are located is heterogeneous or contaminated by image artifacts. This circumstance can be addressed by measuring the matrix in the area immediately surrounding each feature, and utilzing the local value when calculating the attenuation surplus or deficit associated with it. Typically, this local measurement can be done in the voxel annulus immediately beyond the region with CT numbers affected by the feature, which extends a half-PSF length from the feature true edge.

Another complication arises when there is more than one feature type of similar attenuation and size; for example, multiple small, high-attenuation trace phases are commonly present in geological samples. In this case the CT number data can become ambiguous, as it is a function of both material and size, and even potentially the surrounding material. Much of this ambiguity can be removed, and features correctly identified and measured, by plotting the maximum (or minimum) voxel value against total volume, or minimum best-fit ellipsoid axis if particles are

significantly non-equant. The larger particles will achieve the end-member CT-number values for their respoctive materials, and smaller particles have maximum CT numbers that extend from these end-members on a curved trend toward the origin, representing the progressive onset of blurring. Examples of two-component and three-component systems are given.

References :
Ketcham, R.A., and Hildebrandt, J. (2014) Characterizing, measuring, and utilizing the resolution of CT imagery for improved quantification of fine-scale features. Nuclear Instruments and Methods in Physics Research B, 324, 80-87.
Ketcham, R.A., Slottke, D.T., and Sharp, J.M.J. (2010) Three-dimensional measurement of fractures in heterogeneous materials using high-resolution X-ray CT. Geosphere, 6(5), 499-514.

(179) Material discrimination using dual energy computed tomography

*M. PAZIRESH[1], B. RECUR[1], G. MYERS[1], A. KINGSTON[1]
mahsa.paziresh@anu.edu.au

[1] Dept. Applied Mathematics, RSPE, ANU 6201, Australia

3D material discrimination enables more accurate modeling of the properties of imaged samples. For example in petrophysics, identifying Quartz from Feldspar or Calcite from Dolomite improves understanding of diagenesis, Geo-mechanical properties and modeling. Micro-Computed Tomography (μ-CT) provides higher spatial resolution and higher signal to noise ratio than other methods in determining the morphology or structure of samples.

Dual energy imaging techniques are being adopted for material discrimination and provide more information than conventional CT for medical, luggage screening and reservoir industry applications. Although single energy CT is applicable for discrimination of materials which have different attenuation coefficients, samples (e.g. rocks) can contain materials which have similar attenuation coefficients while their properties are different. Dual energy imaging can help material discrimination in this case because the attenuation coefficients may vary differently with energy.

In dual energy CT, images are captured at two distinct energy bands. There are several mechanisms by which X-rays interact with matter. The photoelectric effect dominates at lower energies, while Compton scattering is more prevalent at the intermediate energy range. Other mechanism are negligible in a typical micro-CT X-ray energy range of zero to 120 KeV. The material discrimination application of dual energy CT relies on the fact that Photoelectric absorption depends strongly on atomic number (Z) and Compton scattering is proportional to density (ρ) which are material characterization parameters. One can split the attenuation coefficient into two basis function to model these effects.

The two basis model has been used in various simplified forms (e.g., Alvarez 1976, Heismann 2002, Siddiqui 2003, Derzhi 2012). Alvarez (1976) simplifies his attenuation coefficient two basis model with polynomials. Siddiqui (2003) simplified two basis model with the assumption of two monochromatic energies. Derzhi (2012) applied a post-correction technique on siddiqui's method. Heismann (2002) quantitatively estimated density, as a weighted difference of attenuation coefficients at two distinct energies, and atomic number as non-linear functions of the ratio of dual energy attenuation coefficients.

In this presentation, we investigate the two basis model using an un-simplified form for material discrimination in our rock samples. This model in its full form can account for beam hardening effects. It needs some *a priori* information about spectra so we describe our spectra measurement and the appropriate corrections required (e.g., detector scintillator material conversion, heel effect correction, etc). The model also requires severalparameter values. We demonstrate parameter estimation for a given setup using a set of reference materials. Finally, we calculate the properties of constituent materials of rock sample images by applying the above estimations.

During presentation, we will show that proposed method is able to identify sample constituent materials from ρ and $\mathcal{Z}$ images even if the materials have similar attenuation coefficients. We will also demonstrate that the method reasonably well correct beam hardening artifacts in ρ and $\mathcal{Z}$ reconstructions. Finally, even-though the proposed full model requires precise knowledge of

spectra and reference materials, we will illustrate that our method outperforms state-of-the-art since estimated ρ and Z vary less than 5% from expected (See Table 1).

Material (Berea)	Estimated $\rho\,(gr/cm^3)$	Theoretical $\rho\,(gr/cm^3)$	Estimated Z	Theoretical Z
Quartz	2.7	2.6	12.4	11.8
Feldspar	2.6	2.6	13.8	13.4
Calcite	3.1	2.9	16	15.7

Table 1. Estimated material properties

References :
Alvarez, R. E. and Macovski, A. (1976). "Energy-selective reconstructions in x-ray computerised tomography," Physics in medicine and biology 21(5), 733.
Heismann, B., Leppert, J., and Stierstorfer, K. (2003). "Density and atomic number measurements with spectral x-ray attenuation method," Journal of Applied Physics 94(3), 2073–2079.
Siddiqui, S., Khamees, A., et al. (2004). "Dual-energy ct-scanning applications in rock characterization," SPE.
Derzhi, N. (2012). "Method for estimating effective atomic number and bulk density of rock samples using dual energy x-ray computed tomographic imaging," US Patent App. 13/527,660.

(198) Recent advances in X-ray Computed Tomography and potential impact for non-medical applications

P. DESPRÉS[1]
philippe.despres@phy.ulaval.ca

[1] Laval University, Québec, Qc. Canada

X-ray Computed Tomography (CT) did not change significantly since the advent of multisclice scanners and helical acquisitions. This technology nevertheless kept evolving at a steady pace and now offers features allowing innovative applications in medicine but also in other fields of research. This presentation will focus on three technological advances in CT that might have a significant impact in non-medical applications: advanced tomographic reconstructions, dual-energy CT and 4D applications.

From a computational perspective, CT image reconstruction can nowadays rely on larger processing resources. Massively parallel Graphics Processing Units (GPUs), for instance, can be used to offset the numerical burden of advanced reconstruction algorithms relying on complex physical models of image acquisition. These algorithms and models can potentially yield better images with fewer artifacts, thanks to a priori knowledge injected into the problem. Another promising research avenue is dual-energy CT, either with dual-tube or kV-switching systems. Dual-energy CT, in the context of non-destructive testing, can potentially improve material identification. Finally, sub-second full rotation of the X-ray tube allows time-resolved (4D) applications that are very useful in the study of dynamical systems. The current state and limitations of 4D gating in CT will be presented along with possible applications in non-destructive testing.

(061) Evaluation of phase correction algorithms outside the validity boundaries

*M. N. BOONE[1], L. VAN HOOREBEKE[1]
matthieu.boone@ugent.be

1 UGCT – Dept. Physics and Astronomy, Ghent University, Proeftuinstraat 86/N12, B-9000 Gent, Belgium

In recent years, high resolution X-ray CT (micro-CT) has gained importance in many research domains, including materials science. For low-density materials such as composites or organic materials, the attenuation of X-rays is relatively low, and the real part of the refractive index of materials can provide more image contrast. Several methods have been developed to measure this refractive index accurately, which however usually require highly coherent sources or X-ray optics such as gratings. However, as for visual light, the phase shift induced by the refractive index difference causes refraction, which can be visualized by beam propagation and is as such inherent to the imaging process.

After propagation (within certain limits), the phase shift results in an edge-enhancement effect which is superimposed over the attenuation signal. In the reconstruction process, this phase contrast effect yields artificial effects when left unprocessed. Although this edge enhancement can be beneficial for visual inspection, it often hinders proper analysis and can lead to false conclusions. To correct for or even exploit the phase contrast, several algorithms have been developed to cope with single-image in-line phase contrast data, each with specific advantages and disadvantages.

The methods discussed in this presentation are the Modified Bronnikov Algorithm (MBA), the Simultaneous Phase and Amplitude Retrieval (SPAR), the Bronnikov Aided Correction (BAC) and the Post-Processing Phase Correction (PPPC). The first three are implemented as pre-processing filters, operating on the projection data, the last one is a post-processing method, operating on the 3D reconstructed volume. They are all derived from an inversion of the Transport of Intensity Equation (TIE), which yields an upper limit for the propagation distance. Furthermore, it is known that these methods all require homogeneous objects in order to reconstruct both phase and attenuation information from only one propagation distance. The MBA method additionally requires a low-attenuating object.

In this presentation, the influence of a violation of one or more of these requirements is discussed. It is shown that MBA is very sensitive to remaining attenuation in the sample, resulting in a cupping effect. Despite being very similar, SPAR does not suffer from this cupping artefact and can be used for strongly attenuating samples as well. On the other hand, both are affected similarly by heterogeneity of a sample. In this case, the edge enhancement can not be completely compensated in some regions, and alternatively strong smoothing occurs. Similar effects occur for PPPC and BAC, although the latter is less prone to image smoothing.

Another parameter which has been investigated is the propagation distance. In synchrotron-based CT, the propagation distance can be chosen more or less arbitrarily, allowing for minimization or optimization of this parameter. In lab-based CT on the other hand, the propagation distance is linked to the geometric magnification and X-ray flux, hence it can not be altered drastically. As such, the propagation distance and consequently the validity of the TIE is investigated as well.

References :
If you want to add references, please use an author/date style.

(095) Effect of an initial solution in iterative reconstruction of dynamically changing objects

M. HEYNDRICKX[1], T. DE SCHRYVER[1], M. DIERICK[1], *M. N. BOONE[1], T. BULTREYS[2], L. VAN HOOREBEKE[1]
matthieu.boone@ugent.be

1 UGCT – Dept. Physics and Astronomy, Ghent University, Proeftuinstraat 86/N12, B-9000 Gent, Belgium
2 UGCT / PProgRess – Dept. Geology and Soil Science, Ghent University, Krijgslaan 281/S8, B-9000 Gent, Belgium

The Simultaneous Algebraic Reconstruction Technique (SART) is an iterative algorithm to reconstruct volumes from CT-scans (Beister *et al.,* 2012). An empty volume is initiated and improved by back-projecting the difference between a simulated projection of this (empty) initial solution and the measured projection at the same viewing angle. This is done for every measured projection. The resulting volume is then used in the next iteration step, where the projection/back projection process is repeated using the intermediate solution. After a number of iterations, the solution converges to a final reconstructed volume.

Instead of an empty volume, an initial solution can be used in the first step. This can be the reconstruction of an earlier scan of the same object or another volume resembling the one that's being reconstructed. An initial solution may improve the convergence speed and the quality of the resulting reconstruction (Brabant, 2013).

The SART-reconstruction using an initial solution is compared with the conventional SART-reconstruction using an empty volume as initial solution for a number of parameter values. Specifically, the projection angle, the relaxation factor, the number of projections, the number of iterations and the strength of the simulated noise are varied. Most work is performed using phantom data, where a slightly modified phantom version of the projected one is used as the initial solution. Because these are phantoms, the reconstruction can be compared with a ground truth to quantitatively evaluate the reconstruction. Two effects are investigated: when the initial phantom has a part that has a different attenuation coefficient or when it has a slightly different morphology. Both effects give rise to artefacts when the relaxation factor, the projection angle, the number of projections or the number of iterations is too low. Noise can obscure the artefacts if it is strong enough.

If the non-empty initial solution improves the reconstruction quality for a low number of projections, it may be used for the reconstruction of dynamic processes, where subsequent scans of a changing sample are acquired. Using only a small number of projections, even partial CT-scans can be reconstructed at an improved quality.

An example of such a dynamic process is fluid flow through porous media such as geomaterials. A high-quality scan of the dry sample is acquired before the dynamic process is initiated. This is reconstructed with conventional SART. The result is used as an initial solution for the scans acquired during the process. The fluid presumably follows the pores in this rock, further limiting the regions where the reconstruction can differ from the initial solution. Again, the result is compared with conventional SART to evaluate whether the initial solution is an improvement.

References :
Beister M., Kolditz D., Kalender W.A. 2012. *Iterative reconstruction methods in X-ray CT* Physica Medica 28, 94-108.
Brabant L. 2013 *Latest developments in the improvement and quantification of high resolution X-ray tomography data* UGent, http://hdl.handle.net/1854/LU-4193900.

(117) Semi-empirical beam-hardining correction of dense materials using a bio-medical scanner

*D. R. EDEY[1], S. I. POLLMANN[2], D. LORUSSO[2,4], M. DRANGOVA[2,5,6], R. L. FLEMMING[3], D. W. HOLDSWORTH[2,5,6]
dave.edey@utexas.edu

1 Department of Geological Sciences, University of Texas at Austin, Austin, TX, 78712-9000
2 Imaging Research Laboratories, Robarts Research Institute, Schulich School Of Medicine & Dentistry, Western University, 1151 Richmond Street North, London, ON, N6A 5B7
3 Department of Earth Sciences, Western University, 1151 Richmond St., London, ON, N6A 5B7
4 Department of Physiology and Pharmacology, Schulich School Of Medicine & Dentistry, Western University, 1151 Richmond St., London, ON, N6A 5C1
5 Department of Surgery; Schulich School of Medicine & Dentistry, Western University 1151 Richmond Street, London, ON, N6A 3K7
6 Department of Medical Biophysics; Schulich School of Medicine & Dentistry, Western University, 1151 Richmond Street, London, ON, N6A 3K7

Biomedical micro-computed tomography (micro-CT) scanners are the ideal machines to utilize in various material analysis; this is because they are: 1) more common than highenergy machines; 2) are installed at various university research centers; 3) exhibit high spatial resolution on small specimens; and 4) allow the specimen to remain stationary during imaging. Unfortunately, many biomedical scanners do not have an adequate dynamic range to study dense objects due to a lower peak voltage (90 – 120 kVp) when compared with industrial scanners (>200 kVp). Artifacts due to dense materials can lead to incorrect reconstructed signal levels in the interior of specimens, and can also lead to streak artifacts that obscure details both on the interior and exterior of the specimens, confounding analysis. The major sources of these errors include: beam hardening, an artifact due to the preferential removal of low- energy photons in a polyenergetic spectrum; photon scatter; and underranging, inadequate dynamic range manifested as inadequate recording of very dark signals.

We discuss a simple correction for X-ray beam hardening and scatter that can be readily applied to available biomedical scanners. The calibration data are acquired using materials of known composition and thickness at specific acquisition protocols. Two phantom materials were chosen: PMMA (Poly[methylmethacrylate]), due to its water-like radiodensity and tissue-level attenuation; and aluminum, to mimic dense objects like bone, silicate minerals, and other materials with similar electron densities. The correction takes the form of a semiempirical calibration algorithm that can be applied to X-ray transmission data. Numerical fits to the empirical calibration data are generated to produce a correction function that is able to linearize the log transmission CT data and a custom-written software routine corrected each transmission projection view in a pixel-by-pixel fashion, linearizing the transmission values from the previously observed values. The calibration phantoms are designed and manufactured in house. They are each a single object comprised of eight coaxial cylinders with diameters ranging from 4.5 mm to 60 mm. The calibrators are designed in an alternating step configuration to mimic the irregular nature of specimens, in an effort to simulate typical scatter profiles. Alternatively, many materials can be used to create various calibration phantoms for intended needs; for example, concrete forms of several thicknesses could be used to calibrate for scans of concrete cylinders. These calibration scans must be performed at the same acquisition parameters that the object is to be scanned, particularly with respect to kVp.

The proposed correction algorithm is described, implemented, and tested on two modern biomedical CT scanners. The fits are explored for two separate calibration materials and

evaluated for their ability to reduce or remove the cupping artifacts. This method results in aluminum as a single calibration material for all materials with similar or lower attenuation values to significantly reduce or remove signal intensity errors (i.e. cupping) that occur as a result of beam hardening artifacts. Results show that it is possible to determine an effective method of artifact correction for specified protocols using this implementation and reducing or removing artifacts (such as cupping and streaks) is possible.

This method is applied post data collection and therefore can be retroactively applied to data previously collected, as long as projection data are preserved. Here we show it is possible to obtain calibration data with a single projection using a novel alternating step calibration phantom that is constructed of a material that mimics the attenuation coefficient of the materials that require.

(140) A provenance management system for tomography data processing and visualization

*G. KNAPP[1], J. YUAN[2], L. BUTLER[3], J. GE[4]
gknapp1@tigers.lsu.edu

[1] Department of Mechanical Engineering, Louisiana State University – gknapp1@tigers.lsu.edu
[2] Department of Chemistry, Louisiana State University – jyuan4@tigers.lsu.edu
[3] Department of Chemistry, Louisiana State University – lbutler@lsu.edu
[4] Department of Chemistry, Louisiana State University – jinghuage@cct.lsu.edu

In computerized tomography the algorithms used for data processing are constantly evolving and improving. Each research group has its own preferred platforms, be it Python, Mathematica, or MATLAB scripts, which can make it hard to integrate someone else's code into your data processing pipeline. These factors can also make it difficult to recall, years later, how any given dataset was processed. Which algorithm was used? Which version of software?

Provenance management systems help to track the history of data processing. VisTrails, freeware developed at New York University, allows for the creation of modules that encompass each step of data processing and the creation of a history tree that tracks changes to the workflow as it is developed. Modules can call other programs, which can help integrate multiple pieces of software into a single workflow. The history tree allows for exploratory actions to be logged so that they can be easily returned to in the future. It is a great step towards making the development of tomography data processing more accessible and shareable.

Here we will showcase two workflows we developed that show the utility of the VisTrails software. The first is an X-ray grating interferometry dataset of a foraminifera gathered at the Advanced Photon Source beam line. The second is a collection of multi-energy (12 keV to 32 keV) scans of a burnt flame retardant/polymer blend. A definite need was noted for an active sample position control system to account for the sample consumption and motion out of the field of view.

The foraminifer data processing involves the evaluation of absorption, phase-contrast, and dark-field images from raw stepped-grating interferometry. The history tracking and visualization methods of VisTrails were useful in carrying out comparisons of various tomography reconstructions. It was also possible to integrate modules to export the dataset to a mobile visualization platform KiwiViewer (developed by KitWare), which allowed for facile viewing and sharing of the results.

Data obtained for the burnt flame retardant presented different issues. The large and multiple data sets required extensive use of high performance computing---a system with solid-state storage and 12 core, 196 GB RAM node---and the management of files between local and remote servers. Also, while the reconstruction methods were similar to the foraminifera project, additional processing was needed in MATLAB and Mathematica to convert the absorptions near K-edge into relative volumen percent of constituent materials.

Through the use of custom Python scripting modules, VisTrails was able to handle the switching between applications well. The modules that were developed for the processing of these two datasets should lead to the development of a custom package for our research group that will then be available to the VisTrails community. Easy sharing of packages allowed by VisTrails should encourage openness of data processing techniques between research groups.

(168) CT reconstruction with automated component and specimen motion corrections

*B. RECUR[1], A. KINGSTON[1], S. LATHAM[1], G. MYERS[1], A. SHEPPARD[1]
benoit.recur@gmail.com

[1] Australian National University, Dept. Applied Maths, RSPE, Canberra, Australia

Motions encountered during a CT-scan lead to blurry reconstructed images or multiple edge artefacts, penalizing image analysis (segmentation for instance) and quantization. Motion errors can be divided into three classes: i) source movement, ii) stage errors, and, iii) specimen motion. i) is typically associated with the X-ray source reaching thermal equilibrium during a scan. Supposing it is stable at the end of the scan, an additional fast- or reference-scan (with a few number of projections compared to the full-scan) can be performed. Projections of full and fast scans are registered [1] and each fullscan projection image is corrected by interpolating motion parameters of the two closest reference projections. ii) is due to the inaccuracies of the translation and rotation stages of the system. Despite a higher-and-higher mechanical accuracy, some stage errors remain significant enough, leading to artefacts in reconstructed tomogram. Since these errors are often repeatable, they can often be addressed using a misalignment map (determined experimentally). Finally, iii), if specimen motion is repeatable or stable at the end of the scan, it can be corrected by projection registration or mapping as with source movement. However, some source and stage errors cannot be corrected using existing techniques, and specimen motion is almost always unpredictable. Since scanner calibration and reference-scan are useless in these cases, the only remaining solution consists of including a motion error correction in tomographic reconstruction.

Each motion error can be considered as somehow complementary to each other. For instance, any source drift parallel to the detector leads to a translational misalignment between acquired and expected projections, similar to inverse specimen motion. Similarly, any source or specimen motion orthogonal to the detector leads to a scale change between acquired and expected projections. More complex object motions are partially depicted by a planar rotation.

Iterative CT reconstruction updates the tomogram, μ_t at iteration t, by comparing acquired projection, R_θ, with corresponding projection $R_{\theta,t}$, computed from the volume estimated at previous iteration. The error-projection obtained by such a comparison is back-projected into μ_t, and the overall process is performed until solution convergence. The proposed method is thus implemented by considering: i) $R_{\theta,t}$ as reference image since it is more correctly aligned (compared to R_θ) with the latest volume estimate μ_{t-1}, and, ii) corresponding R_θ as sensed image to register and realign prior to the projection comparison made by CT reconstruction. In our implementation, we use the Ordered Subsets Convex (OSC) algorithm [2,3] as iterative CT basis and the log-polar phase correlation (LPPC) to register projections [4,5]. LPPC is able to estimate translation, (t_i,t_j), rotation angle, φ, and scale rate, Λ, between two images.

The first proposed method, denoted OSC-LPPC, can be improved by modelling all motions as an unique source drift, $(\delta_x,\delta_y,\delta_z)_\theta$, on each projection θ, estimated from $(t_i,t_j,\varphi,\Lambda)_\theta$ (knowing CT scanner geometry). By updating $(\delta_x,\delta_y,\delta_z)_\theta$ at each iteration, we obtain a correction feedback since each motion corrected at iteration t is assessed at sub-sequent iterations throughout the new source position (used as anchor point to compute $R_{\theta,t+1}$). We denote this method OSC-LPPC-DE (Drift Estimation). During presentation, we will discuss reconstruction results given by the different investigated methods from simulated acquisitions as well as real data having

experienced a random source or specimen motions. We will also present how these motion estimations can be adjusted for practical implementation in a non-iterative reconstruction.

References :
1. B. Zitova and J. Flusser, Image and vision computing, 2003.
2. C. Kamphuis and F. J. Beekman, Medical Imaging, IEEE Transactions on, 1998.
3. H. Erdogan and J. A. Fessler, Physics in medicine and biology, 1999.
4. H. Foroosh, J. B. Zerubia, and M. Berthod, Image Processing, IEEE Transactions on, 2002.
5. K. Takita, Y. Sasaki, T. Higuchi, and K. Kobayashi, IEICE transactions on fundamentals of electronics, 2003.

(101) X-ray tomography imaging application for the study of soft matter systems

C. XIA[1], J. LI[1], Y. CAO[1], B. KOU[1], *Y. WANG[1], X. XIAO[2], K. FEZZAA[2]
yujiewang@sjtu.edu.cn

[1] Department of Physics and Astronomy, Shanghai Jiao Tong University, 800 Dong Chuan Road, Shanghai 200240, China
[2] Advanced Photon Source, Argonne National Laboratory, 9700 South Cass Avenue, Argonne, IL 60439, USA

It is important to understand both static and dynamic properties of soft matter systems. Studying them with x-ray imaging technology, including x-ray computed tomography (CT), has great superiority. Due to the penetrating properties of x-ray, internal structures of soft matter systems could be obtained. Using x-ray CT technology, we studied packing problems with various systems, such as mono-dispersed hard spheres, wet spheres, rods, poly-dispersed foams, etc. These experimental works will contribute to revealing some important properties of soft matter systems. We also suggest that with the rapid development of x-ray tomography technique especially with the high-spatial and temporal resolution, it shows great promises for the study of many soft matter systems including foam, emulsion, and colloids whose study have been previously dominated by scattering techniques and visible light microscopy.

Reference :
C.J. Xia, Y.X. Cao, B.Q. Kou, J.D. Li, Y.J. Wang, X.H. Xiao, and K. Fezzaa, *Phys. Rev. E* 90, 062201 (2014).
J.D. Li, Y.X. Cao, C.J. Xia, B.Q. Kou, X.H. Xiao, K. Fezzaa, and Y.J. Wang, *Nature Communications* 5, 5014 (2014).
Y.J. Wang, C.J. Xia, Y.X. Cao, B.Q. Kou, J.D. Li, X.H. Xiao, and K. Fezzaa, *Proc. SPIE* 9212, 92120E (2014).
Y.X. Cao, X.D. Zhang, B.Q. Kou, X.T. Li, X.H. Xiao, K. Fezzaa, and Y.J. Wang, *Soft Matter* 10, 5398 (2014).
X.D. Zhang, C.J. Xia, X.H. Xiao, and Y.J. Wang, *Chinese Phys. B* 23, 044501 (2014).
C.J. Xia, K. Zhu, Y.X. Cao, H.H. Sun, B.Q. Kou, and Y.J. Wang, *Soft matter* 10, 990 (2014).
Y.X. Cao, B. Chakrabortty, G.C. Barker, A. Mehta, and Y.J. Wang, *Europhys. Lett.* 102, 24004 (2013).
Y. Fu, Y. Xi, Y.X. Cao, and Y.J. Wang, *Phys. Rev. E* 85, 051311 (2012).

Session 202 - Geotechnic

(025) Influence of particle morphology on strain localization of sheared sand

A. M. DRUCKREY[1], K. A. ALSHIBLI[2], M. JARRAR[3]
adruckre@vols.utk.edu

[1] Graduate student, Dept. of Civil & Env. Engineering, University of Tennessee, Knoxville, TN 37996, USA,
[2] Professor, Dept. of Civil & Env. Engineering, 324 John Tickle Building, University of Tennessee, Knoxville, TN 37996, USA, Email: Alshibli@utk.edu
[3] Graduate student, Dept. of Civil & Env. Engineering, University of Tennessee, Knoxville, TN 37996, USA

The failure mode of sheared soils when they are tested under Axisymmetric triaxial condition is commonly described as diffuse bifurcation (bulging) or via single or multiple shear bands. Desrues et al. (1996) and Alshibli et al. (2003) reported that the bulging on specimen surface is just the external manifestation or rather complex failure mode of triaxial specimens. They utilized computed tomography to visualize multiple shear bands that developed inside the specimens. This paper discusses the influence of particle morphology on the failure mode of sheared triaxial sand specimens by comparing the behavior of a specimen composed on spherical glass beads with a specimen of angular sand. 3D synchrotron microtomography (SMT) technique was used to acquire multi *in situ* scans of the specimens at multiple axial strain levels. The paper will compare the onset and evolution of failure modes of the two specimens and discuss them in relation to particle morphology.

(104) Wormhole development in carbonate rocks during CO_2 acidized water flow

A. P.S. SELVADURAI, C. COUTURE
patrick.selvadurai@mcgill.ca

Department of Civil Engineering and Applied Mechanics, McGill University, 817 Sherbrooke Street West, Montréal, QC, Canada H3A 0C3

The deep geologic sequestration of greenhouse gases in fluidized forms is regarded as the most favourable option for mitigating climate change. The target reservoirs identified for such sequestration activities are primarily sandstone formations that have natural geologic barriers in the form of caprock that can enhance hydrodynamic trapping. While pure sandstone formations are considered to be the ideal sequestration horizon, these are not universally available and on occasions, the sequestration strategy could include carbonate geological formations. The amount of carbonate content will therefore be a critical factor that will ensure the integrity of the storage formation during long term injection activities. Even with sandstone formations, it is likely that seams of carbonate rocks can be encountered. The behaviour of such carbonate rocks is also important to the sequestration strategy. To this end, an experimental research program was initiated to examine the behaviour of Indiana Limestone during acidized CO2 migration. Indiana Limestone has a carbonate content of 98% and this is intended to provide a worst case scenario in terms of the impact of acidized CO2 migration. Experiments were conducted on 50 mm diameter and 100 mm long samples of Indiana Limestone. The development of “Wormholes” is a characteristic feature of the breakdown of the fabric of the Indiana Limestone. The dissolution pathways can enhance the CO2 migration in such rock and the dissolved carbonates could be trapped in locations impeding the efficiency of injection and the potential for hydraulic fracture with continued injection. CT scanning techniques provided a clear picture of the final stages of wormhole development when complete breakthrough occurs compromising the storage capacity of the formation. The work is also being extended to identical experiments conducted on grey sandstone and dolomite. These experiments complemented by CT scanning techniques provide benchmarks for determining the efficiency of geologic sequestration of greenhouse gases.

(120) Characterisation of force chains in granular media through combined 3DXRD and X-ray tomography

*S. A. HALL[1,2], R. C HURLEY[3], J. WRIGHT[4]
stephen.hall@solid.lth.se

[1] Division of Solid Mechanics, Lund University, Lund Sweden
[2] European Spallation Source AB, Lund, Sweden
[3] Mechanical and Civil Engineering, California Institute of Technology, Pasadena, CA, USA
[4] European Synchrotron Radiation Facility, Grenoble, France

The development of “force chains” in granular media, i.e., spatially continuous lines of force between contacting grains by which boundary loads are transmitted, and their importance in controlling mechanics at larger scales has received much attention in recent years. To this end, many experiments using photoelastic materials, in 2D, and “numerical experiments” using 2D/3D discrete element method (DEM) simulations have been used to investigate the development of force distributions through granular assemblies. However, measuring 3D force distributions real granular materials remains a challenge.

New results from a novel experimental method for characterising structural evolution, deformation and 3D force distribution in real granular materials will be presented. The method involves in-situ mechanical testing with “three-dimensional x-ray diffraction” (3DXRD combined with x-ray tomography). These measurements provide data on individual tensor grain strains, from 3DXRD, at different applied-load levels through a loading test in addition to the grain shapes, positions and contacts, from the tomography. From these data the transmission of forces through the granular network can be inferred to allow force chains to be identified and characterised. Results for samples of nearly spherical quartz single crystals undergoing 1D compression will be presented.

(204) Characterization of rock discontinuity morphology during shearing using X-ray micro-CT

B. S. A. TATONE[1], *N. TISATO[2], G. GRASSELLI[2]
nicola.tisato@utoronto.ca

[1] Geomechanica Inc.,Toronto, 90 Adelaide St. West, Suite 300, Toronto, ON, Canada, M5H 3V9
[2] Department of Civil Engineering, University of Toronto, 35 St. George street, Toronto, ON, Canada, M5S 1A4

Rock mass discontinuities represent planes of relative weakness and enhanced hydraulic conductivity and, thus, have a substantial influence on the hydro-mechanical behaviour of rock masses. While the shearing of rock mass discontinuities has been extensively studied in the past, there remains uncertainty surrounding the mechanisms by which surface asperities deform and degrade during shear and how this degradation influences the aperture distribution. Although many studies have attempted to investigate asperity failure mechanisms, they have been hampered by the lack of appropriate visualization tools. In particular, until recently it was not possible to observe asperity damage without physically separating the joint specimen following shearing.

The objective of the current work is to outline a recently developed methodology to non-destructely study asperity degradation mechanisms and discontiniuty morphology during direct shear tests using micro X-ray Computed Tomography (µCT) (Tatone, 2014). As part of this methodology, replicated discontinuity specimens were designed such that specimens could be shear tested to different incremental displacements and subsequently relocated to a 240 kV industrial micro-CT system to obtain 3D imagery of the internal structure. Via image processing and analysis using a series of newly written plug-ins and macros for FIJI, the damage and void space in each specimen was quantitatively characterized (Tatone, 2014; Tatone & Grasselli, 2015). Specifically, measurements of the statisitical and spatial aperture distributions, fracture surface areas, and preferential void space orientation as a function of shear displacement and different normal loading conditions were obtained.

In presenting the experimental methodology, selected results are presented and discussed in detail. These results provide unprecedented insight into the rock discontinity shearing process, which is of key interest to several rock engineering and hydrogeology practioners; including those concerned with preventing shear displacement (e.g., excavation, slope, and dam stability analyses) and those concerned with changes in hydraulic transmissivity resulting from shear displacement (e.g., EDZ around long-term radioactive waste repositories and reservoir stimulation via hydraulic fracturing).

References :
Tatone B. S. A. (2014) Investigating the evolution of rock discontinuity asperity degradation and void space morphology under direct shear. PhD, University of Toronto, Toronto, Canada
Tatone B. S. A., & Grasselli G. (2015). Characterization of the effect of normal load on the discontinuity morphology in direct shear specimens using X-ray micro-CT. Acta Geotechnica, 10(1), 31-54.

(024) Insight into 3D fracture behavior of silica sand

M. B. CIL[1], K. A. ALSHIBLI[2]

[1] Postdoctoral Research Fellow, Dept. of Civil & Env. Engineering, Technological Institute, 2145 Sheridan Road, Tech A236, Northwestern University, Evanston, IL 60208, Email: mehmet.cil@northwestern.edu
[2] Professor, Dept. of Civil & Env. Engineering, 325 John Tickle Building, University of Tennessee, Knoxville, TN 37996, USA, Tel. 011-865-974-7728, Email: Alshibli@utk.edu

3D synchrotron microtomography (SMT) was used to investigate the evolution of particle fracture of silica sand subjected to k_o-loading condition. A series of 1D compression laboratory experiments were conducted on uniform silica sand to better understand the fracture behavior of silica sand. The evolution and distribution of particle fracture was analyzed non-destructively at the particle and specimen scales using 3D SMT images. The onset of the fracture pattern of individual sand particles within the granular assembly was also examined at consecutive strain levels using SMT images. The paper will show images of fractured sand particles and will try to shed the light on the mode of fracture of sand particles.

Session 203 - Multi-tissue quantitative Imaging technique

(021) Metal artifact reduction using confidence maps and patch-based method

*L. FRÉDÉRIQUE[1,3], B. RECUR[2], S. GENOT[3], J. P. DOMENGER[1], P. DESBARATS[1]
louis.frederique@labri.fr

1 LaBRI, Université de Bordeaux / CNRS, 351 Cours de la Libération, 33405 Talance Cedex, France
2 Australian National University, Dept. Applied Maths, RSPE, Canberra Australia
3 Tomo Adour, Zone Europa, 5 Rue Johannes Kepler, 64000 Pau, France

In the field of non-destructive testing of materials, computed tomography became a good way to check defects in industrial piece production [1]. However, tomographic analysis is difficult to achieve due to the presence of high density objects (such as metal) in most produced pieces, leading to the wellknown metal artifacts in reconstructed data. In X-Ray tomography, metal artifact is characterized by a local and straight hyper-signal [2]. This observed phenomenon is due to high attenuations of the rays in the high density materials.

Many different approaches have been proposed for metal artifact reduction during the last decade. In the most popular case, developed methods consider the artifact reduction as a missing data problem.

Currently, two kind of methods can be distinguished. The first one is based on projection completion method [3, 4]. Missing data, represented by the metal traces in the sinogram, are replaced by synthetic data computed by interpolation or in-painting methods. The second one considers metal artifact reduction as a penalizing term in an iterative reconstruction method [5, 6]. Such a method is based on local filtering assessing the coherence of a pixel with its neighborhood.

However, these methods start their process from the original projection data. In our context, only the reconstructed image is available due to clinical scanner usage. Thus, we focus our investigations on a solution based on the reconstructed image only. We propose an algorithm that reduces the artifact by directly applying a patch-based image processing. Patches preserve geometry in the image and avoid over-smoothing. However, patch-based method amends all pixels whereas only few of them have to be corrected in our case. Thus, in order to only restore corrupted pixels, we compute confidence maps from a simulated sinogram and apply them as weighting functions determining the amount of correction to perform using the patch-based method.

These maps represent hyper-signal and hypo-signal repartition generated by metal artifact in the reconstructed image. In other words, each map is a probabilistic representation of the amount of hyper or hypo-signal phenomenon that occurs during the initial acquisition / reconstruction process. They are obtained using an iterative reconstruction from a simulated acquisition of metal traces. The overall output function is a combination of these two maps, where negative and positive values represent the hypo-signal and the hyper-signal, respectively.

During the presentation, we will first present our method, the way we generate the maps and we use them to manage the image correction performed by the patch-based method. Then, we will

discuss the results we obtain by comparing them with results from the litterature. We will intent to show that we achieve a competitive artifact correction compared to state of the art techniques which are based on original projection data.

References :
1. J. Baruchel, J.Y. Buffiere, and E. Maire, “X-ray tomography in material science”, 2000.
2. F.E. Boas and D. Fleischmann, “CT artifacts: causes and reduction techniques”, Imaging in Medicine, 2012.
3. Y. Chen, Y. Li, H. Guo, Y. Hu, L. Luo, X. Yin, J. Gu, and C. Toumoulin, “CT metal artifact reduction method based on improved image segmentation and sinogram in- painting”, *Mathematical Problems in Engineering*, 2012.
4. H. Yu, K. Zeng, D.K. Bharkhada, G. Wang, M.T. Madsen, O. Saba, B. Policeni, M.A. Howard, and W. Smoker, “A segmentation-based method for metal artifact reduction”, *Academic radiology*, 2007.
5. B. De Man, J. Nuyts, P. Dupont, G. Marchal, and P. Suetens, “Reduction of metal streak artifacts in x-ray computed tomography using a transmission maximum a posteriori algorithm”, *Nuclear Science Symposium*, 1999.
6. G. Wang, D.L. Snyder, J. O’Sullivan, and M.W. Vannier, “Iterative deblurring for ct metal artifact reduction”, *Medical Imaging, IEEE Transactions on*, 1996.

(091) 3D-imaging by synchrotron X-ray micro tomography of ferroelectric composite materials and numerical modelling of their physical properties

*J. LESSEUR[1,2], C. ELISSALDE[1,2], C. ESTOURNES[3], R. EPHERRE[3], P. VEBER[1,2], M. GAYOT[1,2], M. MAGLIONE[1,2], D. BERNARD[1,2]
lesseur@icmcb-bordeaux.cnrs

[1] CNRS, ICMCB, UPR9048, F-33600 Pessac, France
[2] Univ. Bordeaux, ICMCB, UPR 9048, F33600, Pessac, France
[3] CIRIMAT et Plateforme Nationale CNRS de Frittage flash, PNF2 MHT, Univ. Paul Sabatier, F-31062 Toulouse, France

Ferroelectric materials are widely used to produce passive components such as capacitors for microelectronic and telecom applications. These applications require a well-controlled modulation of physical parameters of the materials (permittivity, temperature transition, dielectric losses…). With the miniaturisation of electronic components, capacitors made only with ferroelectric materials are not suitable with permittivity and dielectric losses requirements. Thus, the way of composite materials is increasingly explored. In this study, new designed three-dimensional composites are presented [1,2]. Low-loss non-ferroelectric inclusions (MgO) with a spheroidal geometry are dispersed in a $Ba_{1-x}Sr_xTiO_3$ (BST) ferroelectric powder matrix, and then sintered by Spark Plasma Sintering (SPS). Optimisation of the process relies on a deep understanding of the critical steps: initial powders preparation, powders mixing, SPS sintering parameters, relation between final architecture after sintering process and physical properties. In a first series of experiments, soft granules are deformed during the sintering process, leading to specific flattened shapes (ellipsoids) (Fig.1a). In a second one, MgO granules, previously densified by heat treatment, preserve their spheroidal morphology during sintering by SPS (Fig. 1b).

This presentation is focussed on the methodology developed to obtain a complete description of the three-dimensional microstructure of our materials and reveal the relationships between the inclusions morphology and the physical properties. Based on 3D-imaging techniques and numerical modelling methods, the procedure is achieved by 1) 3D-imaging obtained by synchrotron X-ray computed micro tomography of both initial mixed powder and sintered material; and 2) Numerical modelling of the effective permittivity computed from 3D micro geometry images. Comparisons between numerical and experimental results are exposed and discussed.

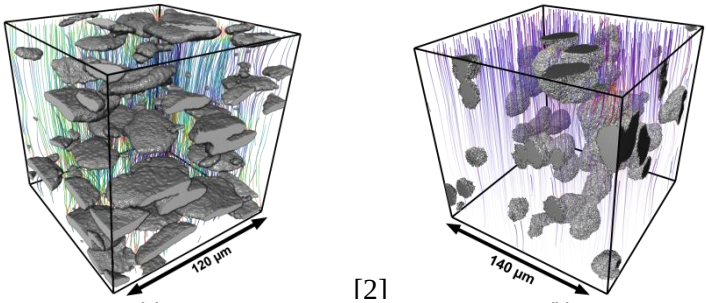

[1] [2]
[3] (a) [4] (b)
[5] Figure 1: Effective permittivity computation in ferroelectric composites with different geometries. Matrix is transparent and MgO inclusions are represented in grey.

References :

- , Ganne JP. Appl Phys Lett 2008;92:042902.
[2] Lesseur J, Bernard D, Chung U-C, Estournès C, Maglione M, Elissalde C. J Eur Ceram Soc 2015;35:337.

(017) Novel contrast agents for contrast-enhanced CT to visualize in 3D the blood vessel network and fat cell distribution in bone marrow

*G. KERCKHOFS[1,2], A. SAP[3], E. PLOUGONVEN[4], N. VAN GASTEL[1,5], M. DURAND[1,2], R. VANGOITSENHOVEN[5], B. VAN DER SCHUEREN[5], A. LÉONARD[4], K. VANDAMME[1,6], G. CARMELIET[1,5], T. N. PARAC-VOGT [3], F. P. LUYTEN[1,2], L. GERIS[1,7,8]
greet.kerckhofs@med.kuleuven.be

[1] Prometheus, Division of Skeletal Tissue Engineering, KU Leuven, O&N 1, Herestraat 49 - PB813, B-3000 Leuven, Belgium
[2] Dept. Development and Regeneration - Skeletal Biology and Engineering Research Center, KU Leuven, O&N 1, Herestraat 49 - PB813, B-3000 Leuven, Belgium
[3] Dept. Chemistry - Molecular Design and Synthesis, KU Leuven, Celestijnenlaan 200f – PB2404, B-3001 Leuven, Belgium
[4] Dept. Applied Chemistry, Université de Liège, Institut de Chimie-Bâtiment B6, Sart Tilman, B-4000 Liège, Belgium
[5] Dept. Clinical and Experimental Medicine - Clinical and Experimental Endocrinology, KU Leuven, O&N 1, Herestraat 49 – PB902, B-3000 Leuven, Belgium
[6] Dept. Oral Health Sciences - BIOMAT, KU Leuven, Kapucijnenvoer 7 blok a - PB7001, B-3000 Leuven, Belgium
[7] Biomechanics Research Unit, Université de Liege, Chemin des Chevreuils 1 - BAT 52/3, B-4000 Liège, Belgium
[8] Dept. Mechanical Engineering - Biomechanics Section, KU Leuven, Celestijnenlaan 300C - PB 2419, B-3001 Heverlee, Belgium

Intro: Long bones consist of a bone and bone marrow compartment. Both contain a complex 3D blood vessel network, which is critical for supply of oxygen, nutrients and minerals to support the process of tissue remodelling and regeneration. A detailed and 3D visualization and quantification of this network might be necessary to be able to link dysfunction or alteration in the blood vessel network with impaired bone remodelling, healing and regeneration. We propose contrast-enhanced nanofocus computed tomography (CE-nanoCT) for 3D multi-tissue imaging to visualize in a single image set the bone and bone marrow compartment including blood vessels and adipose tissue. In this study, we have compared phosphotungstic acid (PTA), a well-known contrast agent, with two novel contrast agents for their non-invasive character and their potential to visualize blood vessels and adipose tissue in the bone marrow compartment.

Methods & results: Both novel contrast agents are metal-substituted polyoxotungstates, and are further referred to as Hf-POT (Hf-substituted) and Zr-POT (Zr-substituted). To investigate whether the staining provoked tissue shrinkage, we used tissue engineering constructs (i.e. calcium phosphate-collagen scaffold with human periosteal derived cells and a growth factor) that were implanted ectopically for 6 weeks. After explantation and fixation in paraformaldehyde, the samples were scanned, stained and rescanned. Using image registration, tissue shrinkage (with focus on bone) was assessed, showing that PTA does induce shrinkage of bone after 24 hours of staining in a 2.5% PTA/PBS (phosphate buffered saline) solution. Both novel contrast agents however did not provoke shrinkage using the same concentration and staining time.

To further assess the non-invasiveness of the contrast agents, we investigated the potential to perform immunological staining after CE-nanoCT imaging. Therefore, we first stained tibias of 4 weeks old mice, scanned these using CE-nanoCT, and processed subsequently for CD31 immunostaining for blood vessel visualisation. We included control samples that were not stained using the contrast agents, and performed blind scoring. PTA staining did not allow CD31staining, while both novel contrast agents showed excellent CD31 tracing. Hf-POT performed better than Zr-POT, not showing any difference with control samples that have not been scanned nor stained with the contrast agents prior to CD31 immunostaining.

Finally, we scanned tibias of old (30 weeks - OLD), young (7 weeks - YNG) and diabetic (30 weeks - diet-induced obese model, DIO) mice to evaluate the potential of the novel contrast agents to visualize the blood vessel network and the fat cell distribution. Both contrast agents were able to pick up differences between the three groups. For the DIO mice, the bone marrow compartment contained more adipose tissue close to the growth plate compared to the YNG and OLD mice. YNG mice showed a higher content of blood vessels compared to the other groups. Full 3D analysis is ongoing to determine the interconnection and thickness distribution of the blood vessels, and to show the added value of CE-nanoCT compared to standard histomorphometry.

Conclusion: CE-nanoCT is a multi-tissue 3D imaging technique that can reveal the 3D structure of different skeletal tissues (i.e. bone, bone marrow, fat cells and blood vessels). Since it is promising for providing additional information to standard histomorphometry, with a spatial dimension, CE-nanoCT might bring novel insights in the biological processes during tissue remodelling and regeneration.

(102) Quantitative three-dimensional tissue imaging of lipid, protein, and water contents via X-ray phase-contrast tomography

*M. WILLNER[1], M. VIERMETZ[1], M. MARSCHNER[1], J. HERZEN[1], C. BRAUN[2], A. FINGERLE[3], P. NOEL[3], E. RUMMENY[3], F. PFEIFFER[1]
marian.willner@ph.tum.de

[1] Department of Physics and Institute of Medical Engineering, Technische Universität München, James-Franck-Strasse 1, 85748 Garching, Germany
[2] Institute of Forensic Medicine, Ludwig-Maximilians-Universität München, Nußbaumstrasse 26, 80336 München, Germany
[3] Department of Diagnostic and Interventional Radiology, Technische Universität München, Ismaningerstrasse 22, 81675 München, Germany

Phase-contrast imaging techniques emerged as essential tool in biomedical research and a broad spectrum of tissue analysis is currently performed by micro computed tomography at synchrotrons and laboratory X-ray sources [Bravin2013].

Besides the high contrast that can be achieved by phase-contrast imaging for small and low absorbing samples, the access to the refractive index decrement in addition to the linear attenuation coefficient enables enhanced evaluation of tissue properties [Willner2013, Willner2014].

In our study, we examined the possibilities to quantitatively assess the content of lipid, protein and water at a subpixel length scale by exploiting the complementary information obtained in attenuation and phase contrast.

Experimental results of dairy products, porcine fat and rind, and different human soft tissue types are presented. The 3D representations of protein, lipid, and water contents open up new opportunities in the fields of biology, medicine, and food science.

References :
A. Bravin et al., Phys. Med. Biol. 58, R1-R35 (2013)
M. Willner et al., Opt. Express 21(4), 4155-4166 (2013)
M. Willner et al., Phys. Med. Biol. 59, 1557-1571 (2014)

Session 204 - 3D imaging

(030) Edge illumination X-ray phase contrast computed tomography: implementations at synchrotrons and in standard laboratories

*C. K. HAGEN[1], A. ZAMIR[1], F. A. VITTORIA[1], P. C. DIEMOZ[1], M. ENDRIZZI[1], A. OLIVO[1]
charlotte.hagen.10@ucl.ac.uk

[1] Department of Medical Physics and Biomedical Engineering, University College London, Malet Place, Gower Street, London WC1E 6BT, United Kingdom

X-ray phase contrast computed tomography (CT) has the potential to overcome the main problem associated with conventional x-ray tomography: limited contrast for samples with weak attenuation properties. This is because contrast is generated from the phase shift that x-rays suffer while they travel through matter, rather than from x-ray absorption. Since phase effects can be much stronger than attenuation ones, this can lead to improved image contrast. Alongside the high spatial resolution and short scan times achievable with x-rays and the three-dimensional nature of tomographic images, this has made phase contrast tomography an attractive modality for a broad spectrum of applications, both from medical and non-medical disciplines. Amongst the latters are, for example, materials science and non-destructive testing of light materials such as plastics and composites.

To date, several approaches to phase contrast tomography have been developed. These can be classified as propagation-based, crystal-based, grating-based interferometric and grating-based non-interferometric methods. Measures to compare these approaches include coherence requirements, phase sensitivity, quantitative accuracy and stability and robustness. Edge illumination x-ray phase contrast tomography, a grating-based non-interferometric method, was demonstrated to provide unprecedented phase sensitivity when it is implemented at synchrotrons (Diemoz et al. 2013). Other advantages are that this method is based on a simple experimental setup, has comparatively weak requirements on stability (Millard et al. 2014), and does not rely on beam coherence (Olivo and Speller 2007). The latter property ensures that the method still works when it is implemented outside synchrotrons with commercially available, non-microfocal x-ray tubes (Hagen et al. 2014).

The working principle of edge illumination phase contrast tomography is schematically shown in Fig. 1(a). A slit collimates the beam in the vertical direction, typically down to 10-20 μm, and an edge positioned in front of the detector stops half of the (here laminar) beam, while the remaining half is allowed through. This “edge illumination” configuration is effectively the sensing mechanism as it creates high sensitivity to refraction, i.e. the spatial derivative of the phase shift: x-rays which are deviated towards (away from) the uncovered detector areas cause an increased (a decreased) measured intensity. By replacing the slit and the edge with appropriate x-ray masks, this configuration is repeated over the entire field of view of an area detector [Fig. 1(b)]. This allows imaging larger samples with a single tomographic scan; hence, it reduces the overall acquisition time.

This talk will introduce the edge illumination x-ray phase contrast tomography and briefly discuss data acquisition and tomographic reconstruction processes. The main focus of the talk will be on the implementation of the method in different setups, including three synchrotron

facitlities and a standard laboratory equipped with a commercial x-ray tube. The respective experimental challenges will be highlighted, and applications in materials science, biomaterials and non-destructive testing will be reviewed, with key examples presented from each.

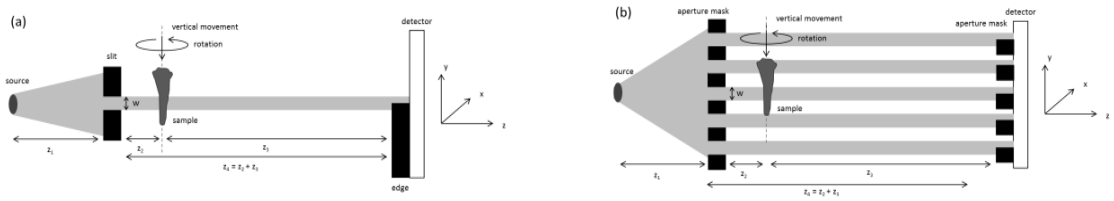

Fig. 1. Schematic of edge illumination x-ray phase contrast tomography using a slit and an edge (a) and a pair of x-rays masks (b).

References :
Diemoz, P.C. et al, Phys. Rev. Lett. 110: 138105 (2013)
Millard, T.P. et al, Rev. Scient. Instrum. 84: 083702 (2013)
Olivo, A. and Speller, R., Appl. Phys. Lett. 91: 074106 (2007)
Hagen, C.K. et al, Med. Phys. 41: 070701 (2014)

(041) Projection-based digital volume correlation: application to crack propagation

T. TAILLANDIER-THOMAS[1], H. LECLERC[1], *S. ROUX[1], F. HILD[1]
thibault.taillandier-thomas@lmt.ens-cachan.fr

1 LMT, ENS-Cachan, CNRS, Univ. Paris-Saclay, 61 Av. Président Wilson, 94235 Cachan Cedex, France

Tomography is not only useful for its ability to reveal the intimate microstructure of material in 3D, but also to track its changes with time, say, during a mechanical test. One useful tool in this context is Digital Volume Correlation (DVC) whose finality is to provide a 3D displacement field that allows for the registration of two 3D images of the same solid at different loadings. However, one limiting feature is the long acquisition time that confines such studies to (quasi) time-independent behaviors. Another limitation of DVC is the presence of artifacts in the tomographic reconstruction that originates from the imperfection and noise of the X-ray detector. Although the latter noise can be considered as white (spatially uncorrelated) the reconstruction algorithm induces long-range correlations. Such correlated noise unfortunately impacts the DVC analysis.

It has been suggested in [Leclerc, 2015] to use a first 3D reconstruction of the reference configuration, and estimate the displacement field from only a few radiographs of the deformed state. Such a procedure was shown on one experimental case study to provide faithful displacement measurements based on a very small number of projections (as small as 2). This procedure of “Projection-based DVC” (or PDVC) offers a large gain in the needed number of projections of *more than two orders of magnitude*. Moreover, as only raw projections are dealt with, the white noise assumption remains valid and hence the detrimental effect of noise can be much reduced.

The example that was used in [Leclerc, 2015] consisted however of a very simple kinematics that could be captured with a very coarse description. As one would move to finer and finer meshes to describe the displacement field, the algorithm showed signs of poorer convergence. Hence, it is natural to raise the question as to what extent such an approach could deal with more complex displacement fields.

The present study deals with such a complex example where a cracked solid is subjected to a tensile test. Not only does the strain field present a singular behavior at the crack tip, but additionally, the crack geometry presents some corrugations that could be evaluated from a full 3D reconstruction performed at the end of (rather than before) the test. The displacement field is decomposed over a 3D finite element mesh that is refined in the vicinity of the crack. Two novel tools are implemented to reach convergence: first, a hierarchical coarsening procedure is used to allow for large displacement corrections; second, a regularization is implemented so as to guide the displacement determination using the solution to a homogeneous elastic problem as a guess. These two procedures have been successfully implemented and the resulting projection residuals show a good convergence to a trustworthy solution based on no more than two projections, in spite of the numerous kinematic degrees of freedom used to describe the displacement field.

References ;
H. Leclerc, S. Roux and F. Hild, (2015) Projection savings in CT-based Digital Volume Correlation, Exp. Mech. in press; http://dx.doi.org/10.1007/s11340-014-9871-5

(056) 4D quantification and tracking of time dependent features

*L. COURTOIS[1,2], P. D. LEE[1,2], K. J. DOBSON[3], Q.LIN[4], S. J. NEETHLING[4]
loic.courtois@manchester.ac.uk

[1] Manchester X-ray Imaging Facility, School of Materials, Oxford Road, University of Manchester, M13 9PL, UK
[2] Research Complex at Harwell, Rutherford Appleton Laboratory, Didcot, Oxfordshire, OX11 OFA, UK
[3] Earth & Environmental Sciences, LMU Munich, Theresienstrasse 41, 80333 Munich, Germany
[4] Department of Earth Science and Engineering, Imperial College London, SW7 2AZ, UK

High flux laboratory and synchrotron tomographic imaging systems, combined with bespoke *in situ* sample environmental rigs has revolutionised our ability to perform 4D imaging, or time-resolved 3D imaging. Experiments ranging from tracking the deformation of high temperature semi-solids (Kareh et al, 2014) through to the fracture of frozen solids (Ní Bhreasail, 2012) can be studied both dynamically and over long time periods, resulting in the acquisition of large 4D datasets (tens of terabytes). Quantification of these datasets offers many advantages over traditional destructive quantification techniques (microscopy), specifically both the motion and the kinetics of reactions can be observed, and ideally quantified. This study presents automated techniques for quantifying these large experimental 4D data sets to gain a better understanding of the process and to inform and validate models of the phenomena. Although we will use data acquired using X-ray micro-computed tomography, the technique it is applicable to any non-destructive 3D imaging technique used for acquiring time dependent images (e.g. Neutron, confocal, or EM tomography…).

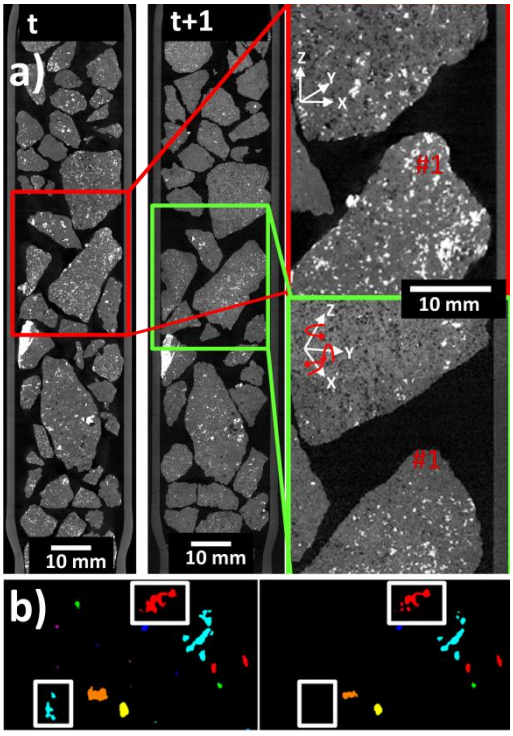

Figure 1: a) Cross section of XMT data of an ore fragment alongside two section at consecutive times. b) segmented and tracked micro-scale particles

In this study, we present a fully automated method to track and quantify motion and morphological changes of particles across a range of scales demonstrated using the evolution

of particle sizes during the processing of rocks over the period of months (Fig. 1.a, see Lin et al, 2014 for details). The key steps include i) denoising, ii) phase segmentation, iii) macro-scale fragment identification, iv) individual macro-scale registration, v) micro-scale track of particles. The analysis is aimed at limiting user-input when processing data, while using consistent algorithms to quantify microstructural parameters.

Histogram-based segmentation methods were used (Tsai, 1985; Kapur, Sahoo & Wong, 1985) to segment both macro-scale fragments and micro-scale particles (bright white spots in Fig. 1.a). A combination of morphological operations and watershed separations were used in order to individually label and identify (volume, shape, diameter,…) fragments before tracking. In such a case where two different scales are easily distinguishable, information from one scale can be used to help the analysis of the second one. Here, macro-scale fragments can be identified through time via the tracking approach described below and a transformation matrix can thus be obtained for all timeframes, resulting physically aligned 3D volumes. However, in order to avoid any further interpolation, volumes are left untransformed and the matrix alone is saved for use in subsequent tracking.

The tracking strategy used here is easily tailored to a specific experiment, using a priori knowledge of the behaviour of the system, e.g.: known displacement field, no volume change, constant shape factor or distance to nearest surface… As a result, features can be matched through time by using both experiment specific information and all identifiers previously defined for each individual feature, thus reducing the number of possible matches for a given particle considerably. A cost function based on weighted distance between matches and specific penalties (e.g. change in volume) is then minimized in order to identify particle matches through time. Figure 1.b shows the result of tracking and subsequent relabelling of particles.

Although we applied this method to the spatially and temporally non-uniform reduction of particles, our method is applicable for tracking flow, porosity, cracks or bubbles, and highlights the attention needed when performing quantification based on 4D datasets.

References :

Kapur, JN; Sahoo, PK; Wong, AKC, "A New Method for Gray- Level Picture Thresholding Using the Entropy of the Histogram", Computer Vision, Graphics and Image Processing, 29: 273–285,1985

Kareh, K.M., Lee, P.D., Atwood, RC, Connolley, T., and Gourlay, C.M., "Semi-solid metal deformation: illuminating new micro-mechanisms with time-resolved synchrotron tomography", Nature Commun., 5:4464, http://dx.doi.org/10.1038/ncomms5464, July 2014.

Lin, Q., Neethling, S.J., Dobson, K.J., Courtois, L., Lee, P.D., "Quantifying and minimising systematic and random errors in X-ray micro tomography based volume measurements, Computers & Geosciences, CAGEO-D-14-00434R1, 2014.

Ní Bhreasail, Á; Lee, P. D.; O'Sullivan, C; Fenton, C.H.; Hamilton, R.; Rockett, P.; Connolley, T, "In situ observation of cracks in frozen soil using synchrotron tomography", Permafrost and Periglacial Processes, Volume 23, Issue 2, pages 170–176, April 2012. DOI: 10.1002/ppp.1737

Tsai, W-H, "Moment-preserving thresholding: A New Approach", Computer Vision, Graphics, and Image Processing, 29: 377–393, 1985

(076) 'Fast shear' phenomena in ductile fracture assessed by digital volume correlation on laminography synchrotron volumes

T. TAILLANDIER-THOMAS[1,2], *T. F. MORGENEYER[2], L. HELFEN[3-4], S. ROUX[1], F. HILD[1]
thibault.taillandier-thomas@lmt.ens-cachan.fr

[1] LMT, ENS-Cachan, CNRS, Univ. Paris-Saclay, 61 Av. Président Wilson, 94235 Cachan Cx., France
[2] MINES ParisTech, PSL Research University, MAT - Centre des matériaux, CNRS UMR 7633, BP 87, F-91003 Evry, France
[3] ANKA/Institute for Photon Science and Synchrotron Radiation, Karlsruhe Institute of Technology (KIT), D-76131 Karlsruhe, Germany
[4] European Synchrotron Radiation Facility (ESRF), BP 220, F-38043 Grenoble Cedex, France

The 'fast shear' phenomena in ductile fracture of thin sheets consist of having a crack that initiates in a plane normal to the loading direction and then tilts to a slanted position when propagating. These phenomena are not well understood despite the wide use of thin sheets in transportation industry. Therefore *in situ* tests are needed to get a better understanding of the relationship between damage and plasticity.

X-Ray computed tomography gives access to the microstructure of a sample but only if it is thin in two directions. As we are dealing with notched plate-like samples, the use of X-Ray computed laminography is needed, even at the cost of additional noise due to the lack of information in the reconstruction process. The natural contrast of the volumes can be exploited to perform 3D volume registration via digital volume correlation (DVC) to measure displacement fields and obtain strain fields between every step of the test.

The studied material is a 2139 T3 aluminum alloy that has already been used to assess the feasability of DVC analyses [Morgeneyer, 2013]. The combination of DVC and laminography allows reliable kinematic fields to be measured despite the low amount of information (~0.45 vol% of intermetallic particles and ~0.34 vol% of initial voids) and the presence of noise and reconstruction artifacts. Strain levels up to 16% can be measured directly and hence give cumulative results around 40% of strain in localized regions. Contrary to another aluminum alloy (i.e., 2198 T8) for which it was shown that strain localization occurs very early on in a single slant band and prior to any nucleation of damage [Morgeneyer, 2014], the present case is much more complex. Due to the hardening of this material, several localized slant bands develop and identifying, right from the beginning, the one that will lead to failure is more challenging.

References :
Morgeneyer, T. F., Helfen, L., Mubarak, H. & Hild, F.(2013), 3D Digital Volume Correlation of Synchrotron Radiation Laminography images of ductile crack initiation: An initial feasibility study. Exp. Mech, 53(4):543–556
Morgeneyer, T.F., Taillandier-Thomas, T., Helfen, L., Baumbach, T., Sinclair, I., Roux, S. & Hild, F.,(2014), In situ 3D observation of early strain localisation during failure of thin Al alloy (2198) sheet. Acta Mat., 69:78-91

(077) THz imaging versus X-Ray tomography: Applications to material inspection

*B. RECUR[1], H. BALACEY[2], J. BOU SLEIMAN[3], J. B. PERRAUD[3], J. P. GUILLET[3], P. MOUNAIX[3]
benoit.recur@gmail.com

1 Australian National University, Dept. Applied Maths, RSPE, Canberra, Australia
2 Noctylio SAS, 59 cours de l'Intendance, 33000 Bordeaux, France
3 IMS, Bordeaux University, CNRS UMR 5218, 351 cours de la Libération, 33405 Talence, France

THz time-domain spectroscopy (THz-TDS) imaging [1] and THz tomography (THz-CT) [2] are two recent imaging techniques allowing contact-free and non-destructive inspection of soft materials, such as paper, wood, plastics or ceramic. THz-TDS imaging is performed using a pulsed laser coupled with a time delay line, providing reflection or transmission images in a range of 0.1 – 4THz, with a frequential resolution of about few GHz. Thanks to a good penetration depth in light or insulating materials, low scattering, free-space propagation, low photon energy and broad spectral bandwidth, a single THz-TDS projection allows one to visualise object interfaces in depth, but also to map its chemical composition using chemometric methods [3]. As illustrations, THz-TDS has been applied in the fields of sigillography science and drug detection [3,4]. Although it is sometimes referred as 3D imaging, such a system only provides a 2.5D images in the sense that the depth-scale is not uniform along the overall acquisition and depends, at each point, on the traversed materials and interfaces. In contrast, THz-CT is based on monochromatic waves (usually 0.1 or 0.3THz, provided by a Gunn diode), which are collimated and focused to a Schottky diode (sensor) by a pair of PTFE lenses. A set of 2D projections, corresponding to the transmitted signal amplitude at different viewing angles around the object, is acquired by raster-scanning. By applying a dedicated tomographic reconstruction algorithm, one can obtain a tomogram of the acquired specimen, allowing 3D visualisation and internal analysis [5], similar to the very well known X-ray tomography.

In the first part of the presentation, we will introduce acquisition setup technologies as well as the related reconstruction and processing methods in order to perform specimen analysis from THz-TDS and 3D THz-CT acquisitions. Both techniques will be illustrated and their advantages and disadvantages will be discussed for various applications, such as porosity detection, non-destructive inspection of multi-layered structures or quantitative analysis of explosives.

Secondly, since: i) THz-TDS provides complete chemical information of the acquired sample, with an additional depth estimation (2.5D imaging); and, ii) THz-CT leads to a coherent 3D tomographic reconstruction, but with highly under-sampled frequency data (at 0.1 and 0.3THz only); we investigate experimental acquisition workflows and corresponding registration techniques in order to combine data from both systems. Two methods are discussed. First, we develop image-based registration techniques mapping the features extracted from THz-TDS spatial data to the 3D volume given by THz-CT. At some point, this approach aims at texturing the 3D THz-CT volume with the complete absorption data when they are correctly registered. Second, we consider THz-TDS acquisition as a spectral absorption dictionary and we try to label each voxel of the THz-CT volume using a bestmatching labeling technique of the data contained in the dictionary, similar to that proposed in [6].

Such a labelling is thus based on chemical features. Then, we detail the advantages and disadvantages of these image-based and chemical-based approaches, and why they are complementary and not exclusive. From the preliminary results, we identify aspects requiring further research in order to achieve a 3D reconstruction combined with a chemical analysis, based on THz waves only. Proposed method perspectives are discussed and compared with existing techniques, such that X-ray dual energy tomography for material characterization.

References :
1. J. El Haddad, B. Bousquet, L. Canioni, and P. Mounaix, Analytical Chemistry, vol. 44, 2013.
2. B. Recur, H. Balacey, J Bou Sleiman, J.-B. Perraud, J.-P. Guillet, A. Kingston, and P. Mounaix, Optics Express, vol. 22, 2014.
3. J. El Haddad, J. Bou Sleiman, F. de Miollis, B. Bousquet, L. Canioni, and P. Mounaix, IRMMW-THz international conference, 2013.
4. K. Kawase, Y. Ogawa, Y. Watanabe, and H. Inoue, Optics Express, vol. 11, 2003.
5. H. Balacey, J.-B. Perraud, J. Bou Sleiman, J.-P. Guillet, B. Recur, and P. Mounaix, SPIE/COS Photonics Asia, 2014.
6. B. Recur, M. Paziresh, G. Myers, A. Kingston, S. Latham, and A. Sheppard, SPIE Optical Engineering+ Applications, 921213-921213-9, 2014.

(080) Scanning-SAXS tensor tomography: accessing the orientation of nanostructures in 3D

*M. LIEBI[1], M. GEORGIADIS[2], A. MENZEL[1], O. BUNK[1], M. GUIZAR-SICAIROS[1]
marianne.liebi@psi.ch

[1] Swiss Light Source, Paul Scherrer Institut, 5232 Villigen, Switzerland
[2] Insitute for Biomechanics, ETH Zurich, Wolfgang-Pauli-Str. 14 8093 Zurich, Switzerland

We have developed a new method combining scanning small-angle X-ray scattering (SAXS) with computed tomography (CT) to access with 3D spatial resolution the three-dimensional ultrastructural orientation.

For 2D scanning SAXS the sample is moved continuously through a focused X-ray beam while a pixel X-ray detector measures the scattering signal. Analysis of these patterns provides information about structures in the size range of nanometers to a few hundreds of nanometers along with their 2D scattering orientation [1]. Using a micrometer-sized beam allows us to gather nanoscale information over areas extending many squaremillimetres.

While scanning SAXS can be combined with CT using filtered backprojection [2], this method provides 3D resolved information describing either the sample's isotropic ultrastructure or its preferential orientation along the axis of rotation only [3]. However, essentially all biological tissues and most specimens investigated in materials science violate this stringent condition. Accessing the three-dimensional orientation of nanostructure is necessary for adequate interpretation of ultrastructure anisotropy, such as the degree of orientation, but is possible thus far only in 2D sectioned samples [4,5].

Compared to, e.g., absorption-based tomography, for which a single rotation axis is sufficient, scanning-SAXS projections are acquired at multiple tilt angles of the tomographic rotation axis with respect to the X-ray beam in order to reconstruct several parameters modeling the ultrastructure in each voxel and the scattering response as function of the sample orientation with respect to the X-ray beam. The reconstruction is carried out through an optimization algorithm, where for each voxel, and for an integrated q-range, the 3D X-ray scattering is modeled using spherical harmonics, which provide a continuous model in q-space where symmetries, such as uniaxial symmetry of, e.g., fibrils, can be explicitly enforced. These modeled intensities are then projected onto the plane of the detector and used to calculate the error metric with respect to the measured projections at different angular positions of the detector. The parameters of the model for each voxel are the spherical angles θ and ϕ, representing the main orientation direction of the ultrastructure and the coefficients a_0, a_1, and a_2 of the spherical harmonics, from which the degree of orientation can be obtained.

We demonstrate the technique using scattering from a model consisting of small carbon fibers, and we show results from biomineralized material from snail shells and characterization of collagen fibril orientation on human trabecular bone, where the anisotropic scattering of mineral

crystals associated to collagen fibrils was analyzed. The information gained with this method is of interest in a broad range of applications in material science and bioimaging as the arrangement and orientation of ultrastructure plays an important role for the mechanical properties of inhomogeneous and anisotropic materials.

References :

Bunk, O., M. Bech, T. H. Jensen, R. Feidenhans'l, T. Binderup, A. Menzel and F. Pfeiffer (2009). "Multimodal x-ray scatter imaging." *New Journal of Physics* **11**.

Jensen, T. H., M. Bech, O. Bunk, M. Thomsen, A. Menzel, A. Bouchet, G. Le Duc, R. Feidenhans'l and F. Pfeiffer (2011). "Brain tumor imaging using small-angle x-ray scattering tomography." *Physics in Medicine and Biology* **56**(6): 1717-1726.

Schroer CG, Kuhlmann M, Roth SV, Gehrke R, Stribeck N, Almendarez-Camarillo A, Lengeler B (2006). "Mapping the local nanostructure inside a specimen by tomographic small-angle x-ray scattering. " *Appl Phys Lett* **88**.

Seidel, R., A. Gourrier, M. Kerschnitzki, M. Burghammer, P. Fratzl, H. S. Gupta and W. Wagermaier (2012). "Synchrotron 3D SAXS analysis of bone nanostructure." *Bioinspired, Biomimetic and Nanobiomaterials,* **1**(2)

Georgiadis, M., M. Guizar-Sicairos, A. Zwahlen, A.J. Trüssel, O. Bunk, R. Müller and P. Schneider (2015). "3D scanning SAXS: A novel method for the assessment of bone ultrastructure Orientation." *Bone* **71**

(161) 3D *in situ* characterisation of the impregnation of model fibre networks using real time synchroton X-ray microtomography

*S. ROLLAND DU ROSCOAT[1,2,3], P. J. J. DUMONT[4,5,6], P. CARION[1,2,4,5,6], L. ORGEAS[1,2], J. F. BLOCH[4,5,6], C. GEINDREAU[1,2], M. TERRIEN[4,5,6], P. CHARRIER[1,2], P. J. LIOTIER[7], S. DRAPIER[7], M. PUCCI[7]
sabine.rollandduroscoat@3sr-grenoble.fr

1 Univ. Grenoble Alpes, 3SR, F-38000 Grenoble, France
2 CNRS, 3SR, F-38000 Grenoble, France
3 ESRF, ID 19 Topography and Microtomography Group, F-38043 Grenoble cedex, France
4 Univ. Grenoble Alpes, LGP2, F-38000 Grenoble, France
5 CNRS, LGP2, F-38000 Grenoble, France
6 Agefpi, LGP2, F-38000 Grenoble, France
7 Ecole des Mines de Saint-Etienne, F-42000 Saint-Etienne, France

Polymer impregnation is a crucial phase of manufacturing processes for polymer composites that are reinforced by fibre bundles. Inhomogeneous impregnation leads to the presence of residual pores within the polymer matrix or to non-impregnated dry zones within the fibre bundles. These defects are detrimental for the end-use properties of composite parts. Most of the theoretical and experimental studies of the impregnation of composite materials are conducted at a mesoscopic scale, *i.e.*, at the scale of an assembly of several fibre bundles or at a macroscopic scale, *i.e.*, at the scale of a composite part. The resulting impregnation models have a structure close to the Lucas-Washburn law where the impregnation phenomena are governed by the permeability of the fibrous media and by capillarity effects for which the polymer-air surface tension and the polymer viscosity are the main parameters. However, these models do not enable a proper prediction of the impregnation of fibrous materials at the fibre scale, *e.g.* within the fibre bundles, as well as of the coupled evolution of the 3D architecture of fibrous materials. Hence, these approaches are not sufficient to understand the presence of residual pores or inhomogeneous infiltration phenomena.

Thus, the objective of this study was to provide an enhanced description of the impregnation phenomena of fibrous and porous media at the fibre scale. For that purpose real time synchrotron X-ray microtomography was used. This technique enables the visualisation and the quantification of the fluid propagation inside model fibrous media as well as the evolution of the fibrous microstructures.

The impregnation of model fibrous networks was studied using a device that was specially designed. This device was equipped with a reservoir filled with the impregnating fluid. The experiments consisted in immersing at constant velocity a model fibrous network in the fluid, and then removing it. This device was also equipped with a force sensor to measure the force that developed during impregnation onto the fibrous network by the impregnating fluid.

A series of tests was conducted using model fibrous networks that consisted of various assemblies of glass fibers with 2D ordered or 3D random microstructures. The fiber surface was also chemically treated to modify their wettability. Distilled water and several silicone oils were used as impregnating model fluids because of their various viscous and capillary properties.

For each impregnation test, several scans were recorded in a few seconds to follow the fluid front propagation inside the fibrous network. The analysis of the obtained images enabled an unprecedented description of the dynamic evolution of the 3D curvature of the fluid-air interface, the advancing and receding contact angles, and the volume fraction of the different constituents (entrapped air and fluid within the fibrous network) during impregnation.

(183) Combining nano X-ray Tomography and X-ray Fluorescence for *In Situ* Observations and 3D Chemical Segmentation

T. LEY[1], Q. HU[1], T. KIM[1], M. MORADIAN[1], J. HANAN[1], V. ROSE[2], R. WINARSKI[3], J. GELB[4]
tyler.ley@okstate.edu

1 Oklahoma State University
2 Argonne National Laboratory, Advanced Photon Source
3 Argonne National Laboratory, Center for Nanoscale Materials
4 Zeiss X-ray Microscopy

Data will be presented that combines the 3D structure and chemical mapping at the nano scale of in-situ hydration with portland cement based systems in a number of different solutions and temperatures. This work uses novel *in situ* reaction cells with both synchrotron and lab scale nano X-ray computed tomography and X-ray fluorescence. For several key samples a novel data fusion technique is presented named Tomography Assisted Chemical Correlation or **TACCo**. This technique combines two dimensional data sets of chemical data with three dimensional data from X-ray computed tomography to build 3D constitutive models. An overview of the method will be presented.

When these observations are combined over time then this allows a powerful five dimensional data set to be created that can investigate how the three dimensional spatial resolution, and chemistry evolve with time. The results are used for both data visualization and quantitative analysis. The results are combined with other experimental techniques and simulations to provide greater insights into these complex reactions.

Although the findings will be of interest to those that study cementitious systems, the presentation will highlight powerful experimental techniques and tools at the nanoscale that can be used on any material where structural and chemical mapping is of importance. The presentation also highlights the power of X-ray imaging to make time resolved and quantitative measurements of volume and material changes in complex systems.

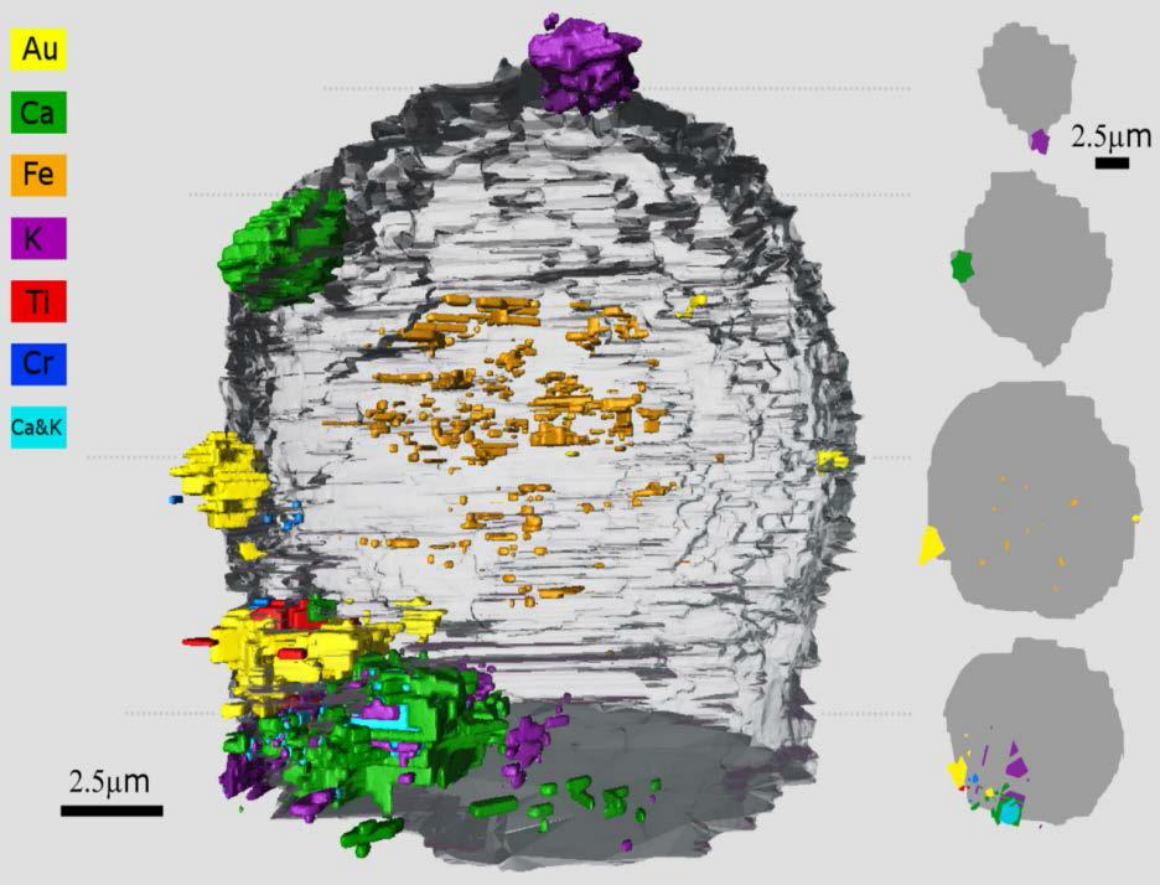

Figure1.Three dimensional chemical and structure analysis of a fly ash particle using TACCo

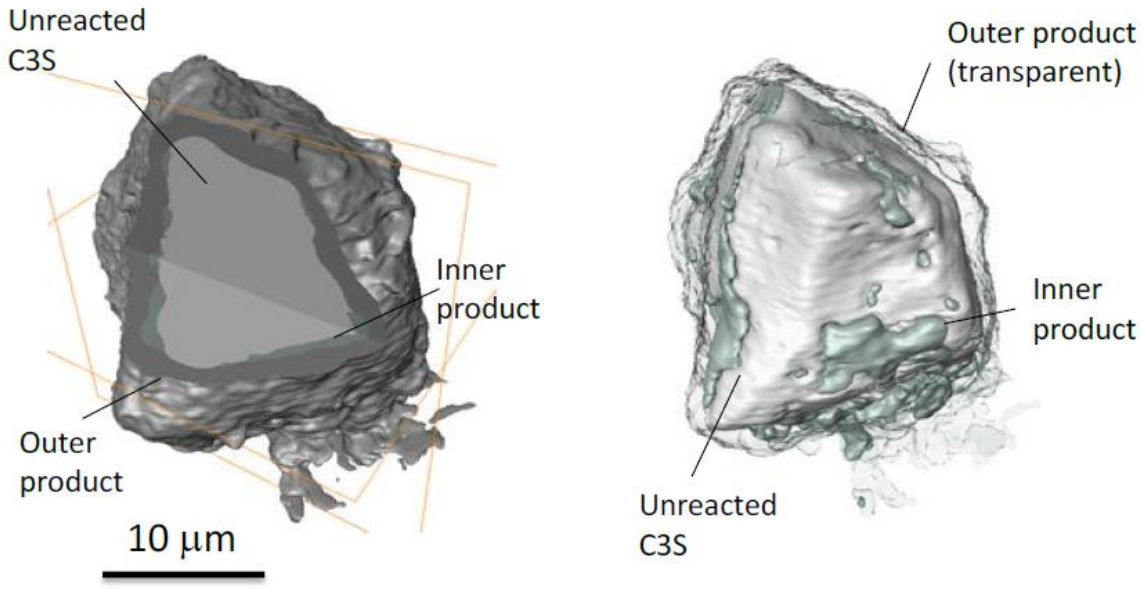

Figure 2. A partially reacted cement grain

(040) A small step beyond resolution

E. ZELINGER[1], D. PODEA[2], V. BRUMFELD[3]
vlad.brumfeld@weizmann.ac.il

The Hebrew University of Jerusalem, Israel
"Vasile Goldis" Western University of Arad, Romania
The Weizmann Institute of Science, Israel

X-ray tomographic microscopy at micron resolution (micro CT) reveals 3D structural details of non-transparent objects that are not accessible by any other experimental methods. However the 1μm resolution limit is frustrating, especially (but not only) when studying biological tissues.

Our work describes some methods for attaining the resolution limits of our instruments and sometimes for exceeding them. We are introducing a new staining agent that helps increasing contrast in samples such as plant meristema, a correlative x-ray and light microscopies that reveals minute structural and functional details of the sexual apparatus of drosophila, a low voltage x-ray source setup that allows visualization of organic crystals in the crayfish eye and a method for the use of image skeletonization for estimating the orientation of nanotubes embedded in different materials.

(066) X-ray Tube Spectrum Determination for Quantitative Interpretation of Reconstructed Micro-CT Images

*O. A. KOVALEVA[1], D. A. KOROBKOV[2], I. V. YAKIMCHUK[2]
okovaleva@slb.com

[1] Moscow Institute of Physics and Technology, Dolgoprudny, Russian Federation
[2] Schlumberger Moscow Research, Russian Federation

Industrial application of X-ray CT (micro-, nano-) involves both data acquisition and the following data interpretation. Undoubtedly, the results of the latter stage strongly depend on the quality of experimental data. Nevertheless, correct interpretation of CT data is still rather independent and challenging field of research. For better understanding and subsequent analysis of the images, obtained by the means of computed tomography, it is essential to be aware of technical characteristics of the laboratory equipment, especially X-ray source properties.

One of such properties that dramatically influence on the interpretation of reconstructed images is X-ray source energy spectrum. As an example, spectrum neglecting or erreneous estimation may lead to mistakes in mineral analysis of the core plugs. This issue originates from the physics of X-ray interaction with studied sample. Experimentally observed attenuations on shadow projections are related to an ‘effective’ absorption of X-ray photons with various energies of the beam spectrum.

The direct measurement of X-ray tube spectrum is rather costly and not trivial procedure, especially for usual CT-scanner end users. Also, it should be taken into account that for the time of X-ray tube usage its spectrum may alter. For these reasons, a simple way for spectrum determination may be required. Tube spectrum reconstruction from transmission data is one of the suitable solutions for that.

The problem of X-ray spectrum reconstruction out of transmission (attenuation) values continues to be acute. We present and analyze several approaches suggested from the early days of X-rays, and propose alternative technique. Proposed idea is based on experiment with a specimen of known mineral (chemical) content and geometrical shape.

(099) Laboratory Nano-CT Using Geometric Magnification

*P. STAHLHUT[1,3], A. HOELZING[1,2], J. ENGELS[1,2], R. HANKE[1,2]
philipp.stahlhut@physik.uni-wuerzburg.de

[1] Chair of X-ray Microscopy, University Wuerzburg, Josef-Martin-Weg 63, 97074 Wuerzburg, Germany
[2] Fraunhofer Development Center X-ray Technology EZRT, Flugplatzstraße 75, 90768 Fuerth
[3] Zentralinstitut fuer Neue Materialien und Prozesstechnik, Dr.-Mack-Str. 81, 90762 Fuerth

We present a computed tomography (CT) setup for material characterization with significantly improved resolution as compared to state-of-the-art micro- or subµ-CT systems. The introduced system is composed of a customized JEOL-JSM7100F scanning electron microscope [1]. By using the focused electron beam of the system with a 30 kV acceleration voltage, we create a very small X-ray source spot in a tungsten or molybdenum tip with a curvature radius of about 30 nm. We formed and optimized the shape of the metal tips by a quick and reliable electrochemical etchingprocess [2]. With the constraints that the object-target distances (under 1 mm) are much smaller than the object-detector distances (over 40 cm) and by using a pixilated detector (55 µm pixelsize), the resolution is only determined by the X-ray sourcespot for geometric magnification.

The detector is a PIXIRAD2 photon counting detector with a 1 mm thick CdTe sensorlayer and 1024x476 pixels. Despite the low flux of the source, the CdTe sensorlayer is rather efficient and due to the case that no optical elements are required in the beampath, the photon saturation of the system is pretty reasonable. As a consequence, exposure times of about 10 to 20 minutes per projection with a spatial resolution below 100 nm are approachable. Due to the ultra small X-ray sourcespot, the system is also capable of inline phase contrast imaging, which comes in handy especially for low contrast imaging.

We will present details about the electrochemical etching process, the experimental setup of the X-ray microscope, as well as some high resolution radiographies and a prospect of 3D nano-CT.

References :
[1] P.Stahlhut, T. Ebensperger, et al.; 2013; J. Phys.: Conf. Ser. 463 012007
[2] M. Fotino; 1992; Rev. Sci. Instrum. 64 159-167

(124) Commerical lithium-ion batteries, neutron tomography and diffraction, PCA-MCR, and SNARK

*A. BROOKS, J. YUAN, L. BUTLER
abroo38@tigers.lsu.edu

Department of Chemistry, Louisiana State University, 232 Choppin Hall, Baton Rouge, LA, 70803, USA

A commercial lithium-ion battery is a challenging sample for neutron tomography. On one hand, a 3D data set of a operating battery would be extremely useful, but hydrogen scattering and lithium absorption conspire against neutron imaging. Herein, we assess these experiments when applied to new 350 mAhr lithium cobalt oxide batteries and corresponding worn batteries. Neutron tomography was performed at FRM II ANTARES and the diffraction studied at SNS VULCAN. Prior neutron radiography has shown sensitivity to the LiC6 Bragg edge at 3.7 Å. Other researchers have used X-ray and neutron diffraction to monitor electrochemistry of non-commerical batteries. Cai, Wang, Rodriguez

Two software packages have been extensively used in this work. The diffraction studies use a Matlab-based PCA MCR-ALS toolbox (http://mcrals.info) to interprete the neutron diffraction data as a function of battery discharge. The initial neutron tomography used the filtered back-projection reconstruction algorithm. However, the low signal-to-noise ratios in the reconstructed slices hinder meaningful image interpretation. The SNARK09 system was used to explore iterative tomography reconstruction options.

The neutron diffraction analysis started with principal component analysis (PCA) based on crystallographic information for the battery constituents: Cu, Al, LiCx, and LixCoO2, including slight modifications to unit cell parameters to match the experimental diffraction. While diffraction data were collected over d-spacings of 0.5 to 2.4 Å, selected regions were chosen for analysis, eliminating, for example, the intense Cu (002) peak. The PCA as a function of battery charge state was followed with the multivariate curve resolution-alternating least squares (MCR-ALS) algorithm. This allowed quantitation of LiC6 conversion to LiC12, LiC18, and to graphite whilst $Li_{0.5}CoO_2$ is converted to $Li_{0.75}CoO_2$ and then to $LiCoO_2$. The MCR-ALS analysis also indicated the electrochemical differences between fresh and worn batteries.

References :
Cai, L., An, K., Feng, Z., Liang, C., Harris, S. J. *J. Power Sources.* **2013**, *236*, 163-168.
Rodriguez, M., Van Benthem, M. H., Ingersoll, D. *Powder Diffr.* **2010**, *25*, 143-148.
Wang, X-L, An, K., Cai, L., Feng, Z., Nagler, S. E., Daniel, C., Rhodes, K. J., Stoica, A. D., Skorpenske, H. D., Liang, C., Zhang, W., Kim, J., Qi, Y., Harris, S. J. *Sci. Rep.* **2012**, *2: 747*, 1-7.

(126) New capabilities in X-ray microscopy for understanding microstructural evolution over time and length scales

*W. HARRIS[1], A. MERKLE[1], J. GELB[1], L. LAVERY[1], C. HOLZNER[1]
william.harris@zeiss.com

[1] Carl Zeiss X-ray Microscopy, Inc., Pleasanton, CA, USA

X-ray tomography is a powerful 3D characterization tool due to its nondestructive operation, accommodation of an array of sample types and sizes, and lack of need for a vacuum environment. However, the traditional projection-based MicroCT architecture, relying on geometric magnification to obtain high resolution, imposes inherent limitations on the detail that can be revealed for large samples/working distances. Conversely, recent X-ray microscopes (XRM) have adopted new designs derived from synchrotron technology to improve the flexibility of laboratory instruments. The resulting instruments, including both sub-micron projection-based and nanofocus transmission X-ray microscopes, are able to effectively de-couple the working distance/resolution dependence, creating new opportunities for resolving small features on both large samples and samples contained within *in situ* stages.

Notably, the nanoscale XRM architecture, which utilizes a quasi-monochromatic X-ray beam directed by a capillary condenser and Fresnel zone plate lens, is now offered at one of two optional X-ray energies, 8.0 or 5.4 keV. As the attenuation of a sample is a function of both density and beam energy, the new flexibility enables system selection that fits the application need, resulting in higher contrast, throughput, and data quality. By accomodating samples on the order of tens to hundreds of microns in size and providing spatial resolution down to 50 nm, these microscopes cover a nondestructive 3D imaging gap between TEM and micron-scale CT, and are also effectively positioned to correlate data with 3D, but destructive, FIB-SEM imaging.

On the larger length scales, a detector architecture consisting of a scintillator-coupled optical magnification step has increased the possibilities of what can be achieved in a polychromatic, high energy, laboratory system. By removing the dependence on high geometric magnification, large samples and working distances can be examined without sacrificing resolution. This architecture also enables new contrast modalities, including propagation phase contrast for enhancing low-Z samples, and diffraction contrast for extracting 3D crystallographic information such as quantitative grain orientation.

Regardless of length scale or platform, a strong advantage of X-ray tomography is the nondestructive nature, which enables imaging of 3D microstructures over time, so-called '4D'. This capability has been leveraged in both *ex situ* and *in situ* arrangements for a variety of samples. While *ex situ* is often simpler from a logistical perspective, *in situ* studies are sometimes essential due to a number of distinct advantages: 1) An *in situ* 4D study eases the experimental challenge of tracking a specific interior volume of interest within the field of view, especially if this volume is contained within a larger sample or changes substantially during sample treatment, 2) The physical transfer of a sample to and from the microscope in an *ex situ* study may introduce unintentional modification (for example due to gas environment, vibration, temperature change, etc.), and 3) In some studies the stimulus must be maintained to provide meaningful results, as is the case for mechanical load and the propagation of cracks.

This work will cover several prominent studies enabled by *in situ* XRM. Two examples will demonstrate mechanical loading, first through application of a tensile rig to generate multiple stages of cracking and pore-scale deformation in a steel laser weld. A second example demonstrates compressive, non-uniform loading of a fibrous gas diffusion layer typical of low

temperature fuel cell electrodes, along with the implications of compression on porosity and transport processes within the structure [1]. A third example will be used to illustrate electrochemical cycling of a lithium ion battery electrode to observe the detailed particle-level degradation effects that occur during the lithiation/de-lithiation processes [2].

References :
[1] Khajeh-Hosseini-Dalasm et al., Journal of Power Sources **266** (2014)
[2] Gonzalez et al., Journal of Power Sources **269** (2014)

(127) Diffraction contrast tomography as an additional characterization modality on a 3D laboratory X-ray microscope

*C. HOLZNER[1], A. MERKLE[1], P. REISCHIG[2], E. M. LAURIDSEN[2], M. FESER[1]
christian.holzner@zeiss.com

1 Carl Zeiss X-ray Microscopy, Inc., 4385 Hopyard Rd. Suite 100, Pleasanton, CA 94566, USA
2 Xnovo Technology ApS, Galoche Alle 15, 4600 Køge, Denmark

We introduce a novel method to add grain position, orientation and size information to absorption 3-D X-ray microscope imaging for poly-crystalline samples. This imaging modality is available on a commercial X-ray microscope and will open the way for routine, nondestructive studies of time-evolution of grain structure to complement 3D EBSD characterization. Grain sizes below 40 micrometers can be studied using this non-destructive imaging modality.

Crystallographic imaging (i.e. imaging of crystallites/grains in polycrystalline materials) are primarily known from electron microscopy, and particularly the introduction of the electron back-scattering diffraction (EBSD) technique in the early 1990's, has made it a routine tool for research and/or development related to metallurgy, functional ceramics, semi-conductors, geology etc. The ability to image the grain structure in such materials is instrumental for understanding and optimization of material properties and processing. However, the destructive nature of 3D EBSD prevents the technique from directly evaluating the microstructure (and grain-orientation) evolution when subject to either mechanical, thermal or other environmental conditions. Non-destructive x-ray imaging methods allow for such '4D' time dependent studies, and to date have been primarily the domain of a limited number of synchrotron facilities.

Here, we present a novel method to acquire, reconstruct and analyze grain orientation and related information from polycrystalline samples on a commercial laboratory x-ray microscope (ZEISS Xradia 520 Versa) that utilizes a synchrotron-style detection system.

Known as laboratory diffraction contrast tomography (DCT), this technique may be efficiently coupled to *in situ* environments within the microscope or subject to an extended time evolution experiment (across days, weeks, months), which remains a unique strength of laboratory (non-synchrotron) experiments. Following an evolution experiment, the sample may be sent to the electron microscope or focused ion beam (FIB-SEM) for destructive but complementary investigation of the same volume of interest. Methodologies for such workflows have also been recently enabled by an advanced correlative workspace environment (ZEISS Atlas 5) [1].

We will show a selection of results of laboratory DCT, discuss the boundary conditions of such a method, and point to the future to discuss ways in which this can be correlatively coupled to related techniques for a better understanding of a materials structure evolution in 3D at multiple length scales.

References :
[1] A. P. Merkle et al., Automated Correlative Tomography Using XRM and FIB-SEM to Span Length Scales and Modalities in 3D Materials, Microscopy and Analysis, 28 (2014), p. S10-S13

(174) Nanoscale 4-D imaging during mechanical testing: application to crack growth in dentin

X. LU[1], R. S. BRADLEY[1], B. HORNBERGER[2], M. LEIBOWITZ[2], A. TKACHUK[2], S. ETCHIN[2], P. J. WITHERS[1]
xuekun.lu@postgrad.manchester.ac.uk

[1] Henry Moseley X-ray Imaging Facility, School of Materials, The University of Manchester, M1 7HS, UK
[2] Carl Zeiss X-ray Microscopy, Pleasanton, CA 94588, USA

High resolution x-ray tomography can enable the evolution of microstructure to be studied on the nanoscale. We report on the development and application of a new in-situ micro mechanical test rig, specifically designed to be accommodated within x-ray nanoCT scanner. The device was used to study progressive crack growth in dentin in different orientations, and thereby provide insights into the relationship between microstructure and anisotropic fracture toughness [1, 2].

Dentin is a nano-composite material which forms the bulk of the mineralised tissue in human teeth. The mineralised component, hydroxyapatite, is believed to provide strength while the organic collagen matrix contributes to toughness [3-5]. A key feature of dentin is the presence of tubules, which run from enamel layer to the pulp chamber, are microscopic channels occupied by odontoblasts during dentinogenesis. The micro mechanical test rig was applied with an indenter to initiate and propagate cracks within elephant dentin parallel and perpendicular to the tubules. At each progressive stage, x-ray nanotomography was used to characterise the evolution of the cracks with respect to the tubules. Quantitative analysis was carried out to provide insight into the anisotropic fracture behaviour and crack shielding mechanisms.

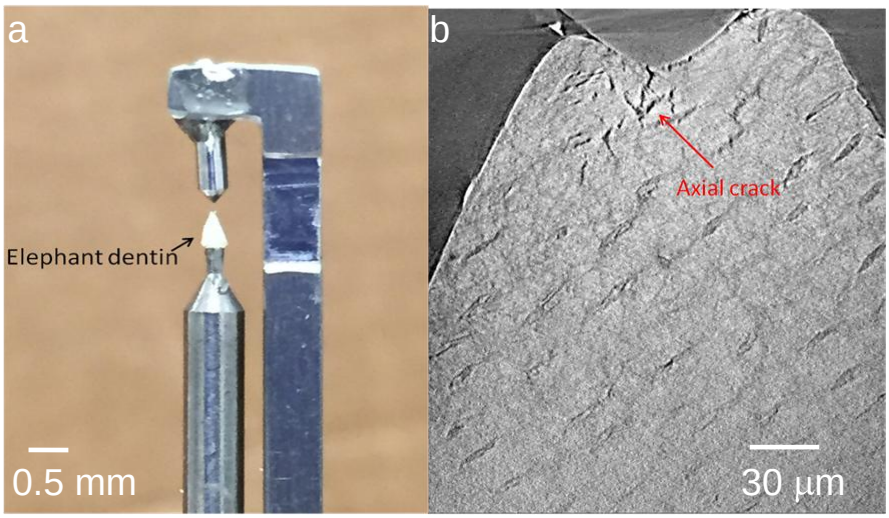

Figure 2 (a) The alignment of the micro indenter and the elephant dentin used for the experiment; (b) An orthoslice of the dentin data showing the crack generated by the indenter in depth direction

References ;
1. Kruzic, J., et al., *Crack blunting, crack bridging and resistance-curve fracture mechanics in dentin: effect of hydration.* Biomaterials, 2003. **24**(28): p. 5209-5221.
2. Nalla, R.K., J.H. Kinney, and R.O. Ritchie, *Effect of orientation on the in vitro fracture toughness of dentin: the role of toughening mechanisms.* Biomaterials, 2003. **24**(22): p. 3955-3968.
3. Arola, D.D. and R.K. Reprogel, *Tubule orientation and the fatigue strength of human dentin.* Biomaterials, 2006. **27**(9): p. 2131-2140.
4. Locke, M., *Structure of ivory.* Journal of Morphology, 2008. 269(4): p. 423-450.
5. Miles, A.E.W. and A. Boyde, Observations on Structure of Elephant Ivory. Journal of Anatomy, 1961. 95(3): p. 450-&.

Session 205 - Developing image analysis tools for synchrotron

(048) A computational toolbox for the data processing pipeline of four-dimensional data from phase contrast X-ray tomography

A. J. SHAHANI[1], E. BEGUM GULSOY[1], J. W. GIBBS[1,2], J. L. FIFE[3], X. XIAO[4], P. W. VOORHEES[1,3]
p-voorhees@northwestern.edu

[1] Department of Materials Science and Engineering, Northwestern University, Evanston, IL 60208, USA shahani@u.northwestern.edu
[2] Materials Science and Technology Division, Los Alamos National Laboratory, Los Alamos, NM 87545, USA
[3] Swiss Light Source, Paul Scherrer Institut, 5232 Villigen, Switzerland
[4] X-ray Science Division, Argonne National Laboratory, Lemont, IL 60439 USA

The growing size of data collected during X-ray computed tomography (XCT), typically on the order of terabytes, renders manual segmentation impractical. Furthermore, processing datasets from phase contrast XCT is nontrivial because of the inherently low-pass characteristics of single image phase retrieval, which results in diffuse interfaces. To circumvent the problems in processing phase contrast images, we have developed a computational toolbox, involving non-linear diffusion filtering and bias-corrected fuzzy c-means algorithm, thereby enabling the automated segmentation of such images.

Once the images have been segmented and meshed, our toolbox also includes methods for quantitative microstructural analysis, such as the calculation of (i) interfacial normal distributions (INDs), the probability of finding an interfacial normal in a certain direction, (ii) interfacial shape distributions (ISDs), the probability of finding a patch of interface with a given pair of principal curvatures, and (iii) interfacial velocity. Using our integrated and fully automated approach, the three-dimensional coarsening morphologies of Al-29.9wt%Si and Al-32wt%Si-15wt%Cu alloys will be presented and discussed.

(049) Advanced noise-reduction and segmentation methods in X-ray computed micro-tomography

*S. S. SINGH[1], J. C. E. MERTENS[1], J. J. WILLIAMS[1], P. HRUBY[1], A. KIRUBANANDHAM[1], X. XIAO[2], F. DE CARLO[2], *N. CHAWLA[1]
nchawla@asu.edu

1 Materials Science and Engineering, Arizona State University, Tempe, AZ 85287-6106, USA
2 Advanced Photon Source, Argonne National Laboratory, Argonne, IL, USA

The study of material structure has been traditionally limited to two dimensional (2D) analyses. This approach is often limited and inadequate for solving many problems. Therefore, there has been an increasing demand for three dimensional (3D) analyses [1, 2]. Moreover, experiments may be performed to resolve time-dependent (4D) evolution of a variety of important phenomena such as fatigue damage and stress corrosion cracking (SCC) [3]. Among these volumetric techniques, X-ray tomography and serial sectioning have been used to characterize microstructure in 3D/4D with high spatial resolution.

A key aspect of microstructure data extraction involves the accurate segmentation of resolved phases. Prior to applying segmentation methods in a grayscale volume, the application of filtering for noise reduction is often critical, either due to the low signal typically achieved in microfocus x-ray imaging or very rapid synchrotron x-ray imaging, particularly in metallic systems. Noise reduction algorithms which have proven particularly effective in noisy metallic tomograms include the anisotropic diffusion, edge-preserving smoothing, and non-local means filters, which have been applied either volumetrically or slice-by-slice. The most effective segmentation method has been observed to vary depending on the contrast mode of the tomography (ex. x-ray phase vs. attenuation contrast modes), the nature of the sample, and the nature of the material phases of interest in multi-phase systems. Segmentation approaches that have demonstrated success include semi-automatic techniques which leverage both the intensity and intensity gradients within volume.

We have performed X-ray tomography (using the synchrotron source at the Advanced Photon Source at Argonne National Laboratory and a lab-scale x-ray source at Arizona State University) and serial sectioning to characterize the microstructure and understand the deformation behavior of several materials. X-ray synchrotron tomography was performed to understand the SCC and fatigue behavior of 7075 aluminum alloys [4-6] and Al-SiC composites [7]. Serial sectioning was performed in combination with electron back scattered diffraction (EBSD) yielding three dimensional crystallographic datasets. Furthermore, by leveraging lab-scale x-ray computed tomography, the 3D microstructure of a eutectic 63Sn-37Pb solder system has been characterized. The use of noise filtering and segmentation algorithms, primarily from within the Avizo® Fire package, will be discussed.

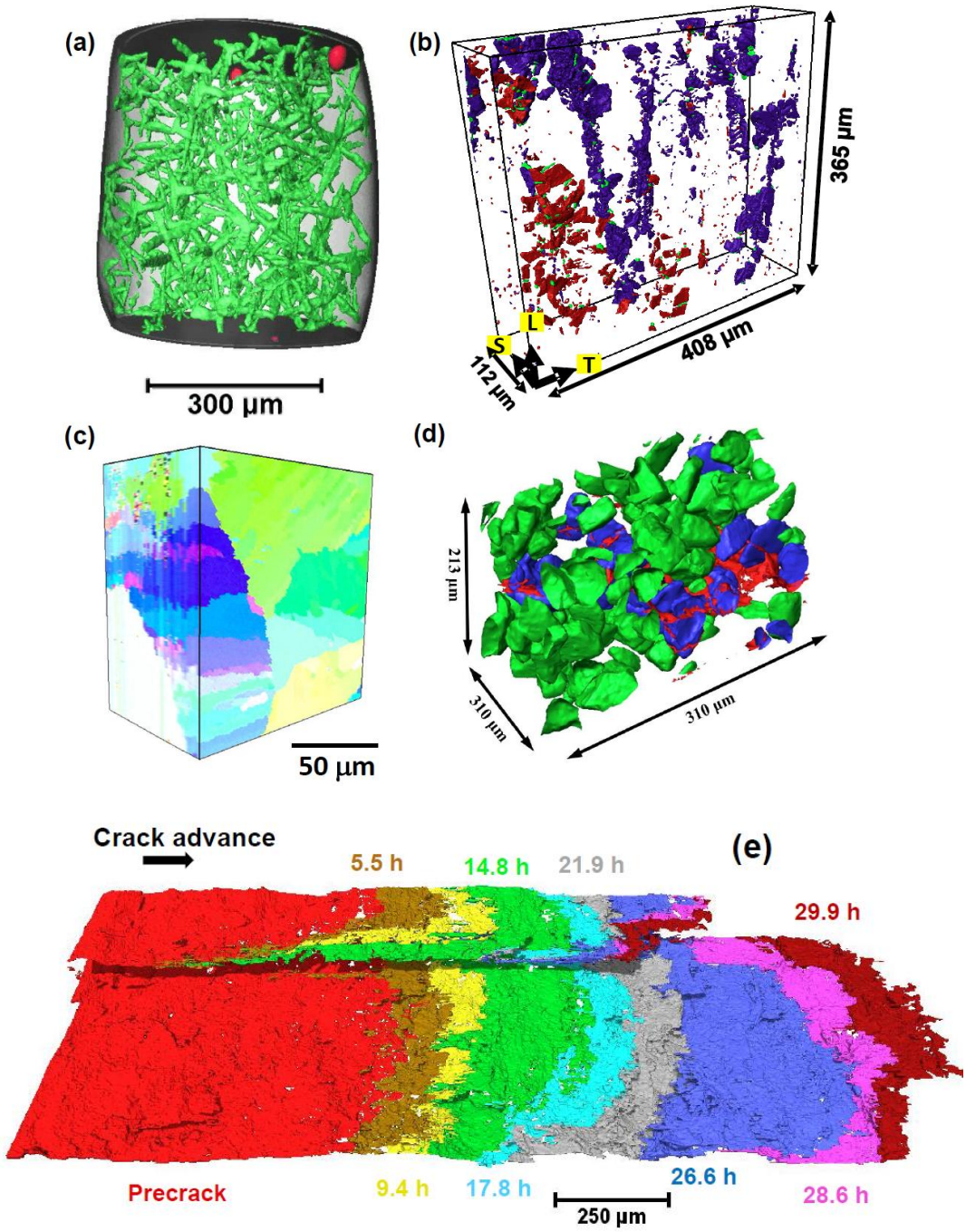

Fig. 1: *(a) Pb dendrites (green) and reflow porosity (red) in a microscale Pb-Sn alloy solder joint, (b) Inclusions and pores in AA7075, (c) A 3D grain map of a Sn-based microscale solder joint through serial-sectioning EBSD, (d) Fatigue crack interaction with SiC particles in an Al-SiC composite, and (e) A moisture induced SCC crack in AA7075.*

Reference :
1. S.S. Singh, C. Schwartzstein, J.J. Williams, X. Xiao, F. De Carlo, N. Chawla, J. Alloys Compounds, 602 (2014) 163-174.
2. J. C. E. Mertens, J. J. Williams, N. Chawla, Mater. Charact. 92 (2014) 36–48.
3. S.S. Singh, J.J. Williams, P. Hruby, X. Xiao, F. De Carlo, N. Chawla, Integr. Mater. Manufac. Innov., (2013) 2014, DOI 10.1186/2193-9772-3-9.
4. S.S. Singh, J.J. Williams, M. Lin, X. Xiao, F. De Carlo, N. Chawla, Mater. Res. Let. (2014) Submitted.
5. S. S. Singh, J. J. Williams, X. Xiao, F. De Carlo, N. Chawla, Fatigue of Materials II: Advances and Emergences in Understanding, Mater. Sci. Tech. (2012) 17-25.
6. J. J. Williams, K. E. Yazzie, E. Padilla, N. Chawla, X. Xiao, F. De Carlo, Int. J. Fatigue, (2013) 57 79-85.
7. P. Hruby, S.S. Singh, J.J. Williams, X. Xiao, F. De Carlo, N. Chawla, Int. J. Fatigue, (2014) Submitted.

(111) Upgraded ID01 @ ESRF: Nanodiffraction, full field diffraction microscopy and coherent diffraction imaging

*S. J. LEAKE[1], P. BOESECKE[1], H. DJAZOULI[1], G. A. CHAHINE[1], J. HILHORST[1], M. ELZO[1], M. I. RICHARD[1], G. BUSSONE[1], R. GRIFONE[1], S. FERNANDEZ[1], T. U.SCHULLI[1]
steven.leake@esrf.fr

[1] ESRF – The European Synchrotron, 71 Avenue des Martyrs, Grenoble, 38000, France

With the completion of the first phase of upgrade of the European Synchrotron Radiation Facility (ESRF), the ID01 beamline has returned successfully to user operation. We offer; scanning diffraction microscopy at 100Hz with 100nm focused x-ray beams [1], full field x-ray diffraction microscopy using compound refractive lenses [2] and coherent beams for coherent diffractive imaging applications [3].

The implementation of the future upgrade of the storage ring [4] and beamline will amplify data rates by a factor of 100 or more. The need for a generic set of tools (inter-synchrotron compatible) is clear given such a data deluge and to make such techniques routinely available to non-expert users. The emphasis from ID01 is to collaborate to generate a framework of such tools to avoid continuously reinventing the wheel.

A detailed breakdown from the data analysis perspective of the existing bottlenecks for all techniques will be provided from both the current and the future decade perspective. In addition the existing data flow from experiment to publication will be analysed.

References :
[1] G. A. Chahine, M.H. Zoellner, M-I. Richard, S. Guha, C. Reich, P. Zaumseil, G. Capellini, T. Schroeder and T. U. Schülli, Applied Physics Letters, 106, 071902 (2015)
[2] J. Hilhorst, F. Marschall, T.N. Tran Thi, A. Last and T. U. Schulli, J. Appl. Cryst. 47, 1882-1888. (2014).
[3] S. T. Haag, M-I. Richard, U. Welzel, V. Favre-Nicolin, O. Balmes, G. Richter, E. Mittemeijer and O. Thomas, Nano Lett., 13 (5), 1883–1889 (2013)
[4] ESRF: Phase II - white paper (http://www.esrf.eu/files/live/sites/www/files/about/upgrade/documentation/whitepaper-upgrade-phaseII.pdf)

(149) Tomography activities at advanced photon source

X. XIAO[1]
xhxiao@aps.anl.gov

1 Advanced Photon Source, Argonne National Laboratory

The non-destructive nature of X-ray tomography makes it a suitable tool in in situ dynamic phenomena studies. At APS, X-ray tomography has seen rapid growth in the past few years and it is spreading to multiple beamlines. In tomography applications image analysis is a key component in extracting quantitative structure information and further structure based modeling. Along with data complexity increase the image analysis tasks also increases and specific image analysis routines need to be designed according to the given data sets. In this presentation few science cases with quantitative image analysis will be shown. A general discussion on quantitative image analysis tasks in tomography works will be given on the end.

Acknowledgment: This research used resources of the Advanced Photon Source, a U.S. Department of Energy (DOE) Office of Science User Facility operated for the DOE Office of Science by Argonne National Laboratory under Contract No. DE-AC02-06CH11357.

(155) Bilateral denoising and region merging segmentation for micro-CT images

*S. J. LATHAM[1], A. M. KINGSTON[1], A. P. SHEPPARD[1]
shane.latham@anu.edu.au

[1] Department of Applied Mathematics, The Australian National University

The multi-class segmentation (classification) of voxels in X-ray micro-tomography images of porous materials is difficult due to image artifacts such as: noise, point-spread and cupping/beam-hardening. While there are a plethora of algorithms and software for de-noising and segmenting images, few of them have the capability to adequately handle tomographic artifacts and/or the large (10's of Gigabytes) image sizes. Typically, high-quality multi-class segmentations are only achieved with significant user input in each of multiple image-processing stages. This has the undesirable effect of introducing user-bias into the image analysis results, further complicating the task of comparing sample-tomograms acquired under diverse imaging conditions or analysed by different users. This paper presents a method for denoising 3D tomograms and a method for subsequent segmentation, both of which require minimal user input.

Our denoising method uses iterated bilateral-filtering [1,2] to increase the micro-CT tomogram contrast-to-noise ratio. In tests on synthetic images, the Gaussian noise standard deviation is decreased by at least a factor of 5 after only a few iterations. Despite this significant level of smoothing, fine features and edges are preserved.

Segmentation on the denoised image is performed using a 3D Statistical Region Merging (SRM) [3] algorithm. Our modified version achieves the following benefits: large salient segments, precise boundary placement, preservation of low contrast features and a contrast-based hierarchy of segmentations. While our modified SRM method does not explicitly account for cupping artefacts, the local nature of region growing combined with the low-gradient variation of cupping mean that this method produces desirable segments in samples with highly connected material phases.

We illustrate the effectiveness of our combined denoising and segmentation methods on synthetic 3D images and micro-CT tomograms of various geomaterials.

References :
[1] Tomasi, C., & Manduchi, R. (1998, January). Bilateral filtering for gray and color images. In Computer Vision, 1998. Sixth International Conference on (pp. 839-846). IEEE.
[2] Milanfar, P. (2011). A tour of modern image filtering. IEEE Signal Processing Magazine, 2.
[3] Nock, R., & Nielsen, F. (2004). Statistical region merging. Pattern Analysis and Machine Intelligence, IEEE Transactions on, 26(11), 1452-1458.

(162) CRAFT, a software tool to standartize CT environment.

*R. VESCOVI[1], E. MIQUELES[1], M. CARDOSO[1]
ravescovi@gmail.com

1 Laboratório Nacional de Luz Síncrotron, Rua Giuseppe Máximo Scolfaro, 10000, Campinas - State of São Paulo, 13083-100

CRAFT, a software tool to standartize the computed tomography environment, stands for Control, Reconstruction and Analisys for Tomography. It consists basically of a collection of python wrappers to generalize every aspect in an CT experiment. A simple dataflow provides the capability to integrate every tomography dataset (from different setups) with reconstruction and analisys algorithms. In the experimental part, it can generate simulated tomograpy experiments to test pre and pos aligment approachs and different reconstructions prograns (pyRAFT, Tomopy, pyHST2, etc). The main use of CRAFT is the control of the IMX Beamline in the LNLS (Brazilian Synchrotron Light Source). It provides the users with a simple python interface to reconstruct and analise the datasets using any after-experiment approach the user finds more suitable.

(176) The study of fluid-rock interaction in 4D

*F. FUSSEIS[1], W. ZHU[2], H. LISABETH[2], J. BEDFORD[3], H. LECLÉRE, X. XIAO
florian.fusseis@ed.ac.uk

[1] School of Geosciences, The University of Edinburgh, Edinburgh, UK
[2] Department of Geology, University of Maryland, College Park, USA
[3] School of Environmental Sciences, University of Liverpool, UK
[4] Advanced Photon Source, Argonne National Laboratory, USA

Fluid-rock interaction is at the core of many geological processes that are of immediate societal interest, including geothermal energy production, nuclear waste storage, CO_2 sequestration and many types of ore mineralisation. Until recently, experimental investigations of these processes relied on hydrothermal cells where reactions inside the vessel could only be indirectly monitored during experiments. This left many details of fluid-rock interaction unnoticed. Fusseis et al. (2014) presented an x-ray transparent hydrothermal cell that allows documenting fluid-rock interaction in 3-dimensional time-series datasets using Synchrotron x-ray microtomography.

In this contribution we use experimental data from novel in-situ studies on olivine carbonation and gypsum dehydration to show the enormous potential of conducting fluid-rock interaction studies in 4D using x-ray transparent cells. Both processes have been investigated in numerous studies, yet our experiments at beamline 2BM at the Advanced Photon Source provide completely new insights.

For the first time, we documented the reaction of forsterite with a $NaHCO_3$-saturated brine to form magnesite and quartz at 200°C and 15 MPa Pc/10 MPa Pf in 379 3-dimensional datasets with a resolution of 1.3 µm. This experiment produced about 20 TB of reconstructed data. Our data enable observing and quantifying the advance of the reaction on the µm-scale (the scale of individual grains) and led to the formulation of a new model for the self-supported carbonation of polycrystalline olivine. These data yielded promising new hints towards the harnessing of this technique to sequester CO_2.

In second series of experiment, we dehydrated polycrystalline gypsum (alabaster) to produce hemihydrate (plaster of Paris) at 115°C, 10 MPa Pc and 7 Mpa Pf. Our study, which yielded 120 3-dimensional datasets, is the first to document the growth of hemihydrate needles from their nucleation to the point of full conversion of our millimetre-sized sample in 4D. Again, the time-resolved 3D data allowed the formulation of a new model for the formation of hemihydrate needles that centred around porous tubes, in which the hemihydrate needles grew.

The large amount of data produced during these time-resolved studies poses challenges for the down-stream analysis and quantification. In this contribution we will also present our workflow from data acquisition through storage and processing to the determination of results that are ready for publication.

References :
If you want to add references, please use an author/date style.

(186) Scikit-image and the Python ecosystem for 3-D image processing

S. VAN DER WALT[1], *E. GOUILLART[2], J. NUNEZ-IGLESIAS[2]
emmanuelle.gouillart@nsup.org

1 Division of Applied Mathematics, Stellenbosch University, Stellenbosch 7600, South Africa
2 Surface du Verre et Interfaces, UMR 125 CNRS/Saint-Gobain, 93303 Aubervilliers, France
3 Victorian Life Sciences Computation Initiative, Carlton, VIC, Australia

Scikit-image [VanDerWalt2014] is a general purpose image processing library for the Python programming language. It is designed to interact efficiently with other popular scientific Python libraries, such as NumPy and SciPy. In particular, scikit-image leverages the powerful data array container of NumPy, that can store images of various dimensions (2-D, 2D RGB, 3D, 4D...).

Most users of scikit-image use the package in order to process 2-D grayscale or color images; however, a large fraction of the available functions are implemented for 3-D images as well, allowing tomography users to process their images directly in 3-D. The different stages of a typical 3-D image processing pipeline are available within scikit-image, with a large choice of filtering algorithms (for example denoising algorithms, that are often necessary for noisy ultrafast tomography data or for the correction of artifacts), mathematical morphology tools, segmentation algorithms, feature detection and measurements on segmented objects. Several standard tools of scikit-image are very common and can be found in other 3-D image processing libraries, such as automatic thresholding with Otsu method, or basic mathematical morphology operations. However, scikit-image also implements a few algorithms that are closer to the state of the art, such as total variation denoising, superpixel segmentation or random walker segmentation. Among the international team of developers (https://github.com/scikit-image/scikit-image/graphs/contributors), many are researchers working with tomography images, ensuring that special care is given to good performances for the processing of large 3-D images.

Users of scikit-image also leverage the Python language, that is both powerful, elegant and easy to use, as well as the “ecosystem” of available scientific libraries. For example, powerful 3-D visualization is provided by the Mayavi [Ramachandran2011] package, that interacts smoothly with scikit-image. Using such packages, tailored interactive interfaces based on 3-D visualization and image processing can be written with a few lines of code. Scikit-image also interacts well with the popular scikit-learn package [Pedregosa2011], making it possible to include machine learning operations in image processing pipelines.

Scikit-image is released under the permissive BSD open-source license, enabling both its free usage, and its inclusion in other softwares, including commercial products. The number of users has been growing steadily over the past year, with the total number of download reaching 150,000 on the PyPI platform. The website of the project (http://scikit-image.org/) offers a comprehensive gallery of images and the associated code for a large variety of image processing operations, allowing users to discover the possibilities of the library in an intuitive and self-learning way.

References :
[VanDerWalt2014] VAN DER WALT, Stefan, SCHÖNBERGER, Johannes L., NUNEZ-IGLESIAS, Juan, et al. scikit-image: image processing in Python. PeerJ, 2014, vol. 2, p. E453.
[Ramachandran2011] RAMACHANDRAN, Prabhu et VAROQUAUX, Gaël. Mayavi: 3D visualization of scientific data. *Computing in Science & Engineering*, 2011, vol. 13, no 2, p. 40-51.
[Pedregosa2011] PEDREGOSA, Fabian, VAROQUAUX, Gaël, GRAMFORT, Alexandre, et al. Scikit-learn: Machine learning in Python. The Journal of Machine Learning Research, 2011, vol. 12, p. 2825-2830.

(196) Multi-resolution characterisation of grain-based measurements from X-ray tomography

*E. ANDÒ[1,2], A. TENGATTINI[1,2,3], M. WIEBICKE[1,2,4], G. VIGGIANI[1,2], S. SALAGER[1,2]
edward.ando@3sr-grenoble.fr

[1] Univ. Grenoble Alpes, 3SR, F-38000 Grenoble, France
[2] CNRS, 3SR, F-38000 Grenoble, France
[3] School of Civil Engineering, The University of Sydney, Sydney, NSW 2006, Australia
[4] Technische Universität Dresden, Institute of Geotechnical Engineering, Germany

In the mechanics of granular media, the ability to perform experiments *in-situ* inside an x-ray scanner is allowing a three-dimensional revolution in the data that can be obtained from experiments. From the 1970s, visionaries such as Oda [1,2] have started to describe the state of a granular medium at the *grain scale*, defining quantities that describe a granular "fabric", *i.e.*, the orientation of the grains, their contacts as well as the pore space around them, which drive the macroscopic (engineering) scale behaviour. This information is readily available from simple numerical (*e.g.* DEM) simulations, but is much more difficult to obtain experimentally. Enter x-ray tomography: allowing not only the measurement of these quantities in 3D on real materials, but also their evolution. This in turn finally opens up the possibility for constitutive models describing the soil behaviour to be created including elements of fabric measured on real 3D granular materials [3], which can be used to greatly improve civil engineering simulations of soil structures.

Previous work on the measurement of granular kinematics [4,5] shows that grain displacements and rotations can be measured individually and accurately in large deformation events such as shear bands, whose grain-scale behaviour can then be related back to macroscopic quantities such as stress and strain. Granular fabric is expected (by the micro-mechanics community in general) to provide a grain scale explanation for more elusive phenomena, such as the enormous change in stiffness upon load reversal, which is manifested at small levels of strain. Such problems, where grains have minuscule displacements, require extremely precise tools: this presentation will cover a number of works-in-progress in this field under way in Grenoble, such as:

- temperature-invariant tools to improve x-ray reconstruction fidelity [6]
- the analytical simulation of the partial-volume-effect of a sphere imaged in 3D, allowing 1) the pore space of a spherical granular medium to be characterised with unprecedented precision and 2) realistic 3D spheres to be easily generated for testing various fabric-measurement algorithms [7]
- the significant improvement in the challenging field of the measurement of orientation of inter-granular contacts, both by improving the output of a watershed [8] and by using 3D Level Sets to smoothly describe grains [9]
- a multi-resolution study of the "snapping" (jumping to some preferred orientations) in the measurement of the major inertial axes defining the grain orientations, by starting from ground-truths obtained by scanning single particles at a pixel size of 350 nanometres/px [10].

These different elements form a strong basis for a 3D granular fabric toolkit being developed in Grenoble.

References :
[1] Oda, M. (1972). Initial fabrics and their relations to mechanical properties of granular material. Soils and foundations, 12:17–36

[2] Oda, M. and Iwashita, K. (1999). Mechanics of Granular Materials, An Introduction. Balkema, Rotterdam, Netherlands, 1st edition
[3] Fu, P., & Dafalias, Y. F. (2011). Fabric evolution within shear bands of granular materials and its relation to critical state theory. International Journal for numerical and analytical methods in geomechanics, 35(18), 1918-1948.
[4] Hasan, A. and Alshibli, K. A. (2012) "Three Dimensional Fabric Evolution of Sheared Sand", Granular Matter, Vol. 14, No. 4, pp. 469-482.
[5] Ando, E., Hall, S. A., Viggiani, G., Desrues, J., & Bésuelle, P. (2012). Grain-scale experimental investigation of localised deformation in sand: a discrete particle tracking approach. Acta Geotechnica, 7(1), 1-13
[6] French Patent 14/53091 (2014). Dispositif de mesure de déplacements parasites dans un tomographe à rayons X
[7] Tengattini, A & Andò, E. (2015) Kalisphera: an analytical tool to reproduce the partialvolume effect of spheres imaged in 3D. Submitted to IOP Measurement Science and Technology, in review
[8] Jaquet, C., Andó, E., Viggiani, G., & Talbot, H. (2013). Estimation of Separating Planes between Touching 3D Objects Using Power Watershed. In Mathematical Morphology and Its Applications to Signal and Image Processing (pp. 452-463). Springer Berlin Heidelberg
[9] Andrade, J. E., Vlahinić, I., Lim, K. W., & Jerves, A. (2012). Multiscale 'tomography-to-simulation' framework for granular matter: the road ahead. Géotechnique Letters, 2(July-September), 13
[10] Wiebicke, M. Andò, E., Viggiani, G, Herle, I. (2015) Towards the measurement of fabric in granular materials with x-ray tomography. Submitted to IS-Buenos Aires, 2015.

(009) Feasibility of iterative phase contrast tomography

*N. T. VO, R. C. ATWOOD, M. DRAKOPOULOS
nghia.vo@diamond.ac.uk

[1] Diamond Light Source, Harwell Science and Innovation Campus, Didcot, Oxfordshire, OX11 0DE, UK

Interative phase retrieval in the Fresnel region based on the random signed feedback (RSF) technique has shown a promising performance on tomographic data as demonstrated in [1,2]. In this report, I present in details the performance of the RSF technique at various conditions and in comparison with other direct phase retrieval methods including the transport-of-intensity equation (TIE), the contrast transfer function (CTF), and the mixed TIE-CTF method. The tomographic data used for demonstration was obtained from beamline I12-JEEP (Joint Engineering, Environmental and Processing) at Diamond Light Source, with 53 keV X-ray beam. The results could help to regain the interest of applying propagation-based methods in phase contrast tomography.

References :
[1] Nghia T. Vo, Robert C. Atwood, Herbert O. Moser, Peter D. Lee, Mark B. H. Breese, and Michael Drakopoulos, "*A fast-converging iterative method for X-ray in-line phase contrast tomography,*" Applied Physics Letters, **101**, 224108 (2012).
[2] https://www.youtube.com/watch?v=r1rHZqBwjyY

(044) Towards the reconstruction of the mouse brain vascular networks with highresolution synchrotron radiation X-ray tomographic microscopy

*A. PATERA[1,2], A. ASTOLFO[1], K. S. MADER[1,3], M. SCHNEIDER[4,5], B. WEBER[5], M. STAMPANONI[1,3]
alessandra.patera@psi.ch

1 Swiss Light Source, Paul Scherrer Institute, Villigen, Switzerland
2 Centre d'Imagerie BioMedicale, Ecole Polytechnique Federale de Lausanne, 1015 Lausanne, Switzerland
3 Institute of Biomedical Engineering, University and ETH Zürich, Switzerland
4 Computer Vision Laboratory, ETH Zurich, Sternwartstrasse 7, 8092 Zurich, Switzerland
5 Institute of Pharmacology and Toxicology, University of Zurich, Winterthurerstrasse 190, 8057 Zurich, Switzerland

The architecture of the cerebral vasculature is currently documented at 100 μm (Lauwers et al., 2008) resolution for human brain and about 10 μm for mouse brain. More recently, Micro-Optical Sectioning Tomography has shown potential in imaging the vessel network of an entire mouse brain with a voxel resolution of 0.35×0.4×2.0 μm^3 (Xue et al., 2014). However, the destructive nature of the technique avoids the potential options of *in-vivo* imaging. Within the context of the Human Brain Project (HBP), we aim at using synchrotron radiation X-ray tomographic microscopy at the Swiss Light Source of the Paul Scherrer Institute (Switzerland) as a key technology for reconstructing, in a non-destructive way, the entire vascular system of the mouse brain at 1 μm resolution. Preliminary experiments exploiting free space propagation X-ray phase-contrast imaging have been performed in this direction.

The tomographic configuration equipped with PCO. Edge detector and 10× objective has been used, thus yielding a pixel size of 0.65 μm. A mouse brain, with a size pproximately of 1 cm^3, has been infused with 50% indian ink and kept in glue to ensure the stability of the sample. In this work, a sub-volume of the sample has been acquired with 5×6×2 scans to cover an axial area of 5.1×7.5 mm^2, with a total scanning time of 9 hours at 25 keV. After reconstruction, the Fourier transform-based phase correlation method (Preibish et al., 2010) has been successfully applied to compute translational offsets between the sub-volumes. A main challenge of the experiment is related to the amount of data to be handled and analyzed. Each reconstructed datasets (with dimensions of 1.7×1.7×1.4 mm^3) consist of 14 GB and the volume of 5.1×7.5×2.8 mm_3 after stitching consists of 188 GB. As example, the maximum intensity of a region of interest with a size of 1.2×0.5 mm_2 is shown in Figure 1.

This preliminary result will be extended into the full reconstruction of the complete cerebrovascular network of the mouse brain, with a final total reconstructed volume of approximatively 7 TB. At this point, these pioneering efforts are pointing towards new horizons in the investigation of large biological samples with 3D high spatial resolution.

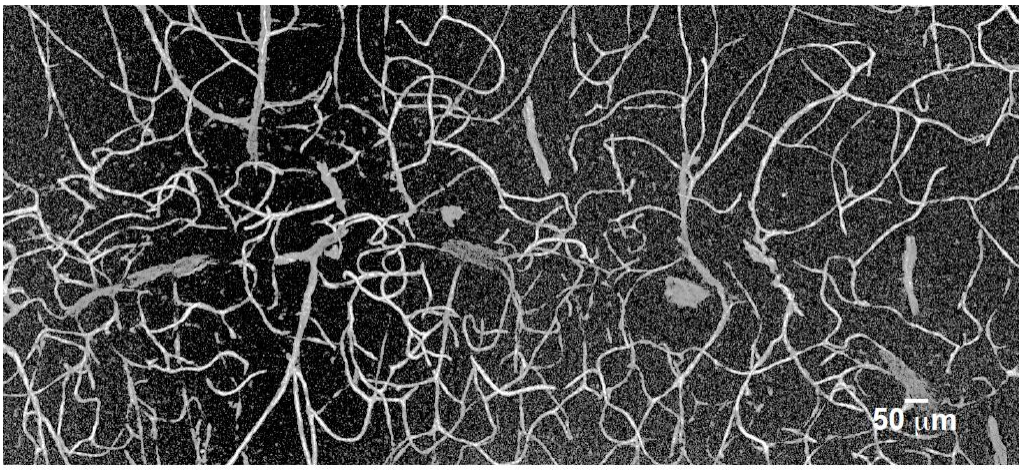

Figure 1: Max. intensity of a region of interest with a size of 1.2×0.5 mm^2 in the brain volume after stitching.

References :
Lauwers F, Cassot F, Lauwers-Cances V, Puwanarajah P, Duvernoy H. Morphometry of the human cerebral cortex microcirculation: general characteristics and space-related profiles. Neuroimage. 2008 Feb 1;39(3):936-48.
Xue S, Gong H, Jiang T, Luo W, Meng Y, et al. (2014) Indian-Ink Perfusion Based Method for Reconstructing Continuous Vascular Networks in Whole Mouse Brain. PLoS ONE 9(1): e88067. doi:10.1371/journal.pone.0088067
Preibisch S, Saalfeld S, Schindelin J and Tomancak P (2010) Software for bead-based registration of selective plane illumination microscopy data, Nature Methods, 7(6):418-419.

(088) Cost-effective image analysis in the cloud: A case study using 1300 mouse femur samples

*K. MADER[1,2,3], M. STAMPANONI[1,2]
mader@biomed.ee.ethz.ch

[1] Swiss Light Source, Paul Scherrer Institut, Villigen, Switzerland
[2] Institute of Biomedical Engineering, Swiss Federal Institute of Technology and University of Zurich, Zurich, Switzerland
[3] 4 Quant, Zurich, Switzerland

Genetic-scale studies in imaging are challenging projects because of both the amount and variety of data involved. In tomography these problems are amplified because data quantities can be 10s of gigabytes per sample and can require anywhere from hours to days to process all of it. Coordination and integration of such complex analyses over so many samples is not easy and requires significant efforts to implement correctly. This raises serious questions about the reliability and reproducibility of not only the study but the analysis.

Using cloud infrastructure from Amazon Web Services (http://aws.amazon.com/), combined with the image processing framework Spark Image Layer (4Quant, Zurich, Switzerland), we perform a genome scale analysis of murine cortical microstructure. The study provides a good example since it involves 1300 samples with comparatively large (~14GB) image data and a number of post-processing tasks, which need to be performed: Gaussian filtration, downsampling, segmentation, contouring, distance map generation, thickness maps, and shape analysis for between 15-60K objects in each sample as described in1. Additionally the step linking the structures to the regions of the genome, required assembling all of the results on a single machine for comparison with the genetic tag data.

The first step in performing such an analysis, and the likely bottleneck for many use cases, was uploading all of the raw image data to cloud storage (Amazon S3 in this case). Our maximum sustained upload rate was 141Mb/s resulting in a upload time of 35 hours if done at once. Once uploaded, a wide variety of hardware and software configurations are available and should be adapted to the size and desired speed of the analysis to perform. Using the "memory-optimized instances" on Amazon's EC2 (r3.2xlarge), our analysis takes between 10-14 hours and produces an additional 4-6GB of data.

The resulting cost per sample for the image processing is around $10 resulting in a total cost of $13,000. The storage of all data (20GB) costs $7.20/sample/year. The final stage of analysis including statistics and genetic linkage was performed for all samples and cannot be as easily divided into a per sample cost. The time consumed was approximately 20 hours costing $15.

In conclusion, we performed an entire genetic study at around the same cost as 2 high performance workstations (without maintenence). These machines would have taken over 100 days to finish the analysis, required maintenance and substantial storage and backup to match the services offered by cloud vendors. In contrast, the limiting factor for the cloud solution is the upload time. After this step, however, the entire analysis could be run on 1300 machines in parallel and the study could be finished within 30 additional hours. Furthermore the cloud approach enables all of the raw data and intermediate results to be made publicly accessible promoting the virtues of open access and reproducible research.

References :
1.Mader, K., Mokso, R. & Raufaste, C. Quantitative 3D Characterization of Cellular Materials: Segmentation and Morphology of Foam. Colloids and Surfaces A: … 415, 230–238 (2012).

(119) Analysis of flame retardancy in polymer blends synchrotron X-ray K-edge tomography and interferometric phase contrast movies

*M. B. OLATINWO[1], H. KYUNGMIN[2], J. MCCARNEY[3], S. MARATHE[4], L. G. BUTLER[1]

[1] Chemistry Department, Louisiana State University, 232 Choppin Hall, Baton Rouge, LA 70803 (molati1@lsu.edu)
[2] Center for Advanced Microstructures & Devices, Lousiana State University, 6980 Jefferson Hwy., Baton Rouge, LA 70806
[3] Albemarle Corporation, PO Box 341, Baton Rouge, LA 70821
[4] Advanced Photon Source, Argonne National Laboratory, Building 401, 9700 S. Cass Avenue, Argonne, IL 60439

High impact polystyrene UL-94 test bars have been imaged with K-edge tomography to assess the spatial distribution of bromine and antimony across char layers of partially burnt samples. Also, single-shot grating interferometry was used to record X-ray movies of test samples during heating (IR and flame) intended to mimic the UL-94 test. One polymer test sample was formulated with sufficient brominated flame retardant, Saytex-8010™ and antimony oxide, a synergist, to pass the UL-94 test; other samples were deficient in one or the other component and did not pass the UL-94 test. The range of sample formulations aided the interpretation of the tomography volumes and X-ray phase contrast movies.

The Br and Sb K-edge absorption tomography experiments started with 5 to 7 data sets acquired over the range of 12 to 32 keV, reconstructed with filtered back-projection, and normalized to the absorption projection images.[1] Fiducial points were used to align the volumes. Linear attenuation coefficients were taken from the NIST XCOM database. Densities of flame retardants are calculated from molecular formulas using the procedure of Cao.[2] The volume fraction composition of each voxel was calculated by a vectorized least squares method [3]; a binary sample mask defined the calculated sample volume. Calculations used a 1024 GPU node for the ASTRA toolbox [4] and a 12-core, 196 GB RAM node for the Mathematica codes.

The phase contrast and dark-field imaging used a 4.8 micron period checkboard phase grating and a high resolution detector. The movie frame rate was 3 Hz. The single-shot interferometry data was processed by 2D FFT and analysis of the image harmonics. Samples were heated with either a 300 W IR lamp or a small flame; soot was collected with a portable smoke extractor. A definite need was noted for an active sample position control system to account for the sample consumption and motion out of the field of view.

Tomography enabled us to observe differences with the sample that pass or fail the UL-94 test. Key features such as char layer, gas bubble formation, micro-cracks, and dissolution of the flame retardant in the char layer regions are used in understanding the efficiency of the flame retardants and synergist. The samples that pass the UL-94 test have a thick, highly visible char layer as well as an interior rich in gas bubbles. Growth of gas bubbles from flame retardant thermal decomposition is noted in the X-ray phase contrast movies as well as an absence of bubbles at the burning surface of the polymer; dark-field images after burning suggest a micro-crack structure between interior bubbles and the surface. The accepted mechanism for flame retardant activity includes free radical quenching in the flame by bromine atoms.

References :
[1] Ham, K. and L. G. Butler (2007). "Algorithms for three-dimensional chemical analysis via multi-energy synchrotron X-ray tomography." Nucl. Instrum. Methods B 262(1): 117-127.
[2] Cao, X., N. Leyva, S. R. Anderson and B. C. Hancock (2008). "Use of prediction methods to estimate true density of active pharmaceutical ingredients." International Journal of Pharmaceutics 355(1-2): 231-237.

[3] Marathe, S., L. Assoufid, X. Xiao, K. Ham, W. W. Johnson and L. G. Butler (2014). "Improved Algorithm for Processing Grating-Based Phase Contrast Interferometry Image Sets." Rev. Sci. Instrum. 85: art. no. 013704.
[4] ASTRA toolbox, iMinds - Vision Lab, University of Antwerp,
http://visielab.uantwerpen.be/research/tomography

(156) Coherent X-ray diffraction imaging of strain on the nanoscale

*R. HARDER[1]
rharder@aps.anl.gov

[1] Argonne National Laboratory, 9700 S Cass Ave, Argonne, IL, USA

In nanoscience, the bulk concepts of lattices and crystal defects must be reconsidered in order to explain why nanomaterials have new and exciting properties. To study these properties, we have developed the method of Coherent X-ray Diffraction (CXD) Imaging to obtain quantitative three-dimensional maps of the deformation of a crystal from its equilibrium lattice spacing. By measuring the coherently scattered photons in the vicinity of Bragg peaks of the samples, and computationally inverting the intensities to an image, we gain this powerful capability.

Very recently we have developed instrumentation and methods that allow us to image, in three dimensions, the total lattice deformation field of micro and sub-micro meter size crystals with high spatial resolution. Using this data, the entire strain tensor of the sample can be determined in three dimensions.

The images being produced by this method have lead to a tremendous need for image analysis in three and even four dimensions. With the advance of ultra high brightness synchrotron sources, like those being planned in an upgrade the Advanced Photon Source of Argonne National Laboratory, coherent imaging is poised to produce sub-nanometer resolution images of vector lattice distortions and strain tensor fields that describe material properties as a function of time during in-situ and operando experiments.

This talk will introduce describe the methods used to acquire such data and include some of the first images of nanoscale strain mapping.

References :
If you want to add references, please use an author/date style.

(175) Use of distance transforms and correlation maps for advanced 3D analysis of impact damage in composite panels

*F. LEONARD[1], J. STEIN[2]
fabien.leonard@bam.de

[1] BAM – Federal Institute for Materials Research and Testing, Division 8.5 - Micro-NDT, Unter den Eichen 87, 12205 Berlin,Germany
[2] TWI Ltd., Granta Park, Great Abington, Cambridge, CB21 6AL, UK

One of the major issues when using composite materials in an industry such has aerospace is their impact behaviour, particularly when subjected to low-velocity impacts. Low-velocity impacts are complex to assess as although significant damage can be generated internally, there can be little indication of external damage, leading to the term barely visible impact damage (BVID). The internal damage appears primarily as matrix cracking and delamination between plies of dissimilar orientation and can lead to loss in strength and stiffness. Ultimately, the load-bearing capabilities can be significantly reduced in both tension and compression, and catastrophic failure can occur under relatively low applied loads. As a result there is a concerted research effort to improve the damage resistance and tolerance of these materials.

When facing a composite damage tolerance problem, the geometric structure of the damage is key in understanding the basic damage mechanisms. It is only when such mechanisms are understood that the critical composites properties in regards to damage can be defined and the damage tolerance improvements implemented. X-ray computed tomography is therefore a technique of choice to deliver a full-field 3D representation of the impact damage non-destructively. However, advanced data processing methodologies are required as the sole segmentation of the damage volume does not provide sufficient information.

Previous work [Léonard2013;Léonard2014] has demonstrated that it was possible to segment the damage produced by a low velocity impact event on a composite laminate; and obtain a through-thickness damage histogram. This histogram was employed to semi-automatically separate the full damage so that the individual ply-by-ply damage could be visualised and assessed independently. The data processing methodology developped was based on a *distance transform* operation to take into account the permanent out-of-plane deformation of the composite panel. However the main limitation of this approach is the degradation of the damage separation for high impact energies, as the out-of-plane deformation becomes greater in the centre than at the edges of the panel.

To obtain a better ply-by-ply separation of the damage, we have employed a combination of distance transform operations and a correlation map using Avizo. This new methodology will be detailled and its advantages and limitations will be discussed based on an investigation of carbon fivre reinforced panels (CFRP) impacted with energies ranging from 5 J up to 20 J.

References :
F Léonard, J Stein, PJ Withers, and A Wilkinson. 3D damage characterisation in composite impacted panels by laboratory X-ray computed tomography. 1st International Conference on Tomography of Materials and Structures. Gent, Belgium, 2013.
F Léonard, Y Shi, C Soutis, PJ Withers, and C Pinna. Impact damage characterisation of fibre metal laminates by X-ray computed tomography. Conference on Industrial Computed Tomography, Wels, Austria, February 2014.

(201) Proposal of a data evaluation chain for the inspection of thermoplast clips

*U. HASSLER[1], W. HOLUB[1], M. REHAK[1], E. PENNE[1], T. GRULICH[1]
ulf.hassler@iis.fraunhofer.de

[1] Fraunhofer IIS/EZRT/AMS/RBV, Flugplatzstraße 75, 90768 Fuerth, Germany;

The Europeen project QUICOM is dealing with the application of X-ray computed tomography methods (CT) to carbon fiber reinforced plastic (CFRP) components from aerospace industry. Here, CT is mainly intended to be an escalation method in certain nondestructive testing situations (NDT), where conventional tests do not produce clear indications. Further, CT is investigated related to a production-integrated quality control. This type of application makes sense for relatively small parts, produced in a large volume. This is the case for so called ‘clips’, manufactured using CFR thermoplastic material. They are mainly used as connecting elements within larger aeronautic structures. Within QUICOM, the capabilities and limits of such an application case are evaluated. In this contribution, we present a specific data evaluation chain, which could be used for an automatic interpretation of such data. Main interest herein is the determination of the local porosity within the parts.

Main challenge using CT for those thermoplastic clips is the relation of object dimension (approx. 200*100*300 mm³) and complex geometry to the minimum size of relevant defects (approx. 10 to 100 µm), which results in very large reconstructed volumes. In this contribution, we rather focus on efficient handling and the principle of the evaluation procedure than on reliable analysis itself. The goals of the usage of the evaluation chain is twofold: to provide a tool for quality assessment of the CT reconstruction itself, in order to be able to optimize scanning and reconstruction parameters, and to show the principle transition of the established ultrasonic inspection procedure to an automated interpretation of CT data in the near future.

The evaluation chain consists of the following steps: (a) multi-clip separation, (b) clip dissection and (c) analysis. The efficiency of the CT inspection raises with the possibility of scanning several parts at the same time. The separation step is then used to create individual volume representations of the clips. The segmentation step is used to reduce the data volume and to subdivide the volume in similar geometrical primitives, which are in the case of clips on one hand the flat and planar main faces and on the other hand the connecting radii. These simple geometric objects are then fed into the analysis step, which consists of (1) detection of surface anomalies, (2) detection of internal inhomogeneities (porosity) and finally (3) determination of geometric properties. Within the contribution, we will focus mainly on the clip dissection and the determination of the internal inhomogeneities by means of a resampling of the volume data relative to the clip surface. The result of the approach is an estimation of the local porosity as a function of depth (distance to the surface). From that, an overall or volume porosity can be deduced and visualised.

Results achieved with the presented approach will be shown using both simulated and real data.

References :
If you want to add references, please use an author/date style.

(210) In-situ 3D nano-imaging at the advanced photon source

V. DE ANDRADE, M. WOJCIK, D. GURSOY, A. DERIY, F. DE CARLO
dgursoy@aps.anl.gov

Advanced Photon Source, Argonne National Laboratory, Lemont, Il-60439, USA

The new in-house Transmission X-ray Microscope (TXM) at Sector 32-ID-C of the Advanced Photon Source (APS) at Argonne National Laboratory has just accomplished a first year of operation. The highest resolution full-field imaging system of Argonne is taking up challenges of nanomaterial science in the field of energy storage, microelectronics, nanoporous materials and environmental science. The TXM is equipped with a fixed exit double crystal monochromator (Si111). It operates from 6 to 14 keV. The available set of optics (in-house 60 and 20 nm Δr_n Fresnel zone plates) offers fields of view ranging from 70 to 20 µm for spatial resolution of 60 and 20 nm. Techniques available include absorption, Zernike type phase contrast and XANES tomography. The design enables operations in a wide range of environments. 3D nano-tomography can be performed under controlled atmosphere, for temperature ranging from -160^{o}C to 1500^{o}C, with ability to supply electric current to the sample. An overview of the first experiments performed at 32-ID will be given.

Session 301 - Hydraulics and sediment transport

(194) X-ray measurement of sand ripples bedload transport

*S. MONTREUIL[1], B. LONG[1]
stephane.montreuil@cll.qc.ca

[1] Institut National de la Recherche Scientifique, 490 rue de la Couronne, Québec (Québec) G1K 9A9 Canada

Sediment transport CT-Scanner-flume experiments provide information about internal bedform structures offering the best setup ever for fundamental and applied research. This innovating technique generates a view inside sediment ripples, revealing the dynamic phenomena acting on internal bedload transport structures. Analysis results have already provided a set of sedimentary parameters defining internal migrating ripple architecture. The aim of this study is focused on the upper bedload transport layer definition providing a new definition of datum used as ripple surface, influencing sediment transport estimation.

The 30 x 30 x 700 cm flume used in this research was specially built to fit into a CT-Scanner room and technically designed to avoid X-ray artefacts. The flume is filled with a 5 cm-thick pure silica sand layer and a 20 cm-high water column at 20 °C. The flow (0 – 80 $cm \cdot s^{-1}$) is measured and controlled by an electro-pneumatic valve inside a recirculating circuit.

Two CT-Scanner measurement techniques have been developed: a global measurement technique uses a 3D matrix of 512 x 512 x 1500 voxels of 0.6 x 0.6 x 0.6 mm, resulting in a view at a precise moment in time (Lagrangian); the second (Eulerian) one is the periodic event technique generating a matrix set of 512 x 512 x 30 voxels separated by a Δt from 30 s to hours. From both techniques, matrixes are considered as vertical density profiles, imaging the density from the water column to the bottom bed, and passing through the boundary suspension-bedload, until bedload transport.

Interpretation of raw data images from CT-Scanner-flume experiments necessitate processing through medical reconstruction software. Best results were obtained with the SpineSpi B20s (Siemens) reconstruction filter. Results in HU based on relative density, are converted in SI units of density following a linear equation. Afterward, SI values are calibrated taking into account flume composition, sand properties and fluid density.

Vertical density profiles for a 3D matrix provide values from the suspension-bedload transition towards the sediment bed's interior (d_{50} = 0.470 mm and U = 28 $cm \cdot s^{-1}$). This reveals the impact of water, penetrating up to 10 mm deep into the sediment. This penetrating process demonstrates the existence of an unknown internal phenomenon present during sediment transport. The thickness of the upper bedload transport layer varies from 0.6 mm to 10 mm respectively for the ripple summit and trough. Density at the upper suspension-bedload boundary varies, respectively for summit and trough, between 1.026 and 1.318 $g \cdot cm^{-3}$ and at its lower end between 1.645 and 1.903 $g \cdot cm^{-3}$.

When observing density profiles along a migrating sand ripple, it appears that the bed surface used as a datum is located deeper into the sediment. Density values and profiles form at the water column base as a conduct to the definition of a boundary density point (former datum) under an upper bedload transport zone. Underneath this bedload transport zone, the maximum density is reached leading to the definition of a stricto sensu ripple surface. This new ripple

surface location is 0.6 to 10 mm deeper than the one used in literature and depends on d_{50}, flow current and position along the ripple. Variation in surface position modify deeply the stoss-side lee-side frontier along sand ripple.

Innovative CT-Scanner results re-open the discussion about suspended and bedload transport during erosion and deposition processes, leading to a new way of looking inside active sediment transport. Protocols and processes developed in this study open new research opportunities in the field of sediment transport.

(199) The internal density structure of sediment-propelled turbidity currents as revealed by CT imagery

M. TILSTON[1], R. W. C. ARNOTT[1], C. D. RENNIE[2], B. LONG[3]
warnott@uottawa.ca

[1] Department of Earth Sciences, University of Ottawa, Ottawa ON
[2] Department of Civil Engineering, University of Ottawa, Ottawa ON
[3] Centre Eau Terre Environnement, INRS, Québec City QC

Turbidity currents are a special kind of density, or buoyancy current, propelled by gravity acting on suspended sediment. In nature turbidity currents are common, and in the deep marine are the principal sediment transporting agents that build up the largest sediment accumulations on Earth. However these powerful currents are notoriously destructive, and as a consequence have been largely unexplored. Accordingly, researchers have turned to analyzing them in the lab. Here it is easy to form a suspended-sediment-propelled turbidity current but because of their inherently dense nature these flows are not amenable to conventional sampling instrumentation. As a consequence most researchers have used variably concentrated saline currents with the implicit assumption, or explicit statement, that they faithfully mimic the dynamics of sediment-propelled currents. Based on that work, two end member kinds of (saline) currents were identified, and differentiated on the basis of flow criticality: subcritical flows have a high velocity maximum below which density is vertically uniform ("plug-like") and above which density decreases rapidly and shows minimal mixing with the overlying fluid; conversely, the velocity maximum of supercritical flows is located at the base of the current, density decreases exponentially away from the bed, and the current as a whole shows extensive vertical mixing. The question, therefore, is under similar hydraulic conditions, are the velocity and density profiles in saline currents representative of those formed in sediment-propelled turbidity currents?

In this study, we created a variety of turbidity currents of varying velocity and sediment concentration. However unlike these other studies, this is the first to accurately measure the density profile (here a surrogate for sediment concentration) in natural, sediment-transporting turbidity currents by passing them through the gantry of a medical grade CT scanner. Given similar hydraulic conditions, the two end-member profiles are controlled exclusively by particle size; specifically the velocity, density and mixing characteristics of fine grained runs were similar to subcritical saline flows whereas coarse-grained runs were similar to supercritical saline flows. Such differences in density and velocity structure will profoundly influence the vertical distribution of momentum through the current, and the degree of vertical mixing, which has important implication for the conservation of flow energy, and therefore run out distance of turbidity currents in the deep sea.

(203) The influence of grain size on the velocity and sediment concentration profiles and depositional record of turbidity currents

M. TILSTON[1], R. W. C. ARNOTT[1], C. D. RENNIE[2,] B. LONG[3]
miketilston@hotmail.com

[1] Department of Earth Sciences, University of Ottawa, Ottawa ON
[2] Department of Civil Engineering, University of Ottawa, Ottawa ON
[3] Centre Eau Terre Environnement, INRS, Québec City QC

Cross-stratified sand and sandstone formed by migrating dunes and ripples is ubiquitous in the fluvial sedimentary record. However in spite of being subjected to similarly unidirectional flows, albeit in this case turbidity currents, these features are comparatively uncommon in the deep-marine sedimentary record. Notwithstanding this obvious difference, open channel flows are commonly viewed as meaningful analogues for turbidity currents. In part this relates to the destructive nature of natural turbidity currents, and the shortcomings of conventional laboratory instrumentation that have hindered the inability to accurately study and properly characterize their internal structure. In this study we use a medical grade Computed Tomography (CT) scanner coupled with a three-dimensional ultrasonic Doppler velocity profiler (UDV) to characterize the flow field and depositional morphology across a range of grain sizes (: 70µm-330µm) and concentrations (5%-17.5% by mass).

Results show that the development of three-dimensional, downstream migrating bedforms is suppressed in all flows with particle concentrations greater than 9.5% by mass, but notably also in all flows made up of particles less than 230µm and sediment concentrations down to at least 5% by mass. Here, bed shear stress far exceeds that required for incipient particle motion, indicating that traditional conceptual models of turbulence as the primary mechanism for their genesis are problematic. Further analysis of the Richardson gradient number shows a distinct temporal oscillation in near-bed stratification stability in the coarse-grained flow that formed three-dimensional bedforms. Notably, these near-bed conditions are absent in the fine-grained but equally concentrated flows that formed planar beds. These data suggest a first order control on the response of the bed to the make-up of the overriding current. More fundamentally, it appears to support the theory that hydrodynamic instabilities are responsible for the generation of three-dimensional bedforms rather than turbulence in waning flows, which to date has been impossible to quantify due to technological limitations. Finally, a conceptual model is proposed to explain how hydrodynamic instabilities are capable of spatially organizing fluid motions that are typically associated with fluid turbulence, thus explaining the spontaneous rather than progressive development of three-dimensional bedforms. Moreover, this provides a mechanism for the development of such features in laminar flows, and unifies the ongoing debate of fluid turbulence versus hydrodynamic instabilities for the origin of three-dimensional bedforms by demonstrating that the two mechanisms result in similar fluid motions, but that the latter is better at organizing them spatially.

(118) Wave-sediment interaction imaging with X-ray tomography: A small-scale experiment to characterize the artefacts

*C. B. BRUNELLE[1], B. LONG[1], P. FRANCUS[1], L. F. DAIGLE[1], M. DES ROCHES[1], H. TAKAYAMA[2]
corinne.bourgault-brunelle@ete.inrs.ca

[1] Institut national de la recherche scientifique, 490, rue de la Couronne, G1K 9A9, Québec, Canada
[2] Kumamoto University, 2-40-1 Kurokami Chuo-ku, Kumamoto City, 860-8555, Japan

The complexity of currents dynamics with porous sand beds has no analytical solutions. Hence, empirical relations are needed to validate fluid-sediment interaction models. The physical model, a reproduction of a system at a different scale, is interesting to use in this case because no simplified assumptions of the equations of movement are required. This way, travelling waves were generated in a small-scale physical model (1:17) to investigate the wave-sediment processes over a sloping beach in the Quebec X-ray Laboratory. A hydraulic flume was inserted into the medical CT-scanner providing a lot of density variation measurements during the experiments. Such physical models have been built similarly in small flumes to characterize the sediment transport (Grasso et al., 2011; Yamada et al. 2013; Montreuil et Long 2007). The main sources of artefacts are discussed in regards of the possible limitations for useful sedimentary parameters.

Two different types of beach sediment mixture were tested: 1) sand, gravel and cobbles and 2) sand only. First, the results show (Figure 1a) that it is possible to characterize grain size sorting for the sand-gravel-cobbles mixture. The regression between the mean grain size (Y) and the HU value standard deviation (X) has a great correlation, $Y=6.96*X+117$ ($R^2=0.98$, $N=3$) with an error of 10%. The density of sediments was not totally homogeneous allowing the detection of HU variability. The resolution of the scan was 200 µm for grain sizes varying between 200 and 3350 µm. There is much more imaging artefacts when the sediment forms a beach (Figure 1b). In this case, the two main sources of artefacts are: 1) the tube power limitation and 2) the geometry of the beach. These limitations are caused by the beach thickness (i.e., up to 20 cm), inducing noise, and the square form of the beach (axial plane), creating black streaks during the image reconstruction (not illustrated). Anyhow, the theory of wave-sediment interaction processes (Butt et al., 2001; Bakhtyar et al. 2011) have been observed and presented here for the sand beach experiment (Figure 1b). After the wave passage, the suspended matter concentrations increase in the water column from the time T_0 to T_4, corresponding to the beach destabilization. The HU values still increase into the beach (T_4) while it decreases in the water column and in the air, corresponding to the water exfiltration (i.e., HU increase) process. Inversely, the wave passage induces water infiltration into the beach (i.e., HU decrease) and the diminution of sediment transport in the water column (T_5 to T_7).

In summary, the image post-treatments provided a better understanding of the artefacts effect and the limitation for HU values interpretation. However, the evolution of the beach morphology, sediment transport processes, air entrapment, suspended matter concentration and grain size distribution were detected and possibly quantified with further investigations. The present work is a contribution to the shore dynamics experimental research using physical models for coastal protection studies.

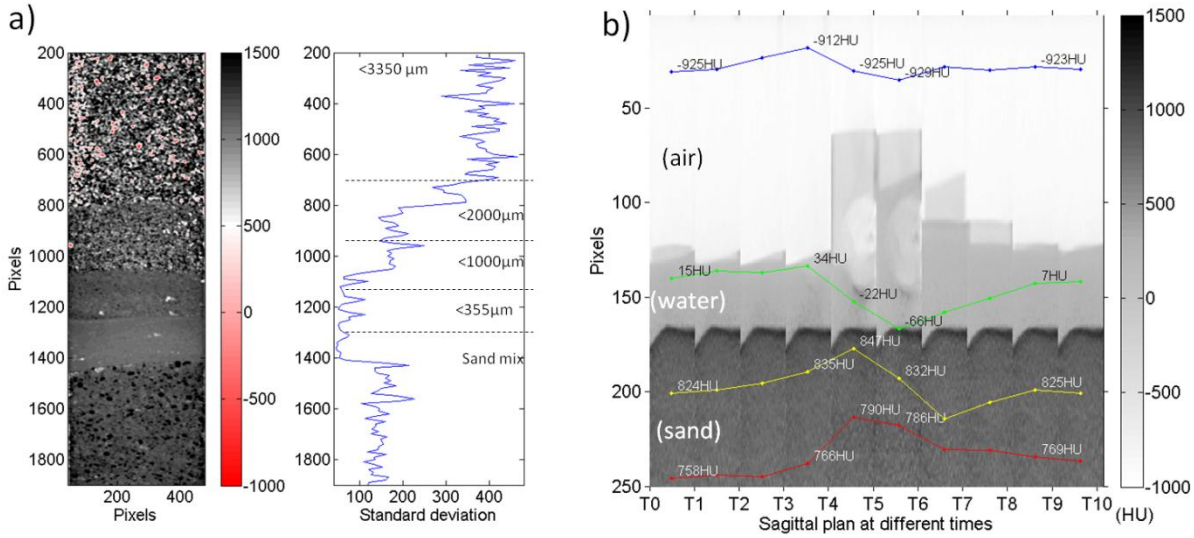

Figure 1. Highest densities are illustrated in black and lowest densities in white (reverse scale), a) sagittal plane of a well-known sorted non-homogenous sediments core (left) with the corresponding standard deviation (SD) of HU values for each grain size class (right), red dot are removed of the SD calculations b) sagittal planes (38.4 mm width) of the homogenous sand beach with temporal mean HU value variations before, during and after the wave passage, illustrated here by pixels in air (10:50), water (140:160), beach surface (180:200) and beach subsurface (225:250).

Acknowledgments

The authors want to thank the Research Chair in Coastal and River Engineering of Quebec, the Canada Foundation for Innovation and the Multidisciplinary Laboratory of CT-Scan for Non-Medical Use (INRS).

References :

Bakhtyar, Roham, Alessandro Brovelli, David Andrew Barry, et Ling Li. 2011. « Wave-induced water table fluctuations, sediment transport and beach profile change: Modeling and comparison with large-scale laboratory experiments ». *Coastal Engineering* 58 (1): 103‑18.

Butt, Tony, Paul Russell, et Ian Turner. 2001. « The influence of swash infiltration–exfiltration on beach face sediment transport: onshore or offshore? ». *Coastal Engineering* 42 (1): 35‑52.

Grasso, Florent, Hervé Michallet, et Eric Barthelemy. 2011. « Experimental simulation of shoreface nourishments under storm events: A morphological, hydrodynamic, and sediment grain size analysis ». *Coastal Engineering* 58 (2): 184‑93.

Montreuil, Stéphane, et Bernard F. Long. 2007. « Flume Experiments under CAT-Scan to measure internal sedimentological parameters during sediment transport ». In *Proceedings Coastal Sediments' 07 Conference, ASCE, New Orleans, LA*, 1:124‑36.

Yamada, Fumihiko, Ryuta Tateyama, Gozo Tsujimoto, Seiya Suenaga, Bernard Long, et Constant Pilote. 2013. « Dynamic monitoring of physical models beach morphodynamics and sediment transport using X-ray CT scanning technique ». *Journal of Coastal Research*, 1617‑22.

(187) Evolution of the ripple field under a wave regime on the offshore of the breaker bar, along the beach profile: Experiment using CT-Scan imaging

B. LONG[2], H. TAKAYAMA[1], T. MUKUNOKI[1], S. MONTREUIL[2], C. B. BRUNELLE[2] , M. DES ROCHES[2], L. F. DAIGLE
bernard.long@ete.inrs.ca

[1]Kumamoto University, 2-40-1 Kurokami Chuo-ku, Kumamoto City, 860-8555, Japan
[2]Institut national de la recherche scientifique, 490, rue de la Couronne, G1K 9A9, Québec, Canada

Beach profile stability is a key factor of the coastal erosion. To understand if a beach profile is stable it is essential to analyze this profile in a physical model. A beach model under waves regime was generated in a small scale model to investigate the formation and the evolution of a ripple field over a sloping (1:15) sand beach with a 0.215 mm sand (Ottawa sand). The aim of this research is to improve the knowledge of the beach profile dynamics and the contribution of the ripple field to the nearshore bar development. This experiment simulates the formation and evolution of ripples from a flat beach profile, with wave of 1.5 second period and 4 cm height. The flume was instrumented with a Siemens CT-Scan in both spiral and perfusion modes and the particle image velocimetry (PIV). These two instruments were covering the offshore of the breaker bar by a series of measurement each 20 minutes during a 5 hours period.

The aims of these studies are to determine the evolution of the suspended sediment concentration by both CT-Scan and PIV, the evolution of the current distribution by PIV and finally the variation of the water concentration under the sand column during wave passage. These evolutions are monitored during the beach profile evolution from a flat bed to a nearshore bar bed. Then, the X-ray tomography method coupled with a PIV method showed promising results to measure the simultaneous evolution of the suspended load zone, the bedload zone and the transition zone.

Session 302 - Geomaterial, Materials, Structures and Mineralogy

(006) Through-porosity induced corrosion under a Fe-based amorphous coating revealed by in-situ X-ray tomography

*S. G.WANG[1], S. D. ZHANG[1], J. Q.WANG[1], S. C.WANG[1], L. ZHANG[1]
wangshaogang@imr.ac.cn

1 Shenyang National Laboratory for Materials Science, Institute of Metal Research, Chinese Academy of Sciences, Shenyang 110016, PR China

In-situ X-ray tomography (XRT) or 4D imaging is one important technique that allows the researchers to track and visualize the internal structure evolution of various materials with the changes of load, temperature or other environment conditions.

Corrosion resistance is one of the basic properties to be evaluated for materials in service. In-situ visualization of corrosion process will be helpful for understanding the corrosion mechanism and improving the material performance.

Thermal sprayed coatings are widely used to protect surfaces of metals and alloys against corrosion and wear in industry. The coating delamination and peeling off caused by corrosion is commonly encountered failure types. It is well known that the corrosion resistance of the materials coated is strongly related to its porosity that normally categorized as through-porosity and non-through porosity. However, the correlation between the porosity and the corrosion behavior of the thermally sprayed coating still remains ambiguous.

In this work, the volume fraction, size and distribution of the porosity in Fe-based amorphous coating were measured and analyzed via 3D XRT technique. Combined with an electrochemical test and the 3D XRT technique using lab-based VersaXRM-500 system, an ingenious in-situ experiment was designed to investigate the correlation between porosity and corrosion. A number of in-situ evidences acquired during the whole corrosion process clearly gave the fact that the preferential substrate corrosion was caused by the through-porosity rather than the other type of porosity. The dissolved volume of substrate was directly observed and calculated from the 3D visualization of the coated sample after potentiostatic polarisation test, and basically matched to the result calculated by measured charge with a negative deviation of about 6%. It was also found that through-porosity is sensitive to the coating thickness. The critical coating thickness for the presence of through-porosity was determined, which could provide a guide for the design of corrosion resistant coatings.

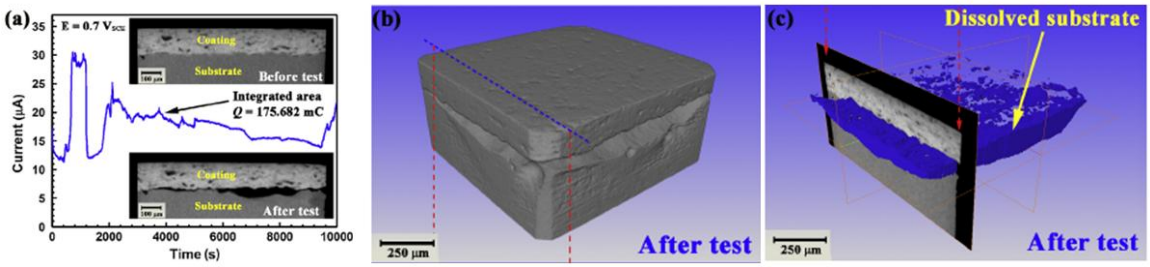

Fig. 1 *(a) Current-time curve of potentiostatic polarisation at 0.7 VSCE for 10,000 s, insets: the cross-sections of the coated sample before and after potentiostatic polarisation test; (b) 3D visualisation of the coated sample after potentiostatic polarisation test; (c) the cross-section indicated by the dashed lines in (b) and 3D visualisation of the volume of dissolved substrate after potentiostatic polarization test.*

(007) Characterization of three-dimensional fatigue pre-crack propagation for 316L stainless steel with lab-based X-ray tomography

*S. G.WANG[1], L. XIONG[1], S. C.WANG[1], L. ZHANG[1]
wangshaogang@imr.ac.cn

1 Shenyang National Laboratory for Materials Science, Institute of Metal Research, Chinese Academy of Sciences, Shenyang 110016, PR China

X-ray tomography (XRT) is a powerful technique to nondestructively characterize the interior structure of the object. Advances in X-ray sources, optical devices and image analysis technologies have enabled the wide application of three-dimensional (3D) XRT in material science with the spatial resolution of micron, even tens of nanometers using either laboratory-based tomographs or synchrotron-based facilities.

It is well known that the development of a new material is highly dependent on the knowledge of its microstructures related with material properties. However, the traditional 2D techniques such as SEM and metallography only provide limited surface information. Instead, the accurate and overall 3D microstructure including certain quantitative information can be acquired by XRT.

In this contribution we will present a non-destructively 3D characterization of complicated crack morphology of single-edge notched bend (SENB) specimen for nanostructured (NS) 316L steel consisting of nano-scale twin bundles embedded in micro-sized grains by means of lab-based XRT. The tests were performed using an Xradia “Versa XRM-500” desktop system with the voltage of 150 kV and a 2048×2048 pixel array CCD detector. The voxel size is 4.2 μm. 3D views of every stage of crack were clearly showed after a reconstruction with Avizo Fire.

Four main components are described and discussed. The first, generally speaking, the plastic zone around the crack tip is either the damage zone in the form of plastic deformation or the process zone in the form of microcracking. As far as the NS 316L steel is concerned, the specific behavior of plastic zone is investigated through a series of slices. In addition, the exactly 3D dimension of the plastic zone is measured. Next, the crack sharpening was verified to originate from the microvoids located ahead of the crack tip. 25% of the sample fractured in plane strain state while 75% is a mixed mode of plane strain and plain stress. The third, three specific zones including tension side, neutral area and compressive side are the typical features of the samples during SENB test. However, we have little knowledge about their 3D shapes associated with the deformability. The visualization and quantitative determination of theses features will give us new insights on the material. At last, we discussed the possible application of XRT technique on the determination of J-integral.

The results of the 3D-XRT analysis indicated that both the intrinsic small 3D plastic zone and the extrinsic minor crack meandering contribute to the relatively low fracture toughness of NS 316L steel (120 MPa·$m_{1/2}$) in comparison with the coarse-grain state (230 MPa·$m_{1/2}$). Such a 3D-XRT technique can also be applied to the complex crack analysis for other materials.

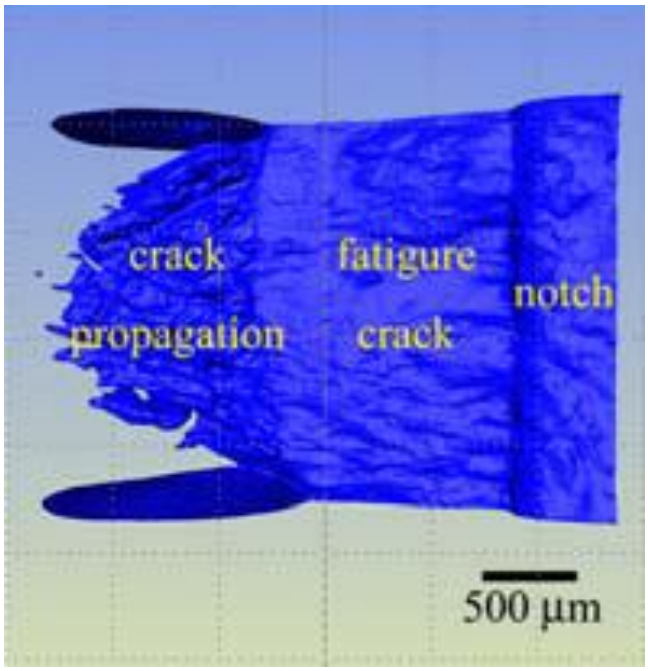

Figure A 3D view of every stage of fatigue pre-crack of a SENB specimen

(020) Microstructural characterization of SiC foams used as solar absorber devices

J. MOLLICONE[1], *B. DUPLOYER[1], P. LENORMAND[1], C. TENAILLEAU[1], J. VICENTE[2], F. ANSART[1]
duployer@chimie.ups-tlse.fr

[1] CIRIMAT, UMR - CNRS 5085, Université de Toulouse, 118 route de Narbonne, 31062 Toulouse Cedex 9, France
[2] Laboratoire IUSTI, Technopôle de Château-Gombert, 5 rue Enrico Fermi, 13453 Marseille cedex 13, France

This work was conducted in the framework of OPTISOL project funded by the French National Agency (A.N.R.). The main purpose of the project was to increase the competitiveness of solar thermal power plant by increasing the solar conversion efficiency at high temperature in particular through the implementation of combined cycles. The key component of such solar process is the solar receiver that must deliver air in the temperature range between 700°C and 1100°C. The optical properties of the porous structures used as receiver must have a selective behaviour in relation to the solar radiation in order to limit the radiative losses of the surface and increase heat transfer by convection.

Receivers usually used are silicon carbide (SiC) foams [1-3]. Increasing the efficiency of such systems is directly related to the geometrical and optical properties of the receivers (ceramic foam, porosity, grain size, additional layer…). Also, the structure and microstructure of the foam have to be controlled at each stage of the process. X-ray Computed Tomography (XCT) was firstly used to characterize the microstructure of various SiC foams. Structural modifications with temperature were then studied by XRD, DTA-TGA and dilatometry [4] since SiC foams are usually used at high temperatures, corresponding to the one required for solar receivers. An oxide has to be formed at the surface of the raw material during the thermal treatment in order to increase radiative transfers and stand such a thermal treatment.

SiC foams cells network are complex (obstructed pores, oriented cells etc…) so the coating process can be difficult. XCT is then a really well suited technique to determine precisely the different foam microstructure features due to the manufacturing process and/or thermal treatment, in a non-destructive manner.

Calculations based on the XCT images collected and further analyzes using the iMorph program showed that cells are not spherical but have an ellipsoidal shape, which can be described by 3 orthogonal axes *a*, *b* and *c* (*a* > *b* > *c*) in a 3D referential O,x,y,z. These three axes have a specific orientation characterized by the elevation angle ϕ and the azimuth angle θ. SiC foams have actually a closed porosity due to the manufacturing process (pyrolysis of a polyurethane template), which is included in the pores analyzes. Porosity is constituted of cells interconnected through throats, which are separated by struts. SiC foam throats are described by 2 parameters *a*' and *b*' corresponding to the equivalent oval included in the throat. Struts have a triangular shape and inner and outer circles can describe them. Note that a filter needs to be applied during image analysis to determine all three axes. This process is also responsible for the closed and intergranular porosities, and closed throats observed. This typical morphology was the main difficulty to consider for the implementation of the coating process. Microstructural information here obtained was of great interest for the understanding and modelling of the radiative properties of these systems.

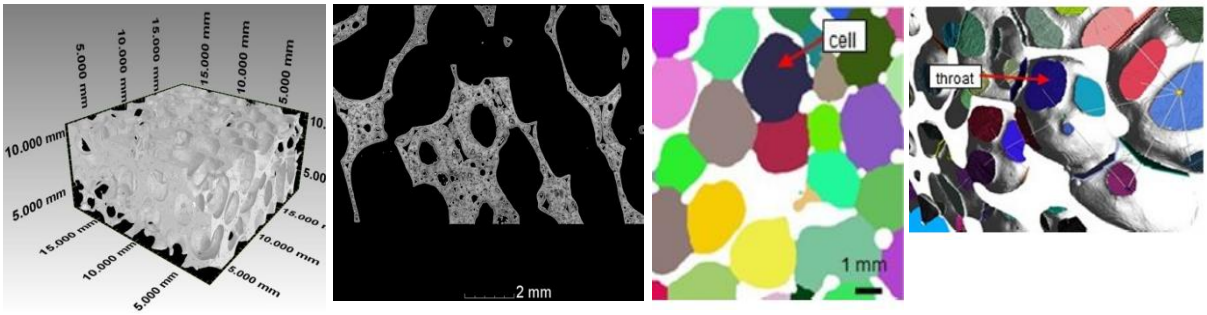

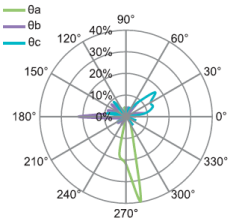

References :
[1] T. Menigault et al., Solar Energy Materials, 24, 192-203, 1991.
[2] R. Pitz-Paal et al., Solar Energy Materials & Solar Cells, 24, 293-306, 1991.
[3] T. Fend et al., Energy, 29, 823-833, 2004.
[4] J. Mollicone et al., J. Eur. Ceram. Soc., 34, 3479–3487, 2014.

(078) *In-operando* fast tomography of lithium-ion batteries during operation and failure

*D. P. FINEGAN[1], M. SCHEEL[2], J. ROBINSON[1], B. TJADEN[1], I. HUNT[3], M. DI MICHIEL[2], G. OFFER[3], G. HINDS[4], D. J. L. BRETT[1], P. R. SHEARING[1]
donal.finegan.13@ucl.ac.uk

Department of Chemical Engineering, University College London, Torrington Place, London, WC1E 6BT, UK
ESRF, The European Synchrotron, 71 Rue des Martyrs, Grenoble, France
Imperial College London, South Kensington Campus, London, SW7 2AZ, UK
National Physical Laboratory, Hampton Rd., Teddington, Middlesex, TW11 0LW, UK

Lithium-ion batteries are recognised as being an integral technology in the process of achieving a clean and sustainable energy future. The safety of Li-ion batteries is of upmost importance particularly as the advancement of electric and hybrid electric vehicles require high energy density batteries to operate under a wide range of conditions. The thermal response of a cell is one of the most important characteristics to understand when assessing the safety of a cell design but little is understood about the dynamic mechanisms associated with thermally induced failures.

X-ray tomography has become a widely used technique for 3D structural analyses of electrochemical materials using either lab based tomography or synchrotron tomography. Two of the major advances in tomography techniques in recent years are the reduction in tomogram acquisition time and the increased spatial resolution. In this study, high frequency tomography imaging of commercial lithium-ion batteries (18650 LG NMC cells) during operation and failure was performed in beam-line ID15A at the European Synchrotron Radiation Facility (ESRF). Tomograms were captured at a rate of up to 2.5 Hz allowing us to study some of the most rapid failure mechanisms including those associated with thermal runaway. Simultaneous thermal imaging and X-ray tomography allowed structural and thermal dynamics to be linked with time.

The evolution of gas pockets, electrode layer delamination and cracking are apparent from the results. Post-mortem tomography analyses of 18650 batteries after thermal runaway reveal a large degree of structural degradation containing features which may be indicative of temperatures reached (>1000 °C) during failure inside the cells. This analysis has provided unprecedented insights into the structural and thermal dynamics leading up to and during thermal runaway and failure of commercial lithium-ion batteries.

(112) Carbon anodes investigation through computed tomography

*D. PICARD[1], H. ALAMDARI[1], D. ZIEGLER[2], L. F. DAIGLE[3], M. FAFARD[1]
donald.picard@gci.ulaval.ca

[1] Université Laval, Aluminium Research Centre, 1065 De la Médecine Avenue, Québec (Québec), G1V 0A6, Canada
[2] Alcoa Primary Metals, Alcoa Technical Center – 100 Technical Drive, Alcoa Centre, PA, 15069-0001, USA
[3] INRS-ETE, Environmental Technology Laboratories, 2605 du Parc-Technologique, Québec (Québec) G1P 4S5, Canada

The aluminium production at industrial scale is done through the electrolysis of alumina, also known as the Hall-Héroult process. This process requires carbon electrodes that can withstand a highly corrosive environment at elevated temperature. The carbon anodes, which are consumed after approximately 26 days of operation, operate in molten cryolite (Na3AlF6) at 960 °C. Given the limited lifespan of the anodes, they are made from low cost raw materials, having high variation of their physical properties over time due to sourcing from different suppliers. Hence, these variations have a direct impact on anode forming process, the green and baked properties and performance in the electrolysis cell. Over the past years, a large research programme has been set-up to investigate the anode properties using different approaches, including non-destructive techniques such as the computed tomography (CT). The CT technique has been used as a diagnostic tool to highlight density gradient in lab scale and industrial scale anodes, metal impurity levels and total porosity percentage. Also, an existing crack detection algorithm based on the percolation method has been adapted to low resolution CT images of large sample obtained with a Siemens Somatom Sensation 64 to detect large cracks in baked anodes.

(187) Coarsening in phase-separated silicate melts observed by in-situ tomography

D. BOUTTES[1], *E. GOUILLART[2], W. WOELFFEL [2], E. BOLLER[3], L. SALVO[4], P. LHUISSIER[4], D. VANDEMBROUCQ[1]
emmanuelle.gouillart@nsup.org

1 Laboratoire PMMH, UMR 7636 CNRS/ESPCI/Univ. Paris 6, UPMC/Univ. Paris 7 Diderot, 10 rue Vauquelin, 75231 Paris cedex 05, France
2 Surface du Verre et Interfaces, UMR 125 CNRS/Saint-Gobain, 93303 Aubervilliers, France
3 European Synchrotron Radiation Facility (ESRF), BP 220, 38043 Grenoble, France
4 SIMAP, GPM2 group, CNRS UMR 5266, University of Grenoble 38402 Saint Martin d'Hères

Many silicate glasses compositions undergo phase separation under a critical temperature, in the stable liquid or undercooled melt state. The resulting microstructure can be used for various applications, such as porous membranes. Numerous theoretical and numerical studies have considered the kinetics and the morphology of the separated phases in the so-called *coarsening* regime, when the composition of the phases is fixed during a isothermal treatment and fixed-composition domains grow with time. However, few experimental results exist for inorganic materials about the 3-D morphology of the phases, and the formation mechanisms of the microstructure.

In this work, we investigate in-situ the coarsening stage of a barium borosilicate-glass forming melt. Our in-situ microtomography experiments are performed on the ID19 beamline of the ESRF synchrotron. Using a PCO Dimax camera and pink beam at a peak energy of 35 keV, tomography scans are realized with a time resolution of 5s for a pixel size of 1.1 microns (corresponding to a true spatial resolution of the order of 5 microns). We use a dedicated high-temperature furnace that allow samples to be imaged in-situ in the course of a thermal treatment. Using image processing, we extract the 3-D geometry of the two separated phases during isothermal treatments in the range 1000-1300°C, far above the glass transition.

Quantitative geometrical measurements and direct observations demonstrate that viscous coarsening is the dominant mechanism governing the evolution of the bicontinuous structure [Bouttes2014]. This mechanism results in a linear growth of domain size with time, much faster than the $t_{1/3}$ growth associated to diffusive mechanisms that have been observed so far in silicates. The activation energy for domain growth is found to be consistent with the one of viscosity.

Interface curvatures between the two phases are measured at different times during a isothermal treatment. We show that histograms of curvatures can be renormalized by the typical domain size, demonstrating that the microstructure evolves in a self-similar way during coarsening. Such measures constitute therefore a convincing evidence of the theoretical hypothesis of *dynamical scaling*. Furthermore, we observe a progressive fragmentation of one of the percolating phases, that we relate to the important viscosity contrast between phases. The rate of fragmentation is found to depend strongly on the volume fraction of the less viscous phase, that is the only one to break up. For a large volume fraction of the less viscous phase, few domains detach from the percolating phase and dynamical scaling persists during coarsening. However, for a less viscous phase in net minority, an important fragmentation takes place and eventually disrupts dynamical scaling, with a complete arrest of coarsening observed in some cases.

References :
[Bouttes2014] Bouttes, D., Gouillart, E., Boller, E., Dalmas, D., & Vandembroucq, D. (2014). Physical review letters, 112(24), 245701

(010) Ptychographic tomography of geological samples – Pushing the spatial resolution limits

*W. DE BOEVER[1], H. DERLUYN[1], J. VAN STAPPEN[1], J. DEWANCKELE[1], T. BULTREYS[1], M. BOONE[2], T. DE SCHRYVER[2], E. T. B. SKJØNSFJELL[3], A. DIAZ[4], M. HOLLER[4], V. CNUDDE[1]
wesley.deboever@ugent.be

[1] PProGRess – UGCT – Dept. Of Geology and Soil Science – Ghent University, Ghent, Belgium – www.pprogress.ugent.be
[2] Radiation Physics group - UGCT – Dept. Of Physics and Astronomy – Ghent University, Ghent, Belgium – www.ugct.ugent.be
[3] Dept. of Physics – Norwegian University of Science and Technology - Norway
[4] Paul Scherrer Institute – Villigen, Switzerland

High resolution X-ray tomography (µ-CT) has proven to be a valuable tool in geosciences (Cnudde and Boone, 2013; Ketcham and Carlson, 2001; Wildenschild and Sheppard, 2013). The development of the method provided new insights on the internal structures of rocks and sediments, adding an extra dimension in comparison with more traditional techniques such as electron and optical microscopy. With µ-CT it is possible to image and analyse samples from the centimeter to the millimeter scale, a key feature for the study of heterogeneous geological materials.

However, the resolution of X-ray tomography is typically limited to a few hundreds of nanometers for standard laboratory setups (Dierick et al., 2014), or just under one hundred nanometer for synchrotron tomography or laboratory systems using optics (Kastner et al., 2010). This leaves an important resolution gap between scanning electron microscopy and µ-CT data. For this reason, the quantitative study of microporous or fine-grained materials is typically not done using µ-CT, although estimations are possible by saturating samples with attenuating liquids.We propose the novel application of ptychographic tomography at synchrotron beam lines for geological samples, to quantitatively study porosity and pore network characteristics of fine-grained clay minerals inside two varieties of sandstone.

Ptychography is a coherent diffraction imaging technique in which a coherent, confined X-ray illumination is used to scan the specimen in such a way that the illumination spot overlaps at consecutive scanning positions. Coherent diffraction patterns are recorded in the far field at each position, and iterative phase retrieval algorithms are then used to reconstruct the complex-valued transmissivity of the specimen (Rodenburg and Faulkner, 2004). The resolution of this technique is only limited by the scattering angles at which diffraction intensities can be reliably recorded, and can be as little as 16 nm (Holler *et al.*, 2014), much better than the size of the illumination or the scanning step size. By combining 2D phase projections acquired at different incident angles of the X-ray beam, quantitative 3D distributions of electron density can be obtained (Diaz et al., 2012; Dierolf et al., 2010). Geological samples are very suited for ptychographic imaging, as they are very stable and do not tend to suffer from radiation damage. This is an important characteristic, as ptychographic tomograms take several hours up to a full day to acquire. However, as in most high-resolution imaging techniques, a drawback is that the samples have to be very small to achieve these extreme resolutions. For example in this study, 50 µm samples where imaged at the cSAXS beam line of the Paul Scherrer Institut in Villigen (www.psi.ch), obtaining a voxel size of 34 nm, and a corresponding spatial resolution of 89 to 120 nm in 3D. In following experiments, two 25 µm sized samples were measured using the setup described in Holler *et al.* (2014), achieving a spatial resolution of 45 nm (voxel size 17 nm) and 60 nm (voxel size 21 nm) in 3D. The resulting images show excellent contrast between pores and grains, and different mineral phases were clearly distinguishable. In this work, we will

show quantitative results on clay microporosity, connectivity and shape of the pore network, and distribution of different mineral phases in these clay clusters.

References :

Cnudde, V., Boone, M.N., 2013. High-resolution X-ray computed tomography in geosciences: A review of the current technology and applications. Earth-Science Rev. 123, 1–17. doi:10.1016/j.earscirev.2013.04.003

Diaz, A., Trtik, P., Guizar-Sicairos, M., Menzel, A., Thibault, P., Bunk, O., 2012. Quantitative x-ray phase nanotomography. Phys. Rev. B 85, 020104. doi:10.1103/PhysRevB.85.020104

Dierick, M., Van Loo, D., Masschaele, B., Van den Bulcke, J., Van Acker, J., Cnudde, V., Van Hoorebeke, L., 2014. Recent micro-CT scanner developments at UGCT. Nucl. Instruments Methods Phys. Res. Sect. B Beam Interact. with Mater. Atoms 324, 35–40. doi:10.1016/j.nimb.2013.10.051

Dierolf, M., Menzel, A., Thibault, P., Schneider, P., Kewish, C.M., Wepf, R., Bunk, O., Pfeiffer, F., 2010. Ptychographic X-ray computed tomography at the nanoscale. Nature 467, 436–9. doi:10.1038/nature09419

Holler, M., Diaz, a, Guizar-Sicairos, M., Karvinen, P., Färm, E., Härkönen, E., Ritala, M., Menzel, a, Raabe, J., Bunk, O., 2014. X-ray ptychographic computed tomography at 16 nm isotropic 3D resolution. Sci. Rep. 4, 3857. doi:10.1038/srep03857

Kastner, J., Harrer, B., Requena, G., Brunke, O., 2010. A comparative study of high resolution cone beam X-ray tomography and synchrotron tomography applied to Fe- and Al-alloys. NDT E Int. 43, 599–605. doi:10.1016/j.ndteint.2010.06.004

Ketcham, R.A., Carlson, W.D., 2001. Acquisition, optimization and interpretation of X-ray computed tomographic imagery: applications to the geosciences. Comput. Geosci. 27, 381–400.

Rodenburg, J.M., Faulkner, H.M.L., 2004. A phase retrieval algorithm for shifting illumination. Appl. Phys. Lett. 85, 4795. doi:10.1063/1.1823034

Wildenschild, D., Sheppard, A.P., 2013. X-ray imaging and analysis techniques for quantifying pore-scale structure and processes in subsurface porous medium systems. Adv. Water Resour. 51, 217–246. doi:http://dx.doi.org/10.1016/j.advwatres.2012.07.018

(038) BaTiO3-based composite materials for electronics characterized by X-ray computed tomography

*C. TENAILLEAU[1], S. DUPUIS[1], P. DUFOUR[1], B. DUPLOYER[1], S. GUILLEMET-FRITSCH[1]
tenailleau@chimie.ups-tlse.fr

[1] CIRIMAT, UMR - CNRS 5085, Université de Toulouse, 118 route de Narbonne, 31062 Toulouse Cedex 9, FRANCE

Barium titanate ($BaTiO_3$, BT) is a well-known material for its excellent dielectric (ε ~ 3500) and piezoelectric properties (190 pC/N), which makes it essential for various electronic applications such as thermistors and capacitors. The high relative permittivity and low dielectric losses are the main targets for the materials to be used in microelectronics allowing device miniaturization. The relative permittivity of BT can be varied in the range of 4000–6000 depending on the grain size of the sintered ceramic, and the maximum relative permittivity can be typically achieved at the grain size of about 1 μm when sintered through conventional sintering methods.

However, we recently reported that abnormally colossal relative permittivity (ε ~ 10^4–10^5) can be induced in the synthesized nano-crystalline (250 nm) BT ceramic using starting nano-crystalline BT powder and spark plasma sintering (SPS) technique.[1] SPS is a fast sintering technique that allows for the densification of ceramics while maintaining small grain size due to the short sintering time and relatively low sintering temperatures used. A number of investigations have reported dielectric properties of SPS BT ceramics.[1-4] Sr-doped BT ceramics exhibit stabilized dielectric constants over a wider range of temperatures and frequencies, though the permittivity value is decreased compared to pure BT ceramics, while the dielectric losses are improved.[5] High relative permittivity has also been found in a number of ceramics and composites such as $CaCu_3Ti_4O_{12}$ (CCTO), $Ba(Zr_{0.2}Ti_{0.8})O_3$-carbon nanotube, and BT-Ni particle composites…

3D mapping of anisotropic ferroelectric/dielectric composites with $Ba_{0.6}Sr_{0.4}TiO_3$ (BST) ferroelectric matrix, in which MgO inclusions were spread, was very recently performed with a synchrotron source.[6] Beyond an accumulation of properties due to the mixture of two different materials, there is a real composite effect that modifies the electronic properties. Thanks to the specific conditions of SPS, it is possible to produce inclusions with a large aspect ratio (ellipsoid) while preserving the chemical integrity of both phases. This is the first step towards realistic mapping of a possible electric field focusing that would fit with the available empirical models. The 3D anisotropy enhanced by the increase of the SPS pressure affects the electric field redistribution between the two phases and appears to be an efficient way to reduce the dielectric permittivity while maintaining electric field tunability. We here present, for the first time to our knowledge, a systematic study of BT-based composites microstructures observed by lab. X-ray Computed Tomography (XCT) in relationships with their dielectric properties. BT-(Ni metal) and BT-(Al_2O_3 insulator) composites were synthesized and sintered by the SPS technique. The influence of inclusions number, shape, size and distribution… determined by XCT over the materials dielectric properties will be discussed.

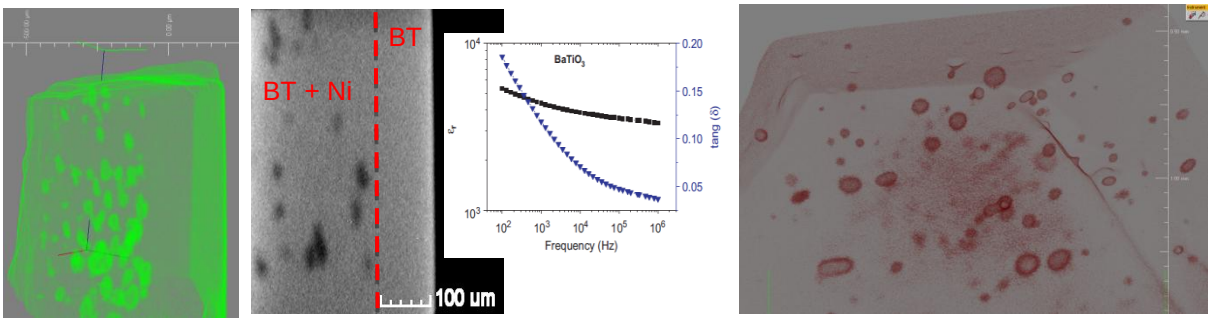

References :
[1] S. Guillemet-Fritsch, Z. Valdez-Nava, C. Tenailleau, T. Lebey, B. Durand, J. Y. Chane-Ching, *Adv. Mater.* 20, 551 (2008).
[2] T. Takeuchi, C. Capiglia, N. Balakrishnan, Y. Takeda, H. Kageyama, *J. Mater. Res.* 17, 575 (2002).
[3] M. T. Buscaglia, V. Buscaglia, M. Viviani, J. Petzelt, M. Savinov,L. Mitoseriu, A. Testino, P. Nanni, C. Harnagea, Z. Zhao, M. Nygren, *Nanotech.* 15, 1113 (2004).
[4] B. R. Li, X. H. Wang, M. M. Cai, L. F. Hao, L. T. Li, *Mater. Chem. Phys*. 82, 173 (2003).
[5] C. Fu, C. Yang, H. Chen, Y. Wang and L. Hu, *Mater. Sci. Eng. B*, 119, 185–188 (2005).
[6] J. Lesseur, D. Bernarda, U.-C. Chunga, C. Estournès, M. Maglione, C. Elissalde, *J. Europ. Ceram. Soc.*, 35, 337 (2015).

(065) Mineralogy mapping on 3D digital rock models based on X-ray Micro-CT and electron microscopy techniques

I. V. VARFOLOMEEV[1,2], *O. A. KOVALEVA[1,2], I. V. YAKIMCHUK[2]
okovaleva@slb.com

[1] Moscow Institute of Physics and Technology, Dolgoprudny, Russia
[2] Schlumberger, Moscow, Russia

Over the time, mineralogical studies have been playing a significant role in development of oil and gas industry in different domains. Knowledge of reservoir mineralogy makes an impact on understanding and predicting behaviour of hydrocarbon reservoir and as a result, enhances oil/gas field development planning. There are several methods for evaluating mineralogy of geologic formation in a laboratory or even *in situ* (downhole using well logging tools). Conventionally, mineralogy of rock samples is being determined in bulk, i.e. for the whole rock sample. To date there are several techniques, which theoretically allow obtaining 3D distribution of chemical and under certain assumptions mineral content of the studied sample. Such capabilities have specific importance in the scope of Digital Rock approach that is being actively developed in the petroleum science. The general idea of Digital Rock consists in constructing 3D model of a rock sample and performing numerical simulations of the processes under interest using the digital model. The most straightforward way for building such models is binarization of rock images into two main classes — voids and solids. In this case, only pore space geometry is taken into account. Evidently, information about spatial distribution of minerals allows making more sophisticated digital rock models (with different solid phases according to mineralogy) that potentially increase the accuracy of calculations.

One of the most efficient imaging techniques for creating digital model of the core plug is X-ray absorption micro-computed tomography (micro-CT), which provides three-dimensional spatial distribution of X-ray attenuation inside the sample according to beam energy spectrum. Most laboratory micro-CT instruments deal with a 'white' (polychromatic) beam using as many photons as possible to obtain statistically reliable images within reasonable amount of time. The energy of the beam should be high enough (>50 keV) to penetrate through dense rock samples. These two facts seriously complicate the problem of recovering the spatial distribution of the minerals constituting the sample. Nevertheless, information about X-ray source spectra and a-priori known bulk mineralogy of the core plug makes it possible to predict the type of mineral in each voxel of reconstructed micro-CT image.

Alternatively, we propose another approach. It is based on combination of X-ray micro-CT data and Scanning Electron Microscopy with Energy Dispersive X-ray microanalysis (SEM-EDX). The essence of the method consists in finding correspondence between the various characteristics of micro-CT image voxels and their mineral content, known from SEM-EDX image. This technique involves spatial registration of 2D elemental or mineral distribution image with 3D micro-CT image. A number of local features is considered to characterise each voxel of 3D micro-CT image: reconstructed X-ray attenuation coefficient value, textural, and morphological properties. Finally, the full 3D micro-CT image is segmented according to its mineral type.

The details of described technique and corresponding results will be presented and discussed.

(115) Measuring in-situ fragment size distributions caused by melt inclusion decrepitation and other mechanisms using HRXCT

*T. CLOW[1], R. A. KETCHAM[1]
travis.clow@utexas.edu

[1] University of Texas at Austin, Department of Geological Sciences, University Station C1100, Austin, Texas 78712, USA.

In comparison to crystal nucleation and growth, fragmentation of crystals has received comparatively little attention in igneous and metamorphic petrology, despite playing an important role in crystal size evolution and overall particle dynamics of magma chambers. Evidence of multiple mechanisms for fragmentation has been observed in previous studies – syn-eruptive fragmentation/shattering due to shockwaves, clot disaggregation, and pre- and syn-eruptive melt inclusion decrepitation – with particular importance placed on the last as the dominant fragmentation mechanism in batholith-sized magma bodies. Each process has been proposed to generate a distinctive fragment size distribution (FSD) that can be distinguished statistically; much can be discovered about fragmentation processes based on these distributions. The present study tests theoretical FSDs for different fragmentation mechanisms as described in Bindeman (2005) by using high-resolution X-ray computed tomography (HRXCT) to analyze plagioclase and hornblende fragments found *in-situ* in dacitic pumice samples from the Popocatepetl stratovolcano in central Mexico. By using HRXCT, we can analyze crystal fragments in a textural context that is lost when samples are disaggregated and sieved, as in previous studies. We interpret unusually large vesicles that have plagioclase and hornblende fragments plating their sidewalls as decrepitation textures, where overheating and/or decompression caused crystals with melt inclusions to explode into fragments lining the vesicle. Crystal fragments that have been fractured without having a large effect on vesicle size are also observed, which we interpret as fragmented due to syn-eruptive shock. HRXCT allows us to quantitatively measure fragment sizes, shapes, distributions, relative positions, and orientations in 3D by isolating individual vesicles within the pumice using *ImageJ* (NIH) and analyzing the associated crystal fragments using *Blob3D* (Ketcham 2005). In addition to long- and short-axis measurements akin to those used in previous work that employed disaggregation, we are able to acquire volumetric measurements that were not possible in previous studies. Frequency versus volume plots show a fractal distribution for melt-inclusion decrepitated plagioclase and hornblende fragments. This may contradict Bindeman (2005), who posited a log-normal size distribution for melt-inclusion decrepitation based on experiments in which isolated quartz fragments were heated until internal melt inclusions expanded and caused breakage. The fractal FSD we observe may signify that rapid depressurization may result in a different character of fragmentation than slow heating. Finally, heavily fragmented hornblende, which is previously reported to have a low susceptibility to fragmentation via melt inclusion decrepitation, is also observed plating the sidewalls of enlarged vesicles.

References :
Bindeman, I.N. (2005) Fragmentation phenomena in populations of magmatic crystals. American Mineralogist, 90, 1801-1815.
Ketcham, R.A. (2005) Computational methods for quantitative analysis of three-dimensional features in geological speciments. Geosphere, 1, 32-41.

(125) Evaluation by Computed Tomography of the Quality of Carbon Anodes Used in Aluminum Industry

S. AMRANI*[1], D. KOCAEFE[1], Y. KOCAEFE[1], D. BHATTACHARYAY[1], M. BOUAZARA[1], B. MORAIS[2]
salah.amrani1@uqac.ca, Duygu_Kocaefe@uqac.ca, Yasar_Kocaefe@uqac.ca, Dipankar_Bhattacharyay@uqac.ca, brigitte.morais@alouette.qc.ca

[1] University of Québec at Chicoutimi 555 Boulevard de l'Université, Chicoutimi, Québec, Canada
2Aluminerie Alouette Inc. 400, Chemin de la Pointe-Noire, Sept-Îles, Québec, Canada

Keywords: Carbon anodes, defects, baking conditions, tomography.

Abstract

Aluminum is produced by the reduction of alumina in an electrolysis cell. The carbon anode is one of the key elements in this process. The quality of these anodes has a considerable impact on the electrolysis process; thus, the evaluation of their quality is important. One problem that is of great interest is the formation of cracks, which affects the quality of anodes. Cracking results in increase in cost as well as in energy and environmental emissions including greenhouse gases. To reduce the cost, the energy consumption, and the impact on environment, aluminum smelters require high quality carbon anodes with a high density and a low electrical resistivity. Anode quality depends on the raw materials and the parameters of the green anode production and the baking processes. Each step may have an impact on the formation of cracks. The physical and chemical properties of the raw materials have a great influence on anode quality and their performance in electrolysis.

In this project, several anodes were made with different raw materials and under various operating conditions. The green anodes produced were characterized using the computed tomography (CT) technique which is a nondestructive method, and the internal defects created during their fabrication were determined. These anodes were baked under different conditions (heating rate, final baking temperature). Then, the baked anodes were again characterized using the CT technique. The principal objective of this study is to evaluate the impact of different anode production parameters on their quality based on the CT analysis. In this article, the results of the CT analysis of various anodes are presented.

(189) Pore engineering of copper foams made by space holder technique through XMCT characterization

A. M. PARVANIAN[1], *M. SAADATFAR[2], M. PANJEPOUR[1], M. H. SHAHZEYDI[1]
a.parvanian@ma.iut.ac.ir

[1] Department of Materials Engineering, Isfahan University of Technology, 84156-83111 Isfahan, Iran
[2] Research School of Physics and Engineering, The Australian National University, Canberra 0200, Australia

Metallic foams are a new class of advanced materials with unique features of mechanical, acoustic, thermal, electrical and chemical. The physical and mechanical properties of foams are mainly affected by their structural features such as porosity percent, pore size distribution and pore shape. In this study, using X-ray micro computed tomography (XMCT) image processing, we produced copper foams via powder metallurgical (PM) process based on using potassium carbonate as sacrificial space holder agent. The geometrical characterization through XMCT showed good agreement between the shape, size and volume percent of the pores and the ones of the potassium carbonate particles revealing that physico mechanical properties of the copper foams made through PM space holder techniques could be reasonably engineered. Results of this survey are applicable in order to tailor the properties of foam products for the specific applications.

(193) Neutron imaging of coupled deformation and fluid flow in sandstones

E. TUDISCO[1], *S. A.HALL[1,2], J. HOVIND[3], N. KHARDJILOV [4], E. M. CHARALAMPIDOU[5], H. SONE[6]
stephen.hall@solid.lth.se

[1] Division of Solid Mechanics, Lund University, Lund Sweden
[2] European Spallation Source AB, Lund, Sweden
[3] Paul Scherrer Institute, Villigen, Switzerland
[4] Helmholtz Zentrum Berlin, Germany
[5] Institute of Petroleum Engineering, Heriot Watt University, Edinburgh, UK
[6] GFZ-Potsdam, Germany

X-ray tomography, in combination with Digital Volume Correlation (DVC), has been used in a number of recent geomechanics investigations to map the 3D heterogeneity of strain fields inside test samples, either during loading ("in-situ" tests performed with the loading device mounted within the imaging set-up) or with imaging before and after loading (pre-/post-mortem tests). In such studies, in-situ measurements have mostly been performed on sand and clays at low confining pressures. However, the poor penetration of x-rays through triaxial pressure cells capable of sustaining elevated fluid pressures limit the use of x-ray imaging for in-situ rock testing. This restriction is reduced by using neutron instead of x-ray imaging, as neutrons are more able to penetrate the metal confining vessels. Furthermore, the high sensitivity of neutrons to hydrogen makes them very useful to study water (or other hydrogen-rich fluid) related phenomena, which paves the way towards coupled deofrmation and fluid-flow studies.

In this work, the use of neutron imaging to measure deformation in sandstone samples and the resultant effect on fluid flow are explored using both pre-/post-mortem and in-situ testing. New results will be presented demonstrating the use of time-lapse neutron tomography in combination with DVC to provide 3D strain field mapping in deformed (pre-post-mortem imaging) and deforming (in-situ tests) sandstone specimens. Furthermore, analysis of fluid flow evolution through the same specimens will be presented. The coupling of the full-field deformation and flow mapping provide previously-inaccesible insight into how fluid-flow properties are changed in the regions where the most significant deformation is actually occuring, as opposed to measuring just bulk changes.

Session 303 - Wood

(045) *In-situ* study of wood hygro-mechanical behaviour by phase contrast X-ray tomography at cellular and sub-cellular scales

*A. PATERA[1,2], D. DEROME[3], J. CARMELIET[3,4], M. STAMPANONI[1,5]
alessandra.patera@psi.ch

1 Swiss Light Source, Paul Scherrer Institute, Villigen, Switzerland
2 Centre d'Imagerie BioMedicale, Ecole Polytechnique Federale de Lausanne, 1015 Lausanne, Switzerland
3 Laboratory for Building Science and Technology, Swiss Federal Laboratories for Materials Science and Technology, EMPA, Dübendorf, Switzerland
4 Chair of Building Physics, ETH Zurich, Switzerland
5 Institute of Biomedical Engineering, University and ETH Zürich, Switzerland

Synchrotron radiation-based phase contrast X-ray tomographic microscopy at the Swiss Light Source, PSI Villigen in Switzerland (Stampanoni et al., 2006), is a powerful technique for studying the response of cellular materials to environmental stimuli. We report on softwood but the presented approach can be applied to other cellular materials. Wood is hygromorphic, thus it responds to changes in environmental humidity by changing its geometry. At the cellular scale, new findings in the anisotropic and reversible swelling behaviour of softwood and in the origin of swelling hysteresis in porous materials are explained from a mechanical perspective (Patera et al., 2013). A main conclusion is that the swelling anisotropy depends exponentially on the porosity. Wood tissues with higher porosity present a more anisotropic swelling behaviour compared with the less porous tissues.

However, the anisotropy of wood tissues is importantly modified in restrained swelling experiments due to the lowering of swelling in the restraining direction. Further investigations on the swelling coefficients highlight that the cellular structure plays an important role on the hygro-mechanical behaviour of wood (Figure 1.a). With the mechanism of swelling identified, the occurrence of hysteresis of moisture content versus relative humidity is discussed.

Hysteresis appears when swelling and moisture content are considered as a function of relative humidity, while it disappears when swelling is plotted versus moisture content. This shows the main origin of hysteresis to be due to sorption, thus leading to the conclusion that the same amount of moisture entering or exiting the cell wall material leads to the same swelling deformation of the cell material. Swelling due to moisture sorption displays also a non-affine component. The results highlight that the mechanical and moisture properties of wood highly depend on sub-cellular features of the wood cell wall. Phase contrast full-field nano-tomography exploits the possibility of capturing the moisture induced deformations in sub-cellular features of wood, such as bordered pits and middle lamella, with 50 nm pixel size and a field of view of 36×36 μm^2 in the horizontal and vertical directions. For these experiments, the total scanning time is of approximately 34 min. Local tomography is performed on toothpick-like pins wood specimens of 50×50 μm^2 and the scans are performed with an energy of 16 keV and no binning factor. High resolution and contrast allow an easy detection of the non-affine swelling deformations occurring in bordered pits of earlywood and the torus movement (which presents a thickness in the order of a few hundred nm) towards the pit surfaces. The middle lamella, obtained by focused ion beam (FIB) milling of an earlywood tissue with cross-sectional dimension equal to 1.3 µm and height of 13 µm, shows an isotropic swelling behaviour (Figure

1.b). The middle lamella is found to swell less than the S2 layer in the wood cell wall. Although the middle lamella shows an isotropic affine deformation behaviour, non-affine strains may occur locally, but more experimental evidence is required to study this phenomenon. Overall, this work presents an experimental approach which aims at bridging the gap from sub-cellular to macroscale in cellular materials.

References :
Patera, A., Derome, D., Griffa, M., & Carmeliet, J. (2013). Hysteresis in swelling and in sorption of wood tissue. Journal of Structural Biology, 182(3), 226–234. doi:10.1016/j.jsb.2013.03.003
Stampanoni, M., Groso, A., Isenegger, A., Mikuljan, G., Chen, Q., Bertrand A., Henein S., Betemps R., Frommherz U., Böhler P., Meister D., Lange M., Abela, R. (2006). Trends in synchrotron-based tomographic imaging: the SLS experience. Proc. S" PIE 6318, Developments in X-Ray Tomography V, 63180M. doi:10.1117/12.679497

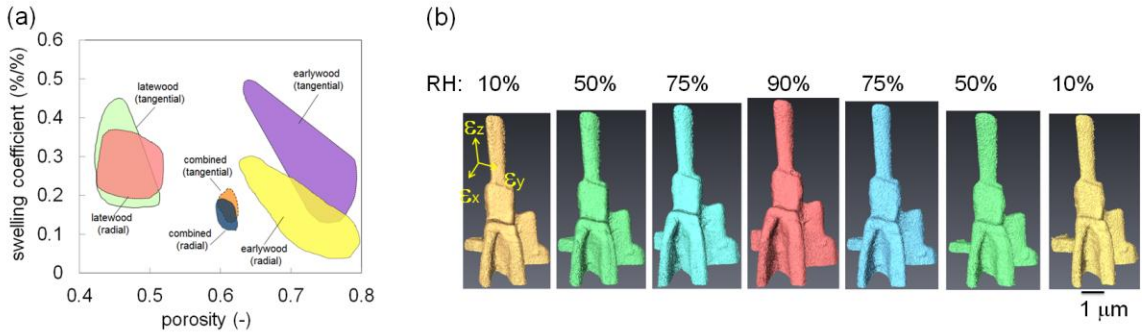

Figure 1: (a) Swelling coefficients of latewood and earlywood for different porosity. (b) Volume renderings of middle lamella in adsorption (10% - 50% - 75% - 90%) and in desorption (75% - 50% - 10%)

(047) Non-destructive research on wooden musical instruments: from macroscale to submicron imaging with lab-based XCT systems

*J. VAN DEN BULCKE[1], D. VAN LOO[2,3], M. DIERICK[2,3], B. MASSCHAELE[2,3], M. N. BOONE[2], L. VAN HOOREBEKE[2], J. VAN ACKER[1]
jan.vandenbulcke@ugent.be

[1] UGCT - Laboratory of Wood Technology, Department of Forest and Water Management, Faculty of Bioscience Engineering, Ghent University, Coupure Links 653, 9000 Gent, Belgium
[2] UGCT – Dept. Physics and Astronomy, Ghent University, Proeftuinstraat 86/N12, B-9000 Gent, Belgium
[3] XRE, X-Ray Engineering bvba, De Pintelaan 111, 9000 Gent, Belgium

Introduction

The use of X-ray CT in wood research has increased considerably during the last decade. Most researchers use commercially available desktop micro-CT scanners. The Ghent University Centre for X-ray Tomography (UGCT) however develops in-house open modular scanners for more experimental freedom, both for applied research in various fields as for research on tomography itself. UGCT is a collaboration between three research groups (physicists, geologists and bio-engineers) operating as an open user facility offering researchers from different fields access to the infrastructure and expertise [Dierick et al. 2014]. The different CT systems at UGCT allow scanning from submicron resolution of very small samples up to scanning of large objects at resolutions depending on sample size. Here we present the possibilities and opportunities of X-ray CT for research on wooden musical instruments using two particular scanners of UGCT: Nanowood and HECTOR.

Methods

Nanowood is a multi-resolution X-ray CT scanner,consisting of an 8-axis motorized stage with two X-ray tubes and two X-ray detectors and is specifically designed to obtain scans with a resolution of 0.2 mm for samples of maximum 37 cm in diameter and a maximal length of approximately 20-30 cm down to a resolution of approximately 400nm for objects that have about the size of a splinter. Nanowood is dedicated to wood research sensu lato [Van den Bulcke et al. 2009, 2011].

The other scanner that is used is HECTOR, the High Energy CT scanner Optimized for Research [Masschaele et al. 2013], and this scanner is built in collaboration with the spin-off company XRE (www.xre.be).

Both systems have a generic in-house developed CT scanner control software platform [Dierick et al. 2010] that allows full control of the scanner hardware. Reconstruction of the scans is performed with Octopus Reconstruction [Vlassenbroeck et al. 2007; www.insidematters.eu].

Results

Different musical instruments (flute, violin, guitar, cello, etc) have been scanned with different acquisition modes (step and shoot, smooth, ROI, helical, tiled) and some of the instruments have been analysed (local thickness analysis, volume labelling, growth ring demarcation, etc). Figure 1 illustrates the potential of both Nanowood and HECTOR for a scanned violin and flute and the accompanying analyses of thickness and internal volume respectively.

[6] (a) [7] (b) [8] (d)

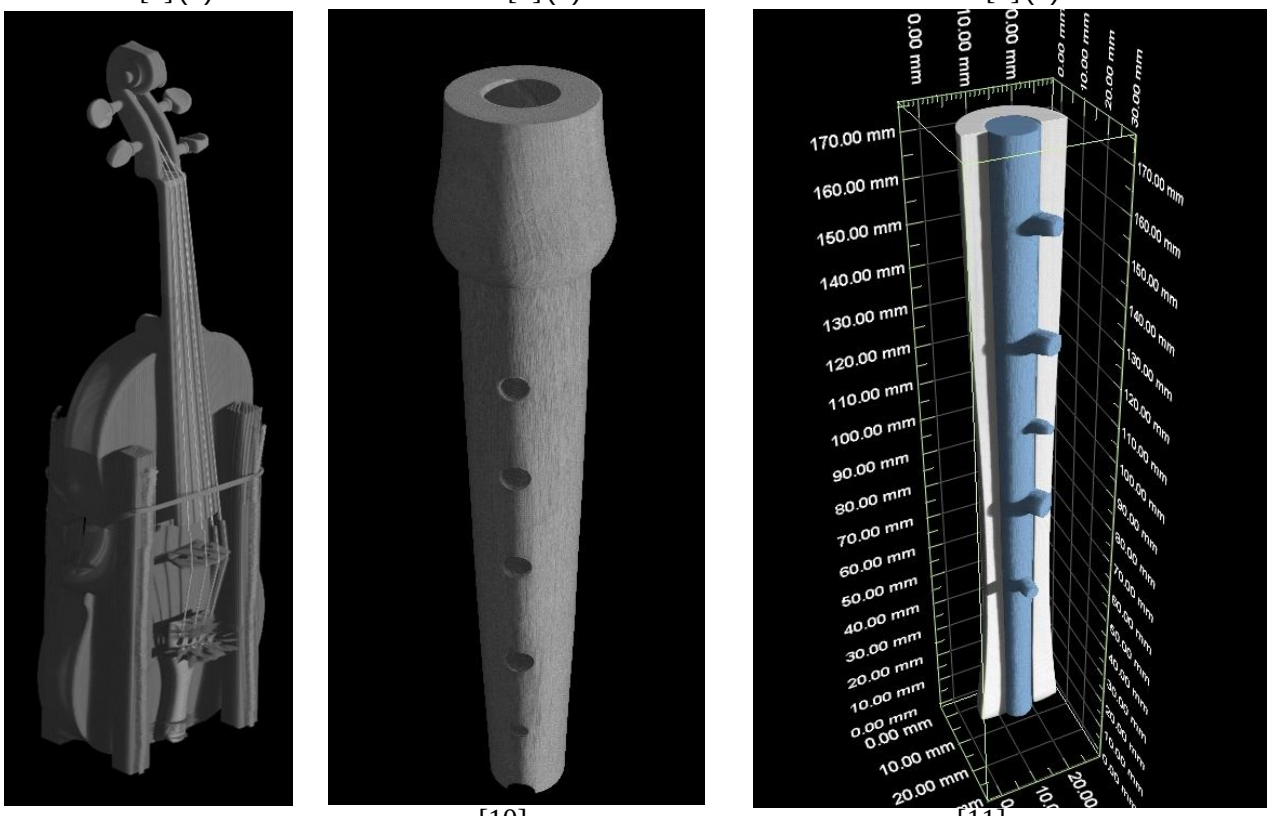

[9] [10] [11]

[12] (c) [13]

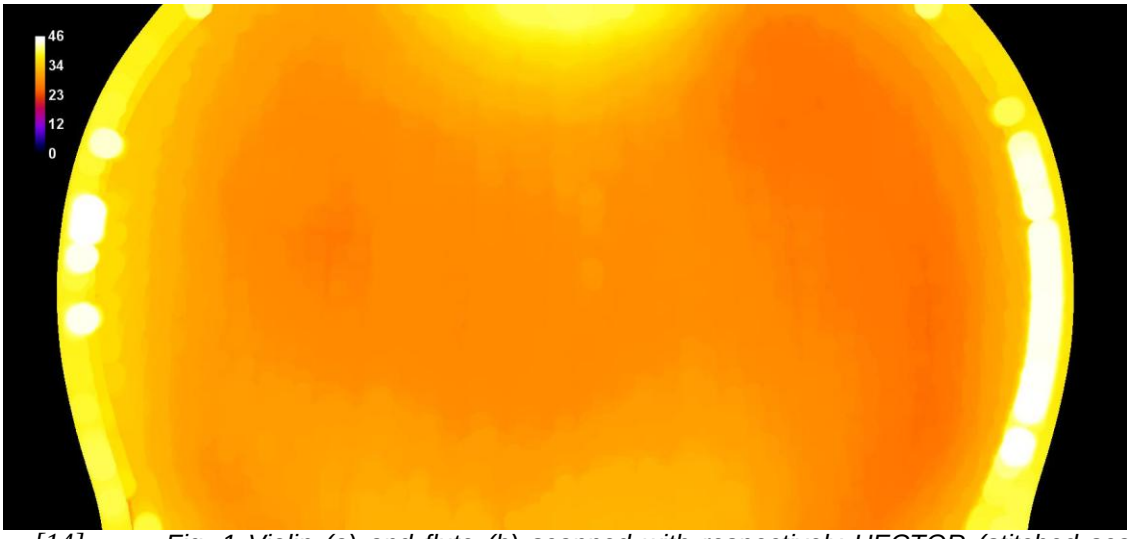

[14] *Fig. 1 Violin (a) and flute (b) scanned with respectively HECTOR (stitched scans) and Nanowood (helical CT). (c) Shows local thickness analysis (in mm) of the violin soundboard and (d) the internal volume of the flute.*

Discussion

The fast evolving field of X-ray computed tomography and its broad employability make it one of the leading techniques for non-destructive visualization and quantification in many different research fields. The flexible Nanowood scanner offers a wide range of opportunities, with specific focus on helical and submicron scanning, yet large object size can be a limiting factor when studying wooden musical instruments. The HECTOR scanner [Masschaele et al. 2013] can be used to scan larger and heavier objects at high resolution and therefore complements the Nanowood scanner. By combination of both scanners a wide range of wooden musical instruments can be analysed for a large range of purposes such as general evaluation, glue line inspection, wood identification, coating inspection, growth ring analysis, etc.

Acknowledgements

The authors acknowledge the fruitful collaboration with all current and former team members of the UGCT, as well as the project SimForTree of IWT Flanders (Strategic Basic Research – SBO 060032) for financial support for obtaining the Nanowood equipment. The authors also acknowledge the financial support of the Flemish community through the Strategic Initiative Materials in Flanders, the special Research Fund of Ghent University and the Research Foundation – Flanders (FWO) for obtaining the HECTOR equipment.

(072) Using X-ray microtomography to assess the vulnerability to drought-induced embolism in plants

*N. LENOIR[1], S. DELZON[2], E. BADEL[3], R. BURLETT[2], B. CHOAT[4], H. COCHARD[3], S. JANSEN[5], J. M. TORRES-RUIZE[2]
nicolas.lenoir@placamat.cnrs.fr

[1] PLACAMAT, UMS3626 CNRS-Univ. of Bordeaux, 87 av. Dr A. Schweitzer, 33600 Pessac (FRANCE)
[2] INRA, UMR BIOGECO, Talence, France
[3] INRA, UMR PIAF, Clermont-Ferrand, France
[4] University of Western Sydney, Sydney, Australia
[5] University of ULM, ULM, Germany

Embolism resistance is a critically important trait for evaluating the ability of plants to survive and recover from drought periods and predicting future drought-induced forest decline. As current methods for measuring xylem embolism in trees are indirect and prone to artifacts, there is ongoing controversy over the capacity of plants to resist or recover from embolism. Indeed, the majority of techniques used to estimate cavitation resistance are indirect and/or invasive. Therefore, artefacts relating to invasive techniques are particularly relevant since xylem sap under tension is in a metastable state and may easily vaporize as a result of disturbance. The debate will not end until we get direct visualization of vessel content. Recently, two distinct technologies have been employed to visualize xylem embolism in intact samples: Magnetic Resonance Imaging (MRI) and X-ray microtomography (micro-CT). MRI systems suffer from poor spatial resolution (20 µm at best) and limited access to the technology. Micro-CT, in contrast, offers a spatial resolution typically around 1 µm, which is more than enough to visualize the lumen content of xylem tracheids or vessels. Thus far, non-invasive imaging on intact plants has only been used to measure cavitation resistance in few species (*Vitis vinifera*, *Quercus* and *Populus*). Further measurement of cavitation resistance using non-invasive imaging on intact plants across a range of species is therefore a high priority.

Synchrotron based microCT produced excellent visualization of xylem tissue in living, intact plants. The high quality of signal and contrast produced by synchrotron based microCT allowed the location and dimensions of both embolised and water filled conduits to be measured to a resolution of 1.62 µm. Our direct observations demonstrate that the four studied species are highly resistant to embolism and not vulnerable to drought-induced embolism in a normal range of xylem tensions. In addition, three dimensional analysis of scan volumes illuminated the fine spatial patterns of embolism spread within each xylem type. We therefore recommend that embolism studies in long-vesseled species should be validated by direct methods such as micro-CT to clear up any misunderstandings on their physiology.

(207) Low-resolution high-speed CT scanning for sawmill log sorting and grading

*Y. AN[1], G. S. SCHAJER[2], C. RISTEA[3], B. LEHMANN[4], D. WONG[5], Z. PIROUZ[6]
yuntao.an@fpinnovations.ca

[1,3,4,5,6] FPInnovations, 2665 East Mall, Vancouver, BC, V6T 1Z4
[2] Department of Mechanical Engineering, UBC, 6250 Applied Science Lane, Vancouver, BC. V6T 1Z4

Significant economic gain can be achieved by grading logs at the inlet of a sawmill so that they can be optimally processed to manufacture the highest possible value products from the available raw material. FPInnovations studies have shown that 8-10% value could be added to each log by simplying being able to detect knots for North American lumber grades. If higher value products and other characteristics were considered, the potenial added value would increase many times. Computed Tomography (CT) has been extensively used as a medical diagnostic tool, and increasingly for scientific and industrial research. For log sanning, CT scanning is of particular interest because it can identify the locations, orientations and sizes of internal quality-controlling features such as knots, heartwood/sapwood extent, cracks, rot and holes. Conventional CT technology is based on medical-style equipment, which needs to have very high spatial and density resolution. Therefore it sets high standards on scanner hardware/software, and thus substantially increases equipment complexity and cost. These features make such equipment unsuited for typical sawmill applications. However, for log scanning applications, high spatial and density resolution and measurement accuracy are not needed because most targeted internal features are fairly large and have specific geometrical shapes. Based on these thoughts, this paper proposes a greatly simplified, mechanically robust and low-cost CT scanning system with ground-breaking geometry-based CT density reconstruction models and algorithms. A generation I lab prototype was designed and built at UBC. Log scanning results compare well with those from an industrial CT scanner using conventional CT reconstruction technique. This good comparison gives confidence in the usefulness and applicability of the proposed approach. FPInnovations is currently researching on upscaling the generation I prototype and developing a commercial ready low-cost high-speed CT scanning system for practical log sorting and breakdown in sawmills.

(212) Effect temperature and tree species on the damage progression of whitespotted sawyer, Monochamus scutellatus scutellatus (Say), larvae in recently burned logs, by X Ray CT measurement.

SÉBASTIEN BÉLANGER[1], ÉRIC BAUCE[2], CHRISTIAN HÉBERT[2], BERNARD LONG[4], RICHARD BERTHIAUME[2], JACQUES LABRIE[4] AND LOUIS-FRÉDÉRIC DAIGLE[4]

1Ministère de la Forêt, de la Faune et des Parcs, 2Laboratoire Entomologie forestière (Consortium iFor), Université Laval, Canada 3Ressources naturelles Canada, Centre de foresterie des Laurentides, Québec, Canada 4Institut national de la recherche scientifique, Centre Eau, Terre & Environnement, Québec Canada

The whitespotted sawyer, *Monochamus scutellatus scutellatus* (Say), is one of the most damaging wood-boring insect in recently burned boreal forest. In Canada, salvage logging can contribute to maintain timber volumes required by the industry but larvae of this insect cause important damage by burrowing galleries into the wood thus reducing the economic value of lumber products. This study aimed to estimate damage progression as a function of temperature in recently burned black spruce and jack pine trees. Using the new axial tomograph technology (CT-Scan), successive pictures of each log were reconstructed in three dimension and galleries depth were determinated with a program developed using Matlab (Natick, MA). These gallery measurements obtained at different time made it possible to model subcortical development, defined as the time elapsed between oviposition and larval entrance into sapwood, as well as gallery depth progression rates as function of temperature for both tree species.

Gallery depth progression was modeled using the Chapman-Richards function. Generally, these rates were slightly higher in black spruce than in jack pine logs. Eggs laid on logs placed at 12°C did not hatched or larvae were unable to establish under bark as no larval development was observed. At 16°C, larvae stayed under the bark for>200 d before penetrating into the sapwood. At 20°C, half of the larvae entered the sapwood after 30-50 d, but gallery depth progression stopped for ≈70 d, suggesting that larvae went into diapause. The other half of the larvae entered the sapwood only after 100-200 d. At 24 and 28°C, larvae entered the sapwood after 26-27 and 21 d, respectively. At 28°C, gallery depth progressed at a rate of 1.44 mm/d. Temperature threshold for subcortical development was slightly lower in black spruce (12.9°C) than in jack pine (14.6°C) and it was 1°C warmer for gallery depth progression for both tree species.

These results indicate that significant damage may occur within a few months after fire during warm summers, particularly in black spruce, which highlights the importance of beginning postfire salvage logging as soon as possible to reduce economic losses.

(206) Cricket bat characterization based on X-ray Computed Tomography and image processing

*J. TAO[1], P. EVANS[2], M. SAADATFAR[1]
jin.tao@anu.edu.au

[1] Department of Applied Mathematics, The Australian National University, Australia
[2] Faculty of Forestry, The University of British Columbia, Canada

This research employed the tomographic technology and related analyzing tools to investigate the unique properties of cricket bat willow/Engilish willow (salix alba var.caerulea), which premium cricket bats are predominantly made from. The cricket bat willow is preferred due to its being lightweight, very tough and shock-resistant, and not being significantly dented nor splintering on the impact of a cricket ball at high speed. Wood, as a major material for construction and sports tools, has not been studied widely by the tomography in terms of relationship between cellular structure and mechanical performance. Micro Computed Tomography (Micro-CT) opens a door for wood scientists to investigate the multi-scale structures of different species in three dimensions.

Wood is a natural composite and porous material, which could inspire various designs of engineered advanced materials in regarding to the layout and binding schemes. It mainly consists of lignin, cellulose and hemi-cellulose, where lignin serves as the adhesive matrix in composite materials while cellulose being the continuous fibre and hemi-cellulose being the non-continuous fibre.

By taking the 3D images of the wood, the interior structure of wood is available as the basis of analysis, e.g. pore inter-connectivity, mass distribution statistics and cell wall orientational anisotropy trend. The image can also be segmented based on binarization of solid and void, and serves as the input for finite element analysis (FEA) method(Saadatfar, Mukherjee, et al., 2012), where the modulii of the sample as a whole are able to be calculated by simulations.

Samples used in this research derive from two cricket bats, one used premium bat and the other brand new first-class bat. Samples are taken from the bats in all three directions of the wood, longitudinal-radial section(LRS), longitudinal-tangential section(LTS) and transverse section (TS). Specimens are conditioned at 65% relative humidity and 20 °C for at least 48 hours prior to mechanical testing.

Specimens are imaged using a Micro-CT facility at 120kV throughout all steps of the in-situ compression with strain interval of 0.005. The series of images obtained are then compared by digital volume correlation (DVC), where we calculate the displacement to the sub-voxel level by locating displaced pixels based on the correlation coefficients of the surrounding pixels (Bay, 1999). Strain tensors of every pixel are also available to generate a strain field map to study the local deformation. The DVC results of displacement and strain are partially displayed in Fig. 1 of a sample before and after in-situ compression from the used bat oriented in LRS. The results from three orthogonal directions will be compared to discover the difference. Then the variance between the new and used bats can be analyzed to distinguish them quantitatively. The ultimate objective of the research is to solve the empirical rule of thumb, that why first-class cricket bat shall be made from English Willow with LRS as the batting surface.

References :
Saadatfar M, Mukherjee M, Madadi M, Schröder-Turk GE, Garcia-Moreno F, Schaller FM, Hutzler S, Sheppard AP, Banhart J, Ramamurty U. (2012) Structure and deformation correlation of closed-cell aluminium foam subject to uniaxial compression. Acta Materialia, 60.8 p. 3604-3615.

Bay BK, Smith TS, Fyhrie DP, SaadM. (1999) Digital volume correlation: three-dimensional strainmapping using X-ray tomography. Exp Mech 39 p. 217–226

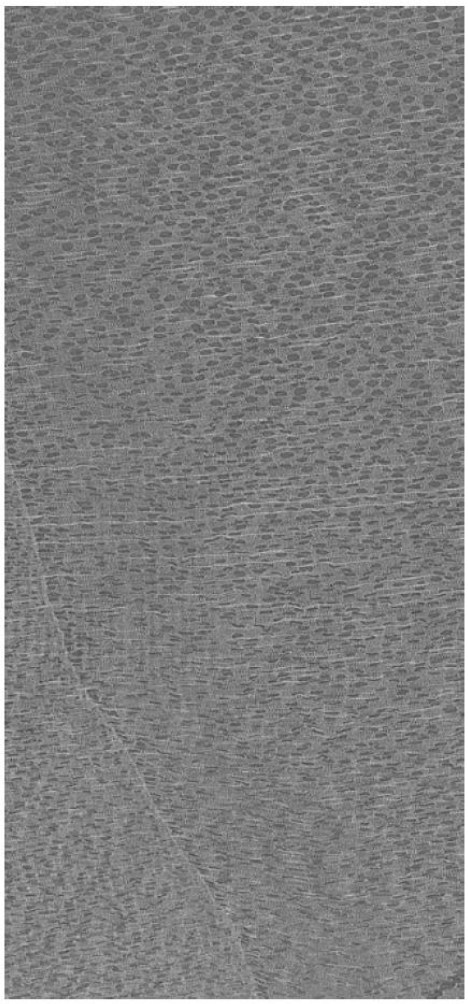

a

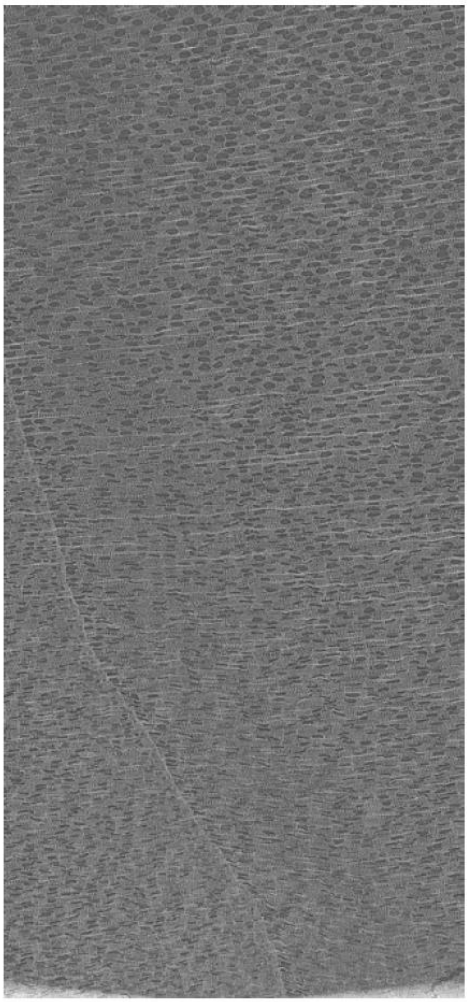

b

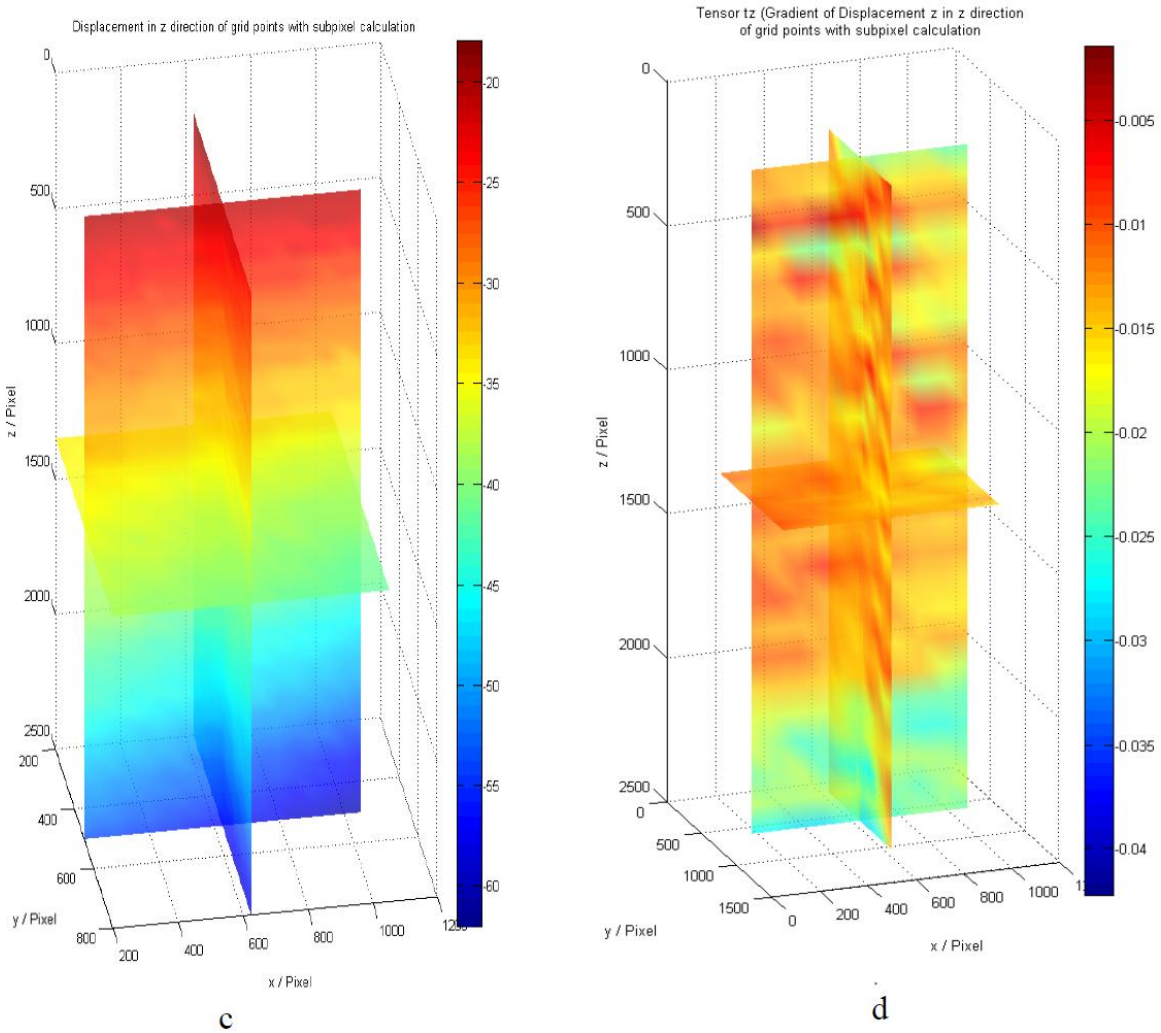

c d

Figure 1. The cross section of the specimen at the same position taken from the tomography at (a)initial step (step 0) and (b)the third step (step 3). The displacement field map in z (compression) direction is shown in (c) and the strain εzz is calculated and presented in (d).

Session 304 - Sedimentary structures: modern and ancients

(029) Dynamic micro-CT analysis of fracture formation in rock specimens subjected to multi-phase fluid flow

*J. VAN STAPPEN[1], T. BULTREYS[1], M. A. BOONE[1], E. VERSTRYNGE[2], V.CNUDDE[1]
jeroen.vanstappen@ugent.be

[1] PProGRess – UGCT – Dept. of Geology and Soil Science – Ghent Universtiy, Ghent, Belgium – www.pprogress.ugent.be
[2] Unit of Architecture and Building Techniques – Campuses Sint-Lucas Brussels and Ghent – Dept. of Architecture – KU Leuven, Leuven, Belgium – www.arch.kuleuven.be

Fractures are widespread in geomaterials throughout the world, contributing to the fluid flow and transport processes in them (Berkowitz, 2002). Not only are they naturally present in many subsurface reservoirs, fractures are also more and more often induced in underground aquifers, thereby affecting the fluids in the earth's crust.Fracture formation in these reservoirs can entail positive consequences, such as a local increase in permeability in the subsurface, intented for enhanced oil recovery or to facilitate CO_2 sequestration; however it can have negative effects if these fractures provide leakage pathways for waste materials. Therefore, it is crucial to understand the process of fracture formation and its influence on fluid distributions in geomaterials. To investigate this at the pore-scale, different add-on modules are combined with the High-resolution X-ray Computed Tomography (μCT) systems available at the Centre for X-ray Tomography at Ghent University (UGCT, www.ugct.ugent.be).

An in-situ load cell, the CT5000 system developed by Deben, United Kindom, is used for the investigation of fracture initiation and propagation in geomaterials. It allows for both compressive and tensile tests with forces up to 5 kN and fits on the High Energy CT system Optimised for Research (HECTOR) at UGCT (Masschaele et al., 2013). Information from acoustic emission testing during compressive tests allows distinguishing different steps in the process of fracture formation and propagation. These are subsequently monitored in the load cell on HECTOR. In these experiments, the analysis of fracture inititiation and propagation is examined on different sedimentary rocks, allowing the determination of the governing features in the rocks influencing these processes.

A second in-situ cell is a state-of-the-art triaxial cell, property of Sintef, Norway. The cell permits cilindrical rock samples of 6 mm in diameter to be subjected to high confining pressures, while multiphase fluid flow is established within them. The cell also allows the induction of fractures in these samples through axial compression. This cell fits on HECTOR and on the Environmental μCT scanner (EMCT) of UGCT (Dierick et al., 2014). This recently refurbished scanner is specifically designed for the investigation of dynamic processes in 3D as a function of time and allows scanning at a frame rate of 12 seconds to permit for 3D time-lapse imaging. With it, multi-phase fluid flow is visualised and analysed at high resolution, before and after the formation of fractures in the rock samples. Consequently, the influence of the induced fractures on the fluid flow is analysed.

This study focuses on experimental monitoring and analysis methods to investigate the dynamic process of fracture formation in rocks and its influence on fluid distributions in them. Through 4D

imaging, the experiments provide insights in the immediate impact of fracture formation in sedimentary rock specimens subjected to multi-phase flow and confining pressures.

Acknowledgement:
Work by these authors was partially supported by FWO, project G.0041.15N and FCWO-UGent.

References :

Berkowitz, B., 2002. Characterizing flow and transport in fractured geological media: a review. *Advances in Water Resources*, 20 (8-12), pp. 861-884.

Dierick, M., Van Loo, D., Masschaele, B., Van den Bulcke, J., Van Acker, J., Cnudde, V., Van Hoorebeke, L., 2014. Recent micro-CT scanner developments at UGCT. *Nuclear Instruments and Methods in Physics Research Section B: Beam Interactions with Materials and Atoms*, 324 (0), pp. 102-112.

Masschaele, B., Dierick, M., Van Loo, D. Boone, M.N., Brabant, L. Pauwels, E., Cnudde, V., Van Hoorebeke, L., 2013. HECTOR: A 240kV micro-CT setup optimized for research. *Journal of physics: Conference Series*, 463 (1), pp. 012012.

(185) CT-Scan analysis of bioturbation structures: from intertidal mudflat to young mangrove forest in French Guiana (South America)

A. ASCHENBROICH[1], E. MICHAUD[1], F. FROMARD[2], L.F. DAIGLE[3], B. LONG[3], G. THOUZEAU[1]
emma.michaud@univ-brest.fr

[1] Laboratoire des Sciences de l'Environnement Marin (LEMAR, UMR 6539, CNRS-IRD-UBO), IUEM, Rue Dumont d'Urville, 29280 PLOUZANE, France
[2] Laboratoire d'écologie fonctionnelle et Environnement (EcoLab, UMR 5245, CNRS-UPS-INPT), Université Paul Sabatier, 118 Route de Narbonne – Bat 4R1, 31062 Toulouse Cedex 9, France
[3] Institut national de la recherche scientifique, Centre – Eau Terre Environnement
2605, boulevard du Parc-technologique, Québec (Québec) G1P 4S5, Canada

Bioturbation activity has considerable impact on ecosystem functioning. By digging and maintaining burrows, transforming and burying organic matter, fauna and roots affect biogeochemical cycles and sedimentary structures at the benthic interface. In French Guiana (South America), the role of bioturbation on mangrove functioning is; however, still unknown. These mangroves are adapted to recurrent sediment disturbances because of huge mud inputs from the Amazon river. The trees colonize new substrata rapidly, which makes it possible to study distinct stages of mangrove development over small spatial scales (i.e., from mudflat to young mangrove). In this study, we expected that biogenic structures (fauna burrows and roots) depend on the benthic fauna and vegetation structure and composition, and may vary with mangrove growth.

Various development stages of the mangrove habitats (mudflat, pioneer and young mangrove) were investigated in order to quantify the biogenic structures according to changes within the benthic fauna and vegetation communities. Vegetation structure was assessed through tree species identification, density measurements as well as biomass calculations, and environmental parameters were determined. For each stage of development, sediment cores were sampled and Ct-scanned for visualizing and quantifying biogenic structures with depth in terms of burrow and root volumes. Vertical sediment characteristics and benthic compositions, and the associated fauna biovolume, were also determined. We present the difficulties encountered with image processing in such mangrove sediments, and compare variations of bioturbation activity and fauna and vegetation structure with environmental conditions.

(110) Computerized coaxial tomography (CT-Scanning) in paleoclimatic studies

P. FRANCUS[1,2], F. LAPOINTE[1,2], C. MASSA[3,] D. FORTIN[4], K. KANAMARU[5], G. ST-ONGE[6,2]
pierre.francus@ete.inrs.ca

[1] Institut National de la Recherche Scientifique, Centre ETE, Québec, Canada
[2] GEOTOP Research Centrer, Québec, Canada
[3] Earth and Environmental Science, Lehigh University, Bethlehem, PA, USA
[4] Earth Sciences and Environmental Sustainability, Northern Arizona University, AZ, USA
[5] Department of Geosciences, University of Massachusetts, Amherst, MA, USA
[6] ISMER, UQAR, Rimouski, Québec, Canada

Medical CT-Scanners allow the rapid 3D visualisation of sediment cores. CT-Scans images correspond to 3-D linear X-ray attenuation pixel or voxel matrix, where higher density and higher atomic numbers result in higher attenuation of X-rays.

This paper illustrates that CT-scanning sediment cores is a powerful tool to identify and visualize, amongst others, physical sedimentary structures (e.g. turbidites), biogenic structures (e.g. bioturbation), coring artefacts, sediment disturbances, hiatus and other erosional features, and therefore is a powerful tool to establish a high-resolution stratigraphy. Moreover, it can be used to establish physical properties of sediments, such as density. This paper presents a comparison of density measurements obtained from CT-Scans images with conventional measurements (Gamma-Ray attenuation, bulk density) over a 100m-long sediment profile and evaluate the quality, sources of error and the comparative advantages of the different methods in terms of accuracy of the signal, and time necessary to perform analyses.

Finally, we applied this technique to the varved sediments of Strathcona Lake sediment, northern Ellesmere Island, in order to obtain annually resolved sedimentary fluxes. Over the last 65 years, annual sediment accumulation rates in Strathcona Lake documented an increase in high-energy hydrologic discharge events from 1990 to 2009. This timing is in agreement with evidence for an increase in the amount of melt on the adjacent Agassiz Ice Cap, as recorded in ice cores.

(136) Assessment of a new method to estimate the thermal conductivity of permafrost using CT scan analyses

*M. A. DUCHARME[1,2], M. ALLARD[1,2], J. CÔTÉ[3], E. L'HÉRAULT[2]

1 Université Laval, Départment de géographie, Faculté de foresterie, géographie et de géomatique, [email: marc-andre.ducharme.1@ulaval.ca ; michel.allard@cen.ulaval.ca]
2 Centre d'études nordiques,[email: emmanuel.lherrault@cen.ulaval.ca]
3 Université Laval, Département de génie civil et de génie des eaux, Faculté des sciences et de génie,[email: jean.cote@gci.ulaval.ca]

Defined as soil or rock that remains at or below 0 °C for a long period of time, permafrost (i.e. perennially frozen ground) covers extensive areas in Arctic regions. It occurs in all types of geological surface material such as solid, fractured and weathered bedrock, gravel, sand, silt, clay or peat and contains ice in various forms and amounts. When building in the Arctic, design considerations require precise knowledge of the thermal and geotechnical properties of the permafrost.Computed tomography provides visualization of the structural organization of permafrost (cryostructure) and to some extent, depending on system resolution, of more intimate soil-particle-ice organization (cryotexture). Previous studies showed great potential in using this technology for classification and volume measurements of permafrost components, i.e. sediment (solid), ice and gas (void) contents.The aims of this study are (1) to developed an innovative and non-destructive approach using CT scan to compute the thermal conductivity of undisturbed permafrost samples and (2) to validate the results computed from CT scan image analysis with proven experimental thermal conductivity tests.

Nineteen permafrost cores from various sedimentary environments (glacial, alluvial, marine, organic, etc.) and with different textures and cryostructure, ranging from homogeneous fine-grained soils with stratified ice lenses to coarse-grained diamictons well-bonded with pore ice, were scanned using a Siemens Somatom 64TM scanner at the Institut National de la Recherche Scientifique (INRS) in Québec city. According to the core diameter (100 mm), a voxel resolution of 0.2 x 0.2 x 0.6 mm was obtained. By selecting a range of TI values corresponding to each of the soil components (sediments, ice, and gas), voxel classification and quantification of the sample components were achieved using ORS Visual© and MatLab ®, therefore providing volumetric contents of the frozen sediments and the bubbly ice (xsoil, xbi) in the permafrost samples. To evaluate thermal conductivity, volumetric CT-scan derived values were then used to feed a three-step thermal conductivity model that takes into account the soil type, the porosity of ground ice and the cryostructure. Futhermore, data from image analysis was used to measure ground ice porosity. For each core, thermal conductivity was measured at the Laboratoire de géotechnique de l'Université Laval using the experimental setup of Côté and Konrad (2005).

Comparisons between CT scan derived conductivities and measured thermal conductivity values show a margin of error of 8,8%. The CT scan used in this study provides voxel resolution larger than the porosity of fine-grained sediments such as silt and clay, yielding an underestimation of pore ice and air content and thereby slightly affecting the prediction of effective thermal conductivity. The very good results obtained so far shall still be significantly improved by the use of a higher resolution CT scanner.

(141) Application of X-ray interferometry to a highly structured calcium carbonate shell (Foraminifera)

G. KNAPP[1], *J. YUAN[2], L. BUTLER[3], N. NAVEJAR[3], M. B. OLATINWO[3], J. GE[4]
gknapp1@tigers.lsu.edu

Department of Chemistry, Louisiana State University, 232 Choppin Hall, Baton Rouge, LA, 70803, USA

Two X-ray tomography/interferometry systems are under construction at LSU. Among the first planned experiments is imaging shells of millimeter-sized foraminifera. We have previously image a foraminifera at a test interferometry beamline at the Advanced Photon Source. The APS work shows an elaborate internal structure, both in absorption and in differential phase contrast. What are the optimal interferometry parameters for the study of a calcium carbonate shell?

The APS data was acquired at 25 keV with a two-grating interferometer; the G0 grating was omitted due to high phase coherence of the bending magnet source at 23 meters downstream of the double multilayer monochromator. The G1 phase grating was optimized for a pi-phase shift at 25 keV with a period of 4.8 micron. The G2 analyzer grating had a period of 2.4 micron; a piezoelectric stage moved the grating in 16 steps over 1.5 periods.

The 100 micron thick LuAG:Ce scintillator was imaged with an optical lens system giving an effective pixel size of 0.645 microns. The interferometry data was analyzed with a vectorized least squares algorithm.

The LSU systems under construction will operate at the LSU CAMD synchrotron and with a lab-based microfocus X-ray tube. The synchrotron beamline is 21 meters downstream from a 7 Tesla, 11-pole wiggler; a double crystal Laue monochromator covers the 40 to 70 keV range. The interferometer thermal and vibration environment is logged. As for the APS system, gratings are purchased from Microworks, but with a design energy of 40 and 70 (phase) keV. The data workflow software consists of Mathematica and Matlab codes within Python wrappers to create modules in a VisTrails workflow. VisTrails Was chosen to serve a wide user base and create a data provenance. The VisTrails workflow uses local computational resources and a special, interactive HPC system. One feature of the VisTrails workflow is export of version of the reconstructed volume, cropped and downsampled, to fit on a tablet and viewed with KiwiViewer (Kitware).

(152) The potential of CT-scan as a high-resolution tool to identify laminated sediments from deep lakes in the Côte-Nord region, Quebec

*O. NZEKWE[1,2], P. FRANCUS[1,2], G. ST-ONGE[2,3], P. LAJEUNESSE[2,4]
obinna_peter.nzekwe@ete.inrs.ca

[1] Institut national de la recherche scientifique, Centre Eau Terre et Environnement, Québec, Canada
[2] GEOTOP Research Centre, Montreal, Canada
[3] Institut des sciences de la mer de Rimouski (ISMER), Université du Québec à Rimouski, Canada
[4] Centre d'etudes nordiques, Départment de géographie, Université Laval, Québec, Canada

This research aims at reconstructing Late Holocene paleoclimate based on annually laminated sediments (varves) from three deep lakes in the Côte-Nord (North Shore) region of Quebec: Lake Walker, Pentecôte and Pasteur. In this region climate data are available from instrumental records covering a 50 years period, and from tree-rings covering 200 years to a millennium. However, the search for laminated sediments in deep lakes offers the possibility to explore this unique paleoenvironmental archive, in order to obtain annually resolved and long records of past climatic conditions. During a two-week fieldwork in June 2014, we obtained 43 short sediments cores ranging from 25 to 75 cm: 16 cores at Lake Walker, 10 cores at Lake Pentecôte and 17 cores at Lake Pasteur. We exposed whole core sections to CT-scan with the aid of a "SIEMENS SOMATOM Definition AS+ 128" Tomography equipment at the INRS Laboratoire Multidisciplinaire de Scanographie. CT-scan allowed for the acquisition of longitudinal and traverse images showing the internal structure of the sediment cores. The resulting images were shown in gray scale, with lighter and darker areas indicating higher and lower X-ray attenuation, respectively. Gray scale values are expressed as Hounsfield units. High quality digital photographs of split-sediment cores were taken with the aid of a GEOTEK Geoscan III line-scan camera that was mounted on a moving frame integrated with a GEOTEK Multi-sensor core logger (MSCL). Photographs were taken immediately after splitting prior to oxidation of the sediment core face. Furthermore, we performed geochemical content analysis of sediment properties using x-ray microfluorescence (µ-XRF). Obtained data show that photographs from digital core imaging capture slight variations in colour and texture but are generally characterized by low contrast. The presence or absence of laminations is better appreciated when digital photos are analyzed alongside CT-scan images. At least 10 out of the16 cores from Lake Walker are visibly characterized by parallel to inclined laminations, while less than 5 cores from Lake Pasteur and Pentecôte shows distinct laminations. CT-scan images and µ-XRF data show good correlation for laminated sections. The annual character of the laminations will be verified by image analysis of thin-sections, and an age-depth model, which will be established by varve counting, supported by radiometric dating (^{210}Pb, ^{137}Cs, ^{14}C) and paleomagnetic measurements.

References

Arseneault, D., B. Dy, F. Gennaretti, J. Autin and Y. Begin (2013). "Developing millennial tree ring chronologies in the fire-prone North American boreal forest." Journal of Quaternary Science **28**(3): 283-292.

Francus, P. (2004). Image analysis, sediments and paleoenvironments. Dordrecht, The Netherlands, Springer.

Jouve, G., P. Francus, S. Lamoureux, L. Provencher-Nolet, A. Hahn, T. Haberzettl, D. Fortin, L. Nuttin and P. S. Team (2013). "Microsedimentological characterization using image analysis and mu-XRF as indicators of sedimentary processes and climate changes during Lateglacial at Laguna Potrok Aike, Santa Cruz, Argentina." Quaternary Science Reviews **71**: 191-204.

Naulier, M., M. M. Savard, C. Begin, J. Marion, D. Arseneault and Y. Begin (2014). "Carbon and oxygen isotopes of lakeshore black spruce trees in northeastern Canada as proxies for climatic reconstruction." Chemical Geology **374**: 37-43.

Nicault, A., E. Boucher, C. Begin, J. Guiot, J. Marion, L. Perreault, R. Roy, M. M. Savard and Y. Begin (2014). "Hydrological reconstruction from tree-ring multi-proxies over the last two centuries at the Caniapiscau Reservoir, northern Québec, Canada." Journal of Hydrology **513**: 435-445.

Ojala, A. E. K., P. Francus, B. Zolitschka, M. Besonen and S. F. Lamoureux (2012). "Characteristics of sedimentary varve chronologies - A review." Quaternary Science Reviews **43**: 45-60.

St-Onge, G., T. Mulder, P. Francus and B. Long (2007). "Continuous physical properties of cored marine sediments." Proxies in Late Cenozoic Paleoceanography. Elsevier: 63-98.

(154) Acquisition of the natural remanent magnetization in varved sediments: Laboratory redeposition experiments, CT-Scan imaging and modeling

*E. G. H. PHILIPPE[1,2], G. ST-ONGE[1], J. P. VALET[2], P. FRANCUS[3]
edouard.philippe01@gmail.com

1 Institut des sciences de la mer de Rimouski (ISMER), Université du Québec à Rimouski, Rimouski, QC, Canada et GEOTOP
2 Institut de Physique de Globe de Paris, Paris, France
3 Institut national de la recherche scientifique, Centre Eau Terre Environnement (INRS-ETE), QC, Canada et GEOTOP

The natural remanent magnetization (NRM) of sediments can be used to reconstruct variations of Earth's magnetic field in the past. Reconstructing variations in Earth's magnetic field is essential for understanding the dynamics of the geodynamo, in addition to serving as a powerful stratigraphic tool. However, the NRM is not only related to the magnetic field behavior and strength, but also depends, to a lesser extent, on the depositional environment and lithology. To accurately determine the paleomagnetic signal from sediments, it is necessary to define the parameters involved in the acquisition of the magnetization. Such parameters include the mineralogy and size of the magnetic particles, as well as other processes which tend to inhibit the alignment of the magnetic grains with the magnetic field such as the deposition of turbidites or debris flows. To succeed in faithfully tracking the geomagnetic variations, it is necessary to determine which processes are involved during the acquisition of the magnetization. We tackle this problematic in three steps: 1) measurement of the NRM of sediments using sediment cores, 2) laboratory redeposition experiments, and 3) modelling. We selected annually laminated sediments (varves) from three deep lakes of the North Shore of the Gulf of St. Lawrence, Quebec (Lakes Walker, Pasteur, and Pentecôte) to perform high-resolution sedimentological, physical, geochemical (^{10}Be) and magnetic measurements. Each core will be checked with CT-Scan imaging to verify the presence of lamination in the sediment. Using this method allows us to see with a high resolution the variation of density in cores. The different properties will be compared in order to identify the factors responsible for the variations of the magnetic signal. Experiments of sediment deposition and compaction will be made in parallel in the laboratory under a controlled magnetic field in order to assess the influence of compaction on the recording of the magnetic signal. CT-Scan imaging will also be used during the experiments to assess the creation and evolution of sedimentary structures and, thanks to the measurement speed, to monitor in real time changes in compaction associated with a varying pressure applied to the sediments. Finally, all the data will be integrated to develop a model of the acquisition of the NRM in laminated sediments.

(209) Ferrous iron in bioturbated sedimentary deposits: a three-dimensional exploratory analysis using planar optodes coupled to tomographic reconstructions

J. SOTO NEIRA[1], E. MICHAUD[2], B. LONG[3], *R. ALLER[1]
emma.michaud@univ-brest.fr

1 Stony Brook University, Stony Brook, NY, 11790, USA
2 Université de Bretagne Occidentale, Institut Universitaire Européen de la Mer, 29238, Brest, France
3 Institut National de la Recherche Scientifique, G1K 9A9, Québec, Canada

Ferrous iron, Fe(II), is abundant in a wide variety of aquatic environments where suboxic and anoxic conditions are developed. In marine sediments, it is typically a product of reduction reactions involving use of Fe(III) as an electron acceptor by microbes during organic matter remineralization, or it is derived from abiotic reactions of Fe(III) with organic and inorganic reducing agents (e.g., thiols, bisulfides). Reactive Fe(III) may be present as both organic complexes and in mineral phases such as ferrihydrite or goethite. Net reduction of Fe(III) often dominates in suboxic regions where manganese oxides are depleted.

Because of the central role of Fe in biogeochemical processes as well as its influence on contaminant distributions in aquatic systems, Fe distributions and cycling patterns in natural sedimentary deposits have been extensively studied. However, most of these studies have emphasized 1-dimensional distributions and associated diagenetic models, and have not considered the complex reaction patterns commonly generated by meio- and macrofaunal activities in organic-rich, bioturbated sediments.

The development of novel planar optical sensors for measurement of Fe(II) and other biogeochemically active solutes in marine sedimentary deposits has allowed our research group to characterize transport – reaction patterns in heterogeneous sediments at high resolution, as well as to evaluate the role of individual macrofaunal species in modifying microhabitats. We have coupled planar optical sensors and tomographic model techniques together with CT-scanning methods, to simultaneously resolve and relate physical and chemical sedimentary structures in 2 and 3-dimensions in marine deposits. Here we present the results of multidimensional measurements of Fe(II) and model flux calculations across the sediment-water interface using a novel planar optical sensor and simultaneous tomographic reconstructions from CT-Scan during laboratory microcosm experiments. These experiments were designed to characterize and more accurately resolve the impact of the polychaete *Nereis* sp. and the bivalve *Macoma* sp. on Fe cycling and redox reactions in the bioturbated zone.

(067) Evaluation of experimental dissolution of dolomite using X-ray computed tomography

*B. BAGLEY[1], B. M. TUTOLO[1], A. J. LUHMANN[1], M. O. SAAR[1,2], W. E. SEYFRIED, JR.[1]
bagley@umn.edu

[1] University of Minnesota, Department of Earth Sciences, Minneapolis, MN 55455
[2] ETH-Zurich, Department of Earth Sciences, Zurich, Switzerland

Flow-through experiments were conducted on nine dolomite cores to simulate CO_2 injection into dolomite reservoirs during geologic carbon sequestration. Experiments at 100 ºC and 150 bar pore-fluid pressure were conducted in single-pass mode using CO_2-charged brine and flow rates that spanned two orders of magnitude. The cores (1.3 cm diameter and 2.6 cm long) were scanned at the University of Minnesota X-ray Computed Tomography (XRCT) facility before and after each experiment to capture mineral volume changes resulting from experimental dissolution. Experimentally-produced dissolution features (i.e., porosity development) were visualized by carefully aligning the pre- and post-experiment cores in three dimensions. Dissolution produced a range of dissolution patterns, including highly permeable flow channels or wormholes.

Previous work provided insight for a porosity-surface area model using the general shapes of the dissolution channels that developed from fluid-rock reaction (Luhmann et al., 2014). Here, we produce a more complete quantification and characterization of the experimentally produced dissolution structures. Specifically, we calculate the diameter, tortuosity, and center of mass of the dissolution structures, and attempt to develop predictive capabilities by calculating correlations between the locations of post-experimental dissolution features and pre-experimental flow properties. By dividing each sample into a 3-dimensional grid of Representative Elementary Volumes (REVs) of various sizes, we attempt to define a characteristic length scale that controls the evolution of dissolution features, and provide important input data sets for high resolution computational fluid dynamics simulations.

The size of the cores limit XRCT resolution to 8 µm, which in turn determines the smallest resolvable features. As a result, our porosity measurements represent the macro porosity in the cores. To capture the micro- and nano-scale porosity, we conducted combined Small and Ultra Small Angle Neutron Scattering ((U)SANS) analyses, which permit investigation of features in the range of ~10 nm to ~10 µm. Simultaneous consideration of calculations based on the invariants of the (U)SANS curves, the XRCT data sets, and full-core porosity measurements demonstrates that ~50% of the pores within the experimental samples are within this lower (<10 µm) pore size range. This combined result suggests that the characteristic length scales for dissolution phenomena in dolomites may be below the resolution of the XRCT measurements, and that a combined approach of this type may be warranted to develop appropriate scaling functions.

References :
A.J. Luhmann, X.Z. Kong, B.M. Tutolo, N. Garapati, B.C. Bagley, M.O. Saar, W.E. Seyfried Jr., (2014) Experimental dissolution of dolomite by CO2-charged brine at 100 °C and 150 bar: Evolution of porosity, permeability, and reactive surface area, Chemical Geology, 380, 145-160, doi:10.1016/j.chemgeo.2014.05.001.

(037) Determination of the REDOX paleoconditions: A MCT study of micro pyrite section 308

*V. CARDENES[1], J. DEWANCKELE[1], W. DE BOEVER[1], J. P. CNUDDE[1], V. CNUDDE[1]
victor.cardenes@ugent.be

[1] Pore-scale Processes in Geomaterials Research Team (PProGRess), Geology Department, Ghent University, Krijgslaan 281 (S8), 9000 Ghent, Belgium

Microscopic pyrite (MPy) is a very common mineral usually found under the form of framboids or euhedral crystals, with an average size between 5 and 60 microns. In sedimentary basins, the ocurrence of MPy in sediments reflects the primitive REDOX conditions (Wilkin et al., 1996).

For euxinic and anoxic conditions, MPy are small and abundant, while with higher contents of oxygen, under dysoxic conditions, MPy are bigger and relatively scarce. The characterization of MPy populations distribution is then a reliable proxy of the environmental paleoconditions (Bond and Wignall, 2010). However, formation of MPy is not restricted to sedimentary environments. In low degree metamorphic and hydrothermal conditions, MPy may also form (Scott et al., 2009). Again, the size and shape of MPy depends on the environment.

In previous works related to this subject, measurement of the MPy populations was done using traditional microscopy techniques (SEM, ore microscopy), which means counting the objects one by one and measuring between 80 and 400 objects per sample. In recent times, the development of micro computed tomography (MCT) techniques has opened a new horizon for measuring MPy. Pyrite usually has a higher X-ray attenuation coeficient than the rest of minerals composing these type of sediments (quartz and mica). In this way, segmentation of MPy is possible. In addition, the use of MCT for characterizing MPy populations is much faster and accurate than the traditional microscopy techniques, since MPy can be classified according to several parameters (maximum diameter, volume, abundance, etc.). Up to several thousands of objects can be measured for each sample, giving much more reliable statistical information than the examination with microscopic techniques.

This work presents the results of the MPy determination in a sample of anchimetamorphic green slate from Brazil, just on the boundary between diagenesis and metamorphism. This slate shows no traces of further metamorphism and keeps the original population of MPy deposited during the sedimentation. Resulting MCT scans were analyzed using Octopus Analysis (Brabant et al., 2011), which is able to perform an accurate estimation of the MPy present in the slate matrix, and hence deduce the paleoconditions of the original basin.

References :
(1) Wilkin, R.T., Barnes, H.L. and Brantley, S.L. (1996): The size distribution of framboidal pyrite in modern sediments: An indicator of redox conditions. Geochimica et Cosmochimica Acta 60, 3897-3912.
(2) Bond, D.P.G. and Wignall, P.B. (2010): Pyrite framboid study of marine Permian-Triassic boundary sections: A complex anoxic event and its relationship to contemporaneous mass extinction. Geological Society of America Bulletin 122, 1265-1279.
(3) Scott, R.J., Meffre, S., Woodhead, J., Gilbert, S.E., Berry, R.F. and Emsbo, P. (2009): Development of framboidal pyrite during diagenesis, low-grade regional metamorphism, and hydrothermal alteration. Economic Geology 104, 1143-1168.
(4) Brabant, L., Vlassenbroeck, J., De Witte, Y., Cnudde, V., Boone, M., Dewanckele, J., Van Hoorebeke, L. (2011): Three-dimensional analysis of high-resolution X-ray computed tomography data with Morpho+. Microscopy and Microanalysis 17(2), 252-263

Session 306 - Innovative Geotechnical Applications

(013) X-ray computed tomography investigation of structures in claystone at large scale and high speed

*G. ZACHER [1], A. KAUFHOLD [2], M. HALISCH [3], J. URBANSKI [4]
gerhard.zacher@ge.com

[1] GE Sensing & Inspection Technologies GmbH, phoenix|x-ray, Niels-Bohr-Str. 7, 31515 Wunstorf, Germany
[2] Federal Institute for Geosciences and Natural Resources, Stilleweg 2, D-30655 Hannover, Germany
[3] Leibniz Institute for Applied Geophysics, Stilleweg 2, D-30655 Hannover, Germany
[4] GE Inspection Technologies, 50 Industrial Park Road, Lewistown, PA 17044, USA.

In the past years X-ray Computed Tomography (CT) became more and more widely used in geosciences from the microscale (microfossils) up to the decimeter scale (cores or soil columns). The method is applied e.g. in structural investigations, *in situ* investigations of processes during tests, porosity and permeability analysis for sediments etc. Hence a variety of systems were adapted to these applications and the investigated specimen size.

In the present paper we investigate CT results from an Opalinus Clay core (diameter ~100 mm) considering the 3D distribution of cracks. Two CT systems are compared, both with specific advantages: the large and flexible phoenix v|tome|x L300 high energy CT scanner and the high throughput speed|scan CT 64 helix CT system (both GE Measurement & Control). The results are compared with regards to contrast resolution, spatial resolution, and scanning speed. The fast medical scanner provides a quick overview whereas the microfocus tube allows a more detailed view on cracks.

For the understanding of deformation processes during mechanical testings detailed information before and after the mechanical testing is required. Thus, it is necessary to obtain micro fabric information of the undisturbed specimen and an overview of the deformed specimen after the mechanical test. Using the overview scans it is possible to select regions of interest (ROIs) which can be analysed in more detail using high resolution CT devices. Suitable position for further micro plugging can be identified from fast 3D scans.

Selected areas are analysed using high-resolution CT techniques as well as mineralogical and geochemical methods. The overall aim of the investigation of the Opalinus Clay (LT-A Project, Mont Terri) is to understand the rock deformation processes upon mechanical stressing. This behaviour is largely governed by the microstructure. CT investigations, therefore, are the key methods for understanding the processes during the mechanical tests.

Additionally, chemical and mineralogical methods are used not only to characterize the material but also to identify homogeneous areas which can be considered representative of the entire rock. Hence, the CT information gathered from a small volume can be used to understand the mechanical processes of the entire rock.

(046) Crack localization in digital volume correlation: Regularization with a damage law

A. BOUTERF[1], *S. ROUX[1], F. HILD[1]
bouterf@lmt.ens-cachan.fr

[1] LMT, ENS-Cachan, CNRS, Univ. Paris-Saclay, 61 Av. Président Wilson, 94235 Cachan Cx., France

Lightweight plasterboard is a product composed of a foamed plaster core whose porosity can reach 75% lined with two sheets of paper. To optimize the compromise between thermal resistance and mechanical strength, it is important to understand and characterize the mechanical behavior of plasterboard. One of the most important properties is a high resistance to bending that has been introduced in the ASTM C11 standard. The analysis of a bending test showed that the failure mode of the sample is quite complex, namely, it combines multiple core cracking and paper facing debonding. It was also shown that the behavior of the plate is controlled essentially by the mechanical properties of the paper and the quality of the paper-plaster interface [Bouterf 2015]. The present study aims to better understand the failure mechanism of the lightweight plasterboard sample subjected to in-situ (i.e. in a tomograph) bending test using regularized digital volume correlation.

To advance the understanding of the failure mechanism, in-situ three point bend test is conducted. The 200 x 13 x 15 mm^3 specimen is prepared from an industrial plasterboard. A cylindrical support (16 mm in diameter) is chosen. The experiment was carried out using a PMMA loading device, which is virtually transparent to X-rays. The specimen is scanned first in an unloaded state and then again at four different loading steps until failure. The experiment has been conducted on an NSI- X50 tomograph located at LMT-Cachan.

The reconstructed volumes are exploited using Regularized Digital Volume Correlation (RDVC) [Taillandier-Thomas 2014] to measure the displacement fields in the bulk of the sample thanks to the very heterogeneous texture of plaster. The sub-volume size used in the correlation analysis is 248 x 200 x 176 $voxels^3$, corresponding to a physical region of the size 6.2 x 5 x 4.4 mm^3. Displacements are decomposed over a regular mesh composed of C8 elements whose size is chosen to be 8 voxels. An elastic regularization allows for a good convergence and reveals the presence of crack through a high strain concentration region. The residual field (difference between the reference and corrected deformed images) confirms that this high strain region does indeed contain a crack.

In order to better localize the crack pattern, a refined calculation is proposed. It consists of implementing a damage law in the regularization instead of an elastic one. The idea is to first be more faithful to the actual mechanical behavior and secondly to relax the smoothing effect of the elastic regularization in regions where strains are already high. The localization property of a softening damage law tends to concentrate damage and hence strain onto the crack surfaces (at the element scale).

References :
Bouterf, A., Roux, S,. Hild, F., Vivier, G., Brajer, X., Maire, E. b. Damage law identification from full field displacement measurement: Application to four-point bending test for plasterboard. European Journal of Mechanics - A/Solids, 49, 60-66, 2015.
Taillandier-Thomas, T., Roux, S., Morgeneyer, T.F., Hild, F. Localised strain field measurement on laminography data with mechanical regularization. Nuclear Instruments and Methods in Physics Research Section B, 324, 70-79, 2014.

(057) A microstructural finite element analysis of cement damaging on Fointainebleau Sandstone

S. NADIMI[1], *J. FONSECA[1], P. BÉSUELLE[2], G. VIGGIANI[2]
joana.fonseca.1@city.ac.uk

1 City University London, UK
2 Laboratoire 3SR, Grenoble, France

This paper presents a micro-scale numerical simulation to predict the effect of inter-particle bonding on the mechanical behaviour of a quartz-cemented, with 6% porosity, specimen of Fontainebleau sandstone. The internal deformation of this sandstone from the Paris basin (France) has been observed from triaxial compression tests operating inside an x-ray scanner. The tomographic images used, had a spatial resolution of 8.5µm, i.e. $0.033 \times d_{50}$, enabling the overall grain arrangement and contact topologies to be captured and their evolution during loading evaluated. Under a confining pressure of 2MPa and an increasing deviatoric loading, the material exhibited brittle behaviour up to peak stress followed by an abrupt drop to an ultimate stress value. Axial splitting was observed to occur in the sample shortly after 2% axial deformation, as a consequence of tensile failure at the grain-to-grain cemented interfaces. The grain-scale phenomena underlying the macro-scale response was observed to involve progressive contact damaging or 'cracking' leading to the debonding along the cemented contacts. These softening processes eventually coalesced into larger geometrical discontinuities or 'vertical ridges', which resulted in the formation of vertical columns of horizontally unbonded grains able to transfer stresses along the direction of the major principal stress (Fonseca *et al*., 2013). The microstructural finite element (µFE) model proposed here combines micro-computed tomography data with finite element analysis. It takes as input a two-dimensional image that was converted to a numerical model using a pixel-to-element approach. The three phases, i.e. solid grains, void space and bonded contacts, were identified and the individual contacts were segmented using an intensity-based threshold technique. This segmented image is the starting point for the image-based mesh. The recreation of the bonding damage and crack formation was carried out by using a constitutive model which allows the identification of the cracking path. For an imposed boundary loading, the onset of the cracks in the cemented contacts is assigned to the integration points by means of weakening of the current strength and stiffness at those points. It is considered that a crack is initiated when the stress at a integration point satisfies a specified condition, e.g. the major principal stress reaching the tensile strength. These small cracks are then connected to form one, or more than one, dominant crack, as deformation progresses. This study contributes towards the modelling of geomaterials that accounts for the effects of the microstructure on the stress transmission mechanisms of bonded granular materials.

References :
Fonseca, J., Besuelle, P. and Viggiani, G. (2013) *Geotechnique Letters* **3**, No. 2, 78–83.

(069) X Ray CT evaluation method for filling of permeable repair material into porous asphalt mixture

*T. FUMOTO[1], S. MOTOMATSU[2], M. OHARA[3], K. UESAKA[4], A. ADACHI[5]
fumoto@civileng.kindai.ac.jp

[1] Kinki University, Faculty of Science and Engineering, Department of Civil & Environmental Engineering 3-4-1 Kowakae, Higashiosaka, Osaka 577-8502, JAPAN
[2] West Nippon Expressway Company Limited, Technical Development Bureau, Dojima Avanza 18F 1-6-20 Dojima Kita-ku Osaka, 530-0003, Japan
[3] West Nippon Expressway Company Limited, Technical Development Bureau, Dojima Avanza 18F 1-6-20 Dojima Kita-ku Osaka, 530-0003, Japan
[4] Showa Rekisei Industries Co.,Ltd. 30-1 Hara Taishi Ibo-gun Hyogo, 671-1502, Japan
[5] Showa Rekisei Industries Co.,Ltd. 30-1 Hara Taishi Ibo-gun Hyogo, 671-1502, Japan

A porous asphalt mixture having continuous pores is a road material with water permeability and sound absorbency. The porous asphalt mixture consists of a high viscosity modified asphalt coating thinly crushed stone surfaces, and the crushed stones bonded to each other. The high viscosity modified asphalt has high durability. However, the asphalt deteriorates due to dynamic fatigue and weather. When the deterioration is small, the porous asphalt mixture is repaired.

One method of repairing the porous asphalt mixture is spraying the repairing material (asphalt emulsion) from the pavement surface. The repairing material coats the inner surface, and collects at the bottom of the porous asphalt mixture. The resultant formation of the water interception layer and the improvement of adhesive strength between coarse aggregates may be the effects of the repair. However, such effects are not understood well, because the visualization in the porous asphalt mixture has been difficult.

The X-ray computed tomography (CT) can visualize the inside of the porous asphalt specimen. At the same time, the X-ray CT method would allow estimation of the mixture ratio of materials in the porous asphalt specimen where the repairing material has been sprayed. This is because the CT value distribution obtained by the X-ray CT is composed of overlapping CT value distributions of different materials. If the CT value distribution of each material has the same shape as a normal distribution, the mixture ratio of the materials is calculated by the method of least squares. Then, the filling distribution in the height direction in the porous asphalt test specimen can be determined based on the change in the mixture ratio of materials. This study shows that the X-ray CT enables determination of the filling distribution in the height direction in the porous asphalt test specimen.

First, the CT value distribution of the specimen was measured before and after saturation of the repair material in the pores of the specimen. The CT value distribution changed from the CT value distribution of the unrepaired specimen because the CT value of the pore increases when the repairing material is saturated. Of such changes, the decrease would relate to the CT value of the pore and the increase would relate to the CT value of the asphalt material. On the other hand, the unchanged distribution would relate to the aggregate. Based on such information, the mixture ratios of three materials in the porous asphalt mixture were calculated by the method of least squares. As the result, the proposed method had a measuring error of 5%.

Next, a porous asphalt specimen of 67.4 mm in height was soaked to the height of 15 mm in the repairing material poured into a cup. The repairing material was then poured to the height of 30 mm from around the specimen. Finally, the repairing material was sprayed over the specimen. The CT value distribution of each specimen was measured at every height of 10 mm. The

difference in the mixture ratio of materials before and after the filling of the repairing material was used to calculate the filling rate of the repair material. The results show that this method can estimate the filling height of the repairing material and the quantity of the repairing material attached to the inner surface.

References :
Takayuki FUMOTO: Development of a New Industrial X-ray CT System and Its Application Compression Test of Polymer Concrete, Journal of Japan Society of Civil Engineers, Division E, Vol. 69, No. 2, pp.182-191, 2013.4 (in Japanese).

(084) Topological characterisation of pore deformations in dense granular packings and geomaterials

*M. SAADATFAR[1], H. TAKEUCHI[2], M. HANIFPOUR[3], N. FRANCOIS[1], V. ROBBINS[1], Y. HIRAOKA[2]
mohammad.saadatfar@anu.edu.au

[1] Department of Applied Mathematics, Research School of Physics and Engineering, Ausralian National University, Canberra – Australia
[2] AIMR, Tohoku University, Japan
[3] Department of Physics, College of Sciences, Tehran University Iran

Geomaterials (granular materials, soils and rocks) have some specific properties, which affect their behaviour and set them apart from conventional solids. Producing mathematical models and constitutive equations to model such properties is extremely challenging due to the multi scale behaviour of granular systems. Understanding properties such as dilatancy, creep and non-affine deformations requires detailed grain-scale knowledge of both short and long range spatial rearrangement mechanisms and pore morphology.

Dense packings of identical spheres are commonly used to model this complex behaviour as well as modelling global ordering transitions. Among the available methods used to characterise sphere packings are the distributions of bond angle and dihedral angle. However, because these distributions only extract configurations up to the third nearest neighbours, they cannot provide a complete description.

In this presentation we demonstrate a new method for the geometric characterisation of amorphous sphere packings called Persistent Homology (PD). We use data from experiments and simulations to explore features of packings using PD. Persistent homology allows us to uniquely quantify topological entities such as loops or cavities in complex structures. We show that it provides an efficient way to quantify grain rearrangement and pore deformation. Additionally, it allows us to distinguish structures with identical packing fractions.

(085) Observation of ground displacement and strain field around the driven open-section piles

*T. SATO[1], K. ONDA[2], J. OTANI[1]
sato@tech.eng.kumamoto-u.ac.jp

[1] X-earth Center, Kumamoto University, 2-39-1, Kurokami, Chuo-ku, Kumamoto, 860-8555, Japan
[2] JFE Steel Corporation, 1-1, Minamiwatarida-cho, Kawasaki-ku,Kawasaki, 210-0855, Japan

In the field of civil engineering, the sheet pile is indispensable structural form for the public works on land development, flood-control, structural foundations and basements. The interlocked sheet piles form a wall for temporary construction as earth retaining structures with reduced groundwater inflow. Sheet piling have the advantages of requiring a little on-site construction, which simplifies on-site work control and shortens work periods. Sheet piles are also a sustainable option since recycled steel is used in their construction, and the piles can often be reused. Further, new sheet pile foundations have been proposed, such as the jacking methods, which can reduce both the noise and vibration during installation. The new sheet piling method can reduce the environmental loads than so far.

Recently, the usability of sheet piles have been re-evaluated, many sheet piling constructions have been proposed for permanent structure as revetments of road, bridge pier foundation. Furthermore, the bulkheads method as continuous impermeable walls have been used as countermeasure for liquefaction on loose sand ground and retarding settlement on soft ground in japan. It is expected that the sheet piling construction will cover wider for public work in the future. Therefore, it will increases that the demand of the development about advanced construction method and form of sheet piles. The sheet piles have been applied to variety ground from the soft clay to dense sand, and the casting depth are various. Also, there are some methods, hammering, vibrating and jacking, for casting sheet piles. As a problem of this sheet piling constructions, according to the ground condition, sometimes happen the deterioration of work efficiency and defective construction. However, the many reasons of these problems are unclear because it is difficult to inspect from appearance on site. The one of the causes of defective construction is expected that the cross sectional shape of the sheet pile. The sheet pile form is not closed as for pipe piles but is open-shaped. Further, the form is not symmetry as for H-type steel pile. It seems that the asymmetric form of the sheet pile causes the occurrence of the stress imbalance in ground. Presumably, the stress imbalance lead to the incline installation of sheet piles.

The paper presents results from a series of laboratory model tests investigating the model ground behavior around the sheet pile on different shape. These tests examined the effects of pile tip shape on the bearing capacity by comparing the measured installation resistance. The analysis results of displacement and strain fields in the penetration test using the X-ray computerized tomography scanner and the digital image correlation.

The tests were carried out in the cylindrical aluminum tank, 50 mm in diameter. The soil used in the tests was dry sand. To compare the effects of cross-sectional shape of model pile for bearing capacity and ground behavior, sheet pile and plate pile ware prepared. Through the whole penetration process, the load and vertically penetration displacement at the pile head was

measured. The soil box was scanned at initial condition and pile penetration depth at 60, 80 and 81 mm. The deformation and strain fields in the model ground analyzed using DIC method. It was shown from the DIC results that the sand around the plate pile deformed at just under the real part of pile. In contrast to plate pile, the sand which exist inside of cross sectional area of sheet pile deformed with pile. Further, the deformation area at the sheet pile tip was wider and deeper than plate piles one. It was revealed that the difference of deformation area at the cross sectional inside and outside of sheet pile.

(005) Study on displacement and strain field analysis in wheel-tracking test of asphalt mixture using X-ray CT and Digital Image Correlation

*S. TANIGUCHI[1], J. OTANI[2], T. SATO[3], T. KIMURA[1]
taniwork1535@gmail.com

[1] Civil Engineering Research Institute for Cold Region, Public Works Research Institute, 1-3-1-34, Hiragishi, Toyohira-ku, Sapporo, 062-8602, JAPAN [e-mail: taniwork1535@gmail.com]
[2] X-earth Center, Graduate School of Science and Technology, Kumamoto University, 2-39-1, Kurokami, Chuo-ku, Kumamoto, 860-8555, Japan
[3] X-earth Center, Faculty of Engineering, Kumamoto University, 2-39-1, Kurokami, Chuo-ku, Kumamoto, 860-8555, Japan

Asphalt mixture is a material composed of coarse aggregate, fine aggregate, filler and bitumen, and mainly used as pavement surface or bituminous course. Asphalt concrete pavement has been subjected to various distresses under various load, temperature conditions and so on. Wheel-tracking test is a dynamic test performed to assess the flow deformation of asphalt pavements. However, wheel-tracking test can only evaluate the deformation on surface of specimens. Since wheel-tracking test does not evaluate within the specimens, internal deformation and strain has hardly been discussed. This paper presents the analysis result of displacement and strain fields in the wheel-tracking test using the X-ray computed tomography (CT) scanner and the digital image correlation (DIC). In addition, this paper mentions the causes of damage in the asphalt concrete pavement such as rutting and cracking from these analysis results.

The mixture types used in the experiments were dense-graded asphalt mixtures using straight and polymer modified asphalt, and a porous asphalt mixture. Their shape was rectangular parallelepiped and size was 150mm width, 300mm length and 50mm height. Each mixture took wheel-tracking test under the conditions of 0.63MPa contact stress and 60°C temperature. X-ray CT scanner used in this study was the industrial one operated by the X-Earth Center of Kumamoto University. The voltage of the X-ray source was set to 300kV to avoid artifact, the beam thickness was set to 1.0mm, and the spacial resolution was set to 0.073 x 0.073 x 1.0 mm^3. X-ray CT scanning was conducted before and after 600 and 2400 times loadings of the solid tire for each specimen. Then, deformation and strain fields for specimens were determined from the conparison of the CT images and DIC analysis using TomoWarp code developed at Laboratoire 3SR at Université Joseph Fourier, France.

The analysis of the displacement field presented following results.

1) The displacement obtained from the CT image and DIC analysis substantially coincided with the result of wheel-tracking test.
2) The vertical and horizontal displacement was increased in the order of dense-graded asphalt mixture using straight asphalt, porous and dense-graded using polymer modified.
3) Radial movement of aggregate around the loading position was confirmed in all specimens at 600 times loading.
4) Uplift of the asphalt mixture has been confirmed in the side of the loading position at 2,400 times loading. This is because the aggregates became dense situation meshed by compaction up to 600 times loading.

In addition, the following results were obtained from horizontal tensile strain that causes longitudinal cracks.

1) In the dense-graded asphalt mixture using straight asphalt, large tensile strain was locally generated. However, tensile strain was overall small.
2) In the dense-graded asphalt mixture using polymer modified asphalt, large tensile strain was generated centrally in the specimen surface at the 600 times loading. This indicates the possibility for occurrence of top-down cracking.
3) In the porous asphalt mixture, large tensile strain was generated in the interior of the specimen at the 600 times loading. This indicates that longitudinal cracking develops not only from the surface or bottom but also within the asphalt concrete.

Therefore, X-ray CT and DIC in order to grasp the inside of the asphalt mixture are very effective in the assessment of asphalt concrete pavement damages. Besides, to evaluate not only the surface but also the internal of the asphalt mixture is preferable in order to evaluate the long-term durability of the asphalt pavement.

(008) Nanoscale mechanical properties of chalk from X-ray tomography

D. MÜTER[1], *H. O. SØRENSEN[1], K. N. DALBY[1], S. L. S. STIPP[1]
mueter@nano.ku.dk

1 Nano-Science Center, Dept. of Chemistry, University of Copenhagen, Denmark

Chalk is a biogenic limestone featured prominently in the coastline of countries bordering the North Sea, e.g. White Cliffs of Dover (UK) or Stevns Klint (DK), and acts as both groundwater aquifers and hydrocarbon reservoirs world wide. It is formed by the microscopic shields (coccoliths) that remain from ancient algae. Even after millions of years, many of the original coccoliths (<10 µm diameter) remain intact. Hence, both particles and pores in chalk are nano metre scale and their geometry is complex, which makes the material properties of chalk, e.g. mechanics hard to predict. On the macroscale, chalk is known to be “very weak”, i.e. its Young’s modulus drops rapidly with increasing porosity.

To understand how the macroscale properties are controlled by the micro- and nanoscale structure in chalk, we recorded high resolution X-ray tomography data from chalk samples with different porosites, at the Swiss Light Source (SLS), using ptychographic X-ray tomography (21 nm voxel size). From the segmented tomography data, we created an adaptive volume mesh for the regions of interest in the material, which can be imported into finite element software to derive mechanical properties. Simulating uniaxial tension, we were able to calculate the Young’s modulus of the chalk matrix and determine its dependence on porosity. Our results show that the Young’s modulus of chalk drops by an order of magnitude at a porosity of 40% in comparison to bulk materials. This can be mainly attributed to the small contact area between the individual calcite grains. The finite element simulations roughly reproduce the trend in the macroscopic measurements but the Young’s modulus in the simulations is higher, especially at medium porosity (10-40%). This can either be caused by a lack of resolution in the tomography data (Müter et al., 2014) or by larger scale fractures that are not present in the samples imaged in tomgraphy which were taken from the rock matrix.

References :
Müter, D., Sørensen, H.O., Jha, D., Harti, R., Dalby, K.N., Suhonen, H., Feidenhans’l, R., Engstrøm, F. & Stipp, S.L.S.: Resolution Dependence of Petrophysical Parameters derived from X-ray Tomography of Chalk. Appl. Phys. Lett. 105 (2014), 043108.

(050) FE-analysis of granular materials based on X-ray CT data

D. TAKANO[1], *Y. MIYATA[2]
takano-d@pari.go.jp

[1] Port and Airport Research Institute, 3-1-1 Nagase Yokosuka JAPAN
[2] National Defence Academy of Japan, 1-10-20 Hashirimizu Yokosuka JAPAN

In geotechnical engineering, analysis of granular materials such as sand, silt and rock is a key-issue. In particular, for failure of soils, strain localization is a phenomenon commonly observed in granular materials including soils and it is a key issue to understand the stability of soils or the interaction between soils and structures. The mechanical properties of the granular materials depend on the shape of particle, its density and structure. For detailed analysis, not only macro but also micro information is very important. However its technical development is not enough.

X-ray Computed Tomography (CT) is a visualisation tool that allows observation of the internal 3D structure of materials and has been applied to study localised deformations of geomaterials in the last two decades.

In experimental studies, quantitative evaluation of localised behaviour from micro- to macro-scale can be achieved through full-field measurements of displacement and strain fields in soil specimens under load. Digital Image Correlation (DIC) is a powerful tool in experimental mechanics that provides full-field measurements of kinematics and strains at the surface of or within an object during its deformation. The combination of both methods provides a quantitative evaluation of 3D deformation process of gramular materials.

In numerical analysis of the failure behavior of soils, the distinct element method (DEM) has been widely used. However, input parameters to specify the characteristics of the spring (i.e., the interaction between particles) cannot be determined systematically.

In this paper, the authors proposed a FE-analysis method based on X-ray CT data for granular materials. Firstly, localized behavior of granular materials is revealed by X-ray CT and digital image correlation. Then, the FE-analysis is implemented with particle discretization, both mesh size and geometry is determined from X-ray CT data. In this research, a series of analysis result for sand is discussed. Laboratory test results and simulation results are compared, and validation of the proposed is discussed. Utilizing micro-data is strongly impressed.

(070) Measurement of three-dimensional deformation inside construction material using X-ray CT and Particle Tracking Velocimetry

*T. FUMOTO[1], K. TAKEHARA[2]
fumoto@civileng.kindai.ac.jp

[1] 3-4-1 Kowakae, Higashi-Osaka, 577-8502 Japan
[2] 3-4-1 Kowakae, Higashi-Osaka, 577-8502 Japan

X-ray CT is one of the most powerful tools which can measure structure in materials without any intrution of sensors. The standard industrial X-ray CT usually has a fixed X-ray tube and detector, and the specimen has to be rotated for the scannning of X-ray. In this case, the size of the specimen becomes relatively small and the load to act on the specimen becomes relatively low. For the measurements of construcion material specimens, it is important to measure deformations under the load which is acting on the actual construction material.

Fumoto (2013) have developed a new X-ray CT system which can measure the interior structure of a specimen of construction material under relatively large load acting on the specimen. In this X-ray CT system, the specimen is fixed on a stage and the X-ray tube and detector turn around the specimen. Large load, which acts on the actual construction, can be loaded on the specimen because the rotatiing X-ray tube and detector system is mechanically separated from the specimen stage. The developed X-ray CT system can measure the three dimensional movements of the aggregates inside the constrauction materials. However, it is very difficult to measure the movements of many aggregate inside the construction material by human eyes.

In the flow measurement techniques, the Particle Image Velocimetry, called PIV, is a very powerful tool to measure temporal and spatial movements of many particles automatically. The advantage of the PIV can measure the instantaneous two dimensional or three-dimensional movement distributions. When video cameras are used for image capturing devices, the two-dimenaional or three-dimensional movement distribution data are acquired as time series data.

Particle Tracking Velocimetry, called PTV, is one of the PIV, which evaluate velocity by measruing a movement of each tracer particle. Takehara et al. (2000) developed the super resolution Particle Tracking Velocimetry, which consists of Kalman filtering theorem and Chi-square test. The developed super resolution PTV is called the super resolution KC method and is one of the highest resolution PIVs. In the super resolution KC method, three dimensional particle movement can be tracked easily, if the three dimensional particle location can be measured.

In this research, the movements of aggregates inside a construction material are measured by the super resolution KC method, which was develped for the measurement of velocimty distribution of fluid flow. The posion of each aggregate is measured by the developed X-ray CT system. The movements of aggregates inside a construction material is caused by large load which is acting on the acutual construction. As the construction materials, aggregates solidified by the sawdust of the cedar with some polymer are used in this research. The results of movement measurement in the construction material show good agreement with those in the elastic body by the compression load.

References :
Fumoto, T.(2013). Development of a New Industrial X-ray CT System and Its Application Compression Test of Polymer Concrete, Journal of Japan Society of Civil Engineers, Division E, Vol. 69, No. 2, 182-191 (in Japanese).
Takehara K., Adrian R.J., Etoh T.G., Christensen, K. T. (2000). A Kalman tracker for super-resolution PIV, Experiments in Fluids, Vol. 29, S34 -S41.

Session 308 - Concrete & building rocks

(026) Non-destructive integrated CT-XRD method developed for hardened cementitious material

*T. SUGIYAMA[1], T. HITOMI[2], K. KAJIWARA[3]
takaf@eng.hokudai.ac.jp

[1] Hokkaido University, Sapporo, Hokkaido, Japan, 060-8628
[2] Obayashi Co. Lt., Kiyose, Tokyo, Japan, 204-8558
[3] Japan Synchrotron Radiation Research Institite, Sayo-cho, Hyogo, Japan, 679-5198

A Non-destructive integrated CT-XRD method (CT-XRD) has been developed to explore hydrated cement system (Sugiyama et al 2014). This technology allows measurement with X-ray CT (CT) followed by X-ray diffraction (XRD) without the removal of a sample from the stage in experimental setup. First 3D image is reconstructed and then several regions of interest (ROI) are determined. For these ROIs XRD is applied so that the mineral information can also be obtained. In addition because of its non-destructive manner hardened cementitious material is measured repeatedly with different times. Therefore the alteration of microstructure in the cementitious material due to a given action can be investigated with elapsed time.

Hardened cement paste in cylinder shape of 5mm in the diameter and 5mm in the length was prepared and splitted so as to form crack. In this study since the specimen was intended as the matrix in a high strength concrete the water to cement ratio was 0.3. The first CT-XRD was conducted to obtain initial state in the specimen. Then a leaching test was carried out with the specimen in which pure water was pumped into the crack space at a constant flow rate. In this way the hydrated cement system would be dissolved. The CT-XRD was again conducted with the same specimen after the leaching test to investigate the physical and chemical alteration in the hydrtade cement system. It was found at the micrometer's order that the density of the matrix near the crack was reduced and the Portlandite was disappeared due to the flow of water.

Although it would take several years to complete the leaching test with the high strength concrete by conventional methodology this newly developed CT-XRD technique exhbits its capacity to explore time dependent change of the hydrated cement system within an accepted period of test.

References :
T. Sugiyama, T. Hitomi and K. Kajiwara (2014), Non-destructive Integrated CT-XRD Method for Reesearch on Hydrated Cement System, 4th International Conference on the Durability of Concrete Structures, 298-303, Purdue University, West Lafayette, Indiana, USA. http://docs.lib.purdue.edu/cgi/viewcontent.cgi?article=1008&context=icdcs.

(096) Salt crystallization dynamics in building rocks: A 4D study using laboratory Xray micro-CT

*H. DERLUYN[1], M. A. BOONE[1,2], M. N. BOONE[3], T. DE KOCK[1], S. PEETERMANS[4], J. DESARNAUD[5], N. SHAHIDZADEH[5], L. MOLARI[6], S. DE MIRANDA[6], V. CNUDDE[1]
hannelore.derluyn@ugent.be

[1] UGCT – PProGRess, Dept. Geology and Soil Science, Ghent University, Krijgslaan 281/S8, B-9000 Gent, Belgium
[2] XRE – X-ray Engineering bvba, De Pintelaan 111, B-9000 Gent, Belgium
[3] UGCT, Dept. Physics and Astronomy, Ghent University, Proeftuinstraat 86/N12, B-9000 Gent, Belgium
[4] NIAG, Spallation Neutron Source Division, Paul Scherrer Insitute, CH-5232 Villigen PSI, Switzerland
[5] Van der Waals-Zeeman Institute, Institute of Physics, University of Amsterdam, Science Park 904, NL-1098 XH Amsterdam, The Netherlands 6 DICAM, University of Bologna, V. le Risorgimento 2, IT-40136 Bologna, Italy

Salt crystallization is a major cause of weathering of building stones and cementitious materials. When saline solutions are present in these materials, changes in climatic conditions, i.e. temperature and humidity variations, may induce the precipitation of salts at the surface (efflorescence) or beneath, in the pore space (subflorescence). Efflorescence leads to aesthetic discomfort. In-pore salt crystallization however may cause pore clogging and permeability changes. Eventually, it may induce deformation and fracturing of the porous building material, drastically reducing its durability. Models have been developed to describe efflorescence and crystallization in pores and to couple the corresponding microscopic phenomena to the macroscopic behavior of the building material. Direct experimental studies of the governing processes at the pore scale are however limited. Experimental data at this scale would aid the advancement of the current models, which would improve the prediction of salt damage risks in building materials.

We employ laboratory X-ray micro-CT during climate-controlled salt weathering experiments to acquire data on the distribution of crystals within the pore space, on the kinetics of salt precipitation and dissolution at the pore scale, and on crystallization-induced fractures. At the Ghent University Centre for X-ray Tomography (UGCT), a climatic chamber was developed, compatible with the centre's high-resolution X-ray micro-tomography scanners. This allows for inducing crystallization under controlled temperature and relative humidity, and for dynamically visualizing salt weathering phenomena in building materials.

This will be illustrated by studies on NaCl crystallization in sandstone and limestone samples, using cylindrical samples of approximately 8 mm in diameter.

To study the effect of different dissolution and drying kinetics on the crystallization pattern, deliquescence-drying cycles and rewetting-drying cycles are visualized in Mšené sandstone.

The samples are initially capillary saturated with a saturated NaCl-solution and the weathering cycles are subsequently imposed using two drying conditions, i.e. drying at 20% RH and at 50% RH, at room temperature. The differences in dissolution and drying kinetics result in different salt precipitation patterns of efflorescence and subflorescence. This is related to the transport and crystallization dynamics and to the pore structure, as revealed by the 4D dynamic X-ray micro-CT datasets.

Crystallization-induced fracturing is studied in Savonnières limestone. Untreated samples, and samples that are treated with a hydrophobic treatment on the upper side to alter their wettability,

are used. The samples are subjected to repeated wetting-drying cycles with a saturated NaCl-solution. During drying, fracture initiation and growth is observed. The hydrophobically treated samples get damaged after one cycle, whereas more cycles are needed to damage the untreated samples. The coupled phenomena of crystallization and fracture dynamics are analyzed through time based on the 4D X-ray micro-CT datasets.

The X-ray micro-CT experiments are complemented with neutron tomography data on Mšené sandstone and Savonnières limestone samples that were precedently subjected to NaCl weathering cycles. Due to the higher microscopic cross section of NaCl for neutrons, NaCl crystals can be clearly distinguished from the stone matrix. These datasets assist in linking the crystal distribution to the pore structure of the stones.

(123) Use of X-ray scan to assess the extent of defects in concrete elements

*J. MARCHAND[1], R. CANTIN[1], E. SAMSON[1]
esamson@simcotechnologies.com

[1] SIMCO Technologies Inc., 2666 boul du Parc-Technologique, Suite 100, Québec (QC) Canada

Stringent durability requirements are now commonly included in tender documents to ensure long-term service-life of concrete structures. Requirements are often expressed as a target duration before major repairs are needed. For instance, the construction protocol for new concrete structures of the US Defence Department asks for a service-life of 75 years before repairs are needed and 60 years before steel reinforcement corrosion starts in waterfront structures. The expected performance of concrete mixtures can be significantly impeded by alterations to the original design occuring during construction. When that occurs, it is important to quantify the extent of defects to see how they affect the targeted durability and eventually propose remediation solutions. The presentation focuses on a case study where X-ray scan was used to investigate concrete cores from a secant wall where defects were observed during construction. The defects translated into reduced concrete cover over the steel reinforcement and compromised the ability of the material to resist steel corrosion before the intended 125-year service-life target. X-ray scan was used to quantify the spatial extent of defects. The information gathered from the observations was then incorporated into a modeling protocol to see if the long-term durability of the concret structural elements was compromised.

(132) A 3D investigation of interface porosity and fracture characteristics of cement-based composites

C. GANGSA, L. FLANDERS, *E. LANDIS
landis@maine.edu

University of Maine, Department of Civil & Environmental Engineering, Orono Maine USA

Properties of the interfacial transition zone (ITZ) in concrete have long been recognized as critical to both transport properties and mechanical properties. The high porosity characteristic of the ITZ can provide a critical flaw that can dictate fracture toughness. Despite its importance, high quality quantitative measurements of ITZ porosity have been limited. In this work, we have employed x-ray microtomography to make 3D measurements of porosity around artificial aggregates in a cement matrix. Within the resolution of the imaging system, we are able to quantify porosity with respect to distance from the aggregate and spatial variation relative to casting direction and load axis. We are also able to look at the spatial variation of interface porosity in the zone of maximum split cylinder tension to partially examine variability of split cylinder strength.

The specimens used for this work were prepared using small glass bead aggregates (nominally 0.5 mm). The glass beads were used for their well-defined geometry, and because the surface can be easily modified to change interface properties. In this work, two different surfaces were considered: smooth (untreated) and etched using an ammonium bifluoride solution. Additionally, a set of specimens without glass beads was prepared to investigate properties of the cement matrix. In the experiments, specimens were scanned in the x-ray beamline while positioned in an *in situ* loading frame that could monitor load and platen-to-platen displacement. The cylindrical specimens were loaded in a split cylinder configuration. Scans were made at nominally zero load and again after fracture.

Image processing techniques were then applied to the acquired 3D images. First, the images were segmented such that both individual aggregate particles could be isolated, as well as the porosity surrounding the aggregates. For the ITZ analysis, varying interfacial zone widths were applied as shells around the beads, and pores within those shells were isolated, resulting in information about ITZ width and porosity.

A porosity analysis at the ITZ showed that the rough surfaced aggregates had lower porosity in the interfacial zone porosity than smooth surfaced aggregates. The implication of the measurement is that the rougher surfaces allow for a slightly more efficient packing density. Further analysis showed that there was no preferential porosity due to casting direction or any other systematic process. This was evaluated by dividing the spherical aggregates into zones relative to a fixed axis. The zones allowed us to additionally measure porosity distribution relative to the direction of maximum tensile stress. Of particular interest were the zones of highest ITZ porosity were located where the maximum tensile stress is the highest. Candidates for the critical flaw that initiated fracture were identified by multipling the volume of each isolated pore space by the tensile stress at that point (as estimated using an elasticity solution for split cylinder loading). While it was not clear we could identify the critical flaw that initiated fracture, we not surprisingly found a strong correlation between the highest pore-stress product and the fracture strength of the specimen. It should be noted that this strength correlation was much stronger than either total porosity or maximum overall flaw size.

(151) Freeze-thaw decay in sedimentary rocks: a laboratory study with CT under controlled ambient conditions

*T. DE KOCK[1], M. A. BOONE[1,2], T. DE SCHRYVER[3], H. DERLUYN[1]., J. VAN STAPPEN[1], D. VAN LOO[2], B. MASSCHAELE[2,3], V. CNUDDE[1]
tim.dekock@ugent.be

[1] UGCT – PProGRess, Dept. of Geology & Soil Science, Ghent University, Krijgslaan 281/S8, 9000 Ghent, Belgium
[2] X-ray Engineering BVBA (XRE), De Pintelaan 111, 9000 Ghent, Belgium
[3] UGCT, Dept. of Physics and Astronomy, Ghent University, Proeftuinstraat 86/N12, 9000 Ghent, Belgium

Freeze-thaw processes play an important role in the physical weathering of porous rocks in cold and humid environments. In the built environment, freeze-thaw related decay threatenss the aesthetic value and structural integrety of natural building stones. Whether or not stones experience freeze-thaw decay depends on their intrinsic stone properties and the environmental conditions to which they are subjected. Two key factors in the susceptibility to freeze-thaw cycles are the pore size distribution and the water saturation of the pore network. The former relates to the stress that can be exerted by an ice crystal growing against the constraints of a pore wall. The latter is rather trivial; water is required for ice crystals to form and grow.

Here we present an experimental X-ray µCT study of the freeze-thaw process in limestone under controlled ambient conditions. The process is studied with time-lapse µCT and dynamic µCT, using the Environmental X-ray CT (EMCT) at the Centre for X-ray Tomography of the Ghent University (www.ugct.ugent.be). The EMCT is a gantry-based system on which full µCT scans were aquired in approximately 80 s. A custom made freezing cell was used for experiments with 9 mm diameter samples subjected to ambient conditions of -5 °C and -15°C. The samples were capillary saturated with water.

The experimental data show that the observed decay is strongly related to the local water saturation and to rock texture, i.e. pore size distribution. The decay is expressed by the developments of cracks in limestone due to ice crystallization. These cracks show a dynamic response to the imposed freeze-thaw cycles. Ice wedging occurs upon the moment of ice crystallization, which is indicated by the release of latent heat. During subsequent thawing, the fractures close. The timing indicates that ice crystallization alone is sufficient to instigate cracking.

The spatial information obtained with CT shows that the crack locations are closely related to the local water saturation in the rock. Assumptions based on the ice crystallization theory allow to calculate the theoretical pore sizes where ice crystallization occurred. This shows that in these experiments, water crystallizes in the nanometric pores, thus under transient conditions. The existence of such pores were validated with other techniques such as nitrogen absorption and SEM and are linked to the rock features observed with CT.

(051) Application of X-ray CT to the observation of cracking in a corroded RC bridge slab

*J. C. KURI[1], I. ZAFAR[2], T. SUGIYAMA[3]

[1] Graduate student, Environmental Material Engineering Laboratory, Graduate School of Engineering, Hokkaido University. (jhutankuri@yahoo.com)
[2] Ph.D. student, Environmental Material Engineering Laboratory, Graduate School of Engineering, Hokkaido University. (izsatti@hotmail.com)
[3] Professor, Environmental Material Engineering Laboratory, Faculty of Engineering, Hokkaido University (takaf@eng.hokudai.ac.jp)

X-ray computed tomography (CT) is a powerful tool to examine the internal structure of an object in three dimensions. In the concrete field, X-ray CT has been applied to a variety of research areas, including pore structure characterization, freeze–thaw and fire damage, and diffusivity in cracks. This technology is quite appropriate to specifically analyze the crack characteristics, as air voids inside concrete, both isolated and connected which are in form of cracks, have little to no X-ray absorption properties, and thus, differ highly from the cement paste and aggregates. However, all these experiments were conducted on the laboratory made specimens and X-ray CT has not been applied to the structures in service like bridges.

In snowy areas like Hokkaido, during the winters the de-icing salts are applied on the bridges to keep the right of way accessible for the traffic. The de-icing salts can penetrate through the bridge deck causing the top rebars to corrode. However, in spite of the thick concrete present between the top and bottom rebars, the bottom rebars have shown corrosion after a certain period of service life. It's still not clear that either the chloride ion penetration from the top surface or the chloride ions travelling from the bottom surface through cracks, formed on the tension fibers, are responsible for the corrosion of bottom rebars.

In this study an effort was made to diagnose the cause of corrosion initiation of the bottom i.e. tension reinforcement in a reinforced bridge slab which has been in service for 38 years. The electrochemical data obtained from the on-site measurement showed the corrosion for both the top and bottom rebars had started. From the visual inspection, few cracks were visible at the bottom surface of the slab. X-ray CT analysis of the core taken at or near the crack was done to evaluate the crack depth, crack width distribution and tortuosity of the cracks. In addition the chloride ion concentration was also calculated along the depth of core. It was found that the maximum crack depth has reached the level of bottom rebar from the bottom surface while majority of the cracks diminished within the concrete cover. The chloride ion concentration remained almost constant till bottom rebar level except for the core having the maximum crack depth, which showed an increase in the chloride ion concentration values. The good correlation was found to exist between the crack characteristics obtained by X-ray CT and the chloride ion concentration measurements.

(058) Evaluation of fiber characteristics and crack structures in conventional and high-performance concretes using X-ray computed tomography

*T. OESCH[1], *E. LANDIS[2], D. KUCHMA[3]
tyler.s.oesch@usace.army.mil

[1] U.S. Army Engineer Research and Development Center (ERDC), Vicksburg, MS 39180
[2] Department of Civil and Environmental Engineering, University of Maine, Orono, ME 04469
[3] Department of Civil and Environmental Engineering, Tufts University, Medford, MA 02155

To make significant advances in concrete engineering, it will be necessary to understand the behavior of cementitious materials at the micro-scale. To reach this goal, the location and orientation of constituent materials within concrete members as well as the nature of damage initiation and growth need to be understood at very small scales. This research program sought to increase that understanding through the use of x-ray computed tomography (CT). The phenomena investigated included the tensile, compression, and reinforcing bar pull-out behavior of both high-strength fiber reinforced concrete (HSFRC) and conventional concrete. These testing efforts yielded a number important results. First, relationships were identified between mechanical performance and cracking parameters that could be quantified mathematically and implemented into future finite element analysis models. Second, these test results demonstrated that the cracking structures of HSFRC samples subjected to the double punch test (DPT) are heavily influenced by fiber anisotropy. This can lead to actual crack structures that are significantly at variance with the theoretical crack structure, which may decrease DPT accuracy in predicting tensile strength. Third, fiber orientations within both small and large samples of HSFRC were demonstrated to be highly anisotropic. Thus, the assumption of randomly oriented fibers within HSFRC could lead to significant over-predictions of strength in some structural members. The results of this research program have the potential to both improve the accuracy and resiliency of numerical models as well as provide insight to the materials engineering and structural design communities about the optimal use of HSFRC.

Session 309 - Porous Material

(133) From 3D X-ray micro tomography images of porous materials to pore network: Image processing and fluid flow modelling

*D. Bernard[1,2], N. Combaret[3], J. Lesseur[1,2], A.K. Diouf[1,2], E. Plougonven[4]
bernard@icmcb-bordeaux.cnrs.fr

[1] CNRS, ICMCB, UPR9048, F-33608 Pessac, France
[2] Univ. Bordeaux, ICMCB, UPR9048, F-33608 Pessac, France
[3] VSG, Visualization Science Group an FEI Company, F-33708, Mérignac, France 4 Univ. Liège, Lab. Chemical Engineering, B-4000, Liège 1, Belgium

Pore network models (PNM) are widely used to study transports in porous media at the pore scale. The basic idea is that the intrinsic complexity of porous media can be addressed considering a large number of simple elements (the pores) connected through simple rules. Most of the PNM are based on building blocks having predetermined geometries positioned on regular grids. Now that 3D imaging techniques allow very precise representations of pore space geometry, it is logical to try building PNM directly from 3D images. But, even if 3D images are now easy to obtain, this appears to be still difficult.

The starting point of the methodology presented in this talk is a 3D binary image of a porous sample. To decompose the pore space in pores, a definition of what is a pore is necessary. Stating a strict definition effective for any 3D voxelized image is very difficult and here we only postulated that at any intersection of potential flow paths there is a porel (pore space element). Skeletonization appears as the natural tool to detect these intersections. Existing algorithms are generally based on homotopic thinning that produces a skeleton defined as a homotopic subset, of lesser dimensionality, of the pore space. Recent works in the field of discrete geometry clarified the mathematical framework and skeletonization can be considered as a reliable process. The main drawback of skeletonization is its sensitivity to noise. The noise affecting binary 3D images obtained by segmentation of noisy grey level images can produce different topological artefacts (surfaces, multiple branches, etc.) that are generally attenuated using classical morphological filters. A different approach has been selected here: all the cases where a single voxel generates a 0D, 1D or 2D artefact have been identified and filtering a 3D image consists in deleting the corresponding voxels present in the image. This approach is more efficient than classical filtering as only voxels producing skeleton artefacts are removed.

From the clean skeleton it is easy to detect the junction points and localize the porels. Discrete nature of the images can induce multiple junctions in the same compact volume, giving an over-partitioning. This is solved defining merging rules between identified porels. Once the number and location of porels are determined, the porel volumes are constructed using a watershed algorithm. The resulting pore space partition covers entirely the pore space and the intersections of its elements (porels) are surfaces. The skeleton can be directly used to build the graph corresponding to the future pore network. Unfortunately this graph is not correct in cases where more than two porels share a limiting surface. In order to handle these cases as well as the porels at the boundaries of the domains, a new graph is built directly from the partition to construct the PNM.

The graph built as presented above is composed of nodes (the porels centres) and branches connecting porels. To compute the permeability of the porous sample, the Stokes equations are

integrated, over porel volumes for mass conservation, and along the connecting branches for momentum conservation. It is easy from these integrations to prove the existence of coefficients linking the local pressure drop and the local flow rates, and from that obtain the linear system to be solved for permeability evaluation. Assuming the uniqueness of these coefficients, a procedure allowing computing them solving a local flow problem is presented. Comparing the results provided by the PNM and the direct numerical modelling of the flow at the global scale, i.e. through the entire domain, we explore the problem of uniqueness for different pore scale geometry.

(134) Phase-contrast synchrotron X-ray fast tomography of wicking in yarns

*M. PARADA[1,2], D. DEROME[2], R. M. ROSSI[3], J. CARMELIET[1,2]
marcelo.parada@empa.ch

[1] Chair of Building Physics. ETHZ, Swiss Federal Institute of Technology in Zurich. Stefano-Franscini-Platz 5, 8093 Zürich, Switzerland
[2] Laboratory for Multiscale Studies for the Built Environment. Empa, Swiss Federal Laboratories for Materials Science and Technology. Überlandstrasse 129, 8600 Dübendorf, Switzerland
[3] Laboratory for Protection and Physiology. Empa, Swiss Federal Laboratories for Materials Science and Technology. Lerchenfeldstrasse 5, 9014 St. Gallen, Switzerland

Understanding wicking in textiles is fundamental to prevent injuries related to inappropriate moisture management in specialized garments, such as firefighter protection (e.g. steam burns) and athlete apparel (e.g. blisters). The transport of liquids in textile materials is a multi-scale phenomenon ranging from the yarn to the multi-layer clothing assembly. To properly investigate wicking it is necessary to study the phenomenon in all of its scales. In this study we present the results of an experiment where the imaging of wicking at the smallest scales (i.e. yarns) was achieved.

There are three challenges for the imaging of the wicking phenomenon in yarns:
a) The yarn complex geometry consists of a bundle of individual fibers twisted together. These fibers are usually made of a flexible synthetic polymer and the interaction with the wicking liquid may result in a changing geometry depending on saturation level or short intertwined natural fibers, e.g. cotton, that can adsorb moisture and swell, further changing the geometry.

b) The wicking process starts with the wetting of the fibers, followed by a film formation and, if the fibers are close together, the formation of a meniscus that advances along the yarn. This is a relatively fast process that happens in a relatively small length scale.

c) The fiber materials investigated are hydro-carbon-based polymers and the liquid tested is water, all of these are ‘light’ materials (i.e. low atomic number) with low X-ray absorption, resulting in poor contrast.

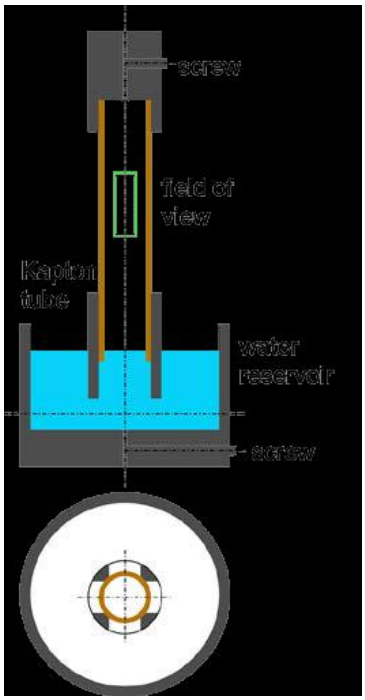

Figure 1: Schematics of sample holder (not to scale). Top: Side view cross section. Bottom: Reservoir cross section. Yarn suspended in the middle and held by two screws. Four holes at the base allow contact with water. Field of view marked in green. Water brought to reservoir during experiment with a syringe.

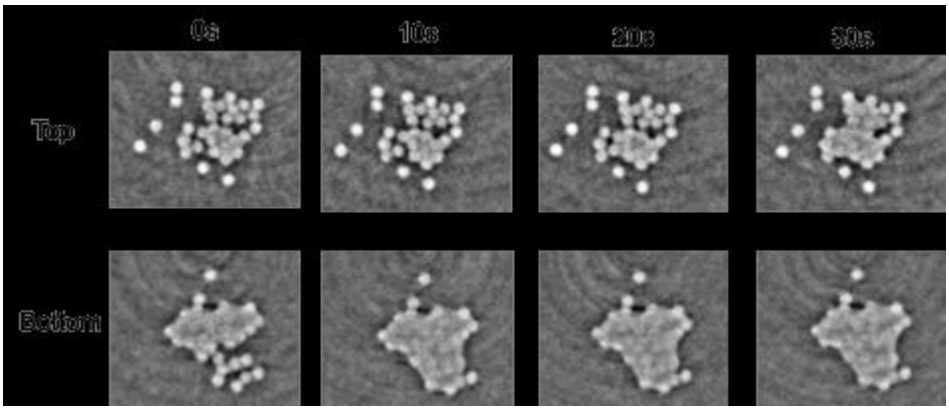

Figure 2: PET yarn during wicking. Top and bottom slices at different time steps.

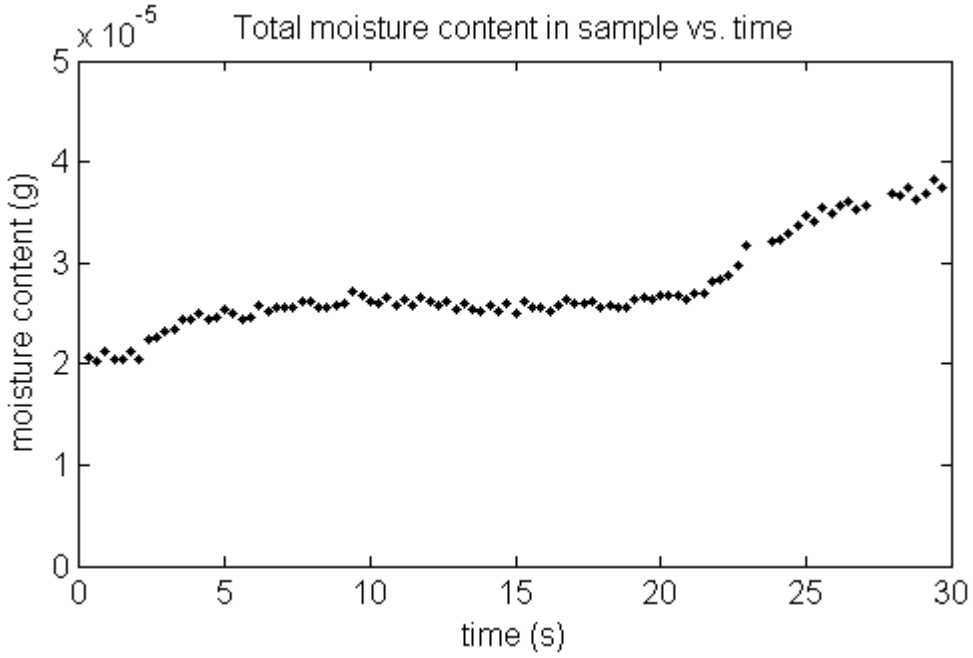

Figure 3: Time evolution of the total moisture content in the field of view for PET sample.

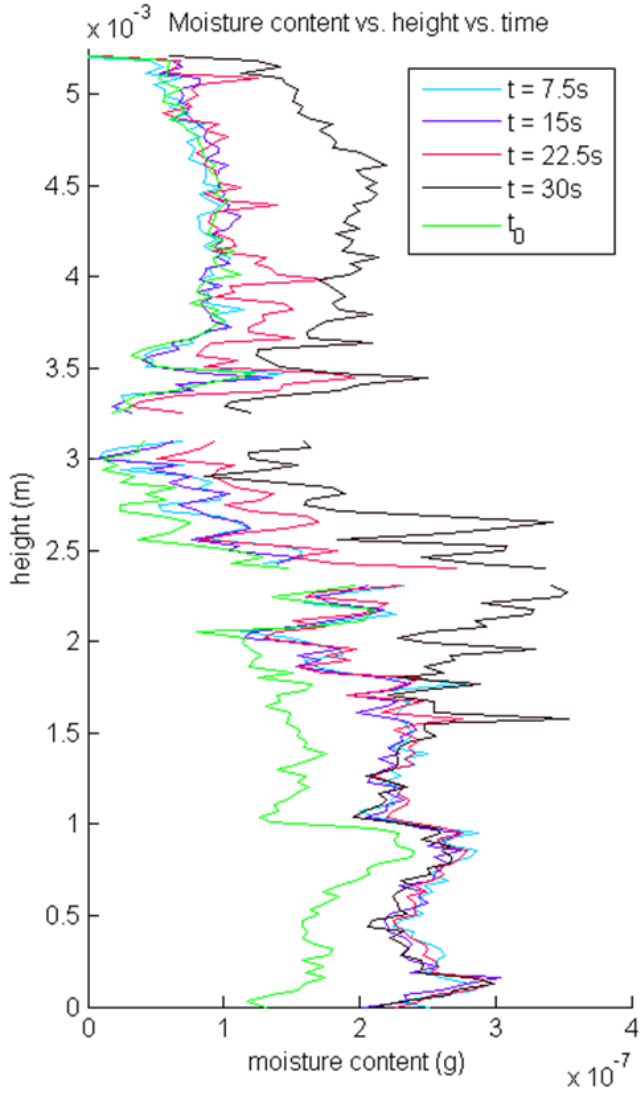

Figure 4: PET sample. Moisture content at different heights for different time steps.

(192) Neutron imaging of coupled deformation and fluid flow in sandstones

E. TUDISCO[1], *S. A. HALL[1,2], J. HOVIND[3], N. KHARDJILOV[4], E. M. CHARALAMPIDOU[5], H. SONE[6]
stephen.hall@solid.lth.se

[1] Division of Solid Mechanics, Lund University, Lund Sweden
[2] European Spallation Source AB, Lund, Sweden
[3] Paul Scherrer Institute, Villigen, Switzerland
[4] Helmholtz Zentrum Berlin, Germany
[5] Institute of Petroleum Engineering, Heriot Watt University, Edinburgh, UK
[6] GFZ-Potsdam, Germany

X-ray tomography, in combination with Digital Volume Correlation (DVC), has been used in a number of recent geomechanics investigations to map the 3D heterogeneity of strain fields inside test samples, either during loading ("in-situ" tests performed with the loading device mounted within the imaging set-up) or with imaging before and after loading (pre-/post-mortem tests). In such studies, in-situ measurements have mostly been performed on sand and clays at low confining pressures. However, the poor penetration of x-rays through triaxial pressure cells capable of sustaining elevated fluid pressures limit the use of x-ray imaging for in-situ rock testing. This restriction is reduced by using neutron instead of x-ray imaging, as neutrons are more able to penetrate the metal confining vessels. Furthermore, the high sensitivity of neutrons to hydrogen makes them very useful to study water (or other hydrogen-rich fluid) related phenomena, which paves the way towards coupled deofrmation and fluid-flow studies.

In this work, the use of neutron imaging to measure deformation in sandstone samples and the resultant effect on fluid flow are explored using both pre-/post-mortem and in-situ testing. New results will be presented demonstrating the use of time-lapse neutron tomography in combination with DVC to provide 3D strain field mapping in deformed (pre-post-mortem imaging) and deforming (in-situ tests) sandstone specimens. Furthermore, analysis of fluid flow evolution through the same specimens will be presented. The coupling of the full-field deformation and flow mapping provide previously-inaccesible insight into how fluid-flow properties are changed in the regions where the most significant deformation is actually occuring, as opposed to measuring just bulk changes.

(015) MicroCT as a tool during the development of pharmaceutical tablets

*J. KLINZING[1]
gerard.klinzing@merck.com

[1] Merck & Co., Inc., West Point, Pennsylvania, USA

The materials used throughout the development of pharmaceutical tablets contain a significant number of pores with sizes spanning nanometers to micrometers. Understanding the processing-porosity-property relationships is of the upmost importance to insure robust processing and a quality product. MicroCT has been used throughout the development process to assess pore structures, pore sizes, and wall thicknesses of materials in order to develop a better understanding of the influence of process on material properties. Moreover, microCT has proven to be invaluable in identifying and correcting the root cause of process errors which allowed for the successful scale up of a unit operation. This talk will highlight several key case studies in the pharmaceutical industry where the use of microCT aided in validating porosity distributions from numerical models, measuring pore size and wall thickness of foam extruded materials which correlate to processing conditions and post production mechanical strength, identifying root cause of tablet impact failures, and pushing the limits of the in-house equipment to <1μm resolution in order to analyze spray dried particles. Also incorporated in the talk will be a discussion on current scanning challenges such as artifacts and discussions on the difficulties of scanning particulate materials at high resolution.

(075) Study on the effects of porous structure on carbon composites manufacture based on synchrotron X-ray CT imaging and 3D visualization analysis

N. VITO[1], M. LEI[1], J. OLSON[2]
mlei@fei.com

[1] FEI-VSG, Houston, USA
[2] Canadian Light Source, Saskatoon, SK, Canada

Carbon composites are being developed for use in a wide variety of applications ranging from sports equipment to aerospace materials. Studying the porous structure in the manufacturing process plays an important role in making better materials with enhanced properties. Using the synchrotron CT capabilities at the Canadian Light Source (CLS) and state of art technology 3D visualization software Avizo, we were able to image the materials non-destructively to visualize and quantify the pore space differences between a cured and uncured sample.

Images were acquired at the BMIT-BM beamline of the CLS, which is a third generation, 2.9 GeV storage ring operating at a ring current of 250 mA. The composites prepared by the Composites Research Network at UBC were mounted onto a piece of polycarbonate and imaged simultaneously at the CLS. The samples were mounted onto a 360 degree rotation stage, where 3750 projections were taken every 0.048 degrees for 180° and captured with a Hamamatsu camera with 4.3 µm pixel resolutions. Avizo 9 was used for image processing. Advanced segmentation and quantification modules were used to analyze the porous structure inside the composite. The combination of BMIT-BM and Avizo techniques are able to accurately demonstrate the 3D composite pore structure qualitatively and quantitatively. In addition to composite samples, the workflow presented here can be potentially applicable to a wide range of general porous media analysis.

(082) Solid-phase structural characterizacion in polymeric foams: Synchrotron µ-CT in the limits of resolution

S. PEREZ-TAMARIT[1], *E. SOLÓRZANO[1], A. HILGER[2], I. MANKE[2], M. A. RODRIGUEZ-PEREZ[1]
saul.perez@fmc.uva.es

[1] CellMat Laboratory, University of Valladolid, Paseo de Belén 7 47011, Valladolid, Spain
[2] Helmholtz-Zentrum Berlin für Materialien und Energie, Lise-Meitner-Campus, Hahn-Meitner-Platz 1 (formerly Glienicker Str. 100) 14109, Berlin, Germany

Foams are two-phase structures in which a gas is dispersed throughout a solid continuous phase. As a consequence both solid and gas local arrangements are important to understand final properties. Gas -pores- are frequently studied while the solid is conventionally less considered. Nevertheless, the architecture of the solid-phase is key to understand most of the final properties since it has a higher influence than the gaseous-phase. µ-CT is one of the most useful tools to this end but it presents certain limits both in the spatial and contrast resolution which difficults carrying out these studies in low density materials (density about 25 kg/m^3) or those with wall thicknesses in the range 1-3 microns. In these situations a complete/exact binarization of the solid-phase is generally not possible thus loosing valuable information. In these conditions watershed reconstruction is not a valid process (an exact reconstruction of those eliminated cell walls is intended) and the only alternative implies a higher resolution, at least 2 times better than the minimum cell wall thickness of the material. As a consequence µ-CT measurements were done at a syncrotron facility.

This work presents the results for a collection closed-cell polymeric foams studied by synchrotron µ-CT and advanced image analysis techniques. The measurements were done at BAM-Line, a synchrotron beamline located at Bessy II facility in Berlin. Measurements were performed using 0.438 microns pixel size and in absorption mode (a minimal phase contrast). Samples under study consisted on a collection of closed-cell polymeric foams with a broad range of solid fractions (from 0.018 to 0.095) and mean pore sizes between 230 and 540 micrometers.

The structural characterization has been focussed on the extraction of different parameters of the solid-phase: local thickness distribution, strut thickness, cell wall thickness, material repartition in cell walls and struts, and local curvatures of these entities by using different methodologies. Conventional parameters of the gas-phase (pore size, anysotropy, etc) were complementarily calculated. Furthermore, a de-structuration -segmentation- process between walls and struts constituting a unique solid phase was implemented. This approach was carried out by different methods reaching similar results. The variance of the methods used will be compared and discussed. The obtained results point to a total different architecture of thermosets (polyurethane) or thermoplastics (polyethylene) that clearly influence both the mechanical and thermal properties and is explained within the analytical models, now with an experimental base not reached before.

(128) 3D detection of damage evolution in porous brittle cement or plaster based materials

T. T. NGUYEN[1,2], M. BORNERT[1], *C. CHATEAU[1], J. YVONNET[2], Q. Z. ZHU[2]
bruns@nano.ku.dk

1 Université Paris-Est, Laboratoire Navier, CNRS UMR8205, ENPC, IFSTTAR, 6 et 8 avenue Blaise Pascal, 77455 Marne-la-Vallée Cedex, France
2 Université Paris-Est, Laboratoire Modélisation et Simulation Multi Echelle, 5 Bd Descartes 77454 Marne-la-Vallée Cedex 2, France

The behaviour of many civil engineering materials is governed by damage caused by microcracking phenomena, the mechanical description of which is still an open issue, in terms of initiation, propagation or localisation leading to macroscopic ruin. A detailed experimental characterisation of damage and its evolution under mechanical loading is necessary to validate 3D models of crack nucleation and propagation in heterogeneous materials (Nguyen et al., n.d.). Such characterisation is made available through X-Ray Computed Tomography (XRCT) combined with Digital Volume Correlation (DVC).

A dedicated experimental set-up was used to perform in-situ compressive tests on an XRCT laboratory scanner available at Laboratoire Navier (Ultratom from RX-Solutions), on cylindrical samples of two different materials (~10 mm in diameter). The first material under investigation is an expanded polystyrene (EPS) lightweight concrete (Miled et al., 2007), made from quartz sand and EPS beads embedded in a cement matrix. The high porosity of this concrete is suitable for crack initiation at relatively low compressive loads and stable propagation. Moreover, specific samples composed of EPS beads embedded in an almost homogeneous plaster matrix have been manufactured. Their simpler microstructure characterized by a limited number of EPS beads is easier to model and will serve for detailed comparisons between new numerical tools and experimental results. Several load levels were successively applied to the specimen and CT images of the whole sample were recorded under constant load. Acoustic emissions were also monitored to detect the beginning of the damage accumulation. Cracks developed progressively during the last loading steps and can be qualitatively observed directly in the CT images. However their precise location and extension are hard to quantify, especially in EPS concrete. In fact, their grey level is very similar to that of the EPS beads. In addition, they are hard to detect in their early stage.

A method to detect and extract cracks more accurately was developped. It is based on DVC techniques, which give access to an evaluation of the mechanical transformation inside a sample, at a scale at which some image contrast is available. In the case of EPS plaster, the latter is provided by the plaster matrix (inclusion, microporosity). In the case of EPS concrete, because grey levels in EPS beads and sand grains are rather uniform, DVC routines have been run on positions in cement matrix only, especially near interfaces. The sparse evaluation of the transformation map can be continuously extended throughout the whole sample, by means of an interpolation procedure: the transformation at any voxel in the reference image is obtained by a first order fit of the displacement of at least 4 near neighbour positions successfully investigated by DVC. Using a tricubic interpolation, the deformed image can then be moved in the same frame as the reference image according to the estimated transformation. Finally, the difference of both reference and deformed images defines the “residuals image”. It reflects the local evolutions of the material, not described by the fit of the coarse evaluation of the transformation. For a brittle material, it essentially gives access to the cracks.

The grey level of the residuals image is almost uniform, except in areas with ring artefacts and at some interfaces. But these features are less pronounced than the signature of cracks, the path of which is clearly visible. Segmentation of cracked areas is possible in the residuals image, while it would have been very hard to separate cracks from porosity in the deformed XRCT images. Moreover, very tiny cracks can also be detected. The crack network and its evolution can thus be characterised and directly compared to numerical simulations.

References :
Miled, K., Sab, K., Le Roy, R., 2007. Particle size effect on EPS lightweight concrete compressive strength: Experimental investigation and modelling. Mech. Mater. 39, 222–240.
Nguyen, T.T., Yvonnet, J., Zhu, Q.-Z., Bornert, M., Chateau, C. A phase field method to simulate crack nucleation and propagation in strongly heterogeneous materials from direct imaging of their microstructure. Submitted to Eng. Fract. Mech.

Session 310 - Hydrogeology, water infiltration and pollution

(121) Evolution of soil hydraulic properties under saturated conditions

*Y. PÉRIARD[1], S. J. GUMIRE[1], B. LONG[2], A. N. ROUSSEAU[2], J. CARON[1]
yann.periard-larrivee.1@ulaval.ca

[1] Department of Soils and Agri-Food Engineering, Laval University, 2480 Hochelaga Blvd, Québec, QC, Canada, G1V 0A6
[2] Institut national de la recherche scientifique : Centre Eau, Terre et Environnement, Québec, QC, Canada

Knowledge of soil hydraulic properties are essential for water flow and solute transport modeling in the vadose zone. These properties are often established assuming the soil is a non-deformable (rigid) porous media in both time and space. However, under real conditions such as those of agricultural systems, the soil is constantly exposed to external stresses induced by farm machinery and wetting and drying conditions leading to volumetric strain and, consequently, non-invariant soil hydraulic properties. The main objective of this work was to propose a methodological framewotk to predict the evolution of the hydraulic properties of a soil sample undergoing hydroconsolidation under saturated conditions. For this study, a cylindrical sandy soil sample was characterized by tomodensitometry during the consolidation process. The results showed a good estimation of the evolution of the soil hydraulic properties. The proposed methodological framework provides a realistic description of water flow through the soil system during hydroconsolidation, a physical process experienced by artificially drained and irrigated soils in carnberry production.

(146) Characterization of intra-aggregate bioaccessible porosity

*A. AKBARI[1], S. GHOSHAL[1]
ali.akbari@mail.mcgill.ca

[1] Department of Civil Engineering, McGill University, Montreal, Québec, Canada

Characterization of soil bacterial habitat advances our knowledge about soil biogeochemistry that could be useful in diverse fields such as greenhouse gas emissions from soil due to decomposition of soil organic matter and, fate and transport of pathogens, remediation of contaminated sites and enhanced oil recovery in petroleum reservoirs. Soils have complex intra- and inter particle pore network characteristics which influence the accessibility of carbon sources, nutrients, oxygen and moisture to soil microorganisms. For example, a major microbial uptake mechanism of poorly soluble hydrocarbon compounds in soil is through direct contact between hydrocarbon and hydrocarbon degrading bacteria. It is expected that biodegradation of poorly soluble hydrocarbons to be severely limited when hydrocarbon compounds are trapped in small pores that are not accessible to soil microbial community.

We characterized the soil pore network of representative aggregates from two soils with distinct textures from two sites contaminated with petroleum hydrocarbons by micro-CT scanning and N_2 adsorption analysis. An image analysis procedure was developed in order to extract intra-aggregate pore network information. Given the complexity of image thresholding in case of heterogeneous porous materials such as soils with constituents with different densities as well particle sizes smaller than scanning resolution, applying simple global thresholding methods which doesn't consider spatial and intensity values of each pixel would not adequately represent the real aggregate micro-structure. Among different thresholding methods investigated (alternating mean thresholding and median filtering, two sigma smoothing and low pass filter and finally indicator kriging (IK)), the IK method provided the most representative images when compared to original gray-scale images. Moreover, the alpha-shape of each single scanned aggregate was determined in order to extract the pore information from whole aggregate body rather than just considering a sub-sample of total aggregate volume as done in most previous studies. Because soil aggregates are usually denser at the center compared to the loose structure near the boundary, considering just the core of aggregate would result in biased porosity calculations. For example, it was found that while CT derived porosity of an aggregate was about 14% calculated from the core sub-sample volume, the porosity of the whole aggregate body was about 26%. N_2 adsorption analyses was performed to determine the volume of pores with diameters less than 1 μm, which are smaller than the resolution of micro-CT scanning (1.04-3.28 μm). Using the data from micro-CT scanning and N_2 adsorption analyses, the bioaccessible pore fraction, which is the fraction of total pore volume of the aggregate accessible to bacteria, were calculated for each aggregate.

The results indicate that more than 90% of total pore volume of aggregates from fine-grained soils were interconnected. Moreover, about 79% of total pore volume were accessible to bacteria (bioaccessible pore fraction). On the other hand, in the case of coarse-grained soils, the bioaccessible pore fraction was significantly higher at 96%. The remarkably significant values of bioaccessible pore fractions of fine and coarse-grained soils may explain the observation that remediation endpoints of high molecular weight petroleum hydrocarbons was significantly higher in fine-grained soils as 525.8 mg/kg than coarse-grained soils which was 102.5 mg/kg soil.

(177) Frequency mapping of local degree of saturation in partially saturated sand subjected to drying and wetting process

*Y. HIGO[1], G. KHADDOUR[2], S. SALAGER[2], R. MORISHITA[3†], R. KIDO[3]
higo.yohsuke.5z@kyoto-u.ac.jp

1 Department of Urban Management, Kyoto University, C1-211 Kyotodaigaku-Katsura, Nishikyo-ku, Kyoto 615-8540 Japan
2 Grenoble-INP, UJF, CNRS UMR5521, Laboratoire 3SR, 1301 rue de la piscine, Domaine Universitaire, Saint Martin d'Hères, BP53 38041 Grenoble, Cedex 9, France
3 Department of Civil and Earth Resources Engineering, Kyoto University, C1-587 Kyotodaigaku-Katsura, Nishikyo-ku, Kyoto 615-8540 Japan
† Currently in Oil, Gas and Metals National Corporation (JOGMEC), Japan

Pore water in unsaturated soils is macroscopically homogeneous but spatially distributed depending upon microscopic natures including particulate structures and history of suction loading. The distribution of degree of saturation is a key to understanding macroscopic hydraulic and mechanical behaviors such as hysteresis during drying and wetting processes. In the present study, in order to clarify the link between distribution of degree of saturation and overall water retention behavior of unsaturated sand, local degree of saturation in unsaturated sand during water retention test was evaluated using micro x-ray tomography and segmentation technique for trinarization into the soil particle phase, the pore water phase and the pore air phase. Two experiments and their image analyses have been done in two laboratories under different but almost the same conditions using different sand samples, Toyoura sand with smaller diameter and Hostun sand with larger diameter. Frequency mpping of the relation between the local porosity and the local degree of saturation for prismatic representative subsets was presented in the two-dimensional histograms through which the effect of the drying and wetting processes and the hysteresis on the distribution of degree of saturation were discussed.

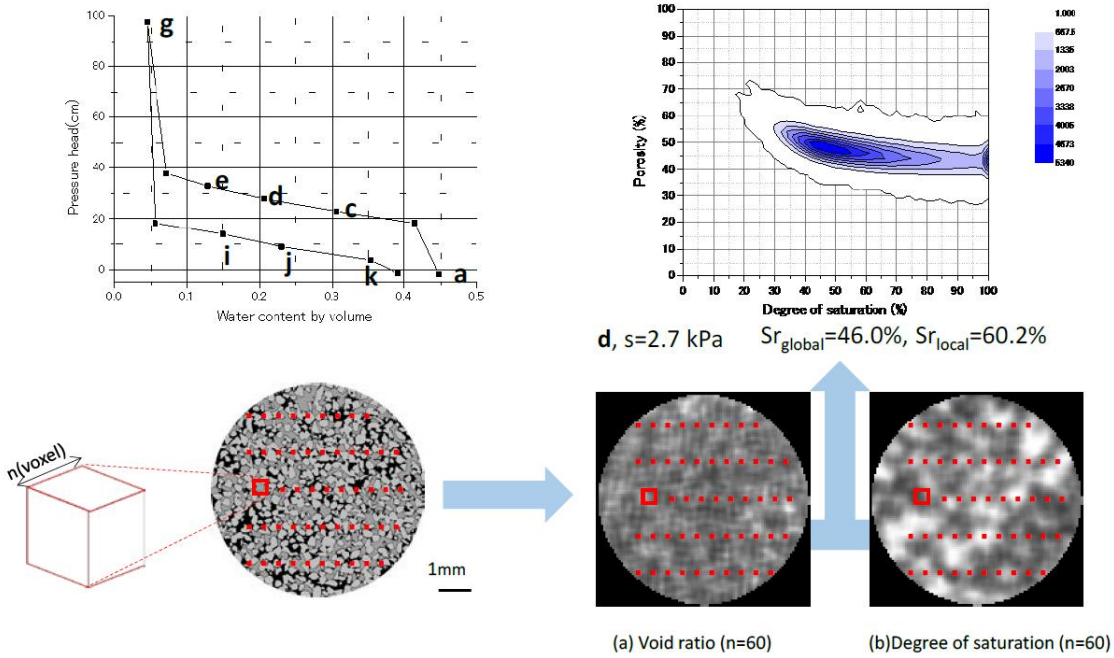

(122) Predicting soil hydraulic properties from tomodensitometric analysis and particle size distribution

*Y. PÉRIARD[1], S. JOSÉ GUMIÈRE[1], A. N. ROUSSEAU[2], J. CARON[1], D. W. HALLEMA[1,3]
yann.periard-larrivee.1@ulaval.ca

[1] Department of Soils and Agri-Food Engineering, Laval University, 2480 Hochelaga Blvd, Québec, QC, Canada, G1V 0A6
[2] Institut national de la recherche scientifique : Centre Eau, Terre et Environnement, Québec, QC, Canada
[3] Eastern Forest Environmental Threat Assessment Center, USDA Forest Service, 920 Main 9 Campus Dr., Raleigh, NC 27606, United States of America

Knowledge of soil hydraulic properties such as water retention and hydraulic conductivity are essential for modelling water flow and contaminant transport in soils. However, characterization of these properties requires many technical manipulations that are very costly and time consuming. Tomographic imagery provides a cost-effective and rapid methodological approach to characterize a number of soil hydraulic properties (Wildenschilds and Sheppard, 2013). Indeed, micro scanning can be used to describe porous media at high spatial resolution and to obtain pore size distribution and pore network. However, the use of micro scanning has limits on sample size making inappropriate to study a representative volume of a specific process described by a macroscopic model. The main objective of this work is to develop a framework to determine soil hydraulic properties using a combination of X-ray tomographic imaging and particle size analysis. A sandy soil samplewas characterized with a medical CT scan at a resolution of 100 µm for a voxel. Water retention and hydraulic conductivity curves were derived using the instantaneous profile method for sorption and desorption curves. A a particle radius distribution was obtained with a LA950v2 Laser Particle Size Analyzer (Horiba). Results showed a good prediction of soil hydraulic properties. The development of this novel framework has provided an opportunity to study the spatiotemporal variability of soil hydraulic properties of a porous media at the soil profile scale (1 m of length) underexperimental conditions inducing hydroconsolidation and particle transport.

References :
Wildenschild, D. and A.P. Sheppard. 2013. X-ray imaging and analysis techniques for quantifying pore-scale structure and processes in subsurface porous medium systems. Advances in Water Resources 51: 217-246. doi:http://dx.doi.org/10.1016/j.advwatres.2012.07.018.

(164) A combination of radiography and micro-tomography X-ray techniques for studying shear-induced migration of particles in yield stress fluids

*S. HORMOZI[1], M. GHOLAMI[1], N. LENOIR[2], G. OVARLEZ[2]
hormozi@ohio.edu

[1] Department of Mechanical Engineering, Ohio University, 251 Stocker Center, Athens, OH 45701-2979, USA
[2] PLACAMAT, UMS3626-CNRS/University of Bordeaux, Pessac, 33608, France

Dense suspensions are materials with broad application both in industrial processes (e.g. waste disposal, concrete, drilling muds and cuttings transport, food processing, etc) and in natural phenomena (e.g. flows of slurries, debris and lava). These suspensions may consist of solid particles with a broad range of sizes. Often the fine colloidal particles interact to form a shear thinning yield stress carrier fluid, i.e., visco-plastic fluid, which itself transports the coarser solid particles. Hereafter, this system will be termed visco-plastic suspension.

From physical perspective, distribution of particles can be attributed to the hydrodynamics and multibody interactions of the particles. In a non-homogeneous shear flow of Newtonian suspensions (i.e., systems of Newtonian carrier fluid and non-colloidal particles), it is observed that particles migrate from the high velocity gradient region to the low velocity gradient region, see Leighton & Acrivos (1987) and Phillips et al. (1992). This phenomenon is called shear-induced migration. Therefore, estimating the particle phase diffusion in visco-plastic suspensions requires understanding of this phenomenon.

We present our preliminary results of an experimental study on visco-plastic suspension flows in a circular Couette configuration. Here, the outer cylinder is rotating and the inner cylinder is stationary. We have used a system of non-Brownian spherical hard particles suspended in a concentrated emulsion with yield stress. A systematic series of experiments were carried out to capture all flow regimes in a wide range of solid volume fraction and outer cylinder rotational speed. The transient evolution of solid volume fraction under shear is measured by an X-ray radiography imaging technique. In addition, an X-ray 3D micro-tomography is performed to scan the exact particles distribution when steady state is established.

In Newtonian suspension, the linearity of the suspending fluid allows to study the shear-induced migration phenomenon at the steady state regime independent of the transient regime. Turning to visco-plastic suspension, the main problem relates to nonlinearity of the constitutive law for the suspending fluid, meaning that many of the analytical results that underlie some Newtonian suspension techniques are not directly applicable. Here, the study of shear-induced migration requires the distribution of particles at the transient regime as well as the steady state regime. To our knowledge, this is the first time that the X-ray radiography imaging technique has been exploited for investigation of such a complex system.

Computational programs are developed to post-process radiography and micro-tomography data with the purpose of calculating the average solid volume fraction during the flow and the exact particles distributions at the steady state. Moreover, we have followed the suspension

balance framework of Nott and Brady (1994) to develop a continuum model for visco-plastic suspension flows. Our experimental results complete a continuum modelling closure perspective for the dispersion of solids in visco-plastic suspension.

References :
Leighton, D., and Acrivos, A. The shear-induced migration of particles in concentrated suspensions. J. Fluid Mech. 181, pp. 415–439, (1987).
Phillips, R., Armstrong, R., Brown, R.A., Graham, A. and Abbott, J.R. A constitu- tive model for concentrated suspensions that accounts for shear-induced particle migration. Phys. Fluids A 4, pp. 30–40, (1992).
Nott, P.R, and Brady, J.F, Pressure-driven flow of suspensions: simulation and theory. J Fluid Mech 275 (1994).

(191) Discrete analysis of water phase evolution within unsaturated soil

*Y. HIGO[1], G. KHADDOUR[2], S. SALAGER[2], R. MORISHITA[3†], R. KIDO[3]
higo.yohsuke.5z@kyoto-u.ac.jp

[1] Univ. Grenoble Alpes, 3SR, F-38000 Grenoble, France
[2] CNRS, 3SR, F-38000 Grenoble, France
[3] Department of Urban Management, Kyoto University, C1-211 Kyotodaigaku-Katsura, Nishikyo-ku, Kyoto 615-8540 Japan

The spatial distribution of the liquid phase within an unsaturated soil involved with the external conditions. This distribution is therefore linked to mechanical and hydraulic states (level of stress and level of suction) and in addition this distribution will affect the mechanical and hydraulic behaviors. The need to describe in details this distribution and its evolution is here clearly highlighted. It is obvious that the solid phase in soils has a discrete nature and recent results imaging unsaturated soils by x-ray tomography shown, that in most of the cases, the liquid phase can be considered as a collection of capillary bridges (pendular domain) or water clusters (funicular domain). From this remark we define several variables that are able to characterize in a discrete manner the state of the liquid phase in soil: number of bridges/clusters, volume of them, distribution in volume, and complexity of their shape.

Drying and wetting paths on two sands were performed and different unsaturated states of the materials were imaged by x-ray tomography. After several steps of images analyses the evolution of water clusters morphology was obtained and analyzed. Finally the different hydraulic domains that were defined historically from macroscopic consideration were reassessed in the light of this new manner for unsaturated soils characterization.

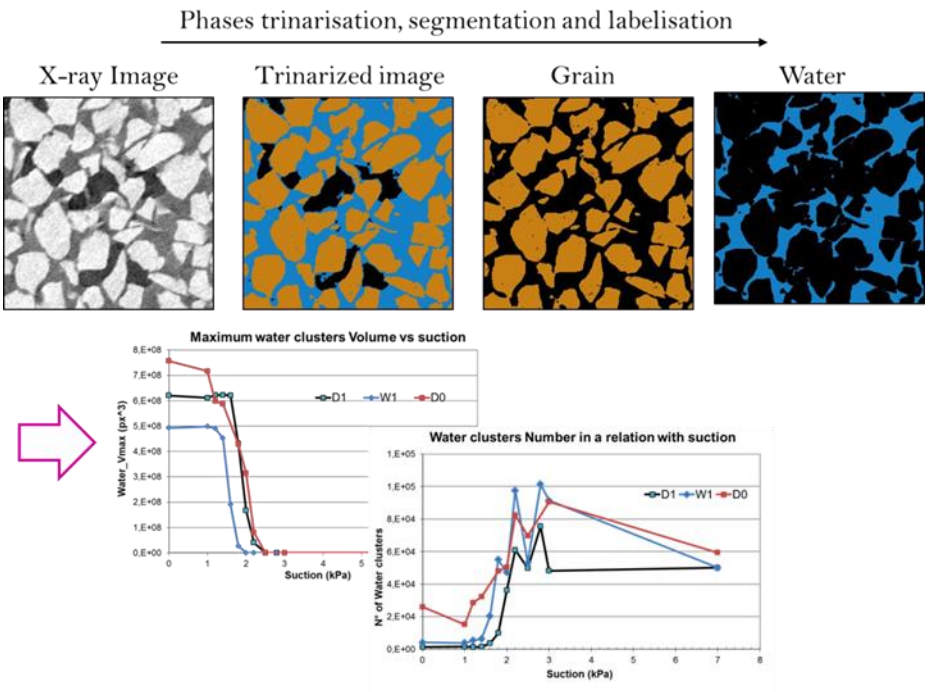

Session 311 - Archaeology

(039) Celtic drum fibula morphology, preparation technique and conservation state determined by X-ray computed tomography

*C. TENAILLEAU[1], E. DUBREUCQ[2], B. DUPLOYER[1], L. SEVERAC[1], P.Y. MILCENT[2], L. ROBBIOLA[2]
tenailleau@chimie.ups-tlse.fr

[1] CIRIMAT, UMR - CNRS 5085, Université de Toulouse, 118 route de Narbonne, 31062 Toulouse Cedex 9, FRANCE
[2] TRACES, UMR - CNRS 5608, Université de Toulouse, 5 allée Antonio Machado, 31058 Toulouse Cedex 9, FRANCE

A celtic bronze drum fibula dating from the middle Iron Age (5th Century BC) and recently excavated from the Corent site in France was characterized in detail for determining the morphology, composition and microstructural features that allow understanding the production method as well as the conservation state. Ancient bronzes (Cu-Sn alloy) are indeed often affected by severe corrosion during long burial periods of time, but can also be preserved when a stable patina is formed.[1-3] Noble patina can indeed well protect the original surface even after several millennia of burying. Investigation of these corroded but preserved surfaces was firstly performed applying a complementary set of non invasive techniques (including SEM, EDS and microRaman spectrometry) to determine composition and structure of natural patina and gilded part. The alloy is a pure tin-bronze with a tin content of about 8 at % (14 wt.%), determined from X-ray microdiffraction measurements applying Vegard's law. The natural patina with a very poor copper content and preserving original surface is of type I patina[4] (also called "noble patina"). It is linked to the internal oxidation of the alloy with a selective dissolution of copper, namely decuprification which is very pronounced here. The gilded aspect is only the result of a desquamation of the outer patina layer at the interface outer/inner corrosion layer, revealing the gold colour of the bronze matrix. Element-specific mapping allowed precise detection of atomic distribution of environmental and alloying elements.

A deeper and original characterization of the celtic bronze drum fibula was performed thanks to X-ray Computed Tomography (XCT) at micrometric level, including detection of mineral/metallic phases. Firstly, XCT is a fantastic tool that provides 3D information of an archeological object in a non destructive manner and makes it possible to investigate the interior surface by preserving the entire original aspect.[5,6] Then, a systematic thickness mapping determination revealed an important homogeneity in the whole structure of the fibula, though widening towards the edges. For the first time, important information on the internal corrosion state is revealed with a network of internal cracks transversally located throughout the thickness of the drum part of the fibula. By compiling these results with historical data it was concluded that this celtic drum fibula was thorougly prepared by stamping of a preform. It was also demonstrated the importance of the decay of bronze even when the external observation prejudge of a well preserved state. Complementary spectroscopic data and imaging information lead us to a clearer insight in the corrosion mechanism that will be discussed.

Additional information was also obtained from iron-based preforms for comparison showing the large potential of XCT when applied to ancient metallic artefacts.

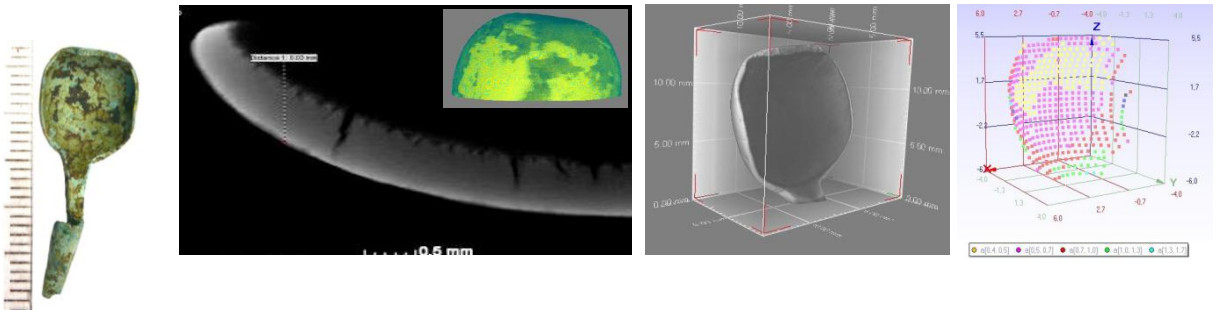

Reference :
[1] F. Koleini et al., Journal of Cultural Heritage 13 (2012) 246–253.
[2] S. Carrara et al., Mobilité des hommes, diffusion des idées, circulation des biens dans l'espace européen à l'âge du Fer (2012) 595-608.
[3] E. Figueiredoa et al., Metal 07, When archaeometry and conservation meet, 1 (2008) 61-66.
[4] L. Robbiola et al., Corrosion Sci. 40 (1998) 2083-2111.
[5] N Ebinger-Rist et al., Metal 2010, Charleston – South Carolina, P. Mardikian et al. Eds, U S A (2011) 342-347.
[6] J. Stelzner et al., Studies in Conservation 55 (2010) 95-106.

(074) Micro-CT characterization of archaeological bones

H. COQUEUGNIOT[1,2], A. COLOMBO[2,1], C. RITTEMARD[3], O. BAKER[3], B. DUTAILLY[1], O. DUTOUR[3,1,4], *N. LENOIR[5]
nicolas.lenoir@placamat.cnrs.fr

[1] UMR 5199 PACEA, Bat B8, Université de Bordeaux, Allée Geoffroy St Hilaire, 33615 Pessac cedex, FRANCE
[2] Department of Human Evolution, Max Planck Institute for Evolutionary Anthropology, Deutscher Platz 6, 04103 Leipzig, GERMANY
[3] Laboratoire d'Anthropologie biologique Paul Broca, Ecole Pratique des Hautes Etudes, FRANCE
[4] Department of Anthropology, University of Western Ontario, CANADA
[5] UMS 3626 PLACAMAT, 87 avenue Docteur Albert Schweitzer, 33608 Pessac cedex FRANCE

Archaeology is developping a growing interest in the use of micro-CT for characterizing its artifacts. Among them, ancient bones studies could take a substantial benefit from micro-CT analyses using both experience from fundamental researches on porous materials and clinical survey on microarchitectural bone changes due to osteoporosis.

In this perspective, we have developed a complete 3D digital chain dedicated to archaeology, going from CT/micro-CT acquisitions to 3D printing (VIRCOPAL® standing for VIRtual COllection of PALeo-specimens). It is based on a specific software program (TIVMI® standing for Treatment and Increased Vision for Medical Imaging) developed by one of us (B.D.). It implements a 3D HMH (Half Maximum Height) algorithm that ensures a high fidelity digital model from CT data of archaeological items.

The goal of this presentation is to illustrate, in 3 case studies, the interest of micro-CT for studying archaeological bones focusing on growth processes, species identification and paleopathological conditions.

Micro-CT acquisitions of artifacts were performed on a GE v|tome x|s device at a resolution ranging from 7 µm to 21 µm; 3D reconstructions were carried out using TIVMI® software program.

First case study: in order to evidence possible trabecular microarchitectural signals of growing processes among archaeological human populations, trabecular bone in humerus upper metaphyses was studied on identified skeletons collections. Tridimensional reconstructions and measures using specific algorithm of skeletonisation, have shown microarchitectural changes linked to 3 major growth periods (Colombo, 2014).

Second case study: in order to differenciate Vertebrate species from skeletal fragments in archaeological context, we analysed the microarchitecture of fragmentary cortical bones from different species of Mammals including Humans. 3D reconstructions of vascular microchannel network revealed specific characteristics allowing possible recognition of Mammal species including Humans (Rittemard et al., 2014).

Third case study: we analysed lumbar vertebra of a young child (ca. 5 years old) coming from Early Pre-Pottery Neolithic B dating from 11000 years BP in the Fertile Crescent. Tridimensionnal reconstructions of micro-CT scans evidenced focal microarchitectural changes (reduction of trabeculae number and thickening) due to early step of tuberculotic vertebral infection (Baker et al., 2015 and Coqueugniot et al., 2015).

These 3 examples underline the great interest of micro-CT in the study of bone as an archaeological artifact.

References :
BAKER O., LEE O.Y-C, WU H.H-T., BESRA G.S., MINNIKIN D.E., LLEWELLYN G., WILLIAMS C.M., MAIXNER F., O´SULLIVAN N., ZINK A., CHAMEL B., KHAWAM R., COQUEUGNIOT E., HELMER D., LE MORT F., GOURICHON L., DUTAILLY B., PÁLFI G., COQUEUGNIOT H., DUTOUR O. Human tuberculosis predates domestication in ancient Syria. Tuberculosis, in press.
COLOMBO A., 2014. "La micro-architecture osseuse trabéculaire de l'os en croissance : variabilité tridimensionnelle normale et pathologique analysée par microtomodensitométrie". PhD, University of Bordeaux.
COQUEUGNIOT H., DUTAILLY B., DESBARATS P., BOULESTIN B., PAP I., SZIKOSSY I., BAKER O., MONTAUDON M., PANUEL M., KARLINGER K., KOVÁCS B., KRISTÓF L.A., PÁLFI G., DUTOUR O. Three-dimensional imaging of past skeletal TB: from lesion to process. Tuberculosis, in press.
RITTEMARD C., BLOSSEVILLE R., DESBARATS P., DUTAILLY B., DUTOUR O., H. COQUEUGNIOT H., 2014. "Interest of 3D microstructural cortical bone canal network analysis in archaeological sciences". 3rd International Congress Biomedical Sciences and Methods in Archaeology, Bordeaux, France, 6–9 November 2014.

(100) The use of metals and metal products on urban and rural archaeological sites: reconstructing technologies employed by native american and european artisans in new france during the 17th and 18th centuries

G.TREYVAUD[1]
genevieve.treyvaud@ete.inrs.ca

[1] INRS-ETE, 490 de la Couronne, Québec, Canada, G1K 9A9

This research aims to document the context in which metallurgy occurred during the transition period and the colonisation of New France, through the application of theoretical concepts to provide a better understanding of an important period in the colonial history of North America.

Topics specific to the processing of metals, the craftsmanship of objects, knowledge concerning metalworkers as well as the social and economic impact of their craft and the influence of technology are discussed in this study. Our work focuses on the study of the *chaînes opératoires* and the metallurgical techniques employed by Native American and European artisans, as well as the technological choices made throughout the process of metal production during a period of technological adaptation to the environment of New France. Artefacts are being studied using tomography, X-ray fluorescence (XRF), and scanning and micro-radiography with the goal of identifying metal sources, the technical signature of the artisans, and technological problems related to climate, fuel and a lack of raw materials.

(205) Mise au point d'une banque de données scannographiques pour l'analyse paléopathologique : exemple du cimetière protestant Saint-Matthew, ville de Québec (1771- 1861)

Z. HOULE-WIERZBICKI[2], G. TREYVAUD[1], E. RAGUIN I[2], R. AUGER[1], I. RIBOT[2]
genevieve.treyvaud@ete.inrs.ca

[1] Université Laval, Ville de Québec
[2] Université de Montréal

Dans le cadre d'analyses paléopathologiques, une cinquantaine de squelettes humains, issus du cimetière protestant Saint-Matthew, datant des 18e et 19e siècles, ont été scannés au laboratoire *Scanographie – Eau Terre Environnement* de l'IRNS de la Ville de Québec. Afin de de palier à un problème central de la bioarchéologie québécoise (ré-inhumation des sépultures et perte des données paléopathologiques), les objectifs principaux étaient les suivants: 1) constituer une banque de données scannographiques sur un échantillon de squelettes les mieux conservés et les plus représentatifs du cimetière étudié (âge, sexe, pathologies); et 2) coupler cette banque de données à des observations macroscopiques, afin d'améliorer l'approche paléopathologique qui permet d'explorer la santé des populations passées.

Grâce au tomodensitomètre *Siemens*, modèle *SOMATOM (Definition AS+ 128*), les 56 squelettes sélectionnés (plus de 50% correspondent à des jeunes adultes) ont été scannés entièrement pour diverses régions anatomiques (crâne, côtes, vertèbres, bras gauche, bras droit, jambe gauche, jambe droite, bassin, mains et pieds). Toutes les images (scans en coupes sagittale, coronale et transversale) ont ensuite été analysées à l'aide du programme *OsiriX*, en quête d'anormalités, et selon un protocole précis pour décrire les lésions (type, distribution). Finalement, elles ont été confrontées aux observations macroscopiques, et des diagnostics possibles ont été proposés dans certains cas.

Issus de ces analyses, les cas paléopathologiques les plus marquants sont présentés ici, afin d'illustrer la nécessité de combiner les observations macroscopiques aux données scannographiques. La mise au point de cette banque de données nous a permis d'approfondir l'approche paléopathologique. Ainsi, elle a pu fournir davantage de données et interprétations possibles sur diverses maladies (ex. rachitisme, ostéomalacie, scorbut), ayant pu affecter en particulier la population urbaine de la Ville de Québec au 19e siècle.

Session 313 - Petroleum core analysis

(052) Construction of complex 3D digital rock models

*I. V. YAKIMCHUK[1], I. A. VARFOLOMEEV[1,2], N. V. EVSEEV[1], B. D. SHARCHILEV[1], O. A. KOVALEVA[2], D. A. LISICIN[1,2], D. A. KOROBKOV[1], S. S. SAFONOV[1]
iyakimchuk@slb.com

[1] Schlumberger, Moscow, Russia
[2] Moscow Institute of Physics and Technology, Dolgoprudny, Russia

The idea of creating digital representation of a reservoir rock sample for further numerical analysis of its petrophysical properties appeared several decades ago. It has a number of benefits and shortcomings with respect to traditional laboratory core analysis. Digital Rock approach is becoming more and more attractive nowadays due to the recent advances in the development of imaging methods, new areas of applications and increasing performance and accuracy of numerical simulations.

Ordinary the digital models are constructed in the simplest way – binarization of greyscale CT images on voids and solids. That is enough to get qualitative results from certain flow simulation experiments. Modern sophisticated numerical simulation techniques allow taking into account a vast set of physicochemical properties during calculation (e.g., mineralogy, mechanical strength, thermal conductivity, wettability) with regards to their volumetric spatial distributions. This information can be obtained using continiously developing experimental imaging techniques.

We present several approaches aimed to extend the content of digital rock models making them more informative. Current results are related to evaluation of 3D mineral map and estimation of 3D distribution of non-resolved pore space. Proposed approaches are based on smart merging of X-ray micro-CT and scanning electron microscopy data. Our first results and implementation in simulation process justify the necessity of the suggested improvements for digital rock model construction workflow.

(063) Sensitivity analysis for micro-tomography data segmentation in digital rock physics

H. BERTHET[1], *M. BLANCHET[1], R. RIVENQ[1]
helene.berthet@total.com

[1] TOTAL, Avenue Larribau 64018 Pau Cedex France

Digital Rock Physics is a fast-growing branch of petrophysics based on the acquisition and analysis of 3D images of small rock volumes at the micrometer scale. For conventional rocks, individual pores and grains can be well resolved leading to the study of the rock porosity, pore-body morphology and flow properties. However, raw data typically suffer from imaging artefacts and noise which are partially removed by filtering before running the segmentation step. Segmentation is the conversion step from greyscale X-ray attenuation image to a binary fit-for-analysis image. Though critical for the reliability of the results, it is known to be extremely user-dependent due to the variety of the available algorithms and to their sensitivity to input parameters. In this work, we performed a converging-active-contour segmentation on a dry Berea sandstone 3D image made available by Andrä *et al.* (2012) for benchmarking purposes. We show that several segmentations can be deemed acceptable according to existing criteria, if a robust workflow is followed, if parameters are carefully chosen and if the image is of sufficient quality. Therefore we propose a method to evaluate the uncertainty brought by the segmentation step in such favourable situations. The underlying principle is that this uncertainty is not an error range that should be reduced with better algorithms; it is rather the true description of the imperfect information available in the image. This method has the advantage of giving probability distributions instead of single values for the computed petrophysical properties, such as porosity, pore surface area, percolation radius and pore throat distribution. The processing workflow followed in this study consisted in median filtering, converging active contours segmentation and black top-hat transform; the resulting porosity ranged from 0.179 to 0.195 for the P90 and P10 porosity cases; surface areas were affected by ±20% and the connectivity indicators by ±10%. The method also provides a set of several good-quality segmentations which can be used as stochastic inputs for more complex image processing such as flow simulations. Such a quantification of uncertainty is however limited to situations were satisfying segmentations can be obtained; it does not quantify the error between any given segmentation and the reality – yet this error is possibly much larger than the parameter-lead uncertainty, e.g. on carbonate images with a lot of sub-resolution porosity.

(145) Characterization of reservoir quality in the upper devonian wabamun group using micro-CT and helical-CT imaging techniques

G. M. BANIAK
greg.baniak@bp.com

BP Canada Energy Group ULC, Calgary, Alberta, Canada

In the Pine Creek gas field of west-central Alberta, Canada, the primary reservoir intervals occur in the Upper Devonian Wabamun Group. A common feature of the Wabamun Group is the presence of the dolomitized burrow fabrics. Notably, the dolomitized burrows have permeabilities ranging between 1 and 350 millidarcies (mD), while the lime mudstone-wackestone matrix adjacent to the burrows has permeabilities of less than 1 mD. Because of the moderate to extreme contrasts in permeabilities between the burrows and matrix, the burrows most likely act as the primary flow pathways within the Pine Creek gas field.

To better understand the impact of bioturbation of bulk reservoir permeability in the Wabamun Group, high-resolution X-ray microtomography (micro-CT) and helical computed tomography (helical-CT) imaging techniques were used. In short, micro-CT and helical-CT images show that the burrows (comparable to examples of *Thalassinoides* and *Palaeophycus*) are spatially heterogeneous and their dimensions and orientations are highly variable at the centimeter to millimeter scale. When viewed in 2D cross-sectional slices at various levels, the overall volumes of dolomite and calcite were found to vary considerably. As a result, the Wabamun Group is composed of an interconnected network of burrows, with the burrow density and burrow interconnectivity varying considerably throughout the sample. Notably however, horizontal burrow connectivity was found to be more common than vertical burrow connectivity, except in the most pervasively bioturbated sections (i.e., 90 to 100% bioturbation). As such, fluid flow within the burrow fabrics is dominantly anisotropic with a preferred bedding parallel flow direction. It was from these high-resolution images that a more detailed and accurate depiction of the bulk reservoir permeability could be constructed using numerical modeling. In short, numerical modeling showed that bulk reservoir permeability is best estimated using the harmonic and geometric mean in scenarios where burrow-associated dolomite is minimal. Conversely, bulk reservoir permeability is best estimated using the arithmetic mean in scenarios where burrow-associated dolomite is moderate to high.

(211) How computerized tomography can improve the remote detection of hydrocarbons using seismic methods?

M. J. DUCHESNE[1], B. GIROUX[2]
mathieuj.duchesne@rncan-nrcan.gc.ca

[1] Geological Survey of Canada
[2] INRS-ETE, 490 de la Couronne, Québec, Canada, G1K 9A9

Physical and mathematical concepts underlying X-ray computed tomography (CT) and reflection seismology are very similar as both electromagnetic and seismic waves propagate through matter to illuminate its internal structure. During their propagation into matter both electromagnetic and seismic waves are attenuated respectively by absorption and scattering of photons and dispersion and partitioning of seismic energy. Although both types of waves interact with the matter in different ways, density is the common physical property which governs propagation behavior and response. Despite this fact, the combined use of CT and seismic reflection data for geological interpretation has been rarely discussed in the literature.

Even if both methods are sharing physical and mathematical similarities, their joint use faces a major hurdle: their different scale of investigation. Effectively, CT provides a nanometer to micrometer-scale resolution whereas seismic reflection generally pictures the subsurface at a meter-scale resolution. Therefore, there is a difference of about 9 orders of magnitude between both methods. Interestingly enough though, this difference is also a strength of their joint use as qualitative and quantitative information brought by CT imaging reveal details about the occurrence and distribution of physical properties influencing the attenuation and reflection of seismic waves. In fact, the scale of heterogeneity of the subsurface that is typically relevant at seismic frequencies is the micrometer-scale also known as the pore-scale. This is particularly true for saturated porous rocks where wave-induced flow mechanism do affect the seismic response. This mechanism occurs over a compression/dilatation cycle of a seismic wave where the elastic behavior of certain fluids is transferred into the rigid matrix leading to increased attenuation. CT has been traditionally used since the late 1980s by the petroleum industry to document porosity distribution in reservoirs and more recently progress has been made for imaging fluids and deriving some of their properties (e.g. saturation and phase). Seismic modeling using poro-elastic and poro-viscoelastic schemes can certainly benefit from CT imaging to quantify information about the skeleton and interstitial fluids forming the media that interact with the wavefront during its propagation and thus contribute to its attenuation. This also has implications for understanding seismic anomalies attributed to the occurrence of hydrocarbons and consequently for providing additional insights into the remote detection of petroleum resources using seismic methods.

(067) Evaluation of experimental dissolution of dolomite using X-ray computed tomography

*B. BAGLEY[1], B. M. TUTOLO[1], A. J. LUHMANN[1], M. O. SAAR[1,2], W. E. SEYFRIED, JR.[1]
bagley@umn.edu

[1] University of Minnesota, Department of Earth Sciences, Minneapolis, MN 55455
[2] ETH-Zurich, Department of Earth Sciences, Zurich, Switzerland

Flow-through experiments were conducted on nine dolomite cores to simulate CO_2 injection into dolomite reservoirs during geologic carbon sequestration. Experiments at 100 ºC and 150 bar pore-fluid pressure were conducted in single-pass mode using CO_2-charged brine and flow rates that spanned two orders of magnitude. The cores (1.3 cm diameter and 2.6 cm long) were scanned at the University of Minnesota X-ray Computed Tomography (XRCT) facility before and after each experiment to capture mineral volume changes resulting from experimental dissolution. Experimentally-produced dissolution features (i.e., porosity development) were visualized by carefully aligning the pre- and post-experiment cores in three dimensions. Dissolution produced a range of dissolution patterns, including highly permeable flow channels or wormholes.

Previous work provided insight for a porosity-surface area model using the general shapes of the dissolution channels that developed from fluid-rock reaction (Luhmann et al., 2014). Here, we produce a more complete quantification and characterization of the experimentally produced dissolution structures. Specifically, we calculate the diameter, tortuosity, and center of mass of the dissolution structures, and attempt to develop predictive capabilities by calculating correlations between the locations of post-experimental dissolution features and pre-experimental flow properties. By dividing each sample into a 3-dimensional grid of Representative Elementary Volumes (REVs) of various sizes, we attempt to define a characteristic length scale that controls the evolution of dissolution features, and provide important input data sets for high resolution computational fluid dynamics simulations.

The size of the cores limit XRCT resolution to 8 µm, which in turn determines the smallest resolvable features. As a result, our porosity measurements represent the macro porosity in the cores. To capture the micro- and nano-scale porosity, we conducted combined Small and Ultra Small Angle Neutron Scattering ((U)SANS) analyses, which permit investigation of features in the range of ~10 nm to ~10 µm. Simultaneous consideration of calculations based on the invariants of the (U)SANS curves, the XRCT data sets, and full-core porosity measurements demonstrates that ~50% of the pores within the experimental samples are within this lower (<10 µm) pore size range. This combined result suggests that the characteristic length scales for dissolution phenomena in dolomites may be below the resolution of the XRCT measurements, and that a combined approach of this type may be warranted to develop appropriate scaling functions.

References :
A.J. Luhmann, X.Z. Kong, B.M. Tutolo, N. Garapati, B.C. Bagley, M.O. Saar, W.E. Seyfried Jr., (2014) Experimental dissolution of dolomite by CO2-charged brine at 100 °C and 150 bar: Evolution of porosity, permeability, and reactive surface area, Chemical Geology, 380, 145-160, doi:10.1016/j.chemgeo.2014.05.001.

(129) Image restoration for oil bearing sandstones

*S. BRUNS[1], S. S. HAKIM[1], H. O. SØRENSEN[1], S. L. S. STIPP[1]
bruns@nano.ku.dk

[1] University of Copenhagen, Department of Chemistry, Universitetsparken 5, 2100 Copenhagen, Denmark

Acquiring synchrotron images takes a lot of time and effort. If we want to be quantitative rather than qualitative in the analysis of these data, we should have the same standards in processing the data as we have in acquiring them. This means image processing should be a restoration procedure rather than merely a sequence of steps where images are enhanced. This is especially important for materials that show nanometer scale details.

From an image processing point of view, sandstone is simpler than more fine grained natural materials, such as chalk. Therefore, sandstone constitutes an ideal environment for developing image restoration methods geared towards tomographic reconstructions of reservoir rock. Apart from a pore network, with much larger pores that are relatively easily resolved, the characteristics that simplify tomogram reconstructions of sandstone are: (i) a crystalline structure with clearly identifiable interfaces between pores and solid and (ii) a range of minerals, each with their own X-ray attenuation coefficients. These characteristics can be used to set up efficient models to simulate the noise characteristics and the impulse response function from the reconstruction to be used for signal restoration.

We used microtomograms taken with synchrotron radiation, of oil bearing sandstones, to develop a nonlocal means and deconvolution framework optimized for tomographic reconstructions of reservoir rock. Notably, noise in these data is a mapping of the detector noise from Radon space to the reconstruction, i.e., it is neither Poissonian nor fully uncorrelated. A data-driven approach was used to characterize the exponential relationship between signal intensity and noise level from the reconstructions. Weak correlations were considered using a two-step filtering approach rather than a direct estimate of the noise-free signal. The approach eliminates the need for regularization almost entirely, i.e., it enabled quantifying the different mineral phases and oil volume ratio of our sandstone samples from greyscale intensity alone. This makes it possible to discern high yield, oil rich zones in the sandstone formation from already depleted zones and/or zones where residual oil is located in regions of low permeability.

The finite resolution of the imaging system was considered by assuming a Gaussian shaped three-dimensional point spread function for the reconstructions. Its dispersion was estimated as a system constant using the denoised datasets. Using the acquired point spread function for iterative image deconvolution yielded volume images of increased contrast and resolution. We consider this step optional for sandstone. Yet, it provides us with an important vantage point for the future analysis of more complex reservoir rocks that can be found in the North Sea oil fields.

(135) Porosity assessment of sandstones of the Potsdam Group, St. Lawrence platform, Québec, Canada: utilisation of the CT scanning techniques

*J. F. GRENIER[1], M. MALO[2], B. LONG[2], D. LAVOIE[3]
mmalo@ete.inrs.ca

[2] INRS-ETE, 490 de la Couronne, Québec, Canada, G1K 9A9
[3] Geological Survey of Canada, 490 de la Couronne, Québec, Canada, G1K 9A9

The tomodensitometry was used to evaluate the porosity of sandstones of the Potsdam Group in the St. Lawrence Platform, Québec, Canada. The Potsdam Group is the basal lithostratigraphic unit of the basin overlying the Precambrian basement and represents the best target for CO_2 geological storage in the Province of Québec (Malo and Bédard, 2012; Bédard et al., 2013). The group is comprised of two formations, the Covey Hill and Cairnside. The Covey Hill is composed of quartz-feldspar-pebble conglomerate, feldspathic and quartz arenites with shale and siltstone intervals deposited in a terrestrial to fluvial and estuarian environments. The Cairnside is composed of a fine- to coarse-grained, massive to laminated, and well-sorted quartz arenite deposited in a littoral to marine environment.

Well A-203 in the St. Lawrence Platform was cored from the top to the bottom in the Precambrian basement. It represents the most complete and uninterupted succession of the platform stratigraphic sequence in Québec. The Potsdam is cored from the base of the overlying Beekmantown Group, 1158 m, to the top of the underlying basement at 1738 m. The Covey Hill Formation in the well was divided into three sub-units. CV1, at the base (1738 to 1672 m), and CV3 (1359 to 1270 m), at the top of the Covey Hill Formation are two heteregenous sub-units with various siliciclastic rocks, conglomerate, sandstone, siltstone and red shale. The middle CV2 sub-unit consists of medium- to coarse grained quartz and feldspathic arenite with local siltstone intervals. The Cairnside Formation is an homogenous fine- to coarse grained quartz arenite of 142 m thick.

The porosity was evaluated by three methods: the density log, a porosimeter and CT scanning techniques using a tomodensitometer Siemens SOMATOM Sensation 64. The two more heterogenous lithologic CV1 and CV3 sub-units show low porosity usually below 2%. The CV2 sub-unit exhibits porosity ranging from 1 to 8%, whereas arenite of the Cairnside Formation shows a more regular porosity between 3 to 4%. The porosity values from the tomodensitometer are usually lower than those obtained from the porosimeter, whereas there is a good correlation with those calculated from the density log.

References :
Bédard, K., Malo, M., Comeau, F.-A. 2013. CO_2 geological storage in the Province of Québec, Canada : Capacity evaluation of the St. Lawrence Lowlands basin. Energy Procedia, 37, 5093-5100.
Malo, M., Bédard, K. 2012. Basin-scale assessment for CO_2 storage prospectivity in the Province of Québec, Canada. Energy Procedia, 23, 487-494.

Centre - Eau Terre Environnement

INRS
UNIVERSITÉ DE RECHERCHE

2nd International Conference on Tomography of Materials and Structures

NOTES:

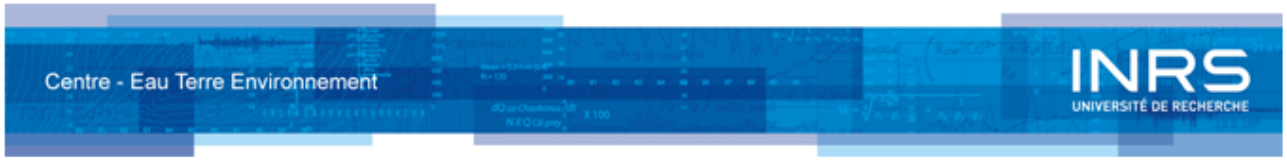

2nd International Conference on Tomography of Materials and Structures

NOTES:

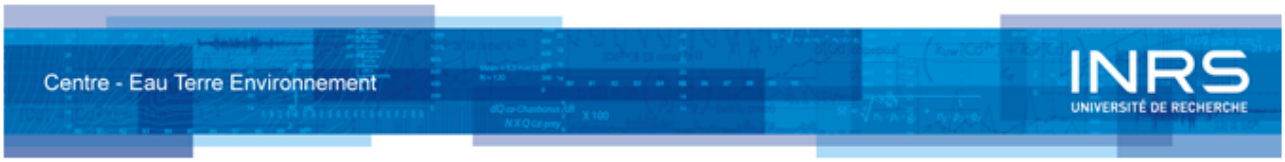

2nd International Conference on Tomography of Materials and Structures

NOTES:

2nd International Conference on Tomography of Materials and Structures

NOTES:

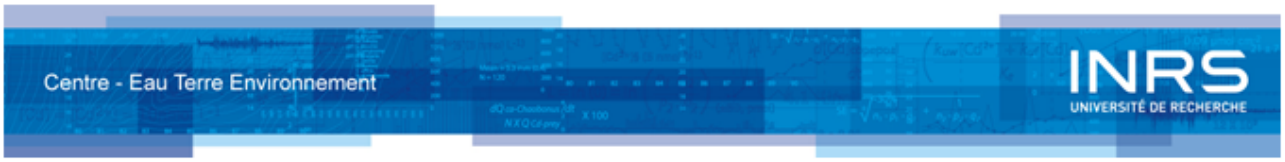

2nd International Conference on Tomography of Materials and Structures

NOTES:

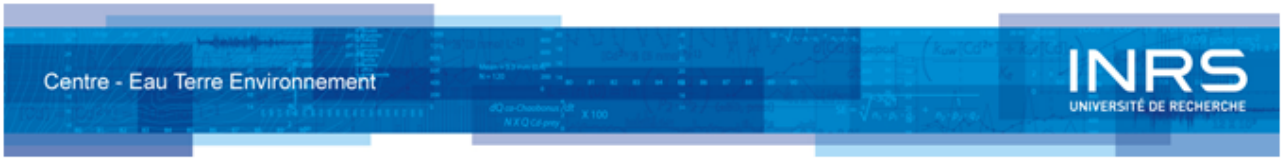

2nd International Conference on Tomography of Materials and Structures

NOTES:

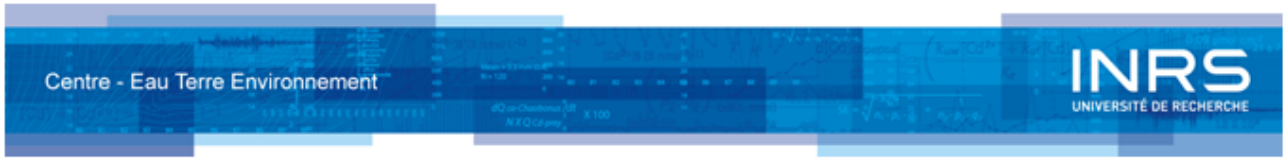

2nd International Conference on Tomography of Materials and Structures

NOTES:

2nd International Conference on Tomography of Materials and Structures

NOTES:

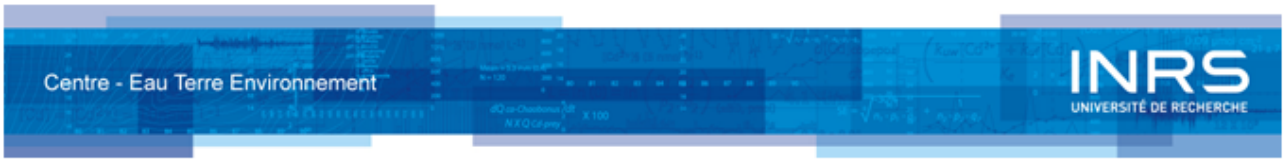

2nd International Conference on Tomography of Materials and Structures

NOTES:

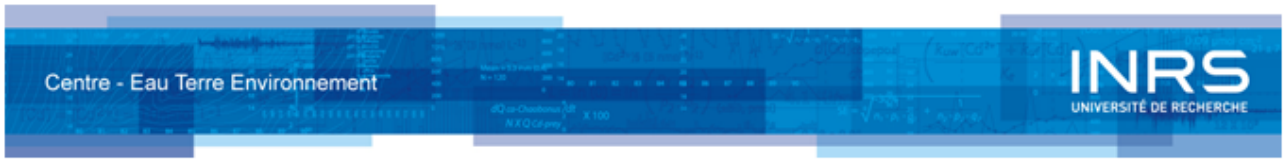

2nd International Conference on Tomography of Materials and Structures

NOTES:

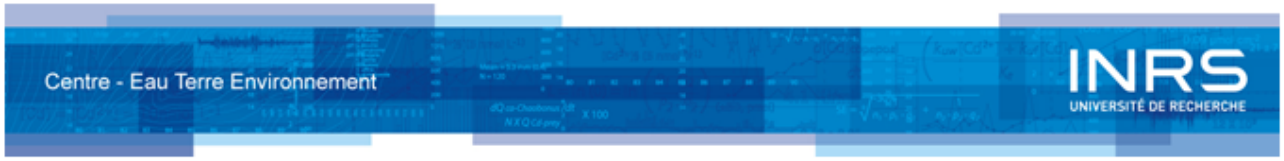

2nd International Conference on Tomography of Materials and Structures

NOTES:

ICTMS 2015

ictms2015.ete.inrs.ca

Lab CT Scan

Laboratoire multidisciplinaire de tomodensitométrie
pour les ressources naturelles et le génie civil

ctscan.ete.inrs.ca

INRS

UNIVERSITÉ DE RECHERCHE
A RESEARCH UNIVERSITY

inrs.ca